UNIVERSITEIT VAN PRETORIA
UNIVERSITY OF PRETORIA
YUNIBESITHI YA PRETORIA

Identification of viral proteins and cellular pathways involved in the induction of apoptosis of African horse sickness virus-infected mammalian cells

by

Elaine Vermaak

Submitted in partial fulfilment of the requirements of the degree
Master of Science
in the Faculty of Natural and Agricultural Sciences
Department of Microbiology and Plant Pathology
University of Pretoria
Pretoria

September 2011

UNIVERSITEIT VAN PRETORIA
UNIVERSITY OF PRETORIA
YUNIBESITHI YA PRETORIA

DECLARATION

I declare that the dissertation, which I hereby submit for the degree M.Sc (Microbiology) at the University of Pretoria, is my own work and has not previously been submitted by me for a degree at this or any other tertiary institution.

Signed: …….. Date: ...……

ACKNOWLEDGEMENTS

I would like to express my sincere appreciation to the following people for their contribution towards the completion of this dissertation:

Prof. J. Theron for granting me the opportunity to complete my M.Sc under his supervision, for his continued support and encouragement.

Mr. A. Hall, Mr. C.F. van der Merwe and Miss. S. Ungerer for their assistance with the confocal laser scanning microscopy and transmission electron microscopy analyses.

Mr. W.A. Barnes for his assistance with the flow cytometric analyses.

Mr. F. Wege for cell culture maintenance and titration of the AHSV-4 strain and recombinant baculoviruses.

The staff and students of the Department of Microbiology and Plant Pathology and Genetics for their support and guidance during this study.

My family and friends for their constant support, love and encouragement.

To Him, through whom all things are possible.

The National Research Foundation for financial assistance.

SUMMARY

Identification of viral proteins and cellular pathways involved in the induction of apoptosis of African horse sickness virus-infected mammalian cells

by

Elaine Vermaak

Supervisor: Prof. J. Theron
Department of Microbiology and Plant Pathology
University of Pretoria

for the degree M.Sc

African horse sickness virus (AHSV) is transmitted by *Culicoides* spp. biting midges to horses, causing serious effusion and haemorrhage in various organs and tissues, but is asymptomatic in the insect host. Likewise, AHSV causes dramatic cytopathic effect (CPE) in infected mammalian cells in culture, but no CPE is observed in infected insect cell cultures despite productive virus replication. The basis for this differential host response has not yet been investigated, but is suggestive of the induction of apoptosis in mammalian cells following virus infection. Consequently, the aims of this investigation were essentially to determine whether AHSV infection induces apoptosis in cultured mammalian cells, and to subsequently identify the initiators and effectors of AHSV-induced apoptosis in mammalian cells.

To determine whether apoptosis is induced in BHK-21 mammalian cells, the cells were infected with AHSV-4 and the key apoptotic indicators of cell morphology, chromosomal DNA fragmentation and caspase-3 activation were monitored. Results were obtained providing evidence that *in vitro* infection of BHK-21 cells with AHSV-4 results in apoptosis at 12 h post-infection with maximal levels of apoptosis at 24 h post-infection. By making use of inhibitors of endosomal acidification and UV-inactivated AHSV-4, it was demonstrated that virus disassembly, but not productive virus replication, is necessary for AHSV-4 to trigger apoptosis in BHK-21 cells. Subsequent studies indicated that extracellular co-administration of VP2 and VP5, which likely results in the uptake of VP2-VP5 complexes into the endosomes, induces apoptosis. These findings therefore suggest that the outer capsid

proteins are sufficient to trigger apoptosis and that they exert their effect during the early events in AHSV cell entry, where cell binding and endosomal membrane penetration is required.

To identify apoptotic pathways triggered during AHSV-4 infection of BHK-21 cells, the enzymatic activity of different cellular caspases in cytoplasmic extracts of infected cells was measured by proteolytic cleavage of caspase-specific chromogenic substrates. Results were obtained indicating the activation of caspases-8 and -9, whereas flow cytometry analyses, following staining of the cells with the lipophilic cation DePsipher™, revealed the loss of mitochondrial membrane potential. This data therefore indicated that both the extrinsic and intrinsic apoptotic pathways are activated in AHSV-infected mammalian cells. Moreover, AHSV-4 infection of BHK-21 cells led to the nuclear translocation of nuclear factor κB (NF-κB) complexes containing the Rel family members p50 and p65, thus suggesting that NF-κB may also play a role in the AHSV apoptotic machinery.

Collectively, the results obtained during the course of this investigation provide evidence for apoptosis induction following AHSV infection of mammalian cells, and are the first to delineate the role of early events in the virus replication cycle in the induction of apoptosis and to demonstrate that both the death receptor and mitochondrial pathways can play an essential role in AHSV-induced apoptosis. These results therefore add an important new dimension to AHSV-host cell interactions and provide a foundation for the future study of apoptosis and the role thereof in viral pathogenesis.

TABLE OF CONTENTS

DECLARATION i
ACKNOWLEDGEMENTS ii
SUMMARY iii
LIST OF ABBREVIATIONS x
LIST OF FIGURES xiv
LIST OF TABLES xvi

CHAPTER ONE 1

LITERATURE REVIEW

1.1 GENERAL INTRODUCTION 2
1.2 AFRICAN HORSE SICKNESS (AHS) 3
1.3 AFRICAN HORSE SICKNESS VIRUS (AHSV) 5
1.3.1 Classification 5
1.3.2 Virion structure 6
1.3.3 Viral genome 7
1.3.4 Viral proteins 8
1.3.4.1 Non-structural proteins 8
1.3.4.2 Inner capsid proteins 10
1.3.4.3 Outer capsid proteins 11
1.4 ORBIVIRUS REPLICATION AND MORPHOGENESIS 12
1.5 APOPTOSIS 15
1.5.1 Caspases 15
1.5.2 Caspase signalling pathways 16
1.5.2.1 Intrinsic apoptotic signalling 16
1.5.2.2 Extrinsic apoptotic signalling 18
1.5.3 Regulation of apoptosis and caspase activation 19
1.5.3.1 Inhibitor of apoptosis proteins (IAPs) 19
1.5.3.2 Bcl-2 protein family 20
1.5.4 Nuclear factor kappa B (NF-κB) 21
1.6 VIRUSES AND APOPTOSIS 22
1.6.1 Initiation of proapoptotic signalling during virus infection 23
1.6.2 Apoptosis and members of the *Reoviridae* family 25
1.7 AIMS OF THIS INVESTIGATION 27

CHAPTER TWO

29

EXPRESSION OF THE OUTER CAPSID PROTEINS VP2 AND VP5 OF VIRULENT AND ATTENUATED AHSV-4 ISOLATES IN EUKARYOTIC CELLS

2.1 INTRODUCTION 30
2.2 MATERIALS AND METHODS 32
2.2.1 Bacterial strains and plasmids 32
2.2.2 DNA amplification 33
2.2.2.1 Primers 33
2.2.2.2 Polymerase chain reaction (PCR) 33
2.2.3 Agarose gel electrophoresis 34
2.2.4 Purification of DNA from agarose gels 34
2.2.5 Cloning of DNA fragments into plasmid vectors 34
2.2.5.1 Ligation reactions 34
2.2.5.2 Preparation of competent *E. coli* cells 35
2.2.5.3 Transformation of competent cells 35
2.2.6 Screening of transformants 36
2.2.6.1 Plasmid DNA isolation 36
2.2.6.2 Restriction endonuclease digestions 37
2.2.6.3 DNA sequencing and sequence analysis 37
2.2.7 Plasmid constructs 38
2.2.8 Transient expression of AHSV-4 VP2 and VP5 proteins in BHK-21 cells 40
2.2.8.1 Cell culture 40
2.2.8.2 Transfection of BHK-21 cells 40
2.2.9 Engineering and characterization of recombinant bacmids 40
2.2.9.1 Transposition 40
2.2.9.2 Isolation of recombinant bacmid DNA 41
2.2.9.3 Analysis of recombinant bacmid DNA 41
2.2.10 Generation of recombinant baculoviruses 42
2.2.10.1 Cell culture 42
2.2.10.2 Transfection of *Sf*9 cells with recombinant bacmid DNA 42
2.2.10.3 Plaque assays 43
2.2.10.4 Preparation of virus stocks 43

2.2.11 Optimization of AHSV-4 VP2 and VP5 protein expression in *Sf*9 cells 44
2.2.11.1 MOI optimization 44
2.2.11.2 Time of harvest optimization 44
2.2.12 Large-scale preparation of soluble baculovirus-expressed AHSV-4 VP2 and VP5 proteins 44
2.2.13 Analysis of recombinant proteins 45
2.2.13.1 SDS-polyacrylamide gel electrophoresis (SDS-PAGE) 45
2.2.13.2 Immunoblot analysis 46
2.3 RESULTS 47
2.3.1 Construction of recombinant pGEM® T-Easy plasmids harbouring full-length AHSV-4 VP2 and VP5 genes 47
2.3.2 Sequencing of the full-length VP2 and VP5 genes derived from virulent and attenuated AHSV-4 isolates 50
2.3.3 Transient expression of AHSV-4 VP2 and VP5 proteins in BHK-21 cells 52
2.3.3.1 Construction of recombinant pCMV-Script® plasmids 52
2.3.3.2 Expression of the AHSV-4 VP2 and VP5 genes in BHK-21 cells 52
2.3.4 Construction of recombinant pFastBac™1 donor plasmids harbouring full-length AHSV-VP2 and VP5 genes 54
2.3.5 Engineering and characterization of recombinant bacmids 56
2.3.6 Recombinant VP2 and VP5 protein expression in *Sf*9 cells 58
2.3.7 Optimization of recombinant VP2 and VP5 protein expression in *Sf*9 cells 61
2.3.8 Large-scale production of soluble recombinant VP2 and VP5 proteins 65
2.4 DISCUSSION 67

CHAPTER THREE **72**

AFRICAN HORSE SICKNESS VIRUS INDUCES APOPTOSIS IN MAMMALIAN CELLS AND IS TRIGGERED BY THE VIRUS OUTER CAPSID PROTEINS

3.1 INTRODUCTION 73
3.2 MATERIALS AND METHODS 74
3.2.1 Cells and virus 74
3.2.2 Microscopic examination of AHSV-4 infected BHK-21 cells 75

3.2.3 Chromosomal DNA fragmentation analysis 76
3.2.4 Quantification of apoptosis 76
3.2.5 Ultra-violet (UV) light inactivation of AHSV-4 77
3.2.6 Transfection of BHK-21 cells 77
3.2.7 Treatment of BHK-21 cells with recombinant AHSV-4 VP2 and VP5 proteins 78
3.2.8 Endosomal acidification inhibition assays 78
3.3 RESULTS 79
3.3.1 Microscopic examination of AHSV-infected BHK-21 cells 79
3.3.2 DNA fragmentation analysis of AHSV-infected BHK-21 cells 83
3.3.3 Induction of apoptosis by AHSV-4 in BHK-21 cells does not require virus replication 85
3.3.4 The outer capsid proteins of AHSV-4 are required for the induction of apoptosis in BHK-21 cells 85
3.3.5 Induction of apoptosis by AHSV-4 in BHK-21 cells requires virion disassembly 89
3.4 DISCUSSION 91

CHAPTER FOUR **95**

AFRICAN HORSE SICKNESS VIRUS INDUCES APOPTOSIS IN MAMMALIAN CELLS BY BOTH EXTRINSIC AND INTRINSIC APOPTOTIC PATHWAYS

4.1 INTRODUCTION 96
4.2 MATERIALS AND METHODS 98
4.2.1 Cells and viruses 98
4.2.2 Caspase inhibition assays 98
4.2.2.1 Treatment of virus-infected BHK-21 cells with caspase inhibitor 98
4.2.2.2 DNA fragmentation analysis 99
4.2.3 Caspase activation assays 99
4.2.4 Detection of mitochondrial membrane depolarization 100
4.2.4.1 Flow cytometry 100
4.2.4.2 Confocal laser scanning microscopy of AHSV-infected BHK-21 cells 101

4.2.5 Detection of NF-κB (p50 and p65) 101
4.2.5.1 Protein extraction 101
4.2.5.2 Immunoblot analysis 102
4.3 RESULTS 102
4.3.1 AHSV-induced apoptosis in BHK-21 cells is caspase-dependent 102
4.3.2 Cellular caspases are activated in AHSV-infected BHK-21 cells 103
4.3.3 The mitochondrial membrane is depolarized in AHSV-infected BHK-21 cells 105
4.3.4 NF-κB is activated in AHSV-infected BHK-21 cells 107
4.4 DISCUSSION 110

CHAPTER FIVE **115**

CONCLUDING REMARKS

REFERENCES **122**

APPENDICES **152**

- A1: Protein binding and internalization assays 153
- A2: Nucleotide and amino acid sequence alignments 158

LIST OF ABBREVIATIONS

A	Absorbance
aa	amino acid
ABTS	2,2-azino-bis[3-ethylbenzothiazoline-6-sulfonic acid]-diammonium salt
AC	ammonium chloride
AHS	African horse sickness
AHSV	African horse sickness virus
Apaf-1	apoptotic protease activating factor-1
ATCC	American Type Culture Collection
ATP	adenosine-5'-triphosphate
att	attenuated
Bcl-2	B-cell lymphoma-2
BH	Bcl-2 homology
BHK	Baby hamster kidney
BIR	baculoviral IAP repeat
BLAST	Basic Local Alignment Search Tool
bp	base pair
BSA	bovine serum albumin
BTV	bluetongue virus
°C	degrees Celsius
C	carboxy
ca.	approximately
CARD	caspase-recruitment domain
cDNA	complementary DNA
CLP	core-like particle
cm^2	cubic centimeter
CMV	cytomegalovirus
CO_2	carbon dioxide
CPE	cytopathic effect
CQ	chloroquine
CRD	cysteine-rich domain
DD	death domain
DED	death effector domain
DEVD	Asp-Glu-Val-Asp
dH_2O	distilled water

DISC	death-inducing signalling complex
DMSO	dimethyl sulfoxide
DNA	deoxyribonucleic acid
DNase	deoxyribonuclease
dNTP	deoxyribonucleoside-5'-triphosphate
DR	death receptor
ds	double stranded
DTT	dithiothreitol
e.g.	*exempli gratia* (for example)
EBSS	Earle's Balanced Salt Solution
EDTA	ethylenediaminetetra-acetic acid
eGFP	enhanced green fluorescent protein
EMEM	Eagle's Minimal Essential Medium
et al.	*et alia* (and others)
FasL	Fas ligand
FBS	foetal bovine serum
FCCP	carbonyl cyanide *p*-[trifluoro-methoxy] phenylhydrazone
Fig.	figure
h	hour
H_2O_2	hydrogen peroxide
i.e.	that is
IAP	inhibitor of apoptosis protein
IB	inclusion body
IKK	IκB kinase
IPTG	isopropyl-β-D-thiogalactopyranoside
IκB	inhibitory protein of κB
JNK	c-Jun N-terminal kinase
kb	kilobase pairs
kDa	kilodalton
KOAc	potassium acetate
LB	Luria-Bertani
M	molar
MCS	multiple cloning site
mg	milligram
min	minute
ml	millilitre
mm	millimetre

mM	millimolar
MOI	multiplicity of infection
Mr	molecular weight
mRNA	messenger ribonucleic acid
N	amino
NaOAc	sodium acetate
NEAA	non-essential amino acids
NF-κB	nuclear factor kappa B
ng	nanogram
nm	nanometer
nM	nanomolar
NTPase	nucleoside triphosphate phosphohydrolase
OD	optical density
OIE	Office International des Epizootics
PAGE	polyacrylamide gel electrophoresis
PBS	phosphate-buffered saline
PCD	programmed cell death
PCR	polymerase chain reaction
pfu	plaque forming units
pmol	picomole
*p*NA	*p*-nitroanilide
PSB	protein solvent buffer
RHD	Rel homology domain
RNA	ribonucleic acid
RNase	ribonuclease
rpm	revolutions per minute
s	second
SD	standard deviation
SDS	sodium dodecyl sulphate
*Sf*9	*Spodoptera frugiperda* clone 9 cells
Smac	second mitochondria-derived activator of caspase
ss	single stranded
TAD	transactivation domain
TEM	transmission electron microscopy
TEMED	N',N',N',N'-tetramethylethylenediamine
TNF	tumour necrosis factor
TNFR	tumour necrosis factor receptor

TRAF	TNF receptor-associated factor
TRAIL	TNF-related apoptosis inducing ligand
U	units
U937	Human leukemic monocyte lymphoma cells
UHQ	ultra-high quality
UV	ultraviolet
V	volts
v.	version
v/v	volume per volume
VIB	viral inclusion body
vir	virulent
w/v	weight per volume
X-Gal	5-bromo-4-chloro-3-indolyl β-D-galactopyranoside
z-VAD-FMK	carbobenzoxy-valyl-alanyl-aspartyl-[O-methyl]-fluoromethylketone
µg	microgram
µl	microlitre
µm	micrometre
µM	micromolar

LIST OF FIGURES

Fig. 1.1 Schematic representation of the BTV particle. 7

Fig. 1.2 Schematic diagram of the replication cycle of BTV. 14

Fig. 1.3 Schematic representation of the extrinsic and intrinsic apoptotic pathways. 17

Fig. 2.1 Agarose gel electrophoretic analysis of recombinant pGEM® T-Easy plasmids harbouring VP2 gene-specific inserts (a) and VP5 gene-specific inserts (b). 49

Fig. 2.2 Schematic representation of recombinant pCMV-Script® vector (a) and agarose gel electrophoretic analysis of recombinant pCMV-Script® plasmids (b). 53

Fig. 2.3 Schematic representation of recombinant pFastBac™1 vector (a) and agarose gel electrophoretic analysis of the recombinant pFastBac™1 plasmids (b). 55

Fig. 2.4 Schematic representation of transposed bacmid DNA (a) and agarose gel electrophoretic analysis of recombinant bacmid DNA following PCR analysis (b). 57

Fig. 2.5 SDS-PAGE and immunoblot analyses of the whole-cell lysates prepared from *Sf*9 cells infected with Bac-VP2att and Bac-VP2vir. 59

Fig. 2.6 SDS-PAGE and immunoblot analyses of the whole-cell lysates prepared from *Sf*9 cells infected with Bac-VP5att and Bac-VP5vir. 60

Fig. 2.7 SDS-PAGE analyses of whole-cell lysates prepared from *Sf*9 cells infected with recombinant baculoviruses at various MOIs. 62

Fig. 2.8 SDS-PAGE analyses of protein fractions prepared at 48 or 72 h post-infection from recombinant baculovirus-infected *Sf*9 cells. 64

Fig. 2.9 Large-scale production of recombinant outer capsid proteins in suspension cultures of *Sf*9 cells. 66

Fig. 3.1 Light microscopy micrographs of BHK-21 cells infected with AHSV-4. 80

Fig. 3.2 Transmission electron micrographs of BHK-21 cells infected with AHSV-4. 82

Fig. 3.3 DNA fragmentation analysis of BHK-21 cells infected with AHSV-4. 84

Fig. 3.4 Enrichment of nucleosomes in the cytoplasm of BHK-21 cells infected with AHSV-4. 84

Fig. 3.5 Effect of UV treatment on induction of apoptosis by AHSV-4 in BHK-21 cells. 86

Fig. 3.6 DNA fragmentation analysis of BHK-21 cells transfected with recombinant pCMV-Script® mammalian expression vectors. 88

Fig. 3.7 Identification of the AHSV-4 proteins required for the induction of apoptosis in BHK-21 cells. 88

Fig. 3.8 Treatment of BHK-21 cells with the endosomal acidification inhibitors ammonium chloride (AC) and chloroquine (CQ). 90

Fig. 3.9 The effect of inhibition of endosomal acidification on DNA fragmentation in BHK-21 cells infected with AHSV-4. 90

Fig. 4.1 The effect of caspase inactivation on DNA fragmentation in BHK-21 cells infected with AHSV-4. 104

Fig. 4.2 Activation of different caspases associated with AHSV-induced apoptosis in BHK-21 cells. 106

Fig. 4.3 Mitochondrial membrane depolarization in BHK-21 cells infected with AHSV-4. 108

Fig. 4.4 Confocal laser scanning microscopy of AHSV-infected BHK-21 cells stained with DePsipher™. 109

Fig. 4.5 Immunoblot analysis of NF-κB translocated to the nuclei in BHK-21 cells infected with AHSV-4. 111

Fig. 5.1 Proposed model of the induction of apoptosis by AHSV in mammalian cells. 118

LIST OF TABLES

Table 1.1 BTV genome segments and their encoded proteins 9

Table 2.1 Primers used in this study to amplify DNA fragments for cloning and sequencing of cloned insert DNA 33

Table 2.2 Amino acid differences between the VP2 sequences of attenuated and virulent AHSV-4 isolates 51

Table 2.3 Yield of soluble baculovirus-expressed AHSV-4 VP2 and VP5 proteins 65

CHAPTER ONE

LITERATURE REVIEW

1.1 GENERAL INTRODUCTION

African horse sickness (AHS), of which African horse sickness virus (AHSV) is the aetiological agent, is an infectious, non-contagious, arthropod-borne viral disease of equids. The first reference to the disease concerns an epidemic that occurred in 1327 in Yemen (Mellor and Hamblin, 2004). However, the virus almost certainly originated in Africa and was first observed on the African continent after the introduction of horses from India in the 16th century for purposes of exploring central and east Africa. The first outbreak of AHS in southern Africa was recorded in 1719 when over 1 700 animals died of the disease in the then Cape of Good Hope. Subsequently, over the next 217 years, at least 10 major outbreaks of AHS have been recorded in southern Africa. The most severe outbreak occurred in the Cape of Good Hope in 1854-1855 in which more than 70 000 horses died (Coetzer and Erasmus, 1994). The frequency and severity of the outbreaks have, however, declined over the last century, probably due to improved surveillance and strict zoning measures, as well as vaccination of horses with polyvalent live attenuated vaccines (Mellor and Hamblin, 2004). Nevertheless, based on its potential economic and international importance, AHS has been classified as a notifiable disease by the Office International des Epizootics (OIE, 2004).

Much of the pioneering research on AHS was performed by Sir Arnold Theiler during the early 20th century. In 1900, he demonstrated the filterability of the pathogen through Berkefield and Chamberland filters, thereby indicating that the pathogen was indeed a virus. Theiler's research also indicated that there existed immunologically distinct strains of the AHS agent, since immunity acquired against one strain did not always protect the horse when challenged by a heterologous virus strain. In 1903, Theiler and Pitchford-Watkins established that AHSV may be transmitted by biting insects and in 1921, Theiler reported the first detailed descriptions of the clinical signs and lesions produced by infections with AHSV (reviewed in Coetzer and Erasmus, 1994). During the late 1960s and 1970s, several studies were undertaken aimed at characterizing the structure and morphology of AHSV (Verwoerd and Huismans, 1969; Oellerman *et al.*, 1970; Bremer, 1976). Consequently, AHSV has been classified as a member of the genus *Orbivirus* in the family *Reoviridae*. This family is comprised of a large number of viruses with segmented double-stranded RNA (dsRNA) genomes and virus particles that have both an inner and outer protein capsid (Urbano and Urbano, 1994; Calisher and Mertens, 1998).

With the advent of gene cloning, genetic engineering and protein expression technologies, much progress has been made regarding structure-function relationships of different AHSV genes and encoded gene products (Uitenweerde *et al.*, 1995; Maree and Huismans, 1997; van Niekerk *et al.*, 2001; de Waal and Huismans, 2005; Stassen *et al.*, 2011). Despite this progress, much still remains to be learned regarding the role of individual AHSV proteins within the context of infected host cells, the interaction of individual viral proteins with host cellular proteins, as well as viral proteins and cellular mechanisms that contribute to the molecular basis of AHS disease and pathogenesis. With regards to the latter, AHS is one of the most lethal diseases of equids and is characterized by clinical signs that develop as a consequence of damage to the circulatory and respiratory systems, thus giving rise to serious effusion and haemorrhage in various organs and tissues (Mellor and Hamblin, 2004). Since the first demonstration by Clem *et al*. (1991) that apoptotic cell death plays a major role in viral disease mechanisms, it is now recognized that many animal viruses are capable of inducing apoptosis in infected cells (Shen and Shenk, 1995; O'Brien, 1998; Clarke and Tyler, 2009) and that apoptosis contributes significantly to their pathogenesis (Oberhaus *et al.*, 1997; O'Donnell *et al.*, 2005; Umeshappa *et al.*, 2010). However, comparatively little is known about the cellular biochemical pathways that modulate virus-induced apoptosis, as well as the identity and nature of the viral intermediates that initiate the signalling of the cell death cascade (Roulston *et al*., 1999; Danthi, 2011).

The review will summarize the current information concerning AHSV and will highlight the role of individual viral proteins in the infectious cycle of the virus. This will be followed by a discussion of apoptosis, including the caspase-dependant signalling pathways involved in virus-induced apoptosis in mammalian cells, and a brief description of the aims of this investigation.

1.2 AFRICAN HORSE SICKNESS (AHS)

African horse sickness (AHS) is an infectious viral disease of equids (horses, donkeys and mules), with horses being the most susceptible (Mellor and Hamblin, 2004; Guthrie, 2007). Although zebra rarely exhibit clinical signs of AHSV infections, they have long been considered the natural vertebrate host and reservoir of AHSV, and are believed to play an important role in the persistence of the virus in Africa (Erasmus *et al.*, 1978; Barnard, 1998).

AHS is endemic in tropical and sub-tropical areas of Africa south of the Sahara, occupying a broad band stretching from Senegal in the west to Ethiopia and Somalia in the east, and extending as far south as northern South Africa (Mellor and Hamblin, 2004). Although AHS was believed to be confined largely to sub-Saharan Africa, except for occasional excursions into North Africa, there have been several outbreaks of the disease in countries of the Persian Gulf and Middle East (Howell, 1960; Brown and Dardiri, 1990). Outbreaks of AHS have also occurred in Spain and Portugal (Lubroth, 1988). Of the nine AHSV serotypes, serotypes 1 to 8 are found only in restricted areas of sub-Saharan Africa, while serotype 9 is more widespread and has been responsible for almost all epidemics outside Africa, the exception being the Spanish and Portuguese outbreaks that were due to serotype 4 (Coetzer and Erasmus, 1994).

AHS is not contagious and the virus is transmitted primarily through the bites of adult female midges belonging to the genus *Culicoides* (du Toit, 1944; Mellor *et al.*, 1975). An adult *Culicoides* becomes infective eight days after feeding on a viraemic animal and stays infected until death. The major vector of AHSV is *C. imicola*, which occurs throughout Africa, much of Southeast Asia and southern Europe (Mellor, 1994). More recently, *C. bolitinos* has also been identified as a potential vector of AHSV (Venter *et al.*, 2000a). *C. bolitinos* has a wide distribution in southern Africa and is common in cooler highland areas where *C. imicola* is rare. Epidemic outbreaks of AHS have been well correlated with climate conditions favoured by the *Culicoides* species, with early heavy rainfall followed by warm, dry spells generally considered as optimal breeding conditions (Venter and Meiswinkel, 1994). Indeed, climate change may expand the range of the vector insect and therefore raises the possibility that AHS may spread more globally (Purse *et al.*, 2005, 2008).

After the transfer of AHSV by the bite of infective midges, AHSV is transported to the lymph nodes of the animal where initial virus replication takes place. The virus particles are subsequently disseminated throughout the body via the blood (primary viraemia) and virus replication in target organs and endothelial cells give rise to a secondary viraemia (Mellor and Hamblin, 2004). According to the extent and severity of clinical symptoms caused by the infection, the disease is classified into four distinct forms. These are the pulmonary or peracute form, the cardio-pulmonary or mixed form, the cardiac or subacute form and horse sickness fever (Coetzer and Erasmus, 1994). In the pulmonary form, a fever is first detected, followed by coughing, dyspnoea and the appearance of a discharge of fluid from the nostrils.

Death usually occurs several hours after the onset of dyspnoea and less than 5% of horses with this form of the disease recover. The mixed pulmonary and cardiac form of the disease is the most common form of the disease with horses occasionally exhibiting signs of respiratory distress. The mortality rate is *ca.* 70% with death occurring within three to six days after the onset of fever. With the cardiac form, the horse suffers subcutaneous oedema of the head, neck and the supraorbital fossae. Approximately 35% of affected horses recover, but mortality rates exceeding 50% have been reported. The horse sickness fever form of the disease is characterized by horses displaying mild to moderate fever, scleral infection and mild depression, which is followed by complete recovery (Coetzer and Erasmus, 1994).

Although there is currently no specific treatment available for AHS, great emphasis has been placed on the control of AHS incidence (House, 1998; Sanchez-Vizcaino, 2004). Since AHSV is non-contagious and can only spread via the bites of infected *Culicoides* species, control is effected through the use of insecticides and repellents to control the vector population, as well as by restricting animal movement to prevent infected animals from initiating new foci of infection, and by slaughtering of viraemic animals to prevent them acting as sources of virus for vector insects (Mellor and Hamblin, 2004). In southern Africa, AHS is controlled by vaccination using polyvalent live attenuated vaccines that are administered twice in the first and second year of life of susceptible animals, and annually thereafter (Erasmus, 1976; Taylor *et al*., 1992; MacLachlan *et al*., 2007).

1.3 AFRICAN HORSE SICKNESS VIRUS (AHSV)

1.3.1 Classification

AHSV is a member of the genus *Orbivirus* in the family *Reoviridae* (Calisher and Mertens, 1998). The family encompasses viruses with segmented dsRNA genomes (10-12 segments) encapsidated within single non-enveloped virus particles with a diameter of 55-80 nm, which exhibit icosahedral symmetry. In addition to *Orbiviruses*, the other eight genera of this family are *Aquareovirus*, *Coltivirus*, *Cypovirus*, *Fijivirus*, *Phytoreovirus*, *Orthoreovirus*, *Oryzavirus* and *Rotavirus* (Roy, 2001). These viruses have broad host ranges and have been isolated from a wide variety of terrestrial and non-terrestrial vertebrates and invertebrates, as well as plants (Francki *et al*., 1991; Gorman, 1992). The orbiviruses can be distinguished from other members of the *Reoviridae* in that they replicate in both insects and vertebrates (Calisher and

Mertens, 1998), show greater sensitivity to lipid solvents and detergents, and virus infectivity is lost in mildly acidic conditions (Gorman and Taylor, 1985). Within the genus, viruses are divided into 21 distinct serogroups based on cross-reactivities in complement fixation tests, and serotypes within a serogroup are recognized by specific serum-neutralization tests (Gorman, 1979, 1983, 1985; Knudson and Monath, 1990; Brown *et al*., 1991; Calisher and Mertens, 1998). Nine different AHSV serotypes have been distinguished serologically (McIntosh, 1958; Howell, 1962).

1.3.2 Virion structure

The AHSV virion is non-enveloped with two concentric protein layers that enclose a dsRNA genome consisting of ten segments (Verwoerd *et al*., 1972; Bremer *et al.*, 1990). The outer capsid is composed of the two major structural proteins VP2 and VP5, while the inner capsid is comprised mainly of the two major proteins VP3 and VP7 that enclose the three minor proteins VP1, VP4 and VP6 (Roy *et al*., 1994).

The structure of the AHSV particle is comparable to that of bluetongue virus (BTV), of which the structure of single- and double-shelled virus particles has been determined by cryo-electron microscopy and by X-ray crystallography (Hewat *et al.*, 1992; Prasad *et al.*, 1992; Grimes *et al.*, 1998). The core particle can be segregated into two distinct layers. A thin inner layer is formed from 120 large triangular plates of VP3 to form a complete shell, while minimizing conformational distortion. The internal scaffold of VP3 is stabilized by the outer layers of the core that comprise a coat of 260 VP7 trimers. The core contains the dsRNA genome and the transcription complexes consisting of VP1 (12 copies), VP4 (20 copies) and VP6 (60 copies), each of which plays an important role in genome RNA replication (Stuart and Grimes, 2006). Cryo-electron microscopy and analyses have also revealed that the outer shell of BTV is highly ordered (Hewat *et al.*, 1992), consisting of 120 globular VP5 regions that are located upon each of the six-membered rings of the VP7 trimers. Moreover, “sail”-shaped spikes of VP2 form triskelion-type motifs that cover nearly all of the VP7 trimers. Together, VP2 and VP5 form a continuous layer surrounding the core, except for holes on the 5-fold axis (Stuart *et al.*, 1998; Nason *et al.*, 2004). A schematic diagram of the BTV particle is presented in Fig. 1.1.

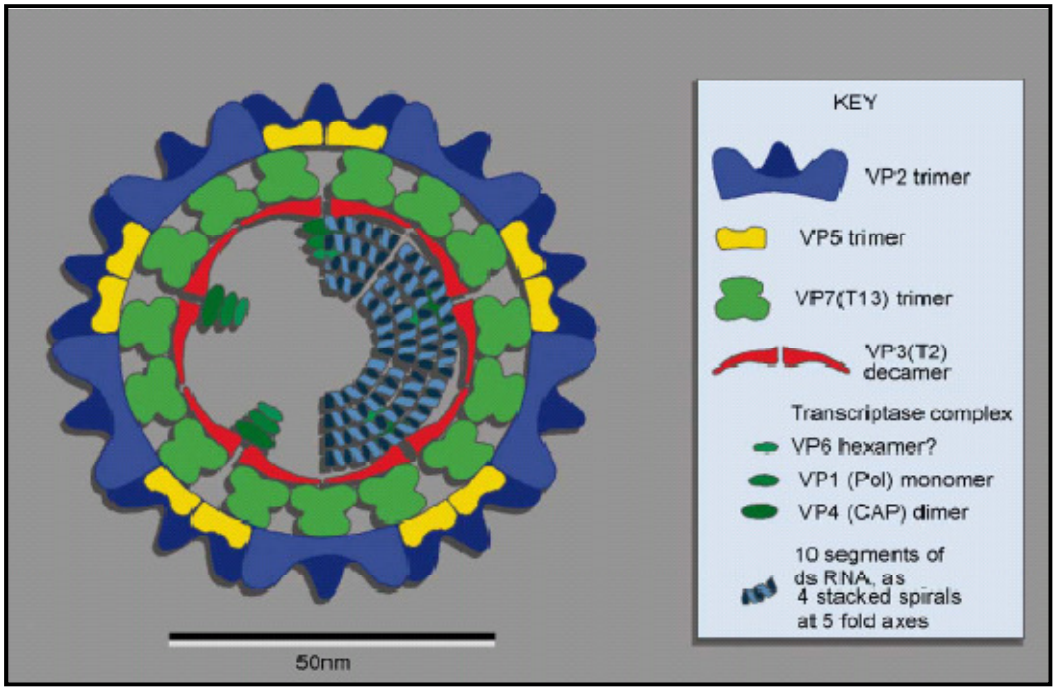

Fig. 1.1: Schematic representation of the BTV particle (Mertens, 2004). The core particle, which comprises VP3 and VP7, encloses the three minor core proteins, namely VP1, VP4 and VP6, and the ten dsRNA viral genome segments. The core is surrounded by the outer capsid composed of VP2 and VP5.

1.3.3 Viral genome

The AHSV genome consists of ten dsRNA segments, which are grouped according to size into large (L1-L3), medium (M4-M6) and small (S7-S10) genome segments (Bremer *et al.*, 1990). Each genome segment is monocistronic, except for S10, which encodes the two related non-structural proteins NS3 and NS3A (van Staden and Huismans, 1991; Grubman and Lewis, 1992). The 5′ non-coding region of the genome segments ranges in size between 12 and 35 base pairs (bp), while the 3′ non-coding regions are 29 to 100 bp in length (Roy *et al.*, 1994). In contrast to BTV, the terminal hexanucleotide sequences of AHSV are not conserved through all the segments (Rao *et al.*, 1983; Roy *et al.*, 1994). Nevertheless, the 5′- and 3′-terminal sequences of each genome segment display partial inverted complementarity. This feature is thought to play a role in determining the secondary structure of the viral mRNA, which may be of importance for initiation of transcription and/or in the sorting and assembly of genome segments during virus replication (Cowley *et al.*, 1992; Mizukoshi *et al.*, 1993).

1.3.4 Viral proteins

In addition to seven structural proteins (VP1-VP7), four non-structural proteins (NS1, NS2, NS3 and NS3A) are also encoded by the viral genome. The ten orbivirus dsRNA genome segments, together with their encoded proteins and likely functions, are summarized in Table 1.1.

1.3.4.1 Non-structural proteins

The NS1 protein of orbiviruses is synthesized abundantly in virus-infected cells and is readily assembled as tubular structures within the cytoplasm. These tubules are biochemically and morphologically distinct from the microtubules and neurofilaments present in normal cells (Huismans and Els, 1979). The tubular structures are formed by helically coiled ribbons of NS1 dimers, but the biophysical character of the tubules differ between BTV and AHSV. In contrast to BTV tubules that have a diameter of 52.3 nm and lengths of up to 1 µm (Hewat *et al.*, 1992), the AHSV tubules have a diameter of 23 nm and vary in length up to 4 µm (Maree and Huismans, 1997). Moreover, whereas BTV tubules exhibit a defined ladder-like appearance, AHSV tubules appear to have a fine reticular "cross-weave" appearance. No function has yet been assigned to NS1, but it has been proposed that the protein may be a major determinant of BTV pathogenesis in the vertebrate host since it augments virus-cell association that ultimately leads to lysis of the infected cell (Owens *et al.*, 2004).

The NS2 protein is the predominant component of virus inclusion bodies (VIBs) (Hyatt and Eaton, 1988; Brookes *et al.*, 1993) and expression of NS2, in the absence of other viral proteins in both insect and mammalian cells, results in the formation of inclusion bodies (IBs) that are indistinguishable from VIBs found in virus-infected cells (Thomas *et al.*, 1990; Uitenweerde *et al.*, 1995; Modrof *et al.*, 2005). The VIBs have been shown to contain ssRNA, dsRNA, NS1, as well as complete and incomplete virus particles (Eaton *et al.*, 1988; Eaton *et al.*, 1990; Brookes *et al.*, 1993). These observations therefore have led to the recognition of VIBs as the sites in which virus assembly occurs. NS2 is also the only virus-specific protein that is phosphorylated in infected cells (Huismans *et al.*, 1987; Devaney *et al.*, 1988). Although the significance of NS2 phosphorylation is not completely understood, a recent report has indicated that phosphorylation of BTV NS2 is important for VIB formation (Modrof *et al.*, 2005). The NS2 protein also has a strong affinity for ssRNA but not for dsRNA, suggesting that it may have a role in the recruitment and packaging of viral ssRNA

Table 1.1: BTV genome segments and their encoded proteins (adapted from Mertens, 2004)

Genome segment (bp)	**Protein**	Location	**Number of amino acids**	**Molecular mass of proteins (Mr)**	**Properties**	*Functions*
Seg-1	VP1	Within the subcore	1305	150292	The largest protein, highly basic with a positively charged carboxyl terminus.	RNA-directed RNA polymerase responsible for RNA transcription/replication.
Seg-2	VP2	Outer capsid	1051	122043	It forms a triskelion spike-like structure, which is found in excess in the outer layer of the core. Together with VP5 it exhibits the greatest variation in sequence between the serotypes, it determines the virus serotype and it is a neutralizing antigen, as well as a hydrophilic protein.	It possesses the viral haemagglutination and neutralization activity, is the cellular receptor protein which allows for the attachment and adsorption of the virus to the cell and is involved in the determination of virulence.
Seg-3	VP3	Within the subcore layer	905	103269	It contains group-specific antigen determinants and it is highly conserved and hydrophobic in nature.	Controls the size and organization of the core structure.
Seg-4	VP4	Component of the inner core	642	75826	Hydrophilic protein, which is highly conserved.	It is a methyl transferase protein that caps and methylates the mRNAs.
Seg-6	VP5	The inner layer of the outer capsid	504	56900	It forms globular structures on the outer layer and is very variable in sequence between the serotypes.	VP5 and VP2 form the outer capsid. VP5 is involved in the permeabilization of the endosomal membrane in a pH-dependent manner during initiation of infection and is also involved in the determination of the virus serotype.
Seg-9	VP6	Within the subcore layer	369	38464	Hydrophilic protein with ssRNA- and dsRNA-binding ability.	May serve as a NTPase and a helicase, which unwinds the dsRNA before replication, and it binds ssRNA and dsRNA.
Seg-7	VP7	Outer core surface	349	37916	It contains group-specific antigen determinants and is rich in hydrophobic regions.	It forms the outer core surface, which is involved in cell entry and in the high infectivity of vector insects and cells.
Seg-5	NS1	Cytoplasm of infected cells	548	63377	Highly conserved and form tubules during replication, which consist of helically coiled ribbons of dimers.	Although the function of NS1 tubules in virus replication is unclear, it may be involved in pathogenesis.
Seg-8	NS2	Cytoplasm of infected cells	365	41193	Only phosphorylated protein, which is largely hydrophilic and has a NTPase function.	It binds to ssRNA and may be involved in enveloping the mRNA during viral assembly and replication, and its NTPase activity might play a role in providing energy for the assortment, movement or packaging of the ssRNA that it binds.
Seg-10	NS3 and NS3A	Cell membranes	217 206	23659 22481	NS3A is a truncated form of NS3, both proteins are glycosylated, highly variable and cytotoxic to cell.	It disrupts cell membranes allowing virus release and may be involved in determination of virulence.

prior to encapsidation (Huismans *et al.*, 1987; Theron and Nel, 1997; Lymperopoulos *et al.*, 2003). Interestingly, BTV NS2 displays phosphohydrolase (NTPase) activity, and can bind and hydrolyse ATP and GTP to their corresponding nucleotide monophosphates (Horscroft and Roy, 2000; Taraporewala *et al.*, 2001). It has been suggested that the NTPase activity of NS2 may play a role in providing energy for the assortment, movement, packaging or condensation of bound ssRNA (Horscroft and Roy, 2000).

In contrast to NS1 and NS2, the two closely related non-structural proteins NS3 and NS3A are synthesized in low abundance in orbivirus-infected cells (Huismans, 1979; French *et al.*, 1989; van Staden *et al.*, 1995). The segment 10 gene, encoding NS3, contains two in-phase translation initiation codons that initiate the synthesis of NS3 and NS3A, respectively (van Staden and Huismans, 1991). The NS3/NS3A proteins are the only virus-encoded membrane-associated proteins (Wu *et al.*, 1992; van Niekerk *et al.*, 2001) and are localized to sites of virus release (Hyatt *et al.*, 1993; Stoltz *et al.*, 1996). NS3 proteins are therefore thought to be involved in the final stages of viral morphogenesis by facilitating the release of progeny virions from infected cells (Han and Harty, 2004; Celma and Roy, 2009; Meiring *et al.*, 2009).

1.3.4.2 Inner capsid proteins

The major core proteins, VP7 and VP3, form the outer layer of the viral core particle. In both BTV and AHSV, VP7 has been demonstrated to be a serogroup-specific antigen (Huismans and Erasmus, 1981; Chuma *et al.*, 1992). However, in contrast to BTV, the AHSV VP7 protein forms flat hexagonal structures in the cytoplasm of both virus-infected (Burroughs *et al.*, 1994) and recombinant baculovirus-infected cells (Chuma *et al.*, 1992; Maree and Paweska, 2005). Although the functional significance of the VP7 crystalline structures is not yet known, it is thought to represent a by-product rather than an essential component of the AHSV replication cycle (Burroughs *et al.*, 1994). The VP3 protein plays a major role in the structural integrity of the virus core and forms the protein scaffold on which the VP7 capsomeres are assembled (Stuart *et al.*, 1998). The BTV VP3 protein has been reported to contain group-specific antigenic determinants (Inumaru *et al.*, 1987) and is capable of interacting with ssRNA (Loudon and Roy, 1992). Co-expression of AHSV VP3 and VP7 genes in insect cells by means of recombinant baculoviruses has been shown to result in their

spontaneous assembly into core-like particles (CLPs), which structurally resemble empty authentic AHSV cores (Maree *et al.*, 1998).

The three minor structural proteins, VP1, VP4 and VP6, are candidates for the virus-directed RNA polymerase and associated enzymes that are responsible for transcription of the ten viral mRNAs during infection. The VP1 protein is considered to be the virus replicase-transcriptase enzyme based on its size (150 kDa), location and molar ratio (estimated at 10-12 molecules per virion) in the core (Stuart *et al.*, 1998), and it possesses motifs characteristic of RNA polymerases (Roy *et al.*, 1988; Vreede and Huismans, 1998). Baculovirus-expressed BTV VP1 has been shown to exhibit detectable RNA-elongation activity in the presence of single-stranded poly(U) template and a poly(A) primer (Roy *et al.*, 1988; Urakawa *et al.*, 1989). More recently, it was reported that soluble recombinant BTV VP1 exhibited a processive replicase activity, synthesizing complete complementary RNA strands of *in vitro*-synthesized BTV ssRNA templates (Boyce *et al.*, 2004). The 5′ ends of the viral mRNA species are believed to be capped and methylated during transcription, thus resulting in stabilization of the viral mRNA synthesized during infection (Roy, 1992). The VP4 protein of BTV has been reported to demonstrate guanylyl transferase (Le Blois *et al.*, 1992) and methyltransferase type 1 and type 2 (Ramadevi *et al.*, 1998) activities. Furthermore, VP4 also binds to GTP and displays nucleoside triphosphate phosphohydrolase (NTPase) activity, which is considered to be of importance for transcription and dsRNA processing (Ramadevi and Roy, 1998). The third minor protein, VP6, has a strong affinity for both ss- and dsRNA (Roy *et al.*, 1990; Hayama and Li, 1994; de Waal and Huismans, 2005). Sequence analysis of BTV and AHSV VP6 sequences has revealed a motif common to helicases (Roy, 1992; Turnbull *et al.*, 1996). In this regard, it has been reported that purified BTV VP6, upon incubation with dsRNA in the presence of ATP, led to the unwinding of the dsRNA template (Stäuber *et al.*, 1997). Thus, VP6 may be involved in the unwinding of the dsRNA genome prior to the initiation of transcription or, based on its RNA-binding ability, it may be involved in the encapsidation of viral RNA.

1.3.4.3 Outer capsid proteins

The VP2 protein, one of the two outer capsid proteins, is the most variable of the viral proteins (Potgieter *et al.*, 2003), and is the major serotype-specific antigen (Huismans and Erasmus, 1981) and viral heamagglutinin (Cowley and Gorman, 1987). Moreover, VP2 is

involved in attachment of the virus to cells and has been reported to bind to sialic acid moieties of cellular receptors prior to internalization of the virus particle (Hassan and Roy, 1999; Zhang *et al.*, 2010). In addition to its role in attachment, VP2 is also emerging as a key player in the control of BTV assembly and egress from infected cells. The amino (N)-terminal of the protein interacts with vimentin and this interaction contributes to virus egress (Bhattacharya *et al.*, 2007; Celma and Roy, 2009). Neutralizing epitopes have been mapped on AHSV VP2 (Bentley *et al.*, 2000; Martínez-Torrecuadrada *et al.*, 2001) and antibodies raised in rabbits to VP2 of AHSV-4 have been reported to neutralize a virulent strain of AHSV-4 (Martínez-Torrecuadrada *et al.*, 1994). It has also been shown that vaccinia- and baculovirus-expressed AHSV VP2 can protect horses against a lethal challenge with the homologous virus serotype (Stone-Marchat *et al.*, 1996; Scanlen *et al.*, 2002).

In contrast to the VP2 protein, the role of VP5 in neutralization has not yet been clearly established. In contrast to BTV (Marshall and Roy, 1990), AHSV VP5 is able to induce neutralizing antibodies, albeit at lower levels than VP2 (Martínez-Torrecuadrada *et al.*, 1999). However, when used in conjunction with VP2, higher titers of neutralizing antibody, compared to immunization with VP2 only, have been reported (Martínez-Torrecuadrada *et al.*, 1996). Consequently, AHSV VP5 may play a supportive role to VP2 in enhancing the immune response. Recent studies of VP5 of BTV and AHSV showed that the protein permeabilizes host cell membranes (Hassan *et al.*, 2001; Stassen *et al.*, 2011) and has the ability to induce cell-cell fusion when expressed on the cell surface (Forzan *et al.*, 2004). Both of these activities are mediated by two N-terminal amphipathic helices and are believed to play a major role in destabilizing the membrane of the endocytosized vesicle, thus allowing release of the viral core into the cytoplasm (Forzan *et al.*, 2007; Zhang *et al.*, 2010). BTV VP5 also interacts with membrane lipid rafts via a WHAL motif, and is likely to play an important part in docking VP5 with plasma membranes for assembly and/or egress via membrane fusion (Bhattacharya and Roy, 2008).

1.4 ORBIVIRUS REPLICATION AND MORPHOGENESIS

Although there are considerable differences in several of the replicative processes of members of the *Reoviridae* family, the overall strategy appears to be the same. Using BTV as a model for orbivirus replication and morphogenesis (Fig. 1.2), four major events in the

replication cycle of orbiviruses have been identified and are discussed below in greater detail. These events are: adsorption and penetration, uncoating and formation of replicative complexes, formation of virus tubules and virus inclusion bodies, and movement of virus to and release from the cell surface (Mertens, 2004; Roy, 2008).

In mammalian cells, binding of BTV to a receptor(s) is mediated by VP2 (Hassan and Roy, 1999; Zhang *et al*., 2010). The virus enters the cell through AP2-dependent clathrin-mediated endocytosis and is incorporated into early endosomes (Forzan *et al*., 2007). The low pH environment within the endosome causes removal of VP2 and triggers conformational changes in VP5 that allows the protein to permeabilize the endosomal membrane (Hassan *et al*., 2001; Zhang *et al*., 2010). Subsequently, the transcriptionally active core is released into the cytoplasm (Forzan *et al*., 2007). The replication of BTV is initiated by the synthesis and extrusion of capped and methylated mRNA from transcriptionally active cores within the cytoplasm. The mRNA transcripts function to encode proteins, and are also used as templates for production of minus-strands to form the dsRNA genome segments encapsidated in the progeny virions (Mertens and Diprose, 2004). However, the mechanism by which viral mRNAs are selected and encapsidated prior to replication is not yet known.

Soon after the initiation of transcription of BTV mRNAs, granular matrix structures accumulate near the core particles (Hyatt *et al.*, 1987). These VIBs increase both in size and number as the viral infection progresses (Eaton *et al.*, 1990). Newly synthesized viral transcripts, the four subcore viral proteins (VP1, VP3, VP4 and VP6), as well as assembled cores and subcores have been identified in the VIBs and therefore appear to be the sites of orbivirus replication and early viral assembly (Hyatt and Eaton, 1988). More recently, co-expression of the BTV structural proteins with NS2 has indicated that VP7 requires co-expression of VP3 to be recruited to the VIBs and that neither of the outer capsid proteins VP5 and VP2 have an affinity for the VIBs (Modrof *et al.*, 2005; Kar *et al.*, 2007). Therefore, it would appear that progeny core particles are first produced in the VIBs, then moved to the periphery of the VIBs where they are coated by the outer capsid proteins VP5 and VP2 (Kar *et al.*, 2007). Little is known of the mechanism whereby VP2 and VP5 are added to the developing virus particle. However, it was recently reported that VP5 of BTV associates with lipid rafts in the plasma membrane and that the core particles are transported to these sites for the final assembly of the outer capsid proteins (Bhattacharya and Roy, 2008). In addition to VIBs, NS1-rich tubules form part of the ‘insoluble’ phase of the cell and become a

characteristic structure of the cell from an early stage of infection (Huismans and Els, 1979; Eaton *et al.*, 1988). It has been reported that NS1 may be a determinant of pathogenesis in the vertebrate host by leading to lysis of infected cells (Owens *et al.*, 2004).

Investigations regarding virus release from mammalian cells have demonstrated a strong correlation between the presence of NS3 and NS3A, and virus release (Hyatt *et al.*, 1993; Stoltz *et al.*, 1996). The virions may leave infected cells by budding through the plasma membrane (Gould and Hyatt, 1994) or virions are extruded through a locally disrupted plasma membrane surface (Hyatt *et al.*, 1989; Han and Harty, 2004). More recently, the NS3 protein of BTV has also been shown to interact with the cellular proteins p11 and Tsg101, and these interactions were furthermore shown to assist in the egress of virus particles from infected cells in a non-lytic manner (Beaton *et al.*, 2002; Wirblich *et al.*, 2006; Celma and Roy, 2009).

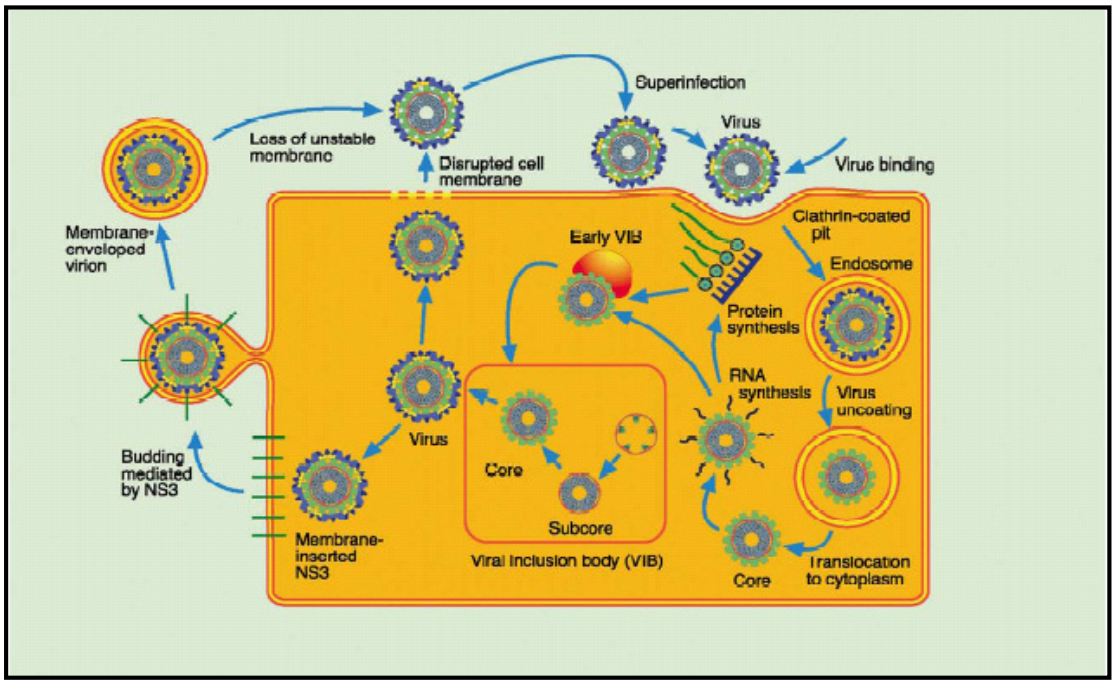

Fig. 1.2: Schematic diagram of the replication cycle of BTV (Mertens, 2004). The adsorption of the virus involves a receptor of unknown nature in the cell membrane of susceptible host cells. The viruses enter the cell via endocytosis, after which clathrin-coated vesicles, containing the virions, form and are drawn to the cell nucleus. The outer capsid proteins are removed to yield core particles in the cell cytoplasm. Transcription of the virion RNA occurs and the proteins generated by translation of the viral mRNA condense with the viral ssRNA around the parental cores to form VIBs. Structural proteins are translated and condense at the VIB periphery to form cores and subcores. The outer capsid proteins are added, after which the virions are released from the cells via lysis, budding or extrusion from the cells.

1.5 APOPTOSIS

Apoptosis, also known as programmed cell death (PCD), is a genetically controlled, energy-dependent process in which individual cells of multicellular organisms activate certain intracellular pathways to terminate themselves in a systematic manner (Kerr *et al.*, 1972; Wyllie *et al.*, 1980). Apoptosis occurs in response to a variety of extracellular and intracellular stimuli and is an essential mechanism in tissue development, the regulation of homeostasis, cellular proliferation and differentiation, and cell fate determination (Elmore, 2007; Lamkanfi *et al.*, 2007; Chowdhury *et al.*, 2008). The induction of apoptosis by viruses is thought to contribute to the tissue injury associated with their pathogenesis (Callus and Vaux, 2007; Clarke and Tyler, 2009). Consequently, knowledge regarding the viral processes and/or proteins that underlie apoptosis induction in infected cells may therefore not only provide a window on critical molecular events in the cell, but also enable the development of new antiviral agents. Since the induction of apoptosis following infection of susceptible host cells with AHSV is a major focus of this investigation, the molecular mechanisms underlying caspase-dependant apoptotic cell death will be discussed specifically in the following sections.

1.5.1 Caspases

A caspase-cascade system plays a central role in the induction, transduction and amplification of intracellular apoptotic signals (Xu and Shi, 2007; Duprez *et al.*, 2009). Caspases belong to a family of highly conserved aspartate-specific cysteine proteases and are members of the interleukin-1β-converting enzyme family (Alnemri *et al.*, 1996; Hengartner, 2000). They exist as inactive precursors, called procaspases, consisting of a large internal domain (p20; 17-21 kDa) that contains the catalytic subunit, a small C-terminal domain (p10; 10-13 kDa) and a N-terminal death domain (DD; 3-24 kDa) (Shi, 2002a; Prior and Salvesen, 2004). An aspartate cleavage site separates the DD from the internal domain, and an interdomain linker, containing one or two aspartate cleavage sites, separates the internal and C-terminal domains (Ashe and Berry, 2003; Li and Yuan, 2008). The DD is involved in the transduction of apoptotic signals (Martinon *et al.*, 2001; Weber and Vincenz, 2001) and has two subdomains, the death effector domain (DED) and the caspase-recruitment domain (CARD) (Deveraux *et al.*, 1998; Fesik, 2000). Upon receiving an apoptotic signal, the inactive procaspases undergo two proteolytic processing events at specific aspartic acid residues to generate two subunits that comprise the active enzyme (Pop and Salvesen, 2009). Active caspases are thus present

in a tetramer, which comprises of two large and two small subunits as heterodimers ($p20_2$-$p10_2$) (Sattar *et al*., 2003; Bao and Shi, 2007).

Both initiator and executioner caspases play key roles in the execution of apoptosis (Duprez *et al*., 2009; Pop and Salvesen, 2009). The initiator caspases contain a long DD (>90 amino acids) with either DED (caspase-8 and -10) or CARD (caspase-2 and -9) domains, which mediate the recruitment of the procaspase to specific death-inducing signalling complexes (Salvesen and Riedl, 2007). Initiator caspases are subsequently autocatalytically activated by a mechanism termed 'proximity-induced' activation, following their oligomerization (Cohen, 1997; Yang *et al*., 1998a, 1998b; Prior and Salvesen, 2004). In contrast, effector or executioner caspases (caspase-3, -6 and -7) contain a short DD (20-30 amino acids) and their activation requires cleavage by activated initiator caspases (Degterev *et al*., 2003; Fuentes-Prior and Salvesen, 2004; Bao and Shi, 2007). Executioner caspase targets include cellular and nuclear structural proteins, DNA metabolism and repair proteins, cytoplasmic proteins, protein kinases and cell cycle proliferative proteins, as well as endonuclease inhibitors (Fischer *et al.*, 2003; Timmer and Salvesen, 2007; Li and Yuan, 2008). The cleavage of several of these substrates by executioner caspases contributes to some of the morphological changes (*e.g.* cell shrinkage and plasma membrane blebbing) and biochemical changes (*e.g.* chromatin condensation and DNA fragmentation) associated with apoptotic cell death (Kerr *et al.*, 1972; Wyllie *et al*., 1981; Earnshaw, 1995; Martelli *et al*., 2001).

1.5.2 Caspase signalling pathways

Two major pathways to caspase activation, presented in Fig. 1.3, have been identified. These pathways are commonly referred to as the mitochondrial-mediated pathway (or intrinsic apoptotic pathway) and the death receptor-mediated pathway (or extrinsic apoptotic pathway), respectively.

1.5.2.1 Intrinsic apoptotic signalling

In the intrinsic pathway, intracellular apoptotic stimuli trigger internal sensors that induce BH3-only domain proteins, such as Bid, to translocate from the cytosol to the mitochondria (Wang *et al*., 1996). Bid binds to the proapoptotic proteins Bax and/or Bak and facilitates their conformational activation, resulting in the permeabilization of the mitochondrial outer membrane (Wang *et al*., 1996; Cheng *et al*., 2001; Danial and Korsmeyer, 2004).

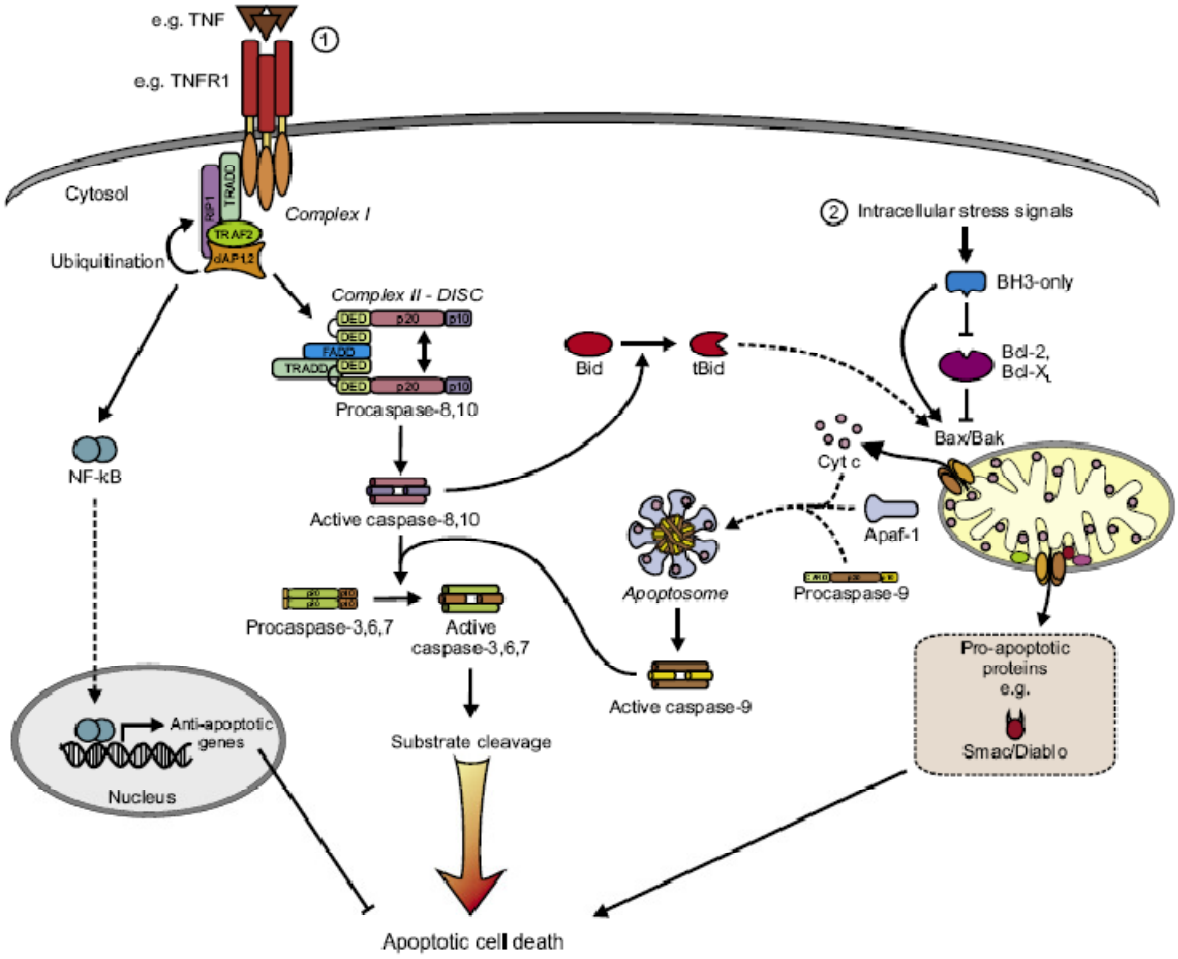

Fig. 1.3: Schematic representation of the extrinsic and intrinsic apoptotic pathways (Duprez *et al.*, 2009). (1) The extrinsic/cell surface death receptor apoptotic pathway. TNF stimulation results in the formation of complex I at the plasma membrane leading to NF-κB activation. A death-inducing signalling complex (DISC; Complex II) is formed after endocytosis of TNFR1, in which caspase-8 and/or -10 are recruited and activated. Downstream effector caspases (caspase-3, -6 and -7) are subsequently activated and their substrates cleaved, leading to cell death. The intrinsic apoptotic pathway (2), occurring at the mitochondrial level, is controlled by the Bcl-2 protein family. Proapoptotic Bak and/or Bax proteins induce the release of cytochrome *c*, and other mitochondrial proapoptotic molecules, leading to the formation of the apoptosome which, in turn, recruits and activates caspase-9. Substrate cleavage and ultimately cell death follows the activation of the downstream executioner caspases. In addition, activation of the intrinsic pathway, by the cleavage of Bid by caspase-8, amplifies the extrinsic apoptotic pathway signal.

Intermembrane space proteins, such as cytochrome *c* and the second mitochondria-derived activator of caspase (Smac), also known as DIABLO, are released from the mitochondrial intermembrane space into the cytosol (Finkel, 2001; Chowdhury *et al*., 2006). Cytochrome *c* interacts with the WD-40 repeat domains of cytosolic, monomeric apoptotic protease activating factor-1 (Apaf-1), resulting in oligomerization of Apaf-1 and formation of the apoptosome complex (Ahmad *et al.*, 1997; Zou *et al.*, 1999). The apoptosome then binds to procaspase-9 via caspase-recruitment domains present within procaspase-9 and Apaf-1, and activates caspase-9 by dimerization and autocleavage (Hu *et al*., 1998; Acehan *et al*., 2002). The activated apoptosome-bound caspase-9 subsequently cleaves and activates the effector caspases (caspase-3 and -7), which are also recruited by the apoptosome (Cain *et al.*, 1999). While cytochrome *c* activates Apaf-1, Smac/DIABLO relieves the inhibition on caspases by binding to and neutralizing the inhibitory activity of inhibitor of apoptosis proteins (IAPs) (Du *et al*., 2000; Ekert *et al*., 2001).

1.5.2.2 Extrinsic apoptotic signalling

The extrinsic cell death pathway is initiated by death receptors of the tumour necrosis factor (TNF) family. The TNF receptor (TNFR) superfamily has three main members, namely (i) Fas and Fas ligand (FasL) (Itoh *et al.*, 1991; Suda *et al.*, 1993), (ii) “death receptors” (DR4 and DR5) and TNF-related apoptosis inducing ligand (TRAIL) (Wiley *et al.*, 1995; Pitti *et al.*, 1996), and (iii) TNF receptors (TNFR1 and TNFR2) and TNFα (Tartaglia *et al.*, 1991; Ashkenazi and Dixit, 1999; Chen and Goeddel, 2002). These cellular death receptors are transmembrane receptors and are characterized by a conserved extracellular cysteine-rich domain (CRD), containing two to four cysteine-rich pseudo-repeats, a single transmembrane region and a conserved intracellular death domain (DD) of *ca.* 80 amino acids (Smith *et al.*, 1994; Huang *et al.*, 1996). Receptor self-association and receptor-ligand interactions occur via the CRD (Siegel *et al.*, 2000), whereas the intracellular DD interacts with specific adaptor proteins signalling cell death (Tartaglia *et al.*, 1993).

Ligation of the death receptor, followed by recruitment of other DD-containing adaptor proteins via electrostatic interactions, form a death-inducing signalling complex (DISC) that is responsible for activating caspase-8 (Boatright *et al*., 2003). The processing of procaspase-8 includes two cleavage events, firstly between the protease domains, and thereafter between the DD and the large protease subunit (Scaffidi *et al*., 1997; Chang *et al*., 2003). Both

cleavage products remain bound to the DISC, where an active caspase-8 heterotetramer is formed. The active caspase-8 is then released to the cytosol and triggers apoptosis. It has been reported that procaspase-10 is also activated at the DISC, but its function remains unclear (Kischkel *et al.*, 2001; Sprick *et al.*, 2002; Takahashi *et al.*, 2006). Although the activation of caspase-8 by the DISC may be sufficient to induce the activation of downstream effector caspases, in cells with an insufficient amount of activated caspase-8, however, death receptor and mitochondrial apoptosis may cross-interact by a mitochondrial amplification step. This step involves caspase-8 cleavage of the Bid protein to generate tBid (Li *et al.*, 1998; Luo *et al.*, 1998) and tBid-mediated release of cytochrome *c* from the mitochondria to the cytosol (Korsmeyer *et al.*, 2000). Subsequent activation of caspase-9 and caspase-3 amplifies the original signal (Luo *et al.*, 1998; Li *et al.*, 2002).

1.5.3 Regulation of apoptosis and caspase activation

A variety of precisely controlled mechanisms regulate the expression, proteolytic processing, activation or inactivation of caspases, thereby modulating the induction or inhibition of apoptosis. Regulation of apoptosis can occur at the level of the DISC, the apoptosome and at each subsequently activated caspase (Salvesen and Duckett, 2002; Golks *et al.*, 2005; Youle and Strasser, 2008). Various proteins, most notably inhibitor of apoptosis proteins (IAPs) and Bcl-2 proteins, have been demonstrated to regulate apoptosis and caspase activity.

1.5.3.1 Inhibitor of apoptosis proteins (IAPs)

The activities exerted by the enzymatically active caspases can be inhibited by conserved cellular caspase-binding proteins of the inhibitor of apoptosis protein (IAP) family (Duckett *et al.*, 1996; Salvesen and Duckett, 2002). Moreover, the overexpression of IAP family proteins inhibits apoptosis induced by Bax and other proapoptotic Bcl-2 family proteins (Deveraux and Reed, 1999). Of the eight mammalian IAPs that have been identified, only XIAP contains all elements required for potent caspase inhibition, whereas overexpression studies demonstrated that NAIP, survivin, c-IAP1 and c-IAP2 are all capable of binding to caspases and effectively modulating caspase activity (Deveraux and Reed, 1999; Srinivasula and Ashwell, 2008). The IAPs are characterized by a novel domain of 70-80 amino acids, termed the baculoviral IAP repeat (BIR) (Birnbaum *et al.*, 1994; Rothe *et al.*, 1995; Shi, 2002b). All members of the family contain one to three N-terminal BIR domains, which bind to the surface of caspases and block the catalyzing grooves of caspases. XIAP, c-IAP1 and c-

IAP2 each contain three BIR domains. Whereas BIR3 interacts with and inhibits the activity of caspase-9 (Johnson and Jarvis, 2004), the linker region between BIR1 and BIR2 targets and inhibits both caspase-3 and caspase-7 (Deveraux *et al*., 1997; Roy *et al*., 1997; Deveraux and Reed, 1999). In the intrinsic pathway, XIAP, c-IAP1 and c-IAP2 bind directly to procaspase-9 and prevent its activation (Deveraux *et al*., 1998). IAPs also inhibit the extrinsic apoptotic pathway by modulating caspase activity (Deveraux *et al*., 1997; Roy *et al*., 1997; Deveraux *et al*., 1998). Although most IAPs bind and directly suppress caspase catalytic activity, some of them function to downregulate caspase expression by acting as E3 ligases for their ubiquitination and degradation (Suzuki *et al*., 2001). IAPs themselves are negatively regulated by IAP antagonists, including Smac/DIABLO (Chai *et al*., 2000), which share a highly conserved N-terminus IAP binding motif and thus function as proapoptotic proteins (Liu *et al*., 2000; Huang *et al*., 2003; Zhou *et al*., 2005).

1.5.3.2 Bcl-2 protein family

The intrinsic apoptotic pathway is also regulated by a second evolutionary conserved protein family, *i.e.* the B-cell lymphoma-2 (Bcl-2) protein family, which is divided into one anti-apoptotic group and two proapoptotic groups (Youle and Strasser, 2008). Anti-apoptotic members of the Bcl-2 family of proteins, such as Bcl-2, Bcl-X_L, Bcl-w, Bcl-B, Bfl-1/A1 and Mcl-1, predominantly prevent mitochondrial changes, and share three or four Bcl-2 homology (BH) domains. One group of the proapoptotic Bcl-2 family members, such as Bax (Oltvai *et al*., 1993) and Bak (Kiefer *et al*., 1995), contain two or three BH domains. The second group of proapoptotic Bcl-2 family members shares only the BH3 domain and includes, amongst others, Bad (Yang *et al*., 1995) and Bid (Wang *et al*., 1996). Bax and Bak activation is triggered by BH3-only proteins, and upon activation function to permeabilize the outer membranes of mitochondria by forming size-indeterminate openings in the outer mitochondrial membrane, resulting in release of proapoptotic factors such as cytochrome *c* (Li *et al*., 1997; Cory and Adams, 2002). The activation of Bax and Bak is inhibited by the anti-apoptotic Bcl-2 family proteins. The anti-apoptotic protein Bcl-2 converges on mitochondria and sequesters the proapoptotic Bax and Bak proteins in order to regulate the release of cytochrome *c* in response to an apoptotic signal (Gross *et al*., 1999; Danial and Korsmeyer, 2004). However, it was recently reported that activated BH3-only proteins, such as Bid, can suppress the capacity of Bcl-2 to inhibit apoptosis by interacting with it to displace and subsequently activate Bax (Kuwana *et al*., 2005).

1.5.4 Nuclear factor kappa B (NF-κB)

The nuclear factor kappa B (NF-κB) family of heterodimeric transcription factors are responsible for regulating the expression of a large array of genes involved in, amongst others, cell growth and survival, as well as apoptosis (Karin and Lin, 2002; Hayden and Ghosh, 2008). The NF-κB family consists of five structurally related proteins, namely p50, p52, p65 (RelA), RelB and c-Rel. Each of these proteins possesses an N-terminal Rel homology domain (RHD) of *ca.* 300 amino acids that mediates dimerization, nuclear localization and DNA binding (Ghosh *et al.*, 1998). To facilitate the transcriptional activation of targeted gene expression, a C-terminal transcription activation domain (TAD) is present in the p65 (RelA), RelB and c-Rel family members (Ghosh *et al.*, 1998). In contrast, the p50 and p52 proteins lack TAD domains in their C-terminal halves and are synthesized as large precursors, p105 and p100, respectively, which undergo proteolytic processing that involves selective degradation of the C-terminal region to generate mature proteins (Liu and Chen, 2011). Both p50 and p52 play critical roles in modulating the specificity of NF-κB function. Although homodimers of p50 and p52 are generally repressors of transcription, both p50 and p52 can participate in target gene transactivation by forming heterodimers with p65 (RelA), RelB and c-Rel (Ghosh *et al.*, 1998; Staal *et al.*, 2011).

Latent, inactive NF-κB dimers are sequestered in the cytoplasm of quiescent cells via non-covalent interactions with the inhibitory proteins of κB family (IκBs) (Baeuerle and Baltimore, 1988; Ghosh *et al.*, 1998). The IκB family has several members, namely IκBα, IκBβ, IκBε, IκB-δ, IκBζ and Bcl-3 (Hayden and Ghosh, 2008). The NF-κB/IκB complexes are activated by site-specific phosphorylation of the IκB proteins by an activated IκB kinase (IKK) complex, composed of two catalytic subunits, IKKα and IKKβ, and the regulatory subunit, IKKγ (Zhang *et al.*, 2000; Devin *et al.*, 2001). Subsequent phosphorylation of the IκB proteins by IKK permits the polyubiquitination of these proteins by an ubiquitin ligase complex and the ubiquitinated IκB molecules are subsequently degraded by the 26S proteosome (Brockman *et al.*, 1995; DiDonato *et al.*, 1996, 1997). The nuclear localization signal of NF-κB is unmasked following the removal of IκB, thus allowing NF-κB dimers to translocate from the cytoplasm to the nucleus where it acts as a transcriptional regulator of target genes containing the 5′-GGGRNNYYCC-3′ consensus sequence (Beg *et al.*, 1992; Pahl, 1999).

NF-κB is capable of activating the transcription of a number of cell death-suppressing genes, thereby antagonizing apoptosis. Genes encoding anti-apoptotic members of the Bcl-2 protein family, such as Bcl-2, Bcl-X_L and Bfl-1/A1, are transcriptionally activated by NF-κB and function to suppress the release of proapoptotic molecules from the mitochondria, including cytochrome *c* (Karin and Lin, 2002; Burstein and Duckett, 2003). Moreover, transcription of the genes encoding the inhibitor of apoptosis proteins XIAP, c-IAP1 and c-IAP2, as well as the adaptor molecules TRAF1 and TRAF2 are also regulated by NF-κB (Kucharczak *et al.*, 2003). XIAP has been implicated in the inhibition of procaspase-9 activation, the inhibition of caspase-3 and caspase-7 activity (Liston *et al.*, 1996; Stehlik *et al.*, 1998; Takahashi *et al.*, 1998) and in the inhibition of TNF-induced JNK activation (Tang *et al.*, 2001), whereas c-IAP1 and c-IAP2 and the TNF receptor-associated factors, TRAF1 and TRAF2, act jointly to suppress TNF-induced apoptosis by inhibiting caspase activity and augmenting NF-κB activation, respectively (Deveraux *et al.*, 1998; Wang *et al.*, 1998).

In addition to its anti-apoptotic role, the transcriptional activity of NF-κB may enhance cell death. Several studies have reported the NF-κB-mediated expression of proapoptotic genes, thereby sensitizing cells to death-inducing signals. Of these genes, NF-κB-dependent activation of the death receptor Fas and its ligand FasL has been noted (Kasibhatla *et al.*, 1999), as well as the NF-κB-mediated expression of the TRAIL receptors DR4 and DR5 (Ravi *et al.*, 2001) and the death receptor ligand TRAIL (Siegmund *et al.*, 2001). The NF-κB-induced expression of proapoptotic Bcl-2 family members has also been observed, thus antagonizing anti-apoptotic Bcl-2 family members and sensitizing cells to TRAIL-induced apoptosis (Chen *et al.*, 2003).

1.6 VIRUSES AND APOPTOSIS

In virus-infected cells, the induction of apoptosis may represent an antiviral mechanism used to limit viral replication and reduce the viral population (Benedict *et al.*, 2002). Therefore, in order to maximize virus progeny, viruses have evolved mechanisms to inhibit apoptosis of the host cell. Many viruses encode proteins that have been shown to suppress apoptosis (O'Brien, 1998; Hay and Kannourakis, 2002). Viral proteins can disrupt apoptosis by degrading p53 (McCarthy *et al.*, 1994; Wang *et al.*, 1995), activating the cell-survival pathways (Nogal *et al.*, 2001; Bagchi *et al.*, 2010), controlling the release of cytochrome *c* by

Bcl-2 family members (Rao *et al.*, 1997; Sundararajan and White, 2001), or encoding orthologs of the anti-apoptotic regulator Bcl-2 (Revilla *et al.*, 1997; White, 1998). In addition, some viruses regulate death receptor signalling by producing neutralizing, soluble TNF decoy receptors (Reading *et al.*, 2002), TRAILR2 orthologs (Brojatsch *et al.*, 1996) or by modulating cell surface amounts of Fas (Shisler *et al.*, 1997) and TRAIL (Benedict *et al.*, 2001). Caspase inhibitors, such as the A224L protein of African swine fever virus (Chacon *et al.*, 1995), the cowpox and vaccinia virus CrmA protein (Renatus *et al.*, 2000; Stennicke *et al.*, 2002), and the baculovirus p35 and p49 proteins (Xu *et al.*, 2001; Clem, 2007) bind to the caspase active sites, forming an irreversible stable complex.

Viruses can also induce apoptosis to facilitate the dissemination of viral progeny to neighbouring cells, while evading host inflammatory responses (O'Brien, 1998; Roulston *et al.*, 1999). In this regard, virions have been shown to be associated with the apoptosome, which aids in their dissemination and protects progeny virions from the host immune response (Barton *et al.*, 2001a; Mi *et al.*, 2001; Hay and Kannourakis, 2002; Courageot *et al.*, 2003). Apoptosis induction can often be ascribed to specific viral proteins. A virus protein, such as the influenza virus NS1 protein, may often exhibit both anti- and proapoptotic activities. In these instances, cells are initially protected from apoptosis to permit viral replication, and during later stages of infection, the spread of virus progeny to neighbouring cells is facilitated by apoptosis induction (Lowy, 2003). In a further example, the adenovirus E1B 19K, E1B 55K, E3 14.7K and E3 10.4/14.5K proteins inhibit apoptosis; however, during late stages of infection, the protective effects of these proteins are overcome by the expression of the adenovirus death protein (ADP) that is required for efficient release of virus from infected cells (Schaack, 2005).

1.6.1 Initiation of proapoptotic signalling during virus infection

Upon viral infection of susceptible host cells, a constant interface exists between the virus and multiple components of the cellular machinery. As viruses are dependent on the host for each stage of the viral replication cycle, the requisition or exploitation of host cellular systems may trigger the induction of apoptosis due to cellular stress or the altered expression of cell survival genes. Viruses may therefore evoke a proapoptotic effect at different stages of the replication cycle (Hay and Kannourakis, 2002; Danthi, 2011). Three distinct stages during viral entry into susceptible host cells have been reported to activate cell death. These

comprise of virus attachment to cellular surface receptors, viral uncoating within the endosomal compartment and/or disruption of the endosomal membrane, and the release of viral components into the cell cytoplasm subsequent to membrane penetration (Danthi, 2011).

Cell surface molecules, such as proteins, carbohydrates and lipids, are frequently used as receptors by viruses for host cell attachment and to ensure efficient internalization of the viral particle (Helenius, 2007). The binding of a virus to a cellular receptor often resembles the binding of the receptor to its native ligand and consequently, similar signalling pathways are activated. Avian sarcosis and leukemia virus (ASLV) (Brojatsch *et al.*, 1996) and bovine herpesvirus-1 (BHV-1) (Hanon *et al.*, 1999) have been shown to initiate apoptotic signalling by direct binding to death receptors. A member of the TNFR family, CAR1, serves as a receptor for cytopathic ASLV, thereby mediating apoptosis (Brojatsch *et al.*, 1996). Although the precise mechanism for the induction of apoptosis by BHV-1 is not known, it is proposed that specific virus-receptor interactions directly trigger death signalling cascades and that the interaction of the BHV-1 gD glycoprotein with one or more cell surface molecules is required for the induction of apoptosis (Hanon *et al.*, 1999).

The utilization of cellular uptake pathways by a virus, following host cell attachment, results in the delivery of the virus into host endocytic compartments. Within the endosomal compartment the virus undergoes uncoating or disassembly, thereby enabling the release of its uncoated genome into the host cell cytoplasm. Different uncoating strategies for enveloped and non-enveloped viruses have been described. Enveloped viruses typically require conformational changes in their envelope glycoproteins, driven by endosomal proteases or by the low pH environment of the endosome, which facilitates viral and host membrane fusion events (Harrison 2008; White *et al.*, 2008). The membrane-penetration apparatus of non-enveloped viruses is typically exposed, following removal of the virus outer coat by endosomal proteases or by low pH-dependent conformational changes in the viral outer capsid proteins. The exposed virally-encoded penetration proteins subsequently destabilize the endosomal membrane through the formation of pores or channels in the membrane, thus allowing the virus genome to enter the host cytoplasm (Tsai, 2007; Banerjee and Johnson, 2008). Cellular stress as a consequence of membrane fusion or rupture during the uncoating events of a virus within the endosome, may initiate apoptotic signalling. The enveloped viruses, murine coronavirus (Liu *et al.*, 2003), Sindbis virus (Jan and Griffin, 1999), iridoviruses, (Chinchar *et al.*, 2003; Chitnis *et al.*, 2008) and vaccinia virus (Ramsey-

Ewing and Moss, 1998) have been reported to induce apoptosis by the early fusion events within the endosome.

The delivery of specific viral components into the host cytoplasm, subsequent to successful membrane penetration, may also initiate proapoptotic signalling cascades. Following low pH-dependent fusion of African swine fever virus and host membranes, the viral nucleocapsid is delivered into the cell cytoplasm and is transported along the microtubules to the perinuclear region for replication (Carrascosa *et al.*, 2002). Although this microtubule-mediated transport requires the dynein-binding viral protein p54 (Alonso *et al.*, 2001), the p54-dynein interaction is proposed to induce proapoptotic signalling (Hernáez *et al.*, 2004). Furthermore, since Bim associates with microtubules via a similar dynein-binding site to that used by p54, it was suggested that p54 displaces Bim from the microtubules. This would result in re-localization of Bim to the mitochondria where it mediates the induction of the intrinsic apoptotic pathway (Puthalakath *et al.*, 1999; Hernáez *et al.*, 2004).

1.6.2 Apoptosis and members of the *Reoviridae* family

Various members of the *Reoviridae* family, including mammalian reovirus, avian reovirus and bluetongue virus (BTV), have been reported to induce apoptosis in infected cultured mammalian cells. Due to its association with various human illnesses and diseases, mammalian reovirus-induced apoptosis has been the most extensively studied (Clarke and Tyler, 2003; Clarke *et al.*, 2005).

The mammalian reovirus attachment protein σ1 and the outer capsid membrane penetration protein μ1 both play essential roles in triggering apoptosis (Tyler *et al.*, 1995; Connolly *et al.*, 2001; Danthi *et al.*, 2008a). Binding of σ1 to cell surface sialic acid and to the junction adhesion molecule (JAM) has been reported to be a critical requirement in order to achieve maximal levels of apoptosis (Barton *et al.*, 2001b; Connolly *et al.*, 2001), and was shown to result in the activation of NF-κB (Connolly *et al.*, 2001). Initiation of apoptosis following infection requires viral disassembly in cellular endosomes (Connolly and Dermody, 2002), furthermore suggesting an important function for the μ1 protein in apoptosis induction. Although membrane penetration may directly initiate proapoptotic signals, the delivery of μ1 cleavage fragments, particularly the C-terminal φ domain, into the cell cytoplasm has been shown to elicit apoptotic signalling (Coffey *et al.*, 2006; Danthi *et al.*, 2008a). In this case,

prodeath signalling is thought to be initiated by localization of the φ domain to mitochondria, thus altering mitochondrial integrity and promoting the release of proapoptotic molecules such as cytochrome *c* (Coffey *et al.*, 2006; Wisniewksi *et al.*, 2010). Alternatively, the φ domain may stimulate the NF-κB apoptotic signalling pathway, thereby mediating the expression of proapoptotic genes (Danthi *et al.*, 2010). Although mammalian reovirus infection activates both the extrinsic and intrinsic apoptotic pathways (Kominsky *et al.*, 2002), activation of the JNK signalling pathway is a prerequisite for activation of the intrinsic apoptotic pathway, albeit that the mechanism whereby this occurs remains undefined (Clarke *et al.*, 2001, 2004). Despite the involvement of the DR4/DR5/TRAIL death receptor pathway in mammalian reovirus-induced apoptosis (Clarke *et al.*, 2000), its full expression requires participation of the intrinsic apoptotic pathway. An important link between these two pathways involves caspase-8 dependent cleavage of the proapoptotic protein Bid. The truncated Bid (tBid) protein translocates to the mitochondria where it facilitates the release of cytochrome *c* and subsequent activation of caspase-9 (Clarke *et al.*, 2000; Kominsky *et al.*, 2002).

In addition to its cellular receptor-binding ability, the avian reovirus cell attachment protein σC was reported to be responsible for the induction of apoptosis in cultured cells (Shih *et al.*, 2004). This virally-encoded apoptin was proposed to induce apoptotic signalling through interaction with death receptor 1 of the TNF superfamily, as well as through interactions with other cell membrane-associated molecules, such as a Src family tyrosine kinase and Ras. More recent studies have, however, shown that viral replication is required for the initiation of signalling pathways that contribute to σC-induced apoptosis, suggesting that σC may induce apoptosis at a later stage in the viral replication cycle (Ping-Yuan *et al.*, 2006). The viral intermediary connecting the entry steps of avian reovirus infection with the apoptotic machinery has not yet been defined. Moreover, as in the case of mammalian reovirus, endosomal disassembly of the avian reovirus virion was reported to be required for triggering an apoptotic response (Labrada *et al.*, 2002).

The outer capsid proteins VP2 and VP5 of BTV have been reported to induce apoptosis of mammalian cells through the activation of caspase-3, and it was furthermore shown that endosomal disassembly of BTV, but not viral replication triggers apoptosis (Mortola *et al.*, 2004). Subsequently, it has been reported that both the extrinsic and intrinsic pathways are involved in the induction of apoptosis by BTV, as was evidenced by the activation of

caspase-8 and caspase-9, respectively, during BTV infection (Nagaleekar *et al.*, 2007; Stewart and Roy, 2010). In contrast to mammalian reovirus (Kominsky *et al.*, 2002), the proapoptotic protein Bid is not cleaved by caspase-8 in BTV-infected cells, thus indicating that the activation of the extrinsic and intrinsic apoptotic pathways during BTV infection occurs independently from each other (Stewart and Roy, 2010). The induction of apoptosis by BTV furthermore requires signalling via JNK and the activation of NF-κB (Mortola *et al.*, 2004; Mortola and Larsen, 2010). Although initially hypothesized to play an important role in the apoptotic machinery of BTV (Mortola *et al.*, 2004), activation of NF-κB was more recently proposed to rather initiate an antiviral cellular environment through the induction of the innate immune responses (Stewart and Roy, 2010).

1.7 AIMS OF THIS INVESTIGATION

From the review of the literature, it is clear that many aspects regarding AHSV biology still need to be elucidated. In addition to a lack of knowledge regarding the role of individual AHSV proteins in processes such as replication, morphogenesis and release, there is a paucity of information regarding the effect that AHSV infection may have on susceptible host cells. As obligate intracellular parasites, viruses are dependent on the host for each stage of replication and therefore constantly interface with various components of the host cell machinery, including cellular receptors and uptake pathways, gene expression mechanisms and cell division apparatus. Viral appropriation of these systems may cause cell stress and activate death signalling pathways or alter expression of genes that control cell survival (O'Brien, 1998; Roulston *et al.*, 1999; Hay and Kannourakis, 2002). The apoptotic pathways leading to cell death can be broadly divided into two signalling cascades involving either mitochondria (intrinsic pathway) or death receptors (extrinsic pathway) (Xu and Shi, 2007; Duprez *et al.*, 2009). Despite their extensive characterization, little is known regarding the specific cellular pathways induced during viral infection or of the viral initiators responsible for inducing these apoptotic pathways (Roulston *et al.*, 1999; Danthi, 2011). Indeed, it is only recently that such studies have been undertaken for orbiviruses and these have focussed primarily on BTV (Mortola *et al.*, 2004; Nagaleekar *et al.*, 2007; Stewart and Roy, 2010). In contrast, no such information exists for AHSV, albeit that previous microscopic analysis of endothelial cells of tissues from AHSV-infected animals suggests that apoptosis may contribute to the pathogenesis of African horse sickness disease in the mammalian host

(Laegreid *et al*., 1992; Gómez-Villamandos *et al*., 1999). Consequently, the aims of this investigation were the following:

- To determine whether AHSV-4 is capable of inducing apoptosis in infected mammalian cells.

- To determine whether the AHSV-4 outer capsid proteins VP2 and/or VP5 can serve as triggers for the induction of apoptosis in mammalian cells.

- To delineate the role of the early events in the AHSV-4 infectious cycle in the induction of apoptosis.

- To determine whether the intrinsic and/or extrinsic apoptotic pathways, as well as NF-κB are activated in mammalian cells infected with AHSV-4.

CHAPTER TWO

EXPRESSION OF THE OUTER CAPSID PROTEINS VP2 AND VP5 OF VIRULENT AND ATTENUATED AHSV-4 ISOLATES IN EUKARYOTIC CELLS

2.1 INTRODUCTION

The genus *Orbivirus* of the family *Reoviridae* comprises a number of important animal pathogens, such as African horse sickness virus (AHSV) and bluetongue virus (BTV). In contrast to other family members, the orbiviruses are transmitted by haematophageous *Culicoides* spp. to vertebrate hosts, and have the ability to replicate in both insect and mammalian hosts (Calisher and Mertens, 1998). However, vastly different cellular responses are produced in insect and mammalian cells. In insect cells, both AHSV and BTV cause persistent and asymptomatic infections despite productive replication (Mirchamsy *et al*., 1970; Guirakhoo *et al*., 1995). In contrast, in infected mammalian cells, these viruses cause severe cytopathic effects and rapid cell death (Osawa and Hazrati, 1965; Castro *et al*., 1989). For BTV, the difference in host cell response was recently ascribed to the induction of apoptosis in virus-infected mammalian cells, and it was furthermore shown that the outer capsid proteins VP2 and VP5 are sufficient to trigger apoptosis (Mortola *et al*., 2004).

The AHSV particle is considered to be structurally similar to that of BTV. The virus particles are composed of seven discrete proteins, which are organized into two capsids that encapsidate the double-stranded RNA (dsRNA) genome segments (Verwoerd *et al*., 1972; Roy *et al*., 1994; Nason *et al*., 2004). In the case of BTV, it has been reported that each of the two outer capsid proteins play a role in virus entry. The outermost capsid protein VP2 is associated with cell binding (Huismans *et al*., 1983; Hassan and Roy, 1999; Zhang *et al*., 2010), whereas the less exposed VP5 protein is involved in membrane permeabilization and translocation of the transcriptionally active core particles into the cytoplasm of virus-infected cells (Hassan *et al*., 2001; Forzan *et al*., 2004). In addition to their roles during the initial stages of infection, the VP2 protein has more recently been implicated in virus release from infected cells via its interaction with vimentin (Bhattacharya *et al*., 2007), while VP5, through its interaction with lipid rafts, is proposed to participate in docking virus particles with the plasma membrane for assembly and/or egress (Bhattacharya and Roy, 2008). Moreover, it has been reported that the extracellular treatment of mammalian cells with a combination of VP2 and VP5 is sufficient to trigger apoptosis (Mortola *et al*., 2004). In contrast to BTV, the biological importance of the AHSV outer capsid proteins has not yet been investigated. The current investigation is therefore aimed at redressing this imbalance by focussing, amongst others, on the role of the AHSV VP2 and VP5 proteins in the

induction of apoptosis in virus-infected mammalian cells. To enable these types of studies, large quantities of the two outer capsid proteins would be required.

The availability of various different biological expression systems, together with gene cloning techniques, has facilitated greatly the production of large quantities of proteins in heterologous hosts. Ideally, heterologous gene expression should result in high-level production of the recombinant protein in a soluble form that can be readily recovered (Baneyx, 1999; Huynh and Zieler, 1999; Jonasson *et al*., 2002; Georgiou and Segatori, 2005; Sørensen and Mortensen, 2005). Therefore, the expression host and choice of expression vector should be considered carefully. Although prokaryotic expression systems have been used extensively, disadvantages of using prokaryotes as expression hosts are their inability to perform post-translational modification on the expressed heterologous protein (Villaverde and Carrío, 2003; Yin *et al*., 2007) and the recombinant protein often accumulates intracellularly as insoluble aggregates (Georgiou and Valax, 1996). Thus, the stability, bioactivity and function of the recombinant protein may be adversely affected (Jung and Williams, 1997; Linskens *et al*., 1999). Consequently, eukaryotic expression systems are often used as an alternative for the production of heterologous proteins.

One of the most popular eukaryotic expression systems is the baculovirus expression system, which allows for the expression of heterologous proteins in insect cells using recombinant baculoviruses. This approach frequently results in the high-level production of correctly folded, post-translationally modified, soluble heterologous proteins (Luckow and Summers, 1988; King and Possee, 1992; O'Reilly *et al*., 1992; Kidd and Emery, 1993). Two dispensable baculovirus genes, the polyhedrin and p10 genes, have strong promoters and their encoded products accumulate to high levels in the late stages of the virus infection cycle (Gombart *et al*., 1989; Weyer and Possee, 1991; Possee, 1997). Since these genes are dispensable, they can be substituted by heterologous genes and the expressed proteins can represent up to 50% of the total cellular protein (Matsuura *et al*., 1987). To allow for expression of heterologous proteins in mammalian cells, various mammalian expression vectors have been constructed (Ramírez-Solís *et al*., 1990; Dirks *et al*., 1994; Hofmann *et al*., 1995; Boyce and Bucher, 1996; Makrides, 1999). One of these, pCMV-Script®, enables constitutive expression of a protein of interest in a variety of mammalian cell lines. The expression vector is derived from a high-copy-number pUC-based plasmid and expression of the cloned gene is driven by the human cytomegalovirus (CMV) immediate early promoter

(Stratagene, 2006). This mammalian expression vector has been used successfully to direct the intracellular expression of a number of viral genes, including individual genes expressed early in infection by *Orf virus* (ORFV) (Wood and McInnes, 2003), the VP7 gene of AHSV (Stassen *et al*., 2007), and the σNS, σ3 and μNS genes of reovirus (Becker *et al*., 2003).

Towards the goal of determining whether the outer capsid proteins of AHSV may stimulate apoptotic responses in mammalian cell culture, the aims of this part of the investigation were to express the VP2 and VP5 proteins in two different eukaryotic expression systems. Expression of the proteins in insect cells, using the Bac-to-Bac® baculovirus expression system, and in mammalian cells, using the pCMV-Script® expression vector, would enable studies aimed at determining whether exogenous addition or intracellular expression of the VP2 and VP5 AHSV proteins are required to trigger apoptosis in mammalian cells. Moreover, for comparative purposes, the VP2 and VP5 genes of both virulent and attenuated AHSV-4 isolates were included in the analyses.

2.2 MATERIALS AND METHODS

2.2.1 Bacterial strains and plasmids

Escherichia coli JM109 and *E. coli* DH10Bac™ cells were routinely cultured in Luria-Bertani (LB) broth (1% [w/v] tryptone; 1% [w/v] NaCl; 0.5% [w/v] yeast extract; pH 7.4) at 37°C with shaking at 200 rpm. Bacterial colonies were maintained on LB agar (LB broth containing 1.2% [w/v] bacteriological agar) at 4°C and cultures were stored at -70°C in 50% (v/v) glycerol. For the selection and maintenance of plasmid DNA in *E. coli*, the medium was supplemented with 100 μg/ml of ampicillin, 50 μg/ml of kanamycin, 7 μg/ml of gentamycin or 10 μg/ml of tetracycline. All antibiotics were obtained from Roche Diagnostics. Recombinant pCR®-XL-Topo® vectors, harbouring cloned cDNA copies of the full-length VP2 and VP5 genes derived from virulent and attenuated AHSV-4 isolates, were obtained from Dr. W. Fick (Department of Genetics, University of Pretoria). The pGEM® T-Easy cloning vector was obtained from Promega, whereas the pFastBac™1 bacmid donor plasmid and pCMV-Script® mammalian expression vector were obtained from Invitrogen and Stratagene, respectively.

2.2.2 DNA amplification

2.2.2.1 Primers

Primers used to amplify the respective full-length VP2 and VP5 genes were designed based on nucleotide sequences obtained from sequencing the 5′- and 3′-termini of the four genes cloned into the supplied recombinant pCR®-XL-Topo® vectors. The primers were designed with DNAMAN v.4.13 (Lynnon Biosoft) software. To facilitate subsequent cloning procedures, unique restriction endonuclease recognition sequences were included at the 5′-terminus of the different primers. The primers, indicated in Table 2.1, were synthesized by Intergrated DNA Technologies.

Table 2.1: Primers used in this study to amplify DNA fragments for cloning and sequencing of cloned insert DNA

Primer	Nucleotide sequence (5′→ 3′)	Enzyme site
PCR amplification[1]		
VP2att/virF	GCC**gaattc**ATGGCGTCCGAGTTTGG	*Eco*RI
VP2attR[2]	GGC**ggtacc**CTATTCCGTTTTTGCGAG	*Kpn*I
VP2virR[2]	GGC**ggtacc**CTATTCTGTTTTTGCGAG	*Kpn*I
VP5att/virF	CCC**gcggccgc**ATGGGAAAGTTCACATC	*Not*I
VP5att/virR[2]	CCC**ctgcag**TCAAGCTATTTTCACACC	*Pst*I
Nucleotide sequencing		
M13-F[2]	CCCAGTCACGACGTTGTAAAACG	
M13-R	CAGGAAACAGCTATGACC	
VP2 642-669[3]	GCTGAGATTTGGAATGATGTACCCACAC	
VP2 1235-1261[3]	GCCAAGTGTCGATCGATGGAGTAAACG	
VP2 1776-1799[3]	GTGGGAGGATGAGGTTGATGATCC	

[1] Restriction endonuclease recognition sequences are indicated in bold lower case letters
[2] Primers used in PCR analysis of recombinant bacmid DNA (Section 2.2.9.3)
[3] Internal VP2 sequencing primers denoting the annealing position (in bp) of the primer

2.2.2.2 Polymerase chain reaction (PCR)

Each PCR reaction mixture (25 µl) contained *ca*. 25 ng of the appropriate recombinant pCR®-XL-Topo® plasmid DNA as template, 1 × PCR buffer (75 mM Tris-HCl [pH 8.8]; 16 mM $(NH_4)_2SO_2$; 0.1% [v/v] Tween-20), 1.5 mM $MgCl_2$, 250 µM of each deoxynucleotide triphosphate (dNTP), 10 µM of each the appropriate forward and reverse primer (Table 2.1), and 1 U of SuperTherm *Taq* DNA polymerase (Southern Cross Biotechnology). The tubes were placed in a GeneAmp® PCR System 2700 (Applied Biosystems) and the thermocycling conditions included an initial denaturation at 94°C for 3 min, followed by 30 cycles of denaturation at 94°C for 30 s, primer annealing at 65°C for 30 s and extension at 72°C for 2

min. After the last cycle, a final extension step was performed at 72°C for 10 min to ensure complete synthesis of all DNA strands. Negative controls were included, in which the template DNA was omitted from the reaction mixtures. Aliquots of the reaction mixtures were analyzed by electrophoresis in a 1% (w/v) agarose gel in the presence of an appropriate DNA molecular weight marker.

2.2.3 Agarose gel electrophoresis

DNA was analyzed by agarose gel electrophoresis (Sambrook and Russell, 2001). For this purpose, horizontal 1% (w/v) agarose gels were cast and electrophoresed at 90 V in 1 × TAE buffer (40 mM Tris-HCl; 20 mM NaOAc; 1 mM EDTA; pH 8.5). The agarose gels were supplemented with 0.5 µg/ml ethidium bromide to enable visualization of the DNA on a UV transilluminator. Where appropriate, a DNA molecular weight marker, FastRuler™ High Range DNA Ladder (Fermentas) or the O'GeneRuler™ 1kb DNA Ladder Plus (Fermentas), was also loaded onto the agarose gel to enable determination of the size of the DNA fragments.

2.2.4 Purification of DNA from agarose gels

The Zymoclean™ Gel DNA Recovery Kit (Zymo Research) was used to extract and purify DNA fragments from agarose gel slices, according to the manufacturer's instructions. Briefly, 3 volumes of ADB buffer was added to each gel slice and incubated for 10 min at 50°C. The melted agarose solutions were then centrifuged through Zymo-Spin™ DNA-binding columns at 10 000 rpm for 1 min. Each column was subsequently washed twice with 200 µl of Wash buffer and the DNA was eluted in 10 µl of UHQ water. An aliquot of each sample was analyzed by agarose gel electrophoresis to assess the purity and concentration of the DNA.

2.2.5 Cloning of DNA fragments into plasmid vectors

2.2.5.1 Ligation reactions

For cloning of PCR amplicons, the pGEM® T-Easy vector system (Promega) was used. The ligation reactions consisted of 5 µl of 2 × Rapid Ligation Buffer, 50 ng of pGEM® T-Easy vector, 80 to 150 ng of purified amplicon, 1 µl of T4 DNA ligase (3 U/µl) and UHQ water to a final volume of 10 µl. Ligation of specific DNA fragments and vector DNA (pCMV-Script® or pFastBac™1) was performed in a 10-µl reaction volume that contained 1 µl of 10 ×

T4 DNA Ligase buffer (660 mM Tris-HCl [pH 7.6]; 66 mM $MgCl_2$; 100 mM DTT; 1 mM ATP; Takara Bio Inc.) and 1 µl of T4 DNA ligase (350 U/µl; Takara Bio Inc.). The ratio of insert to vector in these reactions was typically 2:1. All ligation reactions were incubated overnight at 16°C.

2.2.5.2 Preparation of competent *E. coli* cells

Competent *E. coli* JM109 cells were prepared, as described by Dagert and Ehrlich (1979). A single colony of a freshly streaked *E. coli* JM109 culture was inoculated into 100 ml of LB broth and incubated overnight at 37°C. A volume of 1 ml of the overnight culture was used to inoculate 150 ml of fresh LB broth (prewarmed to 37°C) in an Erlenmeyer flask, and incubated at 37°C until an OD_{600} of 0.70 was reached. The culture was then incubated on ice for 15 min to inhibit further bacterial growth. The cells from 50 ml of the culture were harvested by centrifugation at 5 000 rpm for 8 min at 4°C. The cell pellet was suspended in 10 ml of an ice-cold solution comprising of 80 mM $CaCl_2$ and 50 mM $MgCl_2$, incubated on ice for 10 min and then pelleted as above. This step was repeated once more, after which the cell pellet was suspended in 10 ml of ice-cold 100 mM $CaCl_2$. A volume of 1.5 ml of 50% (v/v) glycerol was added to the cells and aliquots of 400 µl of cells were transferred to chilled 1.5-ml Eppendorf tubes, snap frozen in liquid nitrogen and stored at -70°C until use.

2.2.5.3 Transformation of competent cells

After allowing the competent *E. coli* JM109 cells to thaw on ice, the cells were transformed by the heat shock-method, as described by Sambrook and Russell (2001). An aliquot of the competent cells (200 µl) and the ligation reaction mixture (10 µl) were mixed and incubated on ice for 30 min, followed by a heat shock at 42°C for 90 s. After the heat shock treatment, the tubes were incubated immediately on ice for 2 min. Subsequently, 800 µl of LB broth was added and the cells were incubated at 37°C for 1 h. Aliquots (100 µl) of the transformation mixtures were plated onto LB agar supplemented with the appropriate antibiotic. For plasmids containing a *lacZ'* marker gene (pGEM® T-Easy), the cells were plated together with 10 µl of 100 mM IPTG and 50 µl of 2% (w/v) X-gal. The agar plates were incubated overnight at 37°C. As controls, competent cells were transformed with DNA (pUC18) of a known concentration to determine the transformation efficiency, and untransformed cells were used to test for contamination.

2.2.6 Screening of transformants

2.2.6.1 Plasmid DNA isolation

Small-scale plasmid DNA extractions were performed according to the alkaline lysis protocol, as described by Sambrook and Russell (2001). A single bacterial colony was inoculated into 5 ml of LB broth containing the appropriate antibiotic and incubated overnight at 37°C. The cells from 3 ml of the overnight culture were harvested by centrifugation at 8 000 rpm for 2 min and the cell pellet suspended in 100 µl of ice-cold Solution I (5 mM glucose; 10 mM EDTA; 25 mM Tris; pH 8), followed by incubation at room temperature for 5 min. A volume of 200 µl of freshly prepared Solution II (0.2 N NaOH; 1% [w/v] SDS) was then added and the tubes incubated on ice for 5 min. After incubation, 150 µl of ice-cold Solution III (3 M KOAc; pH 4.8) was added and incubation was continued on ice for 5 min to precipitate bacterial chromosomal DNA, protein-SDS complexes and high-molecular-weight RNA. The cell lysate was clarified by centrifugation at 10 000 rpm for 5 min and plasmid DNA was precipitated from the recovered supernatant by addition of 2 volumes of 96% ethanol. Following incubation on ice for 1 h, the precipitated plasmid DNA was collected by centrifugation at 10 000 rpm for 15 min, rinsed with 70% ethanol, air-dried and then suspended in 30 µl of UHQ water. To remove contaminating RNA, the plasmid DNA preparation was incubated with 1 µl of RNase A (10 mg/ml) at 37°C for 30 min.

Since mammalian cells are sensitive to impurities in plasmid DNA preparations, which can influence transfection efficiencies, highly purified recombinant pCMV-Script® plasmid DNA was prepared with the PureYield™ Plasmid Miniprep System (Promega), according to the manufacturer's instructions. Briefly, the cells from 3 ml of the overnight culture were harvested by centrifugation at 8 000 rpm for 2 min and the cell pellet suspended in 600 µl of 1 × TE buffer (10 mM Tris-HCl; 1 mM EDTA; pH 8.0). Following the addition of 100 µl of Cell Lysis Buffer and 350 µl of Neutralization Solution, the cell lysate was centrifuged at 14 000 rpm for 3 min. The supernatant was recovered and centrifuged through a PureYield™ Minicolumn at 14 000 rpm for 15 s. The column was washed with wash solution and the plasmid DNA eluted in 30 µl of the supplied Elution Buffer. The concentration and purity of the plasmid DNA was determined with a NanoDrop® ND-1000 spectrophotometer and ND-1000 v.3.3 software (Nanodrop Technologies, Inc.).

2.2.6.2 Restriction endonuclease digestions

Restriction enzyme digestion reactions were performed in 1.5-ml Eppendorf tubes in a final volume of 20 µl. The digestion reaction mixtures contained the appropriate concentration of salt, using the 10× buffer supplied by the manufacturer, and 1 U of enzyme per µg of plasmid DNA. The digestion reactions were incubated at 37°C for 1 to 2 h. Digestion reactions, requiring two restriction enzymes with different optimal salt concentrations, were performed first in the buffer of the lowest salt concentration. After incubation, the salt concentration was adjusted and the digestion reaction continued. The restriction digestion reactions were analyzed in a 1% (w/v) agarose gel in the presence of an appropriate DNA molecular weight marker. All restriction enzymes were obtained from Fermentas or Roche Diagnostics.

2.2.6.3 DNA sequencing and sequence analysis

The nucleotide sequence of cloned insert DNA was determined with the ABI PRISM® BigDye™ Terminator v.3.1 Cycle Sequencing Ready Reaction kit (Applied Biosystems), according to the manufacturer's instructions. In addition to the universal pUC/M13 forward and reverse primers, VP2-specific internal primers were also used as sequencing primers (Table 2.1). Each sequencing reaction consisted of 60-100 ng of purified recombinant plasmid DNA, 2 µl of Big Dye™ Terminator mix, 3.2 pmol of sequencing primer, 1 µl of 5 × Big Dye™ Terminator Sequencing buffer and UHQ water to a final volume of 10 µl. Cycle sequencing reactions were performed in a GeneAmp® PCR System 2700 (Applied Biosystems) and consisted of initial denaturation at 94°C for 1 min, followed by 25 cycles of denaturation at 94°C for 10 s, annealing at 55°C for 30 s and extension at 60°C for 4 min. The extension products were precipitated by addition of 31 µl of UHQ water, 2 µl of 3 M NaOAc (pH 4.6) and 60 µl of absolute ethanol. The tubes were incubated at room temperature for 15 min in the dark and subsequently centrifuged at 14 000 rpm for 30 min. The precipitated DNA was washed twice with 70% ethanol. The samples were submitted to the University of Pretoria's sequencing facility for sequencing on an ABI PRISM® Model 3100 DNA sequencer. The nucleotide sequences obtained were analyzed with BioEdit Sequence Alignment Editor v.5.0.6 (Hall, 1999) software. The nucleotide and deduced amino acid sequences were compared against entries in the GenBank database with the BLAST-N and BLAST-P programs (Altschul *et al*., 1997), respectively, available on the National Centre for Biotechnology Information web page (http://www.ncbi.nlm.nih.gov/). The nucleotide and deduced amino acid sequences of the VP2 and VP5 virulent and attenuated genes,

respectively, were aligned using the Pairwise alignment function included in the BioEdit software package.

2.2.7 Plasmid constructs

All molecular cloning techniques used in the construction of the different recombinant plasmids were performed in accordance to the procedures described in the preceding sections. All plasmid constructs were confirmed by nucleotide sequencing, and by agarose gel electrophoresis following restriction endonuclease digestions.

- **pGEM-VP2att**

Primers VP2att/virF and VP2attR were used with plasmid pTopo-attVP2 as template DNA to generate a 3 201-bp amplicon, corresponding to the full-length VP2 gene of an attenuated AHSV-4 isolate. The amplicon was cloned into pGEM® T-Easy to generate pGEM-VP2att.

- **pGEM-VP2vir**

Primers VP2att/virF and VP2virR were used with plasmid pTopo-virVP2 as template DNA to generate a 3 201-bp amplicon, corresponding to the full-length VP2 gene of a virulent AHSV-4 isolate. The amplicon was cloned into pGEM® T-Easy to generate pGEM-VP2vir.

- **pGEM-VP5att**

Primers VP5att/virF and VP5att/virR were used with plasmid pTopo-attVP5 as template DNA to generate a 1 538-bp amplicon, corresponding to the full-length VP5 gene of an attenuated AHSV-4 isolate. The amplicon was cloned into pGEM® T-Easy to generate pGEM-VP5att.

- **pGEM-VP5vir**

Primers VP5att/virF and VP5att/virR were used with plasmid pTopo-virVP5 as template DNA to generate a 1 538-bp amplicon, corresponding to the full-length VP5 gene of a virulent AHSV-4 isolate. The amplicon was cloned into pGEM® T-Easy to generate pGEM-VP5vir.

- **pFB-VP2att**

The full-length VP2 attenuated gene was recovered from plasmid pGEM-VP2att by digestion with *Eco*RI and *Kpn*I and recloned into the *Eco*RI and *Kpn*I sites of the bacmid donor plasmid pFastBac™1 to generate pFB-VP2att.

- **pFB-VP2 vir**

The full-length VP2 virulent gene was recovered from plasmid pGEM-VP2vir by digestion with *Eco*RI and *Kpn*I and recloned into the *Eco*RI and *Kpn*I sites of pFastBac™1 to generate pFB-VP2vir.

- **pFB-VP5att**

The full-length VP5 attenuated gene was recovered from plasmid pGEM-VP5att by digestion with *Not*I and *Pst*I and recloned into the *Not*I and *Pst*I sites of pFastBac™1 to generate pFB-VP5att.

- **pFB-VP5vir**

The full-length VP5 virulent gene was recovered from plasmid pGEM-VP5vir by digestion with *Not*I and *Pst*I and recloned into the *Not*I and *Pst*I sites of pFastBac™1 to generate pFB-VP5vir.

- **pCMV-VP2att**

To construct the recombinant mammalian expression vector pCMV-VP2att, the full-length VP2 attenuated gene was recovered from pGEM-VP2att by digestion with *Eco*RI and *Kpn*I, and cloned into identically digested pCMV-Script® vector DNA.

- **pCMV-VP2vir**

To construct the recombinant plasmid pCMV-VP2vir, the full-length VP2 virulent gene was excised from plasmid pGEM-VP2vir by digestion with *Eco*RI and *Kpn*I and then cloned into pCMV-Script® that had been prepared in an identical manner.

- **pCMV-VP5att**

To construct the recombinant mammalian expression vector pCMV-VP5att, the full-length VP5 attenuated gene was recovered from pGEM-VP5att by digestion with *Not*I and *Pst*I, and cloned into identically digested pCMV-Script® vector DNA.

- **pCMV-VP5vir**

To construct the recombinant mammalian expression vector pCMV-VP5vir, the full-length VP5 virulent gene was recovered from pGEM-VP5vir by digestion with *Not*I and *Pst*I, and cloned into identically digested pCMV-Script® vector DNA.

2.2.8 Transient expression of AHSV-4 VP2 and VP5 proteins in BHK-21 cells

2.2.8.1 Cell culture

Baby Hamster Kidney-21 (BHK-21; ATCC CL-10) cells were propagated and maintained as monolayers in 75-cm^2 tissue culture flasks. The cells were cultured in Eagle's Minimal Essential Medium (EMEM) with Earle's Balanced Salt Solution (EBSS) and L-glutamine (Lonza, BioWhittaker®), supplemented with 5% (v/v) foetal bovine serum (FBS), 1% (v/v) non-essential amino acids (NEAA) and antibiotics (10 000 U/ml of penicillin, 10 000 µg/ml of streptomycin and 25 µg/ml of amphotericin B). The flasks were incubated at 37°C in a humidified incubator in the presence of 5% CO_2.

2.2.8.2 Transfection of BHK-21 cells

BHK-21 cells were transfected with purified parental and recombinant pCMV-Script® plasmid DNA by means of lipofection with Lipofectamine™ 2000 Reagent (Invitrogen), according to the manufacturer's instructions. The cells were seeded in 6-well tissue culture plates to reach 90% confluency within 6 h of incubation at 37°C in a CO_2 incubator. Prior to transfection, the cell monolayers were rinsed twice with incomplete EMEM medium (lacking FBS and antibiotics) and 1.5 ml of incomplete EMEM medium was then added. For each transfection, 2.5 µg of purified plasmid DNA and 7.5 µl of Lipofectamine™ 2000 Reagent were separately diluted in 625 µl of incomplete EMEM medium and incubated at room temperature for 5 min. After incubation, the two solutions were mixed and incubated at room temperature for 20 min. The BHK-21 cell monolayers were overlaid with the DNA-Lipofectamine complexes and the tissue culture plates were incubated at 37°C for 4 to 6 h in a CO_2 incubator before replacing the transfection mixtures with complete EMEM (containing FBS and antibiotics). The tissue culture plates were incubated for a further 36 h. As a control, mock-transfected cells were also included.

2.2.9 Engineering and characterization of recombinant bacmids

2.2.9.1 Transposition

An overnight culture of *E. coli* DH10Bac™ cells, containing the bacmid genome and helper plasmid, was prepared by inoculating a single colony in LB broth supplemented with kanamycin (50 µg/ml) and tetracycline (10 µg/ml). Competent *E. coli* DH10Bac™ cells were prepared, as described previously (Section 2.2.5.2). For transformation, 1 ng of the

recombinant pFastBac™1 donor plasmid DNA was mixed with 100 µl of the competent *E. coli* DH10Bac™ cells and then incubated on ice for 30 min. The cells were heat-shocked at 42°C for 45 s and incubated immediately on ice for 2 min. LB broth (900 µl) was then added to the cells and the transformation mixtures were incubated at 37°C for 4 h to allow transposition to occur. The transformation mixtures were plated in aliquots of 100 µl onto LB agar supplemented with 50 µg/ml of kanamycin, 7 µg/ml of gentamycin and 10 µg/ml of tetracycline in the presence of 10 µl of 100 mM IPTG and 50 µl of 2% (w/v) X-gal. The agar plates were incubated at 37°C for 24 to 48 h. Transformants displaying a white colony-phenotype were selected and re-streaked onto the same agar medium, as above, to confirm the recombinant phenotype.

2.2.9.2 Isolation of recombinant bacmid DNA

Selected colonies were inoculated into 5 ml of LB broth containing antibiotics (50 µg/ml kanamycin, 7 µg/ml gentamycin, 10 µg/ml tetracycline) and cultured overnight at 37°C. The recombinant bacmid DNA was isolated by the following protocol that had been developed for isolating high-molecular-weight plasmid DNA and subsequently adapted for isolating recombinant bacmid DNA (Invitrogen). The bacterial cells from 3 ml of the overnight culture were harvested by centrifugation at 14 000 rpm for 1 min and the cell pellet suspended in 300 µl of Solution I (15 mM Tris-HCl [pH 8.0]; 10 mM EDTA; 100 µg/ml RNase A). A volume of 300 µl of Solution II (0.2 N NaOH; 1% [w/v] SDS) was added, followed by incubation at room temperature for 5 min. Subsequently, 300 µl of 3 M KOAc (pH 5.5) was added and the tubes were incubated on ice for 10 min. Following centrifugation at 17 000 rpm for 10 min, the bacmid DNA was precipitated from the recovered supernatant by addition of 800 µl of isopropanol and incubation on ice for 10 min. The precipitated bacmid DNA was collected by centrifugation at 17 000 rpm for 15 min, washed with 70% ethanol, air-dried and then suspended in 40 µl of 1 × TE buffer. An aliquot of the extracted bacmid DNA was analyzed by electrophoresis in a 0.7% (w/v) agarose gel at 90 V for 30 min in 1 × TAE buffer.

2.2.9.3 Analysis of recombinant bacmid DNA

To confirm successful transposition of the respective AHSV-4 VP2 and VP5 genes into the bacmid DNA, PCR analysis of the extracted bacmid DNA was performed. Each PCR reaction mixture (50 µl) contained 100 ng of bacmid DNA as template, 1 × PCR buffer (75 mM Tris-HCl [pH 8.8]; 16 mM $(NH_4)_2SO_2$; 0.1% [v/v] Tween-20), 1.5 mM $MgCl_2$, 250 µM

of each dNTP, 10 µM of each the pUC/M13 forward and appropriate gene-specific reverse primer (Table 2.1), and 2.5 U of SuperTherm *Taq* DNA polymerase (Southern Cross Biotechnology). The PCR was performed in a GeneAmp® PCR System 2700 (Applied Biosystems). The DNA was initially denatured at 94°C for 3 min, followed by 30 cycles of denaturation at 94°C for 45 s, primer annealing at 55°C for 45 s and extension at 72°C for 5 min. After the last cycle, a final extension step was performed at 72°C for 10 min to ensure complete synthesis of all DNA strands. To test for contamination, a reaction mixture from which the template DNA was omitted was also included. Following PCR, aliquots of the reaction mixtures were analyzed by agarose gel electrophoresis in the presence of an appropriate DNA molecular weight marker.

2.2.10 Generation of recombinant baculoviruses

2.2.10.1 Cell culture

Spodoptera frugiperda clone 9 (*Sf*9) insect cells were propagated and maintained as monolayers or as suspension cultures in Spinner flasks at 27°C in TC-100 medium (Lonza, BioWhittaker®) or Grace's Insect Medium with L-glutamine, lactalbumin hydrolysate, yeastolate and gentamycin (Lonza, BioWhittaker®). The media were supplemented with 10% (v/v) FBS, 10 000 U/ml of penicillin, 10 000 µg/ml of streptomycin and 25 µg/ml of amphotericin B. The cell densities of the suspension cultures were determined with a haemocytometer. Cell viability was determined by staining the cells with Trypan Blue (0.4% [w/v] in 1 × PBS), as described by Summers and Smith (1987). Suspension cultures were seeded at an initial density of 0.3×10^6 cells/ml and subcultured when they reached 2×10^6 cells/ml.

2.2.10.2 Transfection of *Sf*9 cells with recombinant bacmid DNA

For transfection of *Sf*9 cells with the recombinant bacmid DNA, 1×10^6 cells were seeded per well of a 6-well tissue culture plate. The cells were allowed to attach to the tissue culture plate by incubating the plate at 27°C for 1 h. For each transfection, *ca*. 500 ng of recombinant DNA and 6 µl of CellFECTIN® Reagent (Invitrogen) were separately diluted in 100 µl of incomplete TC-100 medium (lacking FBS and antibiotics). The two solutions were then mixed and, following incubation at room temperature for 45 min, 800 µl of incomplete TC-100 medium was added. *Sf*9 cells were prepared for transfection by aspirating the medium from the attached cells and the cells were rinsed twice with 1 ml of incomplete TC-100

medium. The cells were then overlaid with the lipid-DNA complexes and the tissue culture plate incubated at 27°C for 5 h in a humidified environment. After incubation, the transfection mixtures were removed and replaced with 2 ml of complete TC-100 medium (containing FBS and antibiotics). The tissue culture plate was subsequently incubated at 27°C for 72 h. The cells were harvested by centrifugation at 2 500 rpm for 5 min and the cell-free supernatants, containing recombinant baculovirus, were stored at 4°C. Mock-transfected cells and cells transfected with the wild-type bacmid DNA were included as controls whereby infection of the cells could be monitored.

2.2.10.3 Plaque assays

Plaque assays were performed, as described by Browne and Faulkner (1977) with modifications. Cells were seeded in 6-well tissue culture plates and incubated at 37°C in a CO_2 incubator until the monolayers were confluent. The cells were infected with serial 10-fold dilutions of virus in 2 mM Tris buffer and, following adsorption of the virus to the cells for 2 h, the cells were overlaid with 2 ml of a sterile solution of agarose (1:1 ratio of 0.7% [w/v] agarose and 2 × concentrated Earle's salt containing 10% [v/v] FBS and antibiotics). The plates were incubated at 37°C for 5 to 7 days. Following incubation, the monolayers were flooded with Neutral Red (0.1% [w/v] in sterile UHQ water) and incubated for a further 24 to 48 h until plaques became visible. For each recombinant virus, individual plaques were picked as an agarose plug with a pipette and transferred to Eppendorf tubes containing 500 µl of medium. The viruses were eluted from the agarose plugs by vigorous vortexing. Cell monolayers, prepared as above, were infected with each plaque pickup and the plates were incubated for 72 h. The virus-containing supernatant of this passage one stock was collected by centrifugation at 2 500 rpm for 5 min to remove the cell debris. The supernatants were stored at 4°C, titrated as described above, and then used to prepare large-scale virus stocks.

2.2.10.4 Preparation of virus stocks

To prepare stocks of the plaque-purified recombinant baculoviruses, 100 ml of *Sf*9 cells, propagated as a suspension culture at 1×10^6 cells/ml in complete TC-100 medium, were infected at a multiplicity of infection (MOI) of 0.1 pfu/cell. Following incubation at 27°C for 4 days, supernatants were collected by centrifugation at 2 500 rpm for 10 min, filter-sterilized with a 0.2-µm filter (Pall Acrodisc®) and stored at 4°C. The titer of the respective baculovirus stocks was determined by plaque assay, as described above.

2.2.11 Optimization of AHSV-4 VP2 and VP5 protein expression in *Sf*9 cells

2.2.11.1 MOI optimization

Monolayers of *Sf*9 cells in 6-well tissue culture plates (1×10^6 cells/well) were infected with the respective recombinant baculoviruses at a MOI ranging from 1 to 20 pfu/cell and incubated at 27°C for 72 h. As controls, mock-infected cells and cells infected with wild-type baculovirus at a MOI of 5 pfu/cell were included in the analysis. Following incubation, detached and adherent cells were harvested and collected by centrifugation at 1 500 rpm for 8 min. The cell pellet was washed once with 1 × Phosphate Buffered Saline (PBS: 137 mM NaCl; 2.7 mM KCl; 4.3 mM $Na_2HPO_4.2H_2O$; 1.4 mM KH_2PO_4; pH 7.4) and then suspended in 100 µl of 1 × PBS to a cell density of 1×10^7 cells/ml. Aliquots of the whole-cell lysate (10 µl) from each sample were analyzed by 10% SDS-PAGE.

2.2.11.2 Time of harvest optimization

To determine the time of harvest at which maximal levels of soluble VP2 and VP5 proteins could be obtained, *Sf*9 cell monolayers in 25-cm^2 tissue culture flasks (3.8×10^6 cells/flask) were infected with the respective baculoviruses at a MOI of 5 and 10 pfu/cell, respectively, and the flasks were incubated at 27°C for 48 or 72 h. Mock-infected cells and cells infected with the wild-type baculovirus at a MOI of 5 pfu/cell were included in the analyses. Following incubation, the detached and adherent cells were harvested and collected by centrifugation at 1 500 rpm for 8 min. The cell pellets were washed once in 1 × PBS and then suspended in 350 µl of PBS to a density of 1×10^7 cells/ml. An aliquot of 150 µl of each cell suspension was removed and referred to as the whole-cell lysate. The cells were subsequently lysed by two cycles of freezing and thawing, which involved freezing of the cell suspension at -70°C for 1 h, followed by thawing at room temperature. The cell lysates were fractionated by centrifugation at 6 600 rpm for 30 min at 4°C and the supernatants (cytoplasmic or soluble fraction) were transferred to Eppendorf tubes. The cell pellets (particulate or insoluble fraction) were suspended in 200 µl of 1 × PBS. Aliquots of the whole-cell (10 µl), soluble (10 µl) and insoluble (50 µl) protein fractions were analyzed by 10% SDS-PAGE.

2.2.12 Large-scale preparation of soluble baculovirus-expressed AHSV-4 VP2 and VP5 proteins

To prepare sufficient amounts of soluble VP2 and VP5 proteins for subsequent biological assays, suspension cultures of *Sf*9 cells were infected with the respective recombinant

baculoviruses. For this purpose, the *Sf*9 cells were collected by centrifugation at 450 rpm for 10 min. The cell pellet was suspended in 1/10th of the original culture volume in Grace's medium without FBS (1.5 × 10^8 cells/ml) and transferred to a sterile siliconized 100-ml Erlenmeyer flask. The cells were infected with recombinant baculovirus at a MOI of 5 or 10 pfu/cell at room temperature for 1 h, with gentle agitation. Following virus infection, complete Grace's medium supplemented with 0.1% (v/v) Pluronic® F-68 (Gibco BRL) was added to the infected cell suspensions to yield a cell density of 1 × 10^6 cells/ml. As controls, mock-infected cells and cells infected with the wild-type baculovirus at a MOI of 5 pfu/cell were prepared similarly. The flasks were incubated at 27°C for 48 h, except for cells infected with a recombinant baculovirus expressing VP2 of a virulent AHSV-4 isolate that was incubated for 72 h. Following incubation, the *Sf*9 cells were collected by centrifugation at 1 500 rpm for 10 min, washed once in 1 × PBS containing 10% (v/v) glycerol and suspended in 1 × PBS to a final density of 1.5 × 10^7 cells/ml. The cells were lysed by three successive cycles of freezing and thawing, and the cell lysates were fractionated by centrifugation into soluble and insoluble fractions, as described previously. The insoluble pellet fractions were suspended in 15 ml of TN buffer (0.05 M Tris [pH 8.0]; 0.15 M NaCl; 10% [v/v] glycerol) and homogenized with a syringe and 21G needle. Aliquots of whole-cell lysates, as well as soluble and insoluble protein fractions were analyzed by 10% SDS-PAGE. The yield of soluble recombinant proteins was quantified, as compared to a known concentration (2 mg/ml) of bovine serum albumin (BSA), using EZQuant-Gel v.2.1 software (EZQuant Biology Software, EZQuant Ltd.). The protein samples were stored at -70°C until required.

2.2.13 Analysis of recombinant proteins

2.2.13.1 SDS-polyacrylamide gel electrophoresis (SDS-PAGE)

Prior to analysis, protein samples were mixed with an equal volume of 2 × Protein Solvent Buffer (PSB: 125 mM Tris-HCl [pH 6.8]; 4% [w/v] SDS; 20% [v/v] glycerol; 10% [v/v] 2-mercaptoethanol; 0.002% [w/v] bromophenol blue) and then denatured by heating to 95°C for 5 min in a boiling water bath. The proteins were resolved by electrophoresis in a discontinuous gel system, as described by Laemmli (1970). A 5% (w/v) acrylamide stacking gel (0.125 M Tris-HCl [pH 6.8]; 0.1% [w/v] SDS) and a 10% (w/v) acrylamide separating gel (0.375 M Tris-HCl [pH 8.8]; 0.1% [w/v] SDS), with an acrylamide:bisacrylamide ratio of 30:0.8, were polymerized by the addition of 0.08% (w/v) ammonium persulphate and 0.008% (v/v) TEMED. Electrophoresis was performed in a Hoefer® miniVE vertical electrophoresis

system at 100 V for 4.5 h in 1 × TGS electrophoresis buffer (0.025 M Tris-HCl [pH 8.3]; 0.192 M glycine; 0.1% [w/v] SDS). In order to visualize the proteins, the gels were stained for 20 min with 0.125% (w/v) Coomassie brilliant blue (prepared in 50% [v/v] methanol and 10% [v/v] acetic acid) and then counterstained by repeatedly soaking the gels in destaining solution (10% [v/v] methanol; 10% [v/v] acetic acid). The sizes of the resolved proteins were determined by comparison to reference molecular mass proteins (Spectra™ Multicolor Broad Range Protein Ladder; Fermentas).

2.2.13.2 Immunoblot analysis

For immunoblot analysis (Sambrook and Russell, 2001), proteins from an unstained SDS-polyacrylamide gel were electroblotted onto a Hybond™-C$^+$ nitrocellulose membrane (Amersham Pharmacia Biotech AB). Two sheets of filter paper and the nitrocellulose membrane, cut to the same size as the gel, were equilibrated for 10 min in transfer buffer (25 mM Tris; 192 mM glycine). The proteins were electroblotted onto the membrane at 28 V for 3 h with a Mighty Small™ Transphor blotting apparatus (Hoefer). Following transfer, the membrane was rinsed in 1 × PBS for 5 min and non-specific binding sites were blocked by immersing the membrane overnight at 4°C in blocking solution (1% [w/v] fat-free milk powder in 1 × PBS). The membrane was transferred to 1 × PBS containing the primary antibody. These comprised of AHSV-4 VP2 EpiB antiserum or anti-βgal-VP5 (AHSV-4) antiserum, which were each diluted 1:100 in 1 × PBS. Following incubation at room temperature for 2 h with gentle agitation, the unbound primary antibodies were removed by washing the membrane three times for 5 min each with wash buffer (0.05% [v/v] Tween-20 in 1 × PBS). An appropriate secondary antibody was then added to the membrane. These comprised of Protein-A conjugated to horseradish peroxidase (Sigma-Aldrich) for VP2 or anti-chicken IgY (IgG) conjugated to horseradish peroxidase (Sigma-Aldrich) for VP5, which were diluted 1:500 and 1:4000 in 1 × PBS, respectively. Following incubation at room temperature for 1 h with gentle agitation, the membrane was washed three times for 5 min each with wash buffer and once with 1 × PBS for 5 min. To detect immune-reactive proteins, freshly prepared enzyme substrate solution (60 mg 4-chloro-1-naphtol in 20 ml of ice-cold methanol and 60 µl H_2O_2 in 100 ml of 1 × PBS, mixed just before use) was subsequently added to the membrane, followed by incubation at room temperature in the dark until the protein bands became visible. The membrane was then washed with dH_2O and allowed to air dry.

2.3 RESULTS

The primary aims of this part of the investigation were to clone and express the VP2 and VP5 genes of two AHSV-4 isolates in different eukaryotic expression systems. The VP2 and VP5 genes encode the outer capsid proteins of infectious orbivirus particles, which, in the case of BTV, have been reported to trigger apoptosis in mammalian cells (Mortola *et al*., 2004). To determine whether the same holds true for AHSV and also to determine whether intracellular synthesis or exogenous addition of the outer capsid proteins are required for the induction of apoptosis, the VP2 and VP5 genes were thus expressed in both a mammalian and baculovirus expression system. Whereas the mammalian expression system allows for intracellular synthesis of heterologous proteins, the baculovirus expression system enables large-scale production of heterologous proteins that can be used in *in vitro* biological assays. For comparative purposes, the VP2 and VP5 genes of both attenuated and virulent AHSV-4 isolates were included in this study. These virus isolates were derived from an experiment, performed at the Equine Research Centre (Faculty of Veterinary Science, University of Pretoria), in which a virulent AHSV-4 strain was isolated from a diseased horse and subsequently attenuated through repeated passage (13 times) in cell culture. The AHSV-4 isolates were designated AHSV-4 (1) and AHSV-4 (13), respectively. Although only the seed stock virus [AHSV-4 (1)] is available, cDNA copies of the full-length VP2 and VP5 genes of both virus isolates have been cloned previously (Korsman, 2007). The following sections will provide detailed information regarding the cloning and expression strategies that were used in this part of the study, as well as the results that were obtained.

2.3.1 Construction of recombinant pGEM® T-Easy plasmids harbouring full-length AHSV-4 VP2 and VP5 genes

Full-length cDNA copies of the VP2 and VP5 genes of both virulent and attenuated isolates of AHSV-4 had been cloned previously into the pCR®-XL-Topo® vector (Korsman, 2007). To facilitate subsequent directional cloning of the respective VP2 and VP5 genes into different eukaryotic vectors, primers were designed that were extended at their 5′-termini by additional nucleotides to incorporate unique restriction endonuclease recognition sites. The gene-specific primer pairs were subsequently used with the appropriate recombinant pCR®-XL-Topo® plasmid as template DNA to PCR amplify the respective VP2 and VP5 genes, as described under Materials and Methods (Section 2.2.2). An aliquot of each reaction mixture was analyzed by agarose gel electrophoresis and a single amplicon of the expected size for

the VP2 (3.2 kb) and VP5 (1.538 kb) genes were observed. In contrast, no amplification products were observed in the negative control reaction in which template DNA was omitted (results not shown).

The amplicons were purified from the agarose gel and ligated into pGEM® T-Easy vector DNA. Following transformation of competent *E. coli* JM109 cells, recombinant transformants with a Lac$^-$ phenotype were selected from X-gal indicator plates and cultured in LB broth supplemented with ampicillin. The extracted plasmid DNA was analyzed by agarose gel electrophoresis. Plasmid DNA migrating slower than the parental pGEM® T-Easy vector DNA were selected and analyzed for the presence of cloned insert DNA by using restriction enzymes of which the recognition sites had been incorporated during the design of the primers.

Digestion of recombinant plasmid DNA harbouring the respective VP2 genes with both *Eco*RI and *Kpn*I yielded a single DNA fragment. This was most likely due to co-migration of the digested vector DNA (*ca*. 3.0 kb) and excised VP2 insert DNA (3.2 kb). Therefore, to confirm that the respective VP2 genes were indeed cloned successfully, the recombinant plasmid DNA was linearized by digestion with *Kpn*I. Following agarose gel electrophoresis, a restriction fragment of *ca*. 6.215 kb was observed, which is in agreement with the expected size of the linear recombinant plasmid DNA (Fig. 2.1a, lanes 2 and 5, respectively). Digestion of recombinant plasmid DNA harbouring the respective VP5 genes with both *Not*I and *Pst*I yielded two DNA fragments that corresponded in size to the vector DNA (*ca*. 3.0 kb) and the cloned VP5 gene (1.538 kb) (Fig. 2.1b, lanes 1 and 4, respectively). Recombinant plasmids harbouring the VP2 gene of the virulent and attenuated AHSV-4 isolates were designated pGEM-VP2vir and pGEM-VP2att, respectively, whereas recombinant plasmids harbouring the VP5 gene were designated pGEM-VP5vir and pGEM-VP5att, respectively. Once the integrity of the cloned insert DNA had been verified, the recombinant plasmids were used as sources in the construction of recombinant pCMV-Script® mammalian expression vectors and pFastBac™1 donor plasmids.

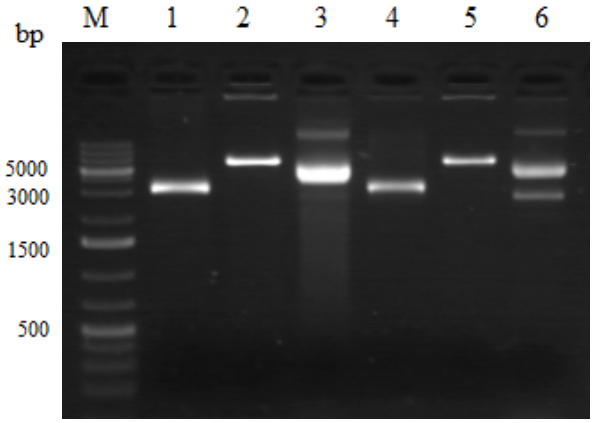

Fig. 2.1a: Agarose gel electrophoretic analysis of recombinant pGEM® T-Easy plasmids harbouring VP2 gene-specific inserts. Lane M, DNA molecular weight marker; lane 1, pGEM-VP2att plasmid DNA digested with both *Eco*RI and *Kpn*I; lane 2, pGEM-VP2att plasmid DNA linearized by digestion with *Kpn*I; lane 3, uncut pGEM-VP2att plasmid DNA; lane 4, pGEM-VP2vir plasmid DNA digested with both *Eco*RI and *Kpn*I; lane 5, pGEM-VP2vir plasmid DNA linearized by digestion with *Kpn*I; lane 6, uncut pGEM-VP2vir plasmid DNA. The sizes of the DNA molecular weight marker, O'GeneRuler™ 1kb DNA Ladder Plus (Fermentas), are indicated to the left of the figure.

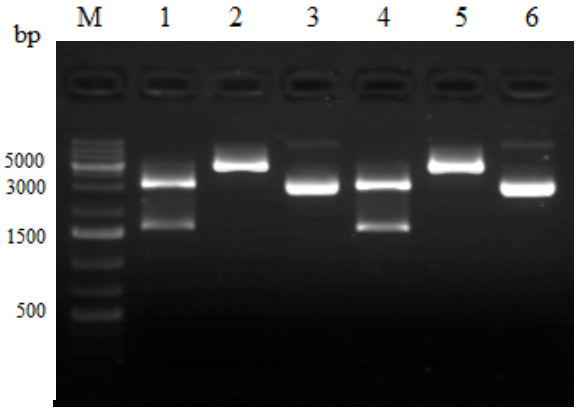

Fig. 2.1b: Agarose gel electrophoretic analysis of recombinant pGEM® T-Easy plasmids harbouring VP5 gene-specific inserts. Lane M, DNA molecular weight marker; lane 1, pGEM-VP5att plasmid DNA digested with both *Not*I and *Pst*I; lane 2, pGEM-VP5att plasmid DNA linearized by digestion with *Pst*I; lane 3, uncut pGEM-VP5att plasmid DNA; lane 4, pGEM-VP5vir plasmid DNA digested with both *Not*I and *Pst*I; lane 5, pGEM-VP5vir plasmid DNA linearized by digestion with *Pst*I; lane 6, uncut pGEM-VP5vir plasmid DNA. The sizes of the DNA molecular weight marker, O'GeneRuler™ 1kb DNA Ladder Plus (Fermentas), are indicated to the left of the figure.

2.3.2 Sequencing of the full-length VP2 and VP5 genes derived from virulent and attenuated AHSV-4 isolates

To confirm the integrity of the cloned insert DNA, the nucleotide sequence of the respective VP2 and VP5 genes was determined. For this purpose, universal and gene-specific internal primers were used to sequence both strands of each of the four cloned insert DNAs. For each of the genes, a consensus sequence was derived from the individual overlapping nucleotide sequences and used in subsequent analyses.

Pairwise alignments of the nucleotide sequences of the respective VP2 and VP5 genes, derived from virulent and attenuated AHSV-4 isolates, revealed multiple nucleotide differences between the sequences of the virulent and attenuated VP2 genes, whereas no nucleotide differences were observed between the respective sequences of the VP5 genes. The deduced amino acid sequence of the respective VP2 and VP5 proteins was also compared in pairwise alignments. The deduced VP2 amino acid sequence of the attenuated AHSV-4 isolate displayed 19 amino acid (aa) dissimilarities with the cognate sequence of the virulent AHSV-4 isolate. Of these, three are present in the N-terminal region (aa 18-110), six in the C-terminal region (aa 464-886) and the remainder are localized to the central region (aa 254-401) of the VP2 protein (Table 2.2). Interestingly, ten of the amino acid differences are located in a previously identified antigenic region (aa 199-414) known to contain neutralization-specific epitopes (Burrage *et al*., 1993; Bentley *et al*., 2000; Venter *et al*., 2000b; Martínez-Torrecuadrada *et al*., 2001). In contrast to the VP2 proteins, no differences were observed between the VP5 amino acid sequences of the attenuated and virulent AHSV-4 isolates. Pairwise alignments of the nucleotide and deduced amino acid sequences of the respective VP2 and VP5 genes, as determined in this investigation, are provided in the Appendix to this dissertation.

Table 2.2: Amino acid differences between the VP2 sequences of attenuated and virulent AHSV-4 isolates

VP2 virulent		VP2 attenuated	
Amino acid[1]	**Amino group**	**Amino acid[1]**	**Amino group**
Leu_{18}	Non-polar	Ile_{18}	Non-polar
Arg_{56}	Basic	Cys_{56}	Polar
Gly_{110}	Polar	Glu_{110}	Acidic
Val_{254}	Non-polar	Ala_{254}	Non-polar
Asn_{265}	Polar	Ser_{265}	Polar
Leu_{299}	Non-polar	Gln_{299}	Polar
Phe_{311}	Non-polar	Cys_{311}	Polar
Gly_{312}	Polar	Asp_{312}	Acidic
Met_{346}	Non-polar	Thr_{346}	Polar
Thr_{355}	Polar	Ala_{355}	Non-polar
Leu_{365}	Non-polar	Phe_{365}	Non-polar
Asp_{380}	Acidic	Gly_{380}	Polar
Leu_{401}	Non-polar	Gln_{401}	Polar
Thr_{464}	Polar	Met_{464}	Non-polar
Asn_{465}	Polar	Asp_{465}	Acidic
Val_{470}	Non-polar	Ile_{470}	Non-polar
Ser_{600}	Polar	Tyr_{600}	Polar
Gln_{822}	Polar	Arg_{822}	Basic
Asn_{886}	Polar	Tyr_{886}	Polar

[1] The amino acid position is indicated by subscript

2.3.3 Transient expression of AHSV-4 VP2 and VP5 proteins in BHK-21 cells

2.3.3.1 Construction of recombinant pCMV-Script® plasmids

To facilitate studies aimed at determining whether intracellular expression of the AHSV outer capsid proteins may result in the induction of apoptosis in mammalian cells, the AHSV-4 VP2 and VP5 genes were cloned into the mammalian expression vector pCMV-Script® (Fig. 2.2a). For this purpose, the respective VP2 and VP5 genes were recovered from the previously constructed recombinant pGEM® T-Easy plasmids and cloned into pCMV-Script® vector DNA that had been digested with the corresponding restriction enzymes. The plasmid DNA extracted from randomly selected kanamycin-resistant transformants were first analyzed by agarose gel electrophoresis. Plasmid DNA that migrated slower than the parental pCMV-Script® vector DNA were selected and the presence of the gene-specific DNA inserts was verified by restriction enzyme digestion.

Digestion of recombinant plasmids pCMV-VP2att and pCMV-VP2vir with both *Eco*RI and *Kpn*I yielded DNA fragments corresponding with the size of the vector DNA (*ca*. 4.3 kb) and the VP2 gene (3.2 kb) (Fig. 2.2b, lanes 1 and 3, respectively), whereas digestion of recombinant plasmids pCMV-VP5att and pCMV-VP5vir with both *Not*I and *Pst*I resulted in excision of the 1.538-kb VP5 gene (Fig. 2.2b, lanes 5 and 7, respectively). These results therefore confirmed that the VP2 and VP5 genes of the attenuated and virulent AHSV-4 isolates had been cloned successfully into the pCMV-Script® vector DNA.

2.3.3.2 Expression of the AHSV-4 VP2 and VP5 genes in BHK-21 cells

To determine whether the respective VP2 and VP5 genes were expressed in BHK-21 cells, cell monolayers were mock-transfected and transfected with purified parental pCMV-Script® vector or the recombinant mammalian expression plasmids. Cell lysates were prepared at 36 h post-transfection, and analyzed by SDS-PAGE and immunoblot analyses. No uniquely expressed proteins could be observed in a Coomassie-stained SDS-polyacrylamide gel when compared to the control transfected cells. Moreover, immunoblot analysis of the cell lysates revealed that the anti-VP2 antibody did not react with immunoreactive bands, whereas the anti-VP5 antibody yielded several non-specific immunoreactive bands (results not shown). These results are most likely due to low levels of transient gene expression, which is often the case when using mammalian expression systems (Isler *et al*., 2005; Hartley, 2005; Yin *et al*., 2007).

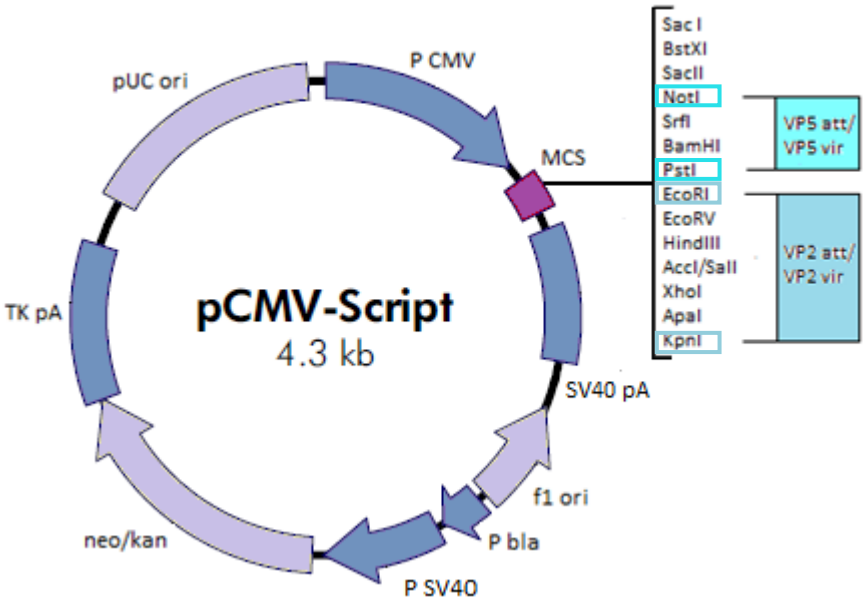

Fig. 2.2a: Schematic representation of the recombinant pCMV-Script® expression vector. The cloning sites, within the multiple cloning site (MCS) of the vector, used for insertion of the different AHSV-4 VP2 and VP5 genes are indicated in blue boxes.

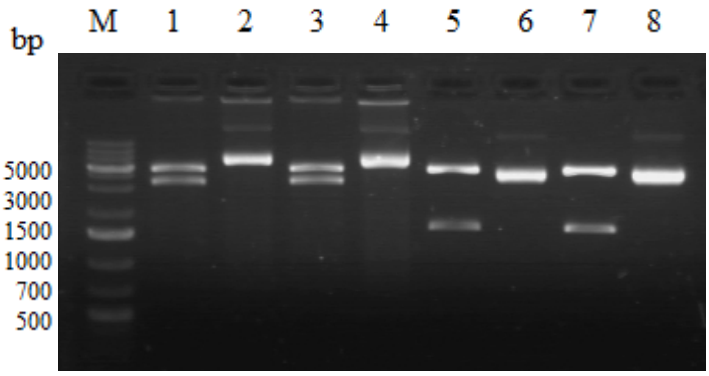

Fig. 2.2b: Agarose gel electrophoretic analysis of recombinant pCMV-Script® plasmids harbouring VP2 and VP5 gene-specific inserts. Lane M, DNA molecular weight marker; lane 1, pCMV-VP2att plasmid DNA digested with both *Eco*RI and *Kpn*I; lane 2, uncut pCMV-VP2att plasmid; lane 3, pCMV-VP2vir plasmid DNA digested with both *Eco*RI and *Kpn*I; lane 4, uncut pCMV-VP2vir plasmid; lane 5, pCMV-VP5att plasmid DNA digested with both *Not*I and *Pst*I; lane 6, uncut pCMV-VP5att plasmid; lane 7, pCMV-VP5vir plasmid DNA digested with both *Not*I and *Pst*I; lane 8, uncut pCMV-VP5vir plasmid. The sizes of the DNA molecular weight marker, O'GeneRuler™ 1kb DNA Ladder Plus (Fermentas), are indicated to the left of the figure.

2.3.4 Construction of recombinant pFastBac™1 donor plasmids harbouring full-length AHSV-VP2 and VP5 genes

To facilitate studies regarding the ability of the AHSV outer capsid proteins to induce apoptosis in mammalian cells when added exogenously, the Bac-to-Bac® baculovirus expression system was exploited for synthesis of the outer capsid proteins of virulent and attenuated AHSV-4 isolates. To enable cloning of the respective VP2 and VP5 genes into the bacmid donor plasmid pFastBac™1 (Fig. 2.3a), both the recombinant pGEM® T-Easy and pFastBac™1 plasmid DNA were digested with the appropriate restriction enzymes. The excised VP2 and VP5 genes, as well as digested donor plasmid DNA were purified from an agarose gel and ligated overnight. Following transformation of competent *E. coli* JM109 cells, plasmid DNA isolated from randomly selected ampicillin-resistant transformants was analyzed by agarose gel electrophoresis. Plasmid DNA migrating slower than the parental pFastBac™1 vector DNA were selected and characterized further by restriction enzyme digestion.

Digestion of the recombinant bacmid donor plasmids pFB-VP2att and pFB-VP2vir with both *Eco*RI and *Kpn*I resulted in the excision of a 3.2-kb DNA fragment, indicating that the full-length VP2 gene of the attenuated and virulent AHSV-4 isolates, respectively, had been cloned successfully (Fig. 2.3b, lanes 1 and 3, respectively). To verify that the VP5 gene of the respective AHSV-4 isolates had been cloned, the recombinant bacmid donor plasmids pFB-VP5att and pFB-VP5vir were characterized by digestion with both *Not*I and *Pst*I. Digestion of the recombinant plasmid DNA excised a DNA fragment corresponding in size with the full-length VP5 gene (1.538 kb) (Fig. 2.3b, lanes 5 and 7, respectively). These recombinant donor plasmids were subsequently used to generate recombinant bacmids, as described below.

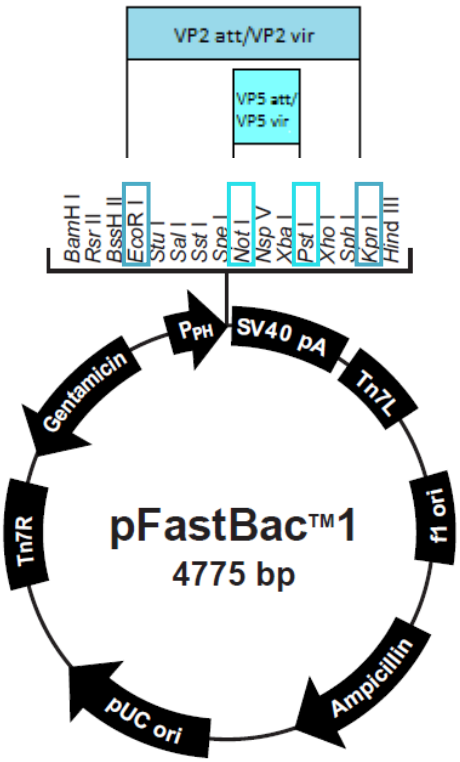

Fig. 2.3a: Schematic representation of the recombinant pFastBac™1 vector. The cloning sites used for insertion of the different AHSV-4 VP2 and VP5 genes into the vector are indicated in blue boxes.

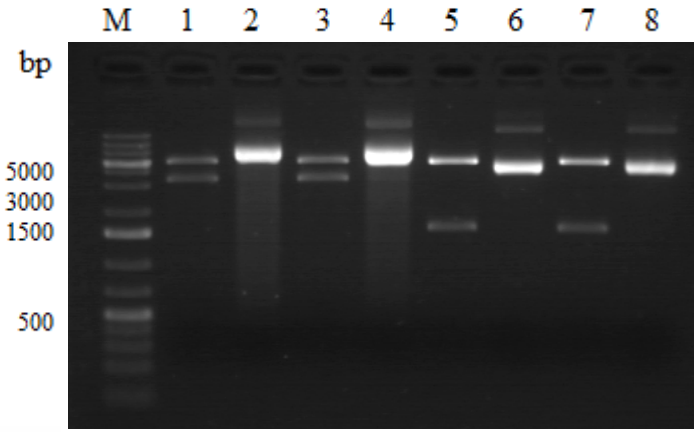

Fig. 2.3b: Agarose gel electrophoretic analysis of the recombinant pFastBac™1 plasmids harbouring VP2 and VP5 gene-specific inserts. Lane M, DNA molecular weight marker; lane 1, pFB-VP2att plasmid DNA digested with both *Eco*RI and *Kpn*I; lane 2, uncut pFB-VP2att plasmid; lane 3, pFB-VP2vir plasmid DNA digested with both *Eco*RI and *Kpn*I; lane 4, uncut pFB-VP2vir plasmid; lane 5, pFB-VP5att plasmid DNA digested with both *Not*I and *Pst*I; lane 6, uncut pFB-VP5att plasmid; lane 7, pFB-VP5vir plasmid DNA digested with both *Not*I and *Pst*I; lane 8, uncut pFB-VP5vir plasmid. The sizes of the DNA molecular weight marker, O'GeneRuler™ 1kb DNA Ladder Plus (Fermentas), are indicated to the left of the figure.

2.3.5 Engineering and characterization of recombinant bacmids

The bacmid DNA propagates as a large plasmid (135 kb) in *E. coli* DH10Bac™ cells and confers resistance to kanamycin, as well as complements a *lacZ′* deletion present on the *E. coli* chromosome to form colonies that are blue in the presence of X-gal. During site-specific transposition of the recombinant donor plasmid, the mini-Tn7 cassette is inserted from the donor plasmid into the mini-*att*Tn7 attachment site on the bacmid DNA, thereby disrupting expression of the LacZα peptide. Thus, colonies containing the recombinant bacmid display a white colony-phenotype and can be readily distinguished from the blue colonies that harbour the unaltered bacmid DNA. The transposase required for the transposition is encoded by the pMON7124 helper plasmid present in the *E. coli* DH10Bac™ cells, which also confers resistance to tetracycline (Luckow *et al*., 1993; Ciccarone *et al*., 1997).

Recombinant bacmid DNA was engineered by transforming competent *E. coli* DH10Bac™ cells with the respective recombinant pFastBac™1 donor plasmids, and selecting for recombinant bacmids by plating the transformed cells onto a selective agar medium. The high-molecular-weight recombinant bacmid DNA was subsequently extracted from selected transformants and used as template DNA in PCR assays to confirm successful transposition of the respective VP2 and VP5 genes into the bacmid DNA. For this purpose, the universal pUC/M13 forward primer and appropriate gene-specific reverse primer were used. Whereas the forward primer anneals to a sequence flanking the mini-*att*Tn7 attachment site within the *lacZ′* gene of the bacmid DNA, the gene-specific reverse primer anneals to the 3′ end of the corresponding VP2 or VP5 gene (Fig. 2.4a).

By making use of recombinant bacmid DNA transposed with either the pFB-VP2att or pFB-VP2vir donor plasmid as template DNA for PCR, bands of *ca*. 4.850 kb were obtained (Fig. 2.4b, lanes 1 and 2, respectively). In the case of recombinant bacmid DNA transposed with either the pFB-VP5att or pFB-VP5vir donor plasmid, PCR amplicons of *ca*. 3.188 kb were obtained (Fig. 2.4b, lanes 3 and 4, respectively). The size of the observed amplicons corresponded with the size of the VP2 (3.2 kb) or VP5 (1.538 kb) gene, together with the size of the transposed mini-Tn7 cassette (1.650 kb). No amplicons were observed in the control reaction from which template DNA was omitted. Recombinant bacmids were selected and designated Bac-VP2att, Bac-VP2vir, Bac-VP5att and Bac-VP5vir, respectively. These recombinant bacmids were used in all subsequent experiments.

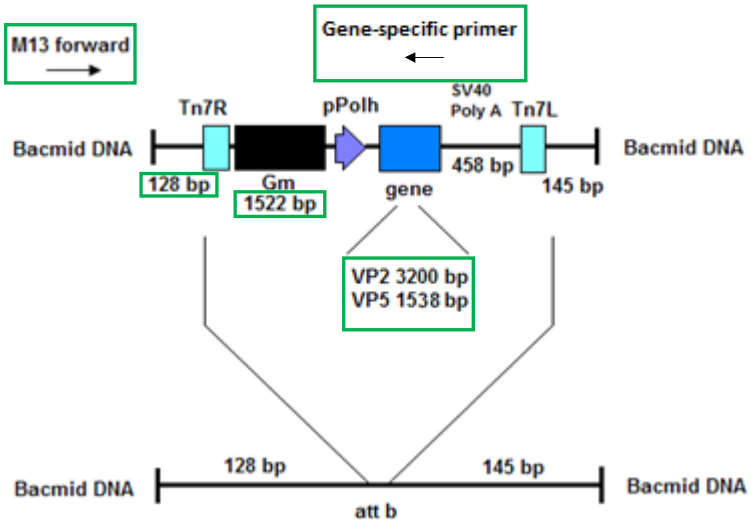

Fig. 2.4a: Schematic representation of transposed bacmid DNA. The annealing positions of the pUC/M13 forward primer and the gene-specific reverse primer are indicated, as well as the size of the mini-*att*Tn7 cassette DNA and the bacmid DNA flanking the cassette. The position of the transposed AHSV-4 VP2 and VP5 genes within the bacmid DNA is also indicated.

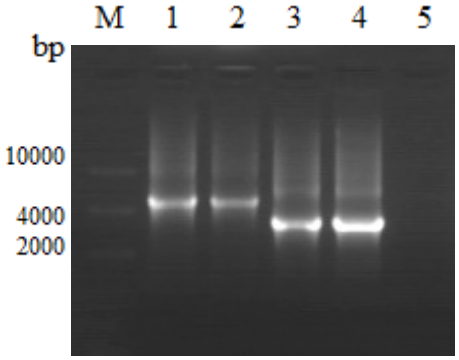

Fig. 2.4b: Agarose gel electrophoretic analysis of recombinant bacmid DNA following PCR analysis with universal pUC/M13 forward and gene-specific reverse primers. Lane M, DNA molecular weight marker; lane 1, amplicon obtained using Bac-VP2att as template; lane 2, amplicon obtained using Bac-VP2vir as template; lane 3, amplicon obtained using Bac-VP5att as template; lane 4, amplicon obtained using Bac-VP5vir as template; lane 5, control reaction from which template DNA was omitted. The sizes of the DNA molecular weight marker, FastRuler™ High Range DNA Ladder (Fermentas), are indicated to the left of the figure.

2.3.6 Recombinant VP2 and VP5 protein expression in *Sf*9 cells

Wild-type and recombinant bacmid DNA were isolated from *E. coli* DH10Bac™ cultures, and transfected into *Sf*9 cells. The progeny viruses were collected at 72 h post-transfection, plaque-purified and then used to prepare virus stocks. The titre of each baculovirus stock was determined by plaque assays and ranged between 3.4×10^7 and 2.1×10^8 pfu/ml. To determine whether the respective AHSV-4 VP2 and VP5 proteins were synthesized in recombinant baculovirus-infected cells, monolayers of *Sf*9 cells were mock-infected and infected with the wild-type or recombinant baculoviruses at a MOI of 5 pfu/cell. Following incubation for 72 h, whole-cell lysates were analyzed by SDS-PAGE and immunoblot analyses.

Analysis of the Coomassie-stained gels indicated the presence of a faint, but apparently unique protein in the lysates prepared from cells infected with the Bac-VP2att and Bac-VP2vir baculovirus recombinants (Fig. 2.5a). An over-expressed protein, which co-migrated with a wild-type baculovirus-expressed protein, was identified in the lysates prepared from cells infected with the Bac-VP5att and Bac-VP5vir baculovirus recombinants (Fig. 2.6a). The molecular mass of these proteins was in agreement with the predicted molecular mass of VP2 (124 kDa) and VP5 (57 kDa). To confirm the identity of these proteins, duplicate unstained SDS-polyacrylamide gels were subjected to immunoblot analysis. The results indicated that the uniquely expressed 124-kDa proteins reacted specifically with the anti-VP2 antibody, thus confirming successful expression of the VP2 attenuated and VP2 virulent proteins by the engineered recombinant baculoviruses (Fig. 2.5b). The anti-VP5 antibody, however, reacted with both the full-length (57 kDa) VP5 proteins and a truncated version of the proteins (*ca.* 50 kDa), which was also present in the cell lysate prepared from BHK-21 cells infected with AHSV-4 (1) (Fig. 2.6b). Both of these proteins reacted specifically with the anti-VP5 antibody, as no cross-reaction with similarly sized proteins were observed in lysates prepared from mock-infected or wild-type baculovirus-infected *Sf*9 cells. The truncated version of VP5 has been noted previously and is thought to be the result of proteolytic cleavage (Martínez-Torrecuadrada *et al.*, 1994). Nevertheless, these results confirmed that the engineered baculoviruses were indeed capable of expressing the VP5 attenuated and VP5 virulent proteins in *Sf*9 cells.

(a)

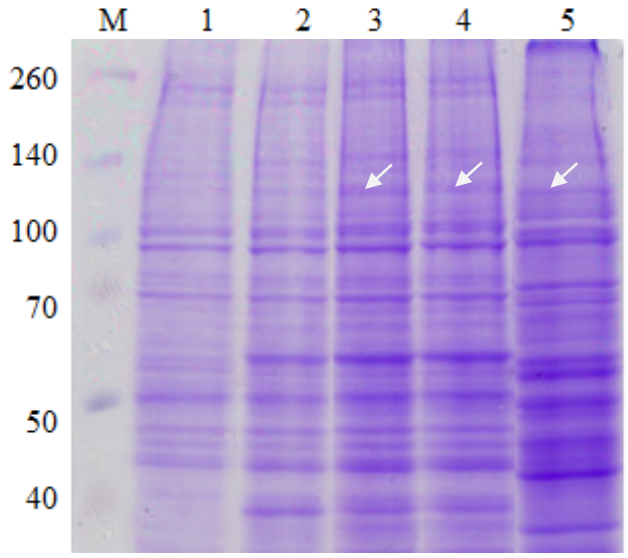

(b)

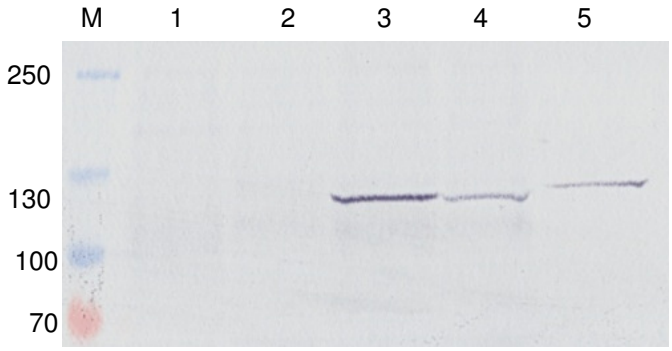

Fig. 2.5: SDS-PAGE and immunoblot analyses of the whole-cell lysates prepared from *Sf*9 cells infected with Bac-VP2att and Bac-VP2vir. Whole-cell lysate proteins were resolved by SDS-PAGE (a) and proteins from a duplicate, unstained gel were electroblotted onto a nitrocellulose membrane and subjected to immunoblot analysis with an anti-VP2 antibody (b). Lanes M, Protein molecular mass marker; lanes 1, mock-infected cells; lanes 2, wild-type baculovirus-infected cells; lanes 3, Bac-VP2att-infected cells; lanes 4, Bac-VP2vir-infected cells; lanes 5, AHSV-4 (1) infected BHK-21 cells. The sizes of the protein molecular mass markers, Spectra™ Multicolor Broad Range Protein Ladder (Fermentas) and PageRuler™ Plus Prestained Protein Ladder (Fermentas), respectively, are indicated in kDa to the left of the figures. Arrows indicate the presence of VP2 in virus-infected BHK-21 cells and of a uniquely expressed protein in cell lysates infected with the recombinant baculoviruses.

(a)

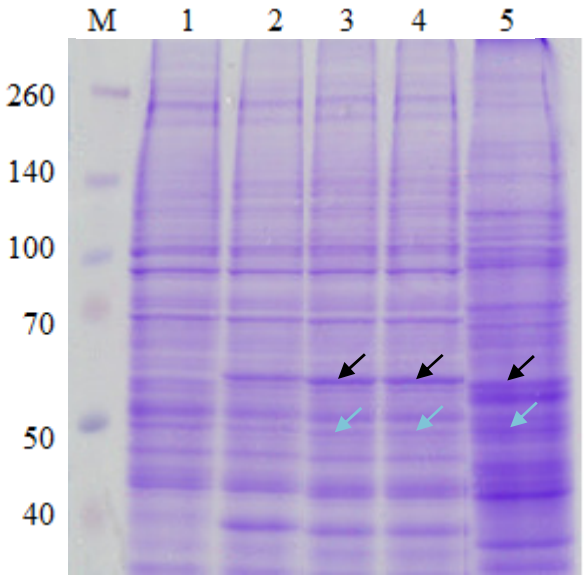

(b)

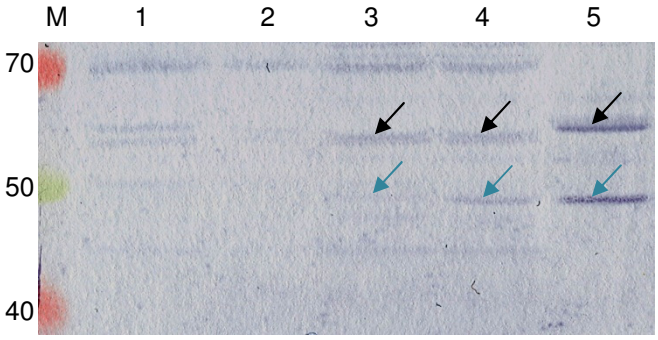

Fig. 2.6: SDS-PAGE and immunoblot analyses of the whole-cell lysates prepared from *Sf*9 cells infected with Bac-VP5att and Bac-VP5vir. Whole-cell lysate proteins were resolved by SDS-PAGE (a), and proteins from a duplicate, unstained gel were electroblotted onto a nitrocellulose membrane and subjected to immunoblot analysis with an anti-VP5 antibody (b). Lanes M, Protein molecular mass marker; lanes 1, mock-infected cells; lanes 2, wild-type baculovirus-infected cells; lanes 3, Bac-VP5att-infected cells; lanes 4, Bac-VP5vir-infected cells; lanes 5, AHSV-4 (1) infected BHK-21 cells. The sizes of the protein molecular mass marker, Spectra™ Multicolor Broad Range Protein Ladder (Fermentas), are indicated in kDa to the left of the figures. Full-length and truncated VP5 proteins that reacted with the anti-VP5 antibody are indicated by black and blue arrows, respectively.

2.3.7 Optimization of recombinant VP2 and VP5 protein expression in *Sf*9 cells

Although the outer capsid proteins of both the attenuated and virulent AHSV-4 isolates were expressed by the engineered recombinant baculoviruses, the yield of synthesized proteins was low. It has been reported previously that baculovirus-expressed AHSV VP2 is highly aggregative and that only *ca*. 10% of the total protein yield of VP2 is soluble, irrespective of the cell line and media used (du Plessis *et al*., 1998; Scanlen *et al*., 2002). Moreover, it has also been reported that expression of AHSV VP5 in *Sf*9 cells is cytotoxic, causing rapid cell lysis and resulting in low levels of protein expression (du Plessis and Nel, 1997; Stassen *et al*., 2011). The insolubility of VP2 and the low level of protein expression generally may therefore present major obstacles in the envisaged biological assays. Thus, to improve the yield of soluble recombinant baculovirus-expressed VP2 and VP5 proteins, the influence of infecting the *Sf*9 cells at different MOIs and of harvesting the infected cells at different times post-infection was subsequently evaluated.

In the first of these approaches, monolayers of *Sf*9 cells were infected with the respective VP2 and VP5 baculovirus recombinants at a MOI ranging between 1 and 20 pfu/cell. Whole-cell lysates of the infected cell monolayers were prepared at 72 h post-infection and analyzed by SDS-PAGE. Analysis of the Coomassie-stained gels indicated distinct differences in the yield of the recombinant proteins. The VP2 protein of the attenuated virus isolate was expressed to a higher level, as compared to that of the virulent virus isolate (Fig. 2.7a and b). However, no noticeable differences were observed in the yield of the recombinant VP2 attenuated protein, irrespective of the MOI used to infect the *Sf*9 cell monolayers. In contrast, the yield of the recombinant VP2 virulent protein was noticeably higher when the *Sf*9 cells were infected at a high MOI (10 to 20 pfu/cell), as opposed to *Sf*9 cells infected at a low MOI (1 to 5 pfu/cell). For *Sf*9 cells infected with the VP5 baculovirus recombinants, the VP5 protein of the attenuated virus isolate was also expressed to a higher level as compared to that of the virulent virus isolate (Fig. 2.7c and d). The recombinant VP5 attenuated protein was expressed to maximal levels when the *Sf*9 cells were infected at a MOI of 1 to 10 pfu/cell, whereas the recombinant VP5 virulent protein was expressed to maximal levels when the *Sf*9 cell were infected at a MOI of 5 to 20 pfu/cell.

(a) VP2 attenuated

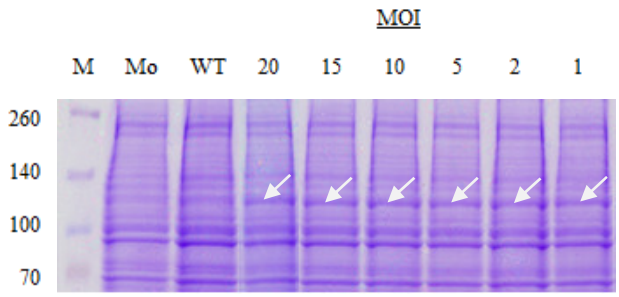

(b) VP2 virulent

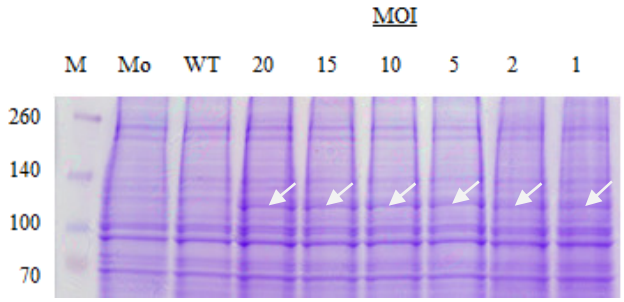

(c) VP5 attenuated

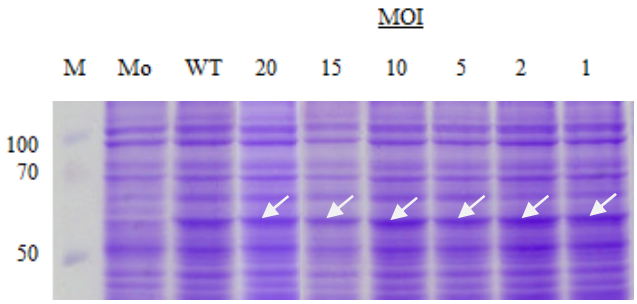

(d) VP5 virulent

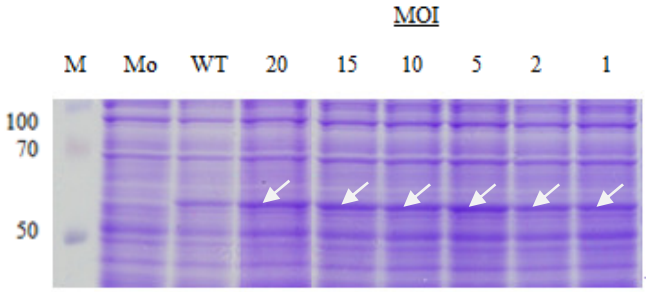

Fig. 2.7: SDS-PAGE analyses of whole-cell lysates prepared from *Sf*9 cells infected with recombinant baculoviruses at various MOIs. Whole-cell lysate proteins, prepared at 72 h post-infection from *Sf*9 cells infected with the respective VP2 and VP5 baculovirus recombinants at MOIs ranging from 1 to 20 pfu/cell, were resolved by SDS-PAGE. Mock-infected (Mo) and wild-type baculovirus-infected *Sf*9 cells (WT) were included as controls. The arrows indicate the recombinant VP2 and VP5 proteins. The sizes of the protein molecular mass markers (lanes M), Spectra™ Multicolor Broad Range Protein Ladder (Fermentas), are indicated in kDa to the left of the figures.

To evaluate the influence of the time of harvest post-infection on the yield of soluble recombinant proteins, monolayers of *Sf*9 cells were infected with the respective recombinant baculoviruses at a MOI of 5 or 10 pfu/cell, based on the results obtained above. At 48 and 72 h post-infection, the cells were harvested and the proteins were fractionated by centrifugation into soluble (cytoplasmic) and insoluble (particulate) fractions. Aliquots of these protein samples, together with the whole-cell lysates, were analyzed by SDS-PAGE. The results of these analyses are presented in Fig. 2.8. Analysis of the Coomassie-stained gels indicated that there was an increase in the amount of aggregated recombinant VP2 upon extended periods of incubation of the infected *Sf*9 cells. Although high levels of aggregated recombinant VP2 virulent protein were observed at 72 h post-infection, greater amounts of the recombinant protein were observed in the whole-cell lysate and soluble protein fraction when compared to that observed in the corresponding protein fractions prepared at 48 h post-infection. Consequently, 48 and 72 h post-infection were respectively selected as the optimal time of harvest for *Sf*9 cells infected with the VP2 attenuated and VP2 virulent baculovirus recombinants. In contrast to recombinant VP2, no apparent differences in the amount of aggregated VP5 protein could be observed at 48 and 72 h post-infection in cells infected with the respective VP5 baculovirus recombinants. To minimize cell lysis due to the cytotoxic properties of AHSV VP5 (Stassen *et al*., 2011), the optimal time of harvest was thus chosen to be 48 h post-infection.

Taking all of the above results into consideration, it was concluded that maximal yields of soluble recombinant VP2 and VP5 proteins could be obtained by infecting *Sf*9 cell monolayers at a MOI of 5 pfu/cell and harvesting the cells at 48 h post-infection (Bac-VP2att and Bac-VP5vir), or by infecting the *Sf*9 cells at a MOI of 10 pfu/cell and harvesting the cells at 48 h post-infection (Bac-VP5att) and at 72 h post-infection (Bac-VP2vir).

(a) VP2 attenuated (MOI of 5 pfu/cell)

(b) VP2 virulent (MOI of 10 pfu/cell)

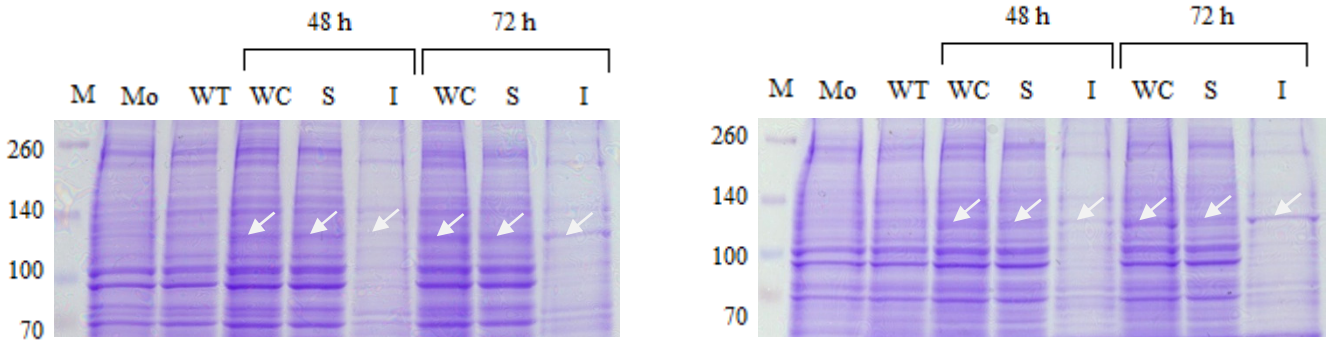

(c) VP5 attenuated (MOI of 10 pfu/cell)

(d) VP5 virulent (MOI of 5 pfu/cell)

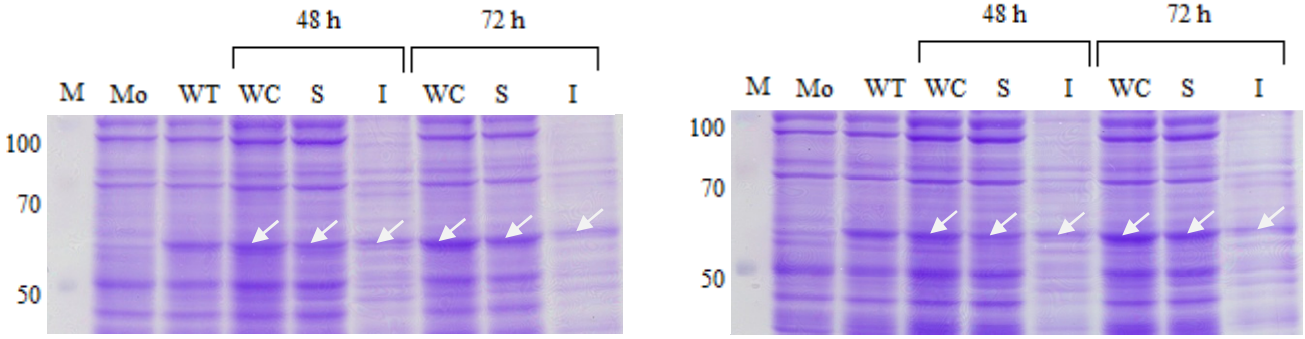

Fig. 2.8: SDS-PAGE analyses of protein fractions prepared at 48 or 72 h post-infection from recombinant baculovirus-infected *Sf*9 cells. Whole-cell lysates (WC), soluble (S) and insoluble (I) protein fractions from *Sf*9 cells infected with the respective VP2 and VP5 baculovirus recombinants at a MOI of 5 or 10 pfu/cell were prepared at 48 or 72 h post-infection, and resolved by SDS-PAGE. Mock-infected (Mo) and wild-type baculovirus-infected *Sf*9 cells (WT) were included as controls. The arrows indicate the recombinant VP2 and VP5 proteins. The sizes of the protein molecular mass markers (lanes M), Spectra™ Multicolor Broad Range Protein Ladder (Fermentas), are indicated in kDa to the left of the figures.

2.3.8 Large-scale production of soluble recombinant VP2 and VP5 proteins

To enable their use in biological assays, soluble recombinant VP2 and VP5 proteins of the attenuated and virulent AHSV-4 isolates were prepared on a large scale in suspension cultures of *Sf*9 cells. The cells were infected and harvested at the appropriate time post-infection, based on the results obtained in the preceding section. Following cell lysis, the lysates were fractionated by centrifugation and the yield of soluble recombinant VP2 and VP5 proteins was quantified from SDS-polyacrylamide gels with EZQuant v.2.1 software (EZQuant Biology Software, EZQuant Ltd.).

The results, presented in Table 2.3 and Fig. 2.9, indicated that the yield of soluble recombinant baculovirus-expressed VP2 of the attenuated and virulent AHSV-4 isolates were 2.39 µg/10^6 cells and 1.56 µg/10^6 cells, respectively. However, the inverse was observed for the recombinant baculovirus-expressed VP5 proteins. In this instance, a lower yield of soluble recombinant VP5 was obtained for the attenuated virus isolate (5.09 µg/10^6 cells) compared with the virulent virus isolate (8.03 µg/10^6 cells). These results compare favourably with those reported by Martínez-Torrecuadrada *et al*. (1994), in which the total yield of baculovirus-expressed AHSV-4 VP2 and VP5 proteins was determined to be 2 µg/10^6 cells and 5 µg/10^6 cells, respectively. Notably, the soluble recombinant VP2 fractions of the attenuated and virulent AHSV-4 isolates represented 72.13% and 38.79% of the total VP2 protein yield, respectively, which are significantly greater than the *ca*. 10% obtained in previous studies (du Plessis *et al*. 1998; Scanlen *et al*., 2002).

Table 2.3: Yield of soluble baculovirus-expressed AHSV-4 VP2 and VP5 proteins

Sample	Concentration of soluble protein (µg/10 µl)	Yield of soluble protein (µg/10^6 cells)	Percentage (%) soluble protein[1]
VP2 att	0.359	2.39	72.13
VP2 vir	0.234	1.56	38.79
VP5 att	0.763	5.09	67.22
VP5 vir	1.204	8.03	80.65

[1] The soluble protein fractions are expressed as a percentage of the total recombinant protein yield

(a)

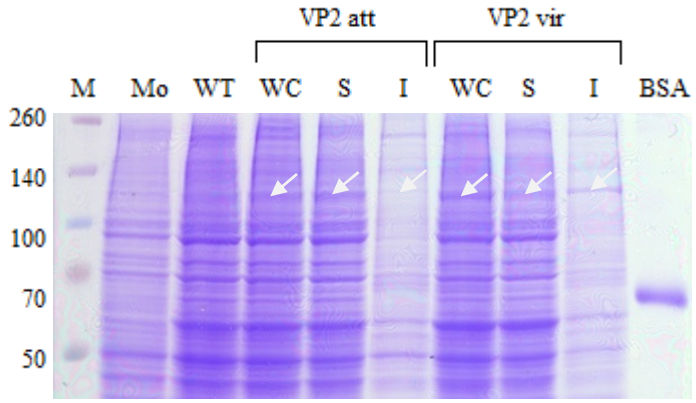

(b)

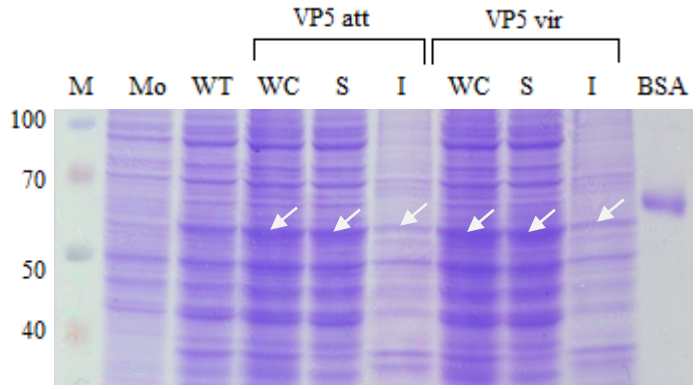

Fig. 2.9: Large-scale production of recombinant outer capsid proteins in suspension cultures of *Sf*9 cells. *Sf*9 suspension cultures were infected with recombinant baculoviruses expressing the VP2 (a) and VP5 (b) proteins of an attenuated and a virulent AHSV-4 isolate using optimized conditions of virus infection. Samples of the whole-cell lysate (WC), soluble (S) and insoluble (I) protein fractions were analyzed by SDS-PAGE, and the yield of soluble baculovirus-expressed VP2 and VP5 proteins were quantified with EZQuant software. Bovine serum albumin (BSA; 2 mg/ml) was used as standard. To ensure accurate quantification, equal cell densities for each sample were loaded onto the gel. The arrows indicate the recombinant VP2 and VP5 proteins. The sizes of the protein molecular mass markers (lanes M), Spectra™ Multicolor Broad Range Protein Ladder (Fermentas), are indicated in kDa to the left of the figures.

2.4 DISCUSSION

Studies regarding the outer capsid proteins VP2 and VP5 of AHSV have focussed almost exclusively on aspects relating to their immunogenicity (Martínez-Torrecuadrada *et al*., 1994, 1996, 1999). Consequently, a considerable amount of research has been undertaken to develop subunit vaccines based on the use of baculovirus-expressed recombinant outer capsid proteins (Martínez-Torrecuadrada *et al*., 1996; Roy *et al*., 1996; du Plessis *et al*., 1998; Scanlen *et al*., 2002). Despite this progress, very little is known regarding the biological importance of the AHSV outer capsid proteins. Notably, the outer capsid proteins of various members of the *Reoviridae* family, such as BTV (Mortola *et al*., 2004), mammalian reovirus (Tyler *et al*., 1995; Connolly *et al*., 2001; Danthi *et al*., 2008a) and avian reovirus (Shih *et al*., 2004), have been implicated in the induction of apoptosis in mammalian cells. Towards the aim of determining whether the AHSV outer capsid proteins are likewise triggers of apoptosis, the VP2 and VP5 genes of an attenuated and a virulent AHSV-4 isolate, respectively, were thus cloned and expressed in different eukaryotic systems.

Differential induction of apoptosis between virus strains has been noted previously for several viruses. Notably, a single amino acid change in the Sindbis virus E2 glycoprotein rendered the virus less virulent and also reduced the ability of the virus to induce apoptosis in 2-week-old mouse brains (Tucker *et al*., 1993; Lewis *et al*., 1996). Similarly, virulent and attenuated Theiler's murine encephalomyelitis virus (TMeV) strains were reported to influence apoptotic levels and survival of infected mice to different extents, with the attenuated strain having a lesser effect. These differences were attributed to several amino acid differences in the sequence of the cell-binding VP2 puff B protein of the two TMeV strains (Tsunoda *et al.*, 1997, 2007). In contrast to these viruses, an avirulent mutant of Sendai virus, which was derived from a highly virulent wild-type Sendai virus isolate and possessed two amino acid mutations, was reported to induce a high degree of apoptotic cell death in mouse pulmonary epithelial cells (Itoh *et al*., 1997). Based on these studies, it was therefore of interest to determine if the virulent and attenuated AHSV-4 isolates differed in their ability to induce apoptosis. In this regard, it is interesting to note that sequence analyses indicated that although the VP5 sequences of the virulent and attenuated AHSV-4 isolates were identical, 19 amino acid differences were observed between the respective VP2 amino acid sequences.

To allow for intracellular expression of the AHSV outer capsid proteins, recombinant pCMV-Script® mammalian expression vectors harbouring the VP2 and VP5 genes of attenuated and virulent AHSV-4 isolates were constructed. However, expression of the proteins could not be confirmed by immunoblot analysis, possibly due to the low levels of expression associated with transient gene expression in mammalian cells. Transient expression involves gene expression from non-integrated plasmid DNA and because only a fraction of the DNA delivered to the cell is transported to the cell nucleus for transcription, expression levels may be lower than cellular expression levels (Yin *et al*., 2007). Similar low levels of gene expression in mammalian cells using this expression vector have been noted previously for other AHSV proteins, including the non-structural proteins NS1 (Roos, 2009), NS2 (Nieuwoudt, 2008) and NS3 (Korsman, 2007), as well as the structural protein VP7 (Burger, 2006). In these instances, intracellular expression of the proteins was observed by fluorescence microscopy only upon construction of chimeric genes in which an eGFP reporter gene was fused in-frame to the 3′-end of the respective viral genes, thus ensuring that transcription of the viral gene would need to occur to obtain a fluorescently tagged viral protein. Although this approach was not pursued, the above results provide supporting evidence for low level expression of heterologous genes in the pCMV-Script® mammalian expression system. Despite these results, note should, however, be taken that the sources of the respective VP2 and VP5 genes used in the construction of the recombinant mammalian expression vectors were identical to those used in the engineering of recombinant baculoviruses, which were subsequently shown to express the respective VP2 and VP5 genes in *Sf*9 cells (see below).

The first manipulation of a baculovirus for the expression of non-baculoviral DNA was described just over 25 years ago (Smith *et al*., 1983). Since then the baculovirus expression system has become one of the most powerful and versatile eukaryotic expression systems for the high-level production of biologically active and functional recombinant proteins (Luckow and Summers, 1988; Kost and Condreay, 1999; Summers, 2006; Yin *et al*., 2007; Jarvis, 2009). Indeed, the expression of individual AHSV proteins in *Sf*9 cells by appropriately constructed baculovirus recombinants has made significant contributions to understanding the biological importance and structure-function relationships of several of the viral proteins, including the non-structural proteins NS1 (Maree and Huismans, 1997), NS2 (Uitenweerde *et al*., 1995) and NS3 (van Niekerk *et al*., 2001), as well as the structural proteins VP5 (Stassen *et al*., 2011), VP6 (de Waal and Huismans, 2005) and VP7 (Basak *et al*., 1996).

Consequently, recombinant baculoviruses were engineered that harboured a transposed copy of the respective AHSV-4 VP2 and VP5 genes under the transcriptional control of the strong polyhedrin promoter in order to produce sufficient amounts of the outer capsid proteins for use in subsequent biological assays. Immunoblot analysis of cell lysates prepared from recombinant baculovirus-infected *Sf*9 cells indicated that an anti-VP2 antibody reacted specifically with the VP2 proteins (124 kDa), whereas an anti-VP5 antibody reacted specifically with the full-length VP5 proteins and a truncated version of the proteins (57 and *ca*. 50 kDa, respectively). The presence of a similarly sized truncated VP5 protein, in addition to the full-length protein, has been noted in previous studies (Grubman and Lewis, 1992; Martínez-Torrecuadrada *et al*., 1994). The truncated VP5 protein may be due to proteolytic cleavage of the full-length protein by a ubiquitous cellular protease present in both insect and mammalian cells, since the truncated protein was present in both recombinant baculovirus-infected *Sf*9 cells and AHSV-4 (1)-infected BHK-21 cells (Fig. 2.6). Alternatively, synthesis of the truncated VP5 protein may have been initiated at an in-frame downstream AUG codon within the VP5 coding sequence, possibly at nucleotide positions 165-167 to yield a 51-kDa protein.

Although the baculovirus expression system is favoured for its high-level production of recombinant proteins, the results obtained during the course of this study indicated that the yield of baculovirus-expressed outer capsid proteins of the attenuated and virulent AHSV-4 isolates was low. The results are nevertheless in agreement with those reported previously for baculovirus-expressed AHSV VP2 (Vreede and Huismans, 1994) and VP5 (du Plessis and Nel, 1997). These low levels of recombinant protein expression, however, can be attributed to the properties of the outer capsid proteins. The AHSV VP5 protein is known to be cytotoxic when expressed in baculovirus-infected *Sf*9 cells (Martínez-Torrecuadrada *et al*., 1994; Stassen *et al*., 2011) and may thus account for its low expression level. Moreover, it has been reported that baculovirus-expressed AHSV VP2 accumulates predominantly as insoluble aggregates (du Plessis *et al*., 1998; Scanlen *et al*., 2002). Although the reasons for the low yield of baculovirus-expressed VP2 are not yet understood, it has been reported that properties of a protein such as charge average, turn-forming residue fraction, cysteine and proline fractions, hydrophobicity and total number of residues may all aid in protein aggregation (Anfinsen, 1973; Dill, 1990; Fink, 1998; Chiti *et al*., 2003; Dobson, 2004). By taking the above into account and considering that biologically active outer capsid proteins

would be required in subsequent assays, attempts were thus made to optimize the synthesis of soluble baculovirus-expressed VP2 and VP5 proteins.

Various approaches have been described to increase the yield of soluble baculovirus-expressed recombinant proteins. In addition to using cell lysis buffers with differing detergent compositions (Schein, 1990; Seddon *et al*., 2004; Privé, 2007) and chemical resolubilization of insoluble proteins (Rudolph and Lilie, 1996; Vallejo and Rinas, 2004), different genetic approaches of preventing protein aggregation have also been described. These typically involve site-directed mutagenesis and amino acid substitutions that increase solubility (Schein, 1993; Malissard and Berger, 2001; Trevino *et al*., 2007), truncation of proteins (Blommel and Fox, 2007) and addition of solubility-enhancing fusion tags (Dyson *et al*., 2004; Waugh, 2006). However, these approaches may not only affect the functionality of the recombinant proteins negatively, but also require extensive experimentation and the yield of soluble protein obtained may be low. Consequently, in this investigation, emphasis was rather placed on approaches aimed at increasing the synthesis of soluble recombinant proteins intracellularly. To this end, the influence of infecting *Sf*9 cells with the respective recombinant baculoviruses at different MOIs and harvesting of the infected cells at different times post-infection were assessed. These infection variables are readily manipulated to maximize recombinant protein yields and are easily amenable to scale-up for the large-scale preparation of recombinant proteins. Several studies have reported the optimization of infection strategies to improve recombinant protein yields (Maiorella *et al*., 1988; Licari and Bailey, 1992; Whitford and Mertz, 1998). To ensure simultaneous infection of all cells it is often necessary to adjust the MOI used, as above a certain threshold an increase in protein yield will not be observed with an increase in the MOI (Madden and Safferling, 2007). Moreover, maximum recombinant protein expression under the control of the polyhedrin promoter is typically observed later than 24 h post-infection, during the very late stages of infection (Madden and Safferling, 2007). Thus, to prevent proteolytic degradation of the protein of interest by released cellular proteases, harvesting of infected cells at time points prior to the onset of significant cell lysis permits the efficient production of high-quality recombinant proteins (Madden and Safferling, 2007).

Based on the results of the above assays (Figs. 2.7 and 2.8), optimal infection and time of harvest conditions were identified for each of the four engineered recombinant baculoviruses. Using these optimized conditions, the recombinant VP2 and VP5 proteins of the attenuated

and virulent AHSV-4 isolates were subsequently prepared in large scale. The yield of soluble outer capsid proteins was quantified following SDS-PAGE analysis of whole-cell lysates, as well as soluble and insoluble protein fractions. The results indicated that the yield of soluble VP5 of the virulent and attenuated AHSV-4 isolates was 8.03 and 5.09 µg/10^6 cells, respectively, and the turnover of soluble protein was *ca*. 80.65 and 67.22%. The yield of soluble VP2 of the virulent and attenuated AHSV-4 isolates (1.56 and 2.39 µg/10^6 cells, respectively) was less compared to that of VP5, but the turnover of soluble proteins was 38.79 and 72.13%, respectively. This represents a major improvement over previous studies in which the maximal yield of soluble AHSV VP2 was reported to be *ca*. 10% (du Plessis *et al*., 1998; Scanlen *et al*., 2002).

In summary, the VP2 and VP5 genes of attenuated and virulent AHSV-4 isolates were cloned into a mammalian expression vector and recombinant baculoviruses expressing the respective genes were engineered. The constructs and soluble recombinant VP2 and VP5 outer capsid proteins were subsequently used to determine whether intracellular expression or exogenous addition of the proteins are involved in the induction of apoptosis in mammalian cells. The details of these studies are presented in the following Chapter.

CHAPTER THREE

AFRICAN HORSE SICKNESS VIRUS INDUCES APOPTOSIS IN MAMMALIAN CELLS AND IS TRIGGERED BY THE VIRUS OUTER CAPSID PROTEINS

3.1 INTRODUCTION

African horse sickness virus (AHSV) is the aetiological agent of African horse sickness (AHS), a highly infectious arthropod-borne disease of equids of which the mortality rate in susceptible horse populations may exceed 90% (Coetzer and Erasmus, 1994; Guthrie, 2007). Reports regarding microscopic examination of endothelial cells of the heart, lung, liver and spleen of AHSV-infected animals noted ultrastructural modifications that included the loss of intercellular junction integrity, the presence of cytoplasmic projections and condensation of the nucleus. In association with these cellular changes, haemorrhages, oedema and microthromboses were observed, predominantly in the myocardium and lung (Laegreid *et al*., 1992; Gómez-Villamandos *et al*., 1999). It has been reported that infection of cells by most viruses triggers apoptosis (O'Brien, 1998; Roulston *et al*., 1999; Hay and Kannourakis, 2002) and in some virus-induced diseases, apoptosis is also a pathogenic mechanism that contributes *in vivo* to cell death, tissue injury and disease severity (Jackson and Rossiter, 1997; DeMaula *et al*., 2001; Martin-Latil *et al*., 2007; Danthi *et al*., 2008b; Umeshappa *et al*., 2010). It is therefore tempting to speculate that apoptosis may likewise contribute to the observed pathogenesis of AHS disease in the mammalian host.

Infection of cultured mammalian cells by AHSV results in dramatic cytopathic effect (CPE) and is associated with irregular-shaped cells, cell rounding, shrinkage and detachment, as well as darkly Giemsa-stained nuclei within the infected cells (Osawa and Hazrati, 1965; Anonymous, 1991). In contrast, propagation of AHSV in *Aedes albopictus* cell lines results in persistent infection and maturation of progeny virions, although no CPE is observed (Mirchamsy *et al*., 1970). This difference in host cell CPE, following virus infection, furthermore suggests that apoptosis may be induced in mammalian cells. However, whether the correlation between CPE and apoptosis holds true for AHSV, as with other arboviruses such as Sindbis virus (Karpf and Brown, 1998), La Crosse virus (Borucki *et al*., 2001, 2002), bluetongue virus (Mortola *et al*., 2004) and West Nile virus (Xiao *et al*., 2001; Yang *et al*., 2002), remains to be determined. Indeed, no investigations regarding the ability of AHSV to induce apoptosis in infected cells have as yet been reported.

Several events during virus replication, including virus attachment to cellular receptors, endosomal virion disassembly, as well as subsequent viral protein synthesis and genome replication, may result in the induction of apoptosis in virus-infected cells (Danthi, 2011).

Indeed, for reovirus, which like AHSV is also a member of the *Reoviridae* family, the outer capsid protein, σ1, was shown to induce apoptosis (Tyler *et al*., 1995; Shih *et al*., 2004). Moreover, it has been reported that receptor binding alone is not sufficient to trigger apoptosis and that virus disassembly in the endosome is also required (Connolly and Dermody, 2002). Similar results have also been reported for bluetongue virus (BTV), the prototype orbivirus (Mortola *et al*., 2004). Since the outer capsid proteins VP2 and VP5 of AHSV are believed to play a role in cell attachment and entry, they may be considered as prime candidates responsible for triggering apoptosis in virus-infected mammalian cells. Studies on the outer capsid proteins of BTV have led to a generalized model of the early events during orbivirus cell entry (Mertens *et al*., 2004; Roy, 2008). According to this model, VP2 mediates attachment of the virion to the cell surface and its subsequent internalization. After internalization, endocytic vesicles are formed within which VP5 may be unmasked following low-pH removal of VP2. The partly denuded virion then causes destabilization of the vesicle membrane to allow the penetration of the uncoated core particles into the cell cytoplasm. The release of the core particles is thought to be mediated by VP5, since the protein has amphipathic helices in its N-terminus that are responsible for membrane permeabilization in a pH-dependent manner (Hassan *et al*., 2001; Zhang *et al*., 2010).

Although there appears to exist circumstantial evidence that AHSV may induce apoptosis in the mammalian host and cultured mammalian cells, no studies in this regard have been undertaken. Consequently, the primary aims of this part of the investigation were to determine whether AHSV is indeed capable of inducing apoptosis in infected mammalian cells, to identify possible initiators of AHSV-induced apoptosis and to delineate the role of early events in the virus infectious cycle in the induction of apoptosis.

3.2 MATERIALS AND METHODS

3.2.1 Cells and virus

Baby Hamster Kidney-21 (BHK-21; ATCC CL-10) cells were propagated and maintained as monolayers in 75-cm^2 tissue culture flasks. The cells were cultured in Eagle's Minimal Essential Medium (EMEM) with Earle's Balanced Salt Solution (EBSS) and L-glutamine (Lonza, BioWhittaker®), supplemented with 5% (v/v) foetal bovine serum (FBS), 1% (v/v) non-essential amino acids (NEAA) and antibiotics (10 000 U/ml of penicillin, 10 000 µg/ml

of streptomycin and 25 µg/ml of amphotericin B). The flasks were incubated at 37°C in a humidified incubator in the presence of 5% CO_2.

A virulent AHSV serotype 4 isolate [AHSV-4 (1)], isolated originally from a diseased horse, was supplied by Mr Flip Wege (Department of Genetics, University of Pretoria) and used for all cell infections. For infections, BHK-21 cell monolayers were rinsed twice with incomplete EMEM medium (lacking FBS and antibiotics) and then infected with AHSV-4 at a multiplicity of infection (MOI) of 1 pfu/cell. Virus infections were performed at 37°C for 1 h, followed by incubation of the cell monolayers in complete EMEM medium.

3.2.2 Microscopic examination of AHSV-4 infected BHK-21 cells

BHK-21 cells were seeded onto coverslips in 6-well tissue culture plates and mock-infected or infected with AHSV-4 at a MOI of 1 pfu/cell. The coverslips were removed at 48 h post-infection and placed on glass slides in the absence of fixatives and sealants. The samples were examined for AHSV-induced cytopathic effect (CPE) with a Zeiss Axiovert 200 inverted microscope at a magnification of 10×. The images were captured with a Nikon DXM 120 digital camera.

For detection of ultrastructural alterations characteristic of apoptosis, confluent BHK-21 cell monolayers were infected in 75-cm^2 tissue culture flasks with AHSV-4 at a MOI of 1 pfu/cell and subsequently prepared for examination by transmission electron microscopy (TEM). Cells from virus-infected and mock-infected cell monolayers were harvested at 12, 24 and 48 h post-infection by centrifugation at 2500 rpm for 10 min. The cells were fixed at room temperature for 1 h in 0.075 M phosphate buffer (pH 7.4) containing 2.5% (v/v) glutaraldehyde, and then post-fixed in 0.5% osmium tetroxide. After fixing, the cells were washed three times with dH_2O and dehydrated through a series of graded ethanol solutions (5 min each in 30%, 50%, 70%, 90% and 100% ethanol). The treatment with 100% ethanol was repeated three times to ensure complete dehydration of the samples. The fixed cells were embedded in Quetol. Ultrathin sections were obtained on an ultramicrotome and collected on copper grids. The samples were stained in a 5% solution of uranyl acetate, rinsed in dH_2O and counterstained in 3% Reynolds' lead citrate. The preparations were examined and photographed in a JEOL JEM 2100F transmission electron microscope.

3.2.3 Chromosomal DNA fragmentation analysis

Chromosomal DNA fragmentation was detected with the Apoptotic DNA-Ladder Kit (Roche Applied Science), according to the manufacturer's instructions. Mock-infected or AHSV-4 infected BHK-21 cells (*ca*. 2.5 × 10^6 cells), in a sample volume of 200 µl of 1 × PBS (137 mM NaCl; 2.7 mM KCl; 4.3 mM $Na_2HPO_4.2H_2O$; 1.4 mM KH_2PO_4; pH 7.4), were incubated with an equal volume of Nucleic Acid Binding/Lysis Buffer (6 M guanidine-HCl; 10 mM urea; 10 mM Tris-HCl; 20% [v/v] Triton X-100; pH 4.4). Following incubation at room temperature for 10 min, 100 µl of isopropanol was added to each sample, mixed thoroughly and pipetted into a DNA-binding column. Following centrifugation at 8000 rpm for 1 min, cellular impurities were removed from the bound DNA by washing the column with Washing Buffer (20 mM NaCl; 2 mM Tris-HCl; pH 7.5) and the DNA was then eluted in 200 µl of prewarmed (70°C) Elution Buffer (10 mM Tris; pH 8.5). As a positive control of chromosomal DNA fragmentation, lyophilized apoptotic U937 cells (supplied in the kit) were suspended in 400 µl of the Nucleic Acid Binding/Lysis Buffer and treated identically. Aliquots of the extracted chromosomal DNA were analyzed by electrophoresis in a 1% (w/v) agarose gel.

3.2.4 Quantification of apoptosis

Apoptosis in BHK-21 cells infected with AHSV-4 was quantified by making use of the Cell Death Detection ELISA^{PLUS} Kit (Roche Applied Science), according to the manufacturer's instructions. This *in vitro* enzyme immunoassay allows for the quantification of histone-associated-DNA-fragments (mono- and oligonucleosomes) that are released into the cytoplasm of cells that have succumbed to apoptosis. BHK-21 cells were seeded in the wells of a 96-well flat-bottom microtitre plate (Cellstar® Greiner Bio-one) and incubated at 37°C in a CO_2 incubator until they reached 100% confluency. The cells were infected with AHSV-4 at a MOI of 1 pfu/cell, while uninfected BHK-21 cells were included as a control in these assays. The cells were harvested at different times post-infection by centrifugation at 1000 rpm for 10 min with a Sigma-Aldrich 4K15C plate centrifuge fitted with a 09100F swing-out rotor. The cell pellets were each suspended in 200 µl of the supplied Lysis Buffer and incubated at room temperature for 30 min to lyse the cells. The cell lysates were centrifuged at 1000 rpm for 10 min and 20 µl of the supernatants were transferred into a streptavidin-coated 96-well microtitre plate. To each well, 80 µl of immunoreagent was added, which comprised of 4 µl of biotinylated anti-histone antibodies, 4 µl of peroxidase-labeled anti-

DNA antibodies and 72 µl of Incubation Buffer (1% [w/v] BSA; 0.5% [v/v] Tween-20; 1 mM EDTA in PBS). The microtitre plate was incubated at room temperature for 2 h on a shaker and unbound antibodies were subsequently removed by three washes each with 250 µl of Incubation Buffer. The peroxidase-labeled complexes retained were incubated with 100 µl of the peroxidase substrate ABTS (2,2′-azino-bis[3-ethylbenzothiazoline-6-sulfonic acid]-diammonium salt). Following colour development for 20 min at room temperature, 100 µl of ABTS stop solution was added to each well. The samples were read at 405 nm against Incubation Buffer (containing ABTS and ABTS stop solution) as the blank with a Multiscan Ascent v1.24 ELISA plate reader. To calculate the specific enrichment factor of nucleosomes released into the cytoplasm of AHSV-infected BHK-21 cells, the absorbance measurements of the samples were averaged and the background value was subtracted from each of these averages. The enrichment factor was then calculated with the following formula: Enrichment factor = mU of the sample (AHSV-infected BHK-21 cells)/mU of the negative control (uninfected BHK-21 cells), where mU = absorbance (10^{-3}). Two independent photometric enzyme immunoassays were performed.

3.2.5 Ultra-violet (UV) light inactivation of AHSV-4

To inactivate AHSV-4, 2 ml of the virus stock was pipetted into sterile Petri dishes, placed on the surface of a UV transilluminator (UVP, model M-15) and exposed to UV light (312 nm) for periods of 1 to 30 min. The effectiveness of the treatment at inactivating the virus was determined by plaque assays, as described previously (Chapter 2, Section 2.2.10.3). To determine whether virus replication may induce apoptosis, confluent BHK-21 cell monolayers were infected with UV-inactivated AHSV-4 at a MOI of 2 and 4 pfu/cell. At 24 h post-infection, the cells were harvested and processed for the detection of chromosomal DNA fragmentation. As a control, mock-infected BHK-21 cells were included in the assays.

3.2.6 Transfection of BHK-21 cells

The construction of recombinant pCMV-Script® mammalian expression vectors, harbouring full-length VP2 and VP5 genes from attenuated and virulent AHSV-4 isolates, has been described previously (Chapter 2). The recombinant plasmid DNA was either transfected or co-transfected into BHK-21 cells using Lipofectamine™ 2000 Reagent (Invitrogen), according to the manufacturer's instructions. BHK-21 cells were seeded in 6-well tissue culture plates to reach 90% confluency within 6 h of incubation at 37°C in a CO_2 incubator.

The cell monolayers were then prepared for transfection by rinsing the cells twice with incomplete EMEM medium, followed by addition of 1.5 ml of the same medium. For each transfection, 2.5 µg of purified recombinant plasmid DNA and 7.5 µl of Lipofectamine™ 2000 Reagent were each diluted in 625 µl of incomplete EMEM medium and incubated at room temperature for 5 min. The two solutions were mixed, incubated at room temperature for 20 min and then used to overlay the BHK-21 cells. Co-transfection of the BHK-21 cells was performed similarly, except that 1.25 µg of each recombinant plasmid DNA was used, mixed and then diluted with incomplete EMEM medium. The tissue culture plates were incubated at 37°C for 6 h in a CO_2 incubator, after which the transfection mixtures were replaced with complete EMEM medium. At various times post-transfection, the cells were harvested and analyzed for chromosomal DNA fragmentation.

3.2.7 Treatment of BHK-21 cells with recombinant AHSV-4 VP2 and VP5 proteins

The expression and quantification of soluble recombinant baculovirus-expressed VP2 and VP5 proteins have been described previously (Chapter 2). For treatment of BHK-21 cells with the soluble proteins, confluent BHK-21 cell monolayers in 6-well tissue culture plates were rinsed twice with incomplete EMEM medium, and then 10 µg of VP2 and/or 5 µg of VP5 were added to the cells. Protein adsorptions were carried out for 1 h at 4°C, after which the protein preparations were aspirated and replaced with 2 ml of complete EMEM medium. The tissue culture plates were incubated at 37°C for 48 h in a CO_2 incubator. Parallel experiments were performed in which the BHK-21 cells were treated with the VP2 and VP5 proteins of either the attenuated or virulent AHSV-4 isolates. BHK-21 cell monolayers treated identically with a soluble protein extract prepared from wild-type baculovirus-infected *Sf*9 cells were included in these assays. Following incubation, the cells were harvested and processed for the detection of chromosomal DNA fragmentation.

3.2.8 Endosomal acidification inhibition assays

Ammonium chloride (AC) and chloroquine (CQ), both obtained from Sigma-Aldrich, were dissolved in 1 × PBS (pH 7.4) at a stock concentration of 1 mM and syringe-filtered through a 0.2-µm pore size filter (Pall Acrodisc®). An experiment was initially performed to determine whether the inhibitors are toxic to BHK-21 cells. For this purpose, cells were exposed to concentrations of AC ranging from 10 µM to 10 mM, and from 10 µM to 200 µM for CQ. The treated cells were subsequently analyzed for DNA fragmentation, the results of

which indicated that these inhibitors did not induce apoptosis in the BHK-21 cells. Consequently, confluent BHK-21 cell monolayers in 6-well tissue culture plates were rinsed twice with incomplete EMEM medium and then exposed to 10 mM AC or 100 µM CQ in incomplete EMEM medium for 2 h prior to AHSV-4 infection, simultaneously with AHSV-4 infection or 1 h following AHSV-4 infection. The inhibitor solutions were aspirated from the cells and replaced with complete EMEM medium containing the appropriate concentration of the respective inhibitor. Following incubation at 37°C for 24 h in a CO_2 incubator, the cells were harvested and processed for the detection of chromosomal DNA fragmentation.

3.3 RESULTS

3.3.1 Microscopic examination of AHSV-infected BHK-21 cells

To characterize the induction of apoptosis by AHSV-4 in BHK-21 cells, the virus-infected cells were analyzed over a time course of 48 h. Light microscopy of the AHSV-infected cells at 48 h post-infection indicated that the virus-infected cells showed signs of severe CPE. In contrast to mock-infected BHK-21 cells, virus infection resulted in cell rounding, shrinkage and surface detachment (Fig. 3.1). To detect ultrastructural alterations associated with apoptosis, the AHSV-infected cells were examined by transmission electron microscopy (TEM). The virus-infected cells showed a continuum of nuclear chromatin alterations, including the formation of dense granular caps underlying the morphologically intact nuclear membrane (Fig. 3.2c, d and e). In addition, plasma membrane blebbing and contortion (Fig. 3.2d and g), cytoplasm vacuolization and compaction (Fig. 3.2d and f), and cellular fragmentation into clusters of apoptotic bodies (Fig. 3.2d, h and i) were also observed in the AHSV-infected BHK-21 cells. In contrast, mock-infected BHK-21 cells did not show any morphological cell alterations (Fig. 3.2a and b).

(a)

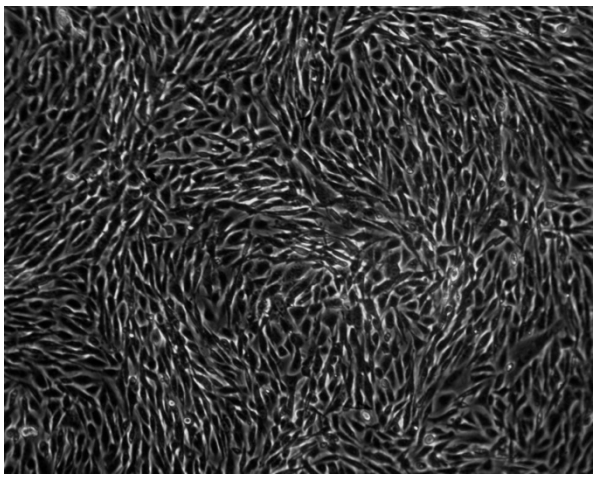

(b)

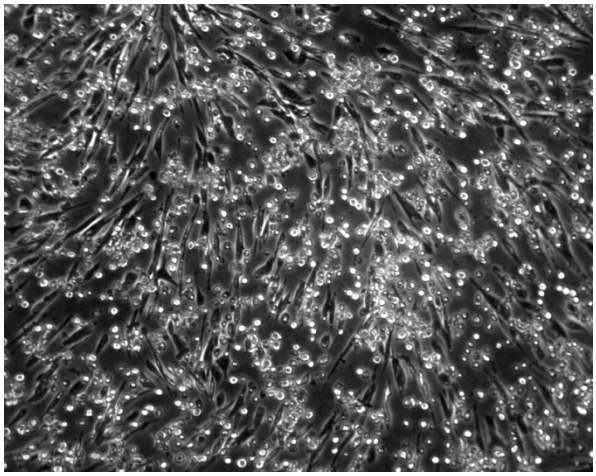

Fig. 3.1: Light microscopy micrographs of BHK-21 cells infected with AHSV-4. Representative micrographs of mock-infected (a) and AHSV-infected (b) BHK-21 cells are shown. The AHSV-infected cells show clear signs of rounding, shrinkage and detachment. Images were captured at a 10× magnification.

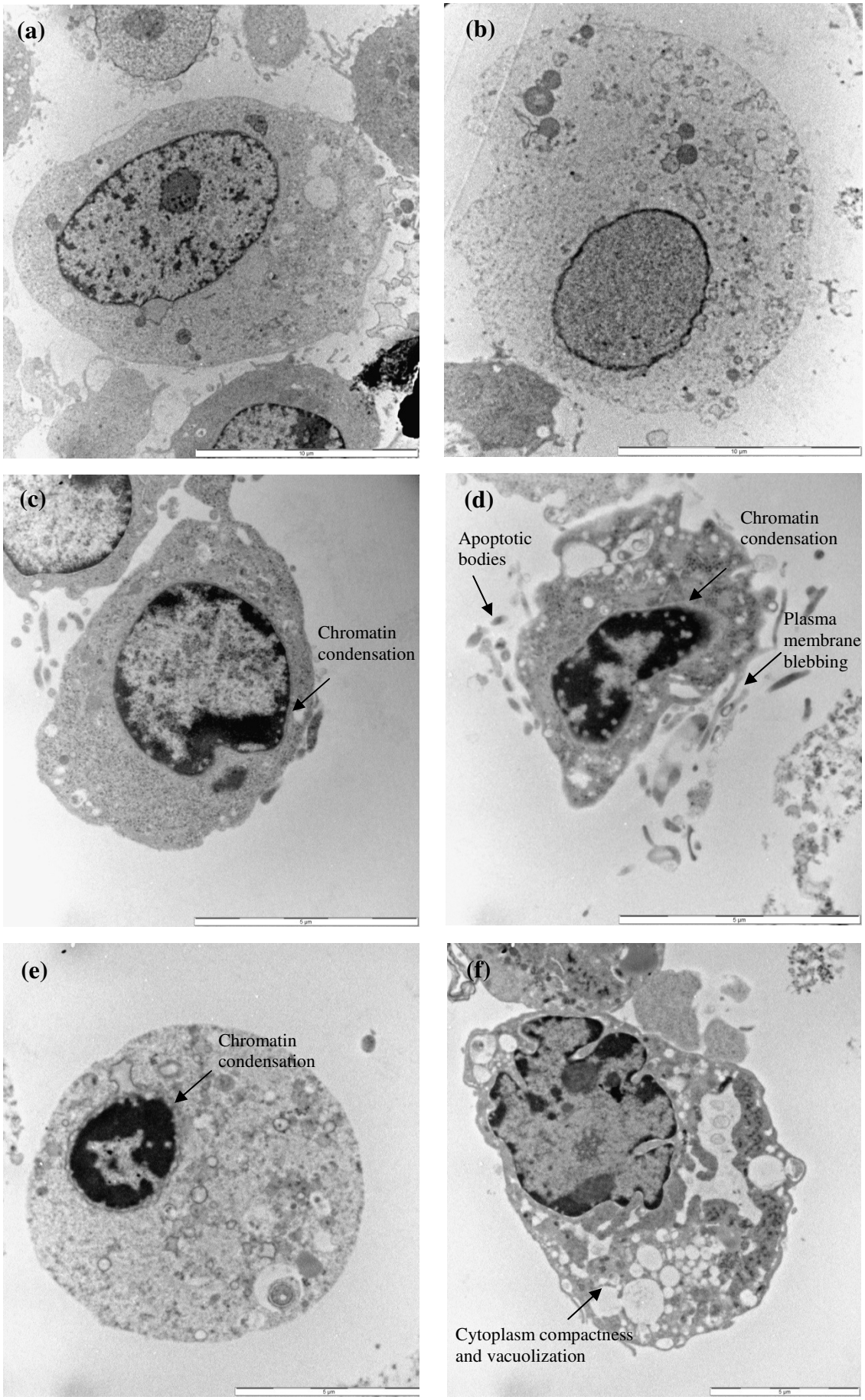

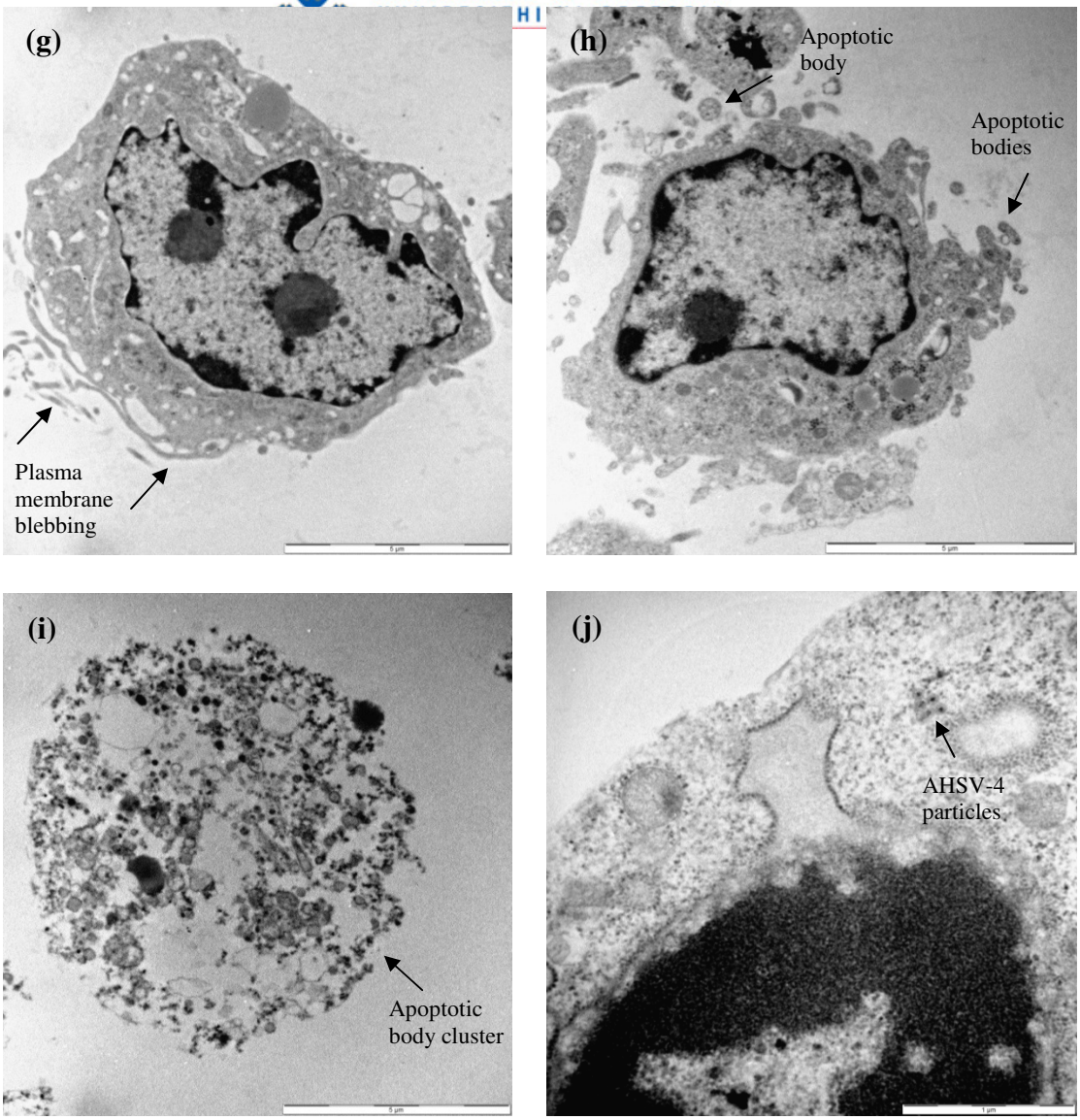

Fig. 3.2: Transmission electron micrographs of BHK-21 cells infected with AHSV-4. In contrast to mock-infected cells (a and b), AHSV-infected cells showed morphological hallmarks of apoptosis, as indicated by the arrows. These included chromatin condensation (c, d and e), cytoplasm compactness and vacuolization (d and f), plasma membrane blebbing (d and g) and the formation of apoptotic bodies (d, h and i). AHSV particles were observed within infected cells (j), as indicated by the arrow.

3.3.2 DNA fragmentation analysis of AHSV-infected BHK-21 cells

In cells undergoing apoptosis, morphological changes such as chromatin condensation are associated with the incidence of nucleosome excisions from chromatin through the activation of intracellular endonucleases (Wyllie, 1980). Since the 180-200 base pairs of DNA wrapped around a histone core are protected conformationally from digestion, the endonuclease-mediated nucleosome excision results in the appearance of a ladder of nucleosomal DNA fragments in agarose gels. This DNA ladder has long been considered the biochemical hallmark of apoptosis (Hewish and Burgoyne, 1973; Kornberg, 1974; Wyllie *et al*., 1980). Thus, to confirm that the morphological alterations observed in AHSV-infected BHK-21 cells were due to apoptosis, the infected cells were analyzed by a DNA fragmentation assay. To investigate, chromosomal DNA was extracted from BHK-21 cells infected with AHSV-4 over a time course of 72 h and analyzed by agarose gel electrophoresis.

In contrast to mock-infected BHK-21 cells, which showed no evidence of DNA fragmentation, a fragmented chromosomal DNA ladder typical of apoptosis was detected in AHSV-infected cells from 12 to 72 h post-infection. The oligonucleosomal DNA ladder resembled that observed in apoptotic U937 cells, which served as a positive control in the assay (Fig. 3.3). These results therefore provided supporting biochemical evidence that the morphological changes observed in AHSV-infected BHK-21 cells were due to the induction of apoptosis in the mammalian cells.

To determine more accurately when apoptosis is induced in the AHSV-infected BHK-21 cells, the nucleosomes present in the cytoplasm of virus-infected cells were quantified over a time course of 48 h with a photometric enzyme immunoassay. This assay is based on a sandwich-enzyme immunoassay principle using monoclonal antibodies directed against histones and DNA, respectively, and allows for the specific detection and quantification of mono- and oligonucleosomes that are released into the cytoplasm of cells that have succumbed to apoptosis.

The results, presented in Fig. 3.4, indicated that there was a limited release of nucleosomes into the cytosol of AHSV-infected BHK-21 cells during the first 6 h of infection. This is reflected by a single-fold increase in the nucleosome enrichment factor from 0 to 6 h post-infection. However, there was a significant increase in the release of nucleosomes between 6

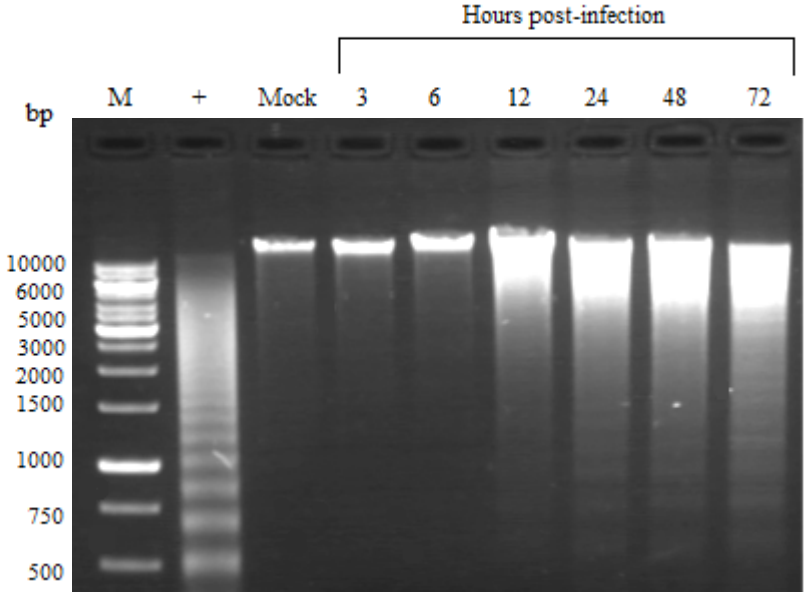

Fig. 3.3: DNA fragmentation analysis of BHK-21 cells infected with AHSV-4. Agarose gel electrophoretic pattern of chromosomal DNA extracted from mock-infected (Mock) and AHSV-infected BHK-21 cells at different times post-infection. Apoptotic U937 cells served as a positive control (+). The sizes of the DNA molecular weight marker, O'GeneRuler™ 1kb DNA Ladder (Fermentas), are indicated to the left of the figure.

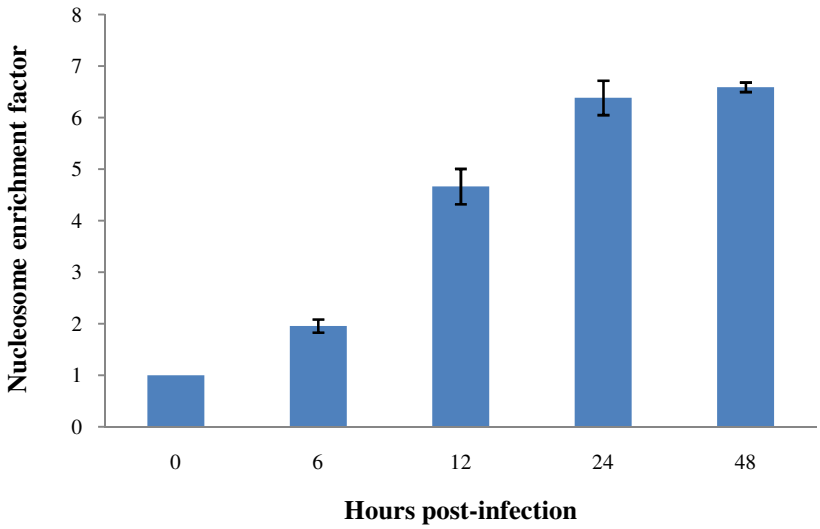

Fig. 3.4: Enrichment of nucleosomes in the cytoplasm of BHK-21 cells infected with AHSV-4. Cytoplasmic extracts were prepared from AHSV-infected BHK-21 cells at different times post-infection and pipetted into a streptavidin-coated microtitre plate. The samples were incubated with a mixture of anti-histone-biotin and anti-DNA-peroxidase antibodies. The biotinylated anti-histone antibody binds to the histone component of the nucleosomes and the streptavidin-coated microtitre plate, whereas the peroxidase-labeled DNA-specific antibody binds to the DNA component of the nucleosomes. After removal of the unbound antibodies, the nucleosomes were detected by measuring peroxidase activity with ABTS as substrate. The nucleosome enrichment factor was subsequently calculated, as described under Materials and Methods. The data are means ± SD of two independent experiments.

and 12 h post-infection, as evidenced by a 2.7-fold increase in the nucleosome enrichment factor over this time period. Between 12 and 24 h post-infection there was a second increase (1.7-fold) in the release of nucleosomes. No further increase in the nucleosome enrichment factor was observed between 24 to 48 h post-infection, possibly as a consequence of complete chromosomal DNA fragmentation in the infected cells (Fig. 3.4). These results therefore indicate that apoptosis is induced at 12 h post-infection and maximal levels of apoptosis are reached at 24 h post-infection. Cumulatively, all of the above data provide evidence that infection of BHK-21 cells with AHSV-4 results in apoptosis at 12 h post-infection.

3.3.3 Induction of apoptosis by AHSV-4 in BHK-21 cells does not require virus replication

To determine whether virus replication is necessary for AHSV-induced apoptosis in BHK-21 cells, the effect of UV treatment on the capacity of the virus to induce apoptosis was investigated. Complete inactivation of AHSV-4 by UV treatment for 30 min was confirmed by a plaque assay prior to its use in further experiments (Fig. 3.5a). Since it was unclear what effect, if any, the UV treatment would have on the outer capsid proteins of the virus particles, at least double as many input virus particles were used as compared to replicating virus. Consequently, BHK-21 cells were infected with UV-inactivated AHSV-4 at a MOI of 2 and 4 pfu/cell. At 48 h post-infection the chromosomal DNA was extracted and analyzed for DNA fragmentation by electrophoresis in an agarose gel. The results indicated that UV treatment had no effect on the ability of virus infection to induce DNA fragmentation (Fig. 3.5b). This data therefore suggests that the full virus replication cycle is not required for the induction of apoptosis by AHSV-4 in BHK-21 cells.

3.3.4 The outer capsid proteins of AHSV-4 are required for the induction of apoptosis in BHK-21 cells

Based on the above data and considering that virus capsid proteins have been reported to trigger apoptosis (Tyler *et al*., 1995; Mortola *et al*., 2004; Shih *et al.*, 2004), the ability of the outer capsid proteins VP2 and VP5 of AHSV-4 to trigger apoptosis was subsequently investigated. In these investigations, the role of each outer capsid protein and their possible synergistic effect in apoptosis was examined when expressed intracellularly and when added extracellularly. For comparative purposes, the outer capsid proteins of attenuated and virulent AHSV-4 isolates were included in the analyses.

(a)

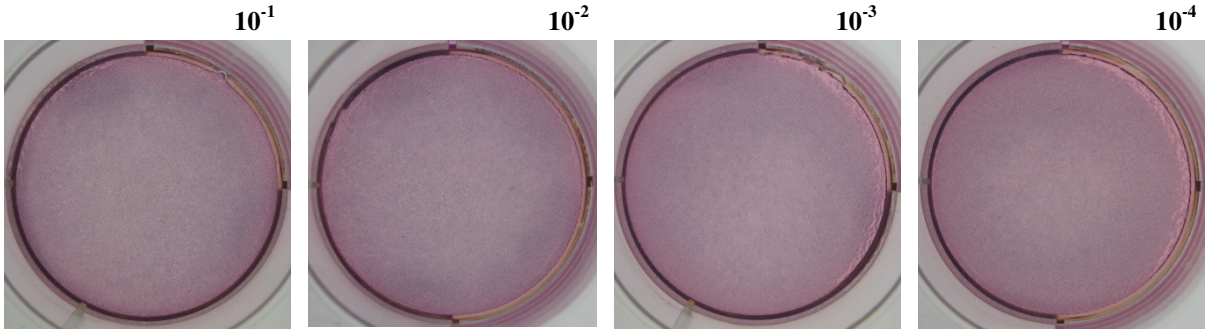

(b)

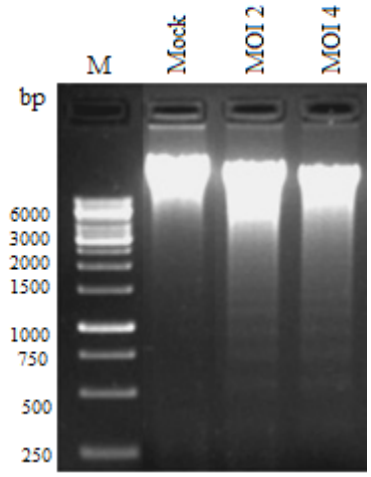

Fig. 3.5: Effect of UV treatment on the induction of apoptosis by AHSV-4 in BHK-21 cells. Inactivation of AHSV-4 by UV treatment for 30 min was confirmed by plaque assay (a). BHK-21 cells were either mock-infected or infected with UV-inactivated AHSV-4 at different MOIs, and fragmentation of the chromosomal DNA was analyzed at 48 h post-infection (b). The sizes of the DNA molecular weight marker, O'GeneRuler™ 1kb DNA Ladder (Fermentas), are indicated to the left of the figure.

To investigate the role of the respective VP2 and VP5 proteins when expressed intracellularly, BHK-21 cells were transfected with recombinant pCMV-Script® mammalian expression plasmids encoding each of the full-length individual proteins. At 12 and 36 h post-transfection, chromosomal DNA was extracted from the transfected cells and analyzed for DNA fragmentation in agarose gels. Under these conditions, no fragmented chromosomal DNA was detected in the cells when the recombinant plasmids were transfected individually. To examine the possible synergistic effect, plasmids expressing the two outer capsid proteins were also co-transfected. However, as with the individual proteins, no sign of apoptosis could be detected (Fig. 3.6).

Based on the premise that the binding of cell receptors might trigger apoptosis, an alternative experimental approach was adopted. In these investigations, uninfected BHK-21 cells were treated extracellularly with soluble recombinant VP2 and VP5 proteins. These recombinant proteins were expressed by using the baculovirus expression system and the concentration of soluble VP2 and VP5 was quantified from SDS-polyacrylamide gels with an appropriate software programme. Since it was not possible to purify the recombinant proteins to homogeneity, cytoplasmic (soluble) protein extracts were used in the experiments. Consequently, an identically prepared cytoplasmic protein extract from wild-type baculovirus-infected *Sf*9 cells was included in the analyses to determine whether host and/or baculovirus proteins are capable of inducing apoptosis when added to BHK-21 cells. Moreover, since VP5 has been reported to be toxic for cells in high concentrations (du Plessis and Nel, 1997; Martínez-Torrecuadrada *et al*., 1994; Stassen *et al*., 2011), and considering the lesser abundance of VP5 relative to VP2 in intact virions, a lower concentration of soluble VP5 was used in the assays.

To investigate, uninfected BHK-21 cells were treated with 10 µg of soluble VP2 and/or 5 µg of soluble VP5, and the chromosomal DNA was extracted at 48 h post-treatment. Analysis of the chromosomal DNA in an agarose gel indicated no signs of DNA fragmentation when the cells were treated with either of the VP2 and VP5 proteins independently. In contrast, when the VP2 and VP5 proteins were added together to the cells, fragmentation of chromosomal DNA was observed (Fig. 3.7). Notably, BHK-21 cells treated with a cytoplasmic protein extract derived from wild-type baculovirus-infected cells did not induce apoptosis in the BHK-21 cells, thus demonstrating that the observed apoptosis can be ascribed solely to the presence of the recombinant VP2 and VP5 proteins.

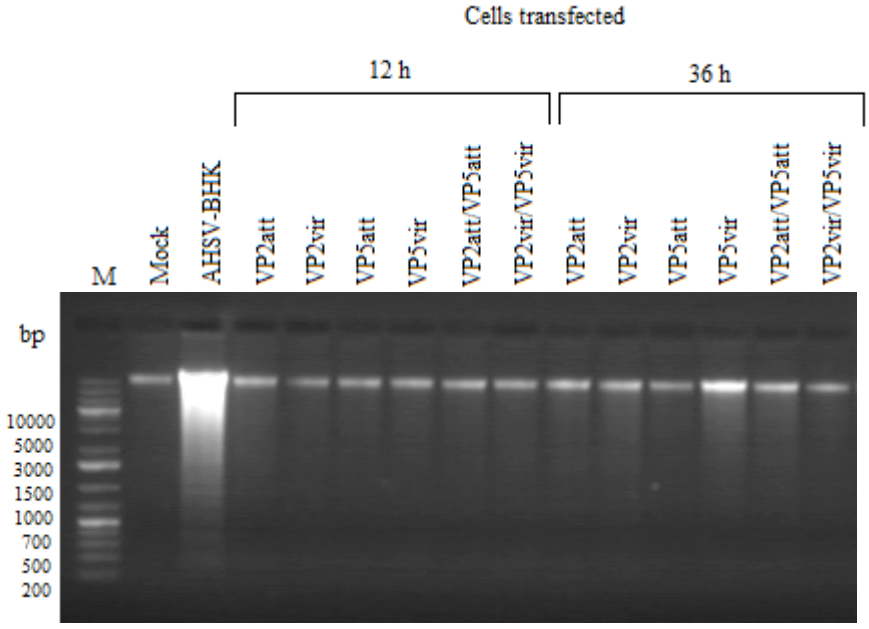

Fig. 3.6: DNA fragmentation analysis of BHK-21 cells transfected with recombinant pCMV-Script® mammalian expression vectors. Agarose gel electrophoretic pattern of chromosomal DNA extracted from BHK-21 cells transfected or co-transfected with the indicated recombinant expression vectors at different times post-transfection (12 and 36 h). Mock-transfected BHK-21 cells and cells infected with AHSV-4 (36 h post-infection) were included as negative and positive controls of apoptosis, respectively. The sizes of the DNA molecular weight marker, O'GeneRuler™ 1kb DNA Ladder Plus (Fermentas), are indicated to the left of the figure.

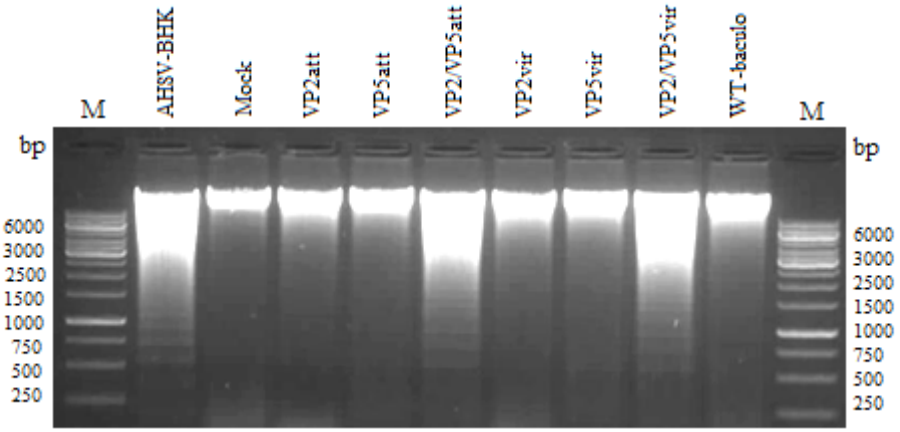

Fig. 3.7: Identification of the AHSV-4 proteins required for the induction of apoptosis in BHK-21 cells. BHK-21 cells were treated with VP2 and/or VP5 derived from attenuated (att) and virulent (vir) AHSV-4 isolates. At 48 h post-treatment, chromosomal DNA was extracted and analyzed in a 1% (w/v) agarose gel. A fragmented ladder of chromosomal DNA typical of apoptosis was found only in cells treated with a combination of the VP2 and VP5 proteins. No DNA fragmentation was induced when the BHK-21 cells were treated with a soluble fraction prepared from wild-type baculovirus-infected cells (WT-baculo). Mock-treated BHK-21 cells and cells infected with AHSV-4 were included as negative and positive controls of apoptosis, respectively. The sizes of the DNA molecular weight markers, O'GeneRuler™ 1kb DNA Ladder (Fermentas), are indicated to the left and right of the figure.

Taken together, the above data therefore indicates that the outer capsid proteins VP2 and VP5 of AHSV-4 are sufficient for the induction of apoptosis in BHK-21 cells. Moreover, the results suggest that early events relating to virus entry into host cells rather than subsequent intracellular expression of viral proteins is required for the induction of apoptosis. Finally, no differences in the results were obtained, irrespective of using the outer capsid proteins of an attenuated or a virulent AHSV-4 isolate in the above assays.

3.3.5 Induction of apoptosis by AHSV-4 in BHK-21 cells requires virion disassembly

For BTV, it has been reported that the virus enters the cell through receptor-mediated endocytosis and is incorporated into early endosomes (Forzan *et al*., 2007). The low pH environment within these endosomes is thought to result in the removal of the VP2 protein and to trigger conformational changes in VP5 that allow the protein to permeabilize the endosomal membrane, thereby releasing the transcriptionally active core into the cell cytoplasm (Hassan *et al*., 2001; Zhang *et al*., 2010). Thus, to determine whether acid-dependent viral uncoating is required for AHSV-4 to trigger apoptosis, the effect of two inhibitors of endosomal acidification, *i.e.* ammonium chloride (AC) and chloroquine (CQ), on the induction of apoptosis in BHK-21 cells was investigated. Preliminary experiments indicated that these inhibitors were not toxic to BHK-21 cells and did not induce an apoptotic response in the cells (Fig. 3.8). BHK-21 cell monolayers were subsequently exposed to 10 mM of AC or 100 µM of CQ at different times, as described in Materials and Methods (Section 3.2.8), and then infected with AHSV-4. Following incubation for 24 h, the chromosomal DNA was extracted and analyzed for DNA fragmentation by electrophoresis in an agarose gel.

The results indicated that each of the inhibitors protected the BHK-21 cells from apoptosis induced by AHSV-4 only when applied as a pre-infection treatment (Fig. 3.9). In contrast, fragmentation of chromosomal DNA was detectable in cells that were treated with the respective inhibitors either during or after virus infection. These results therefore demonstrate that virus uncoating is required for AHSV-4 to trigger apoptosis in BHK-21 cells.

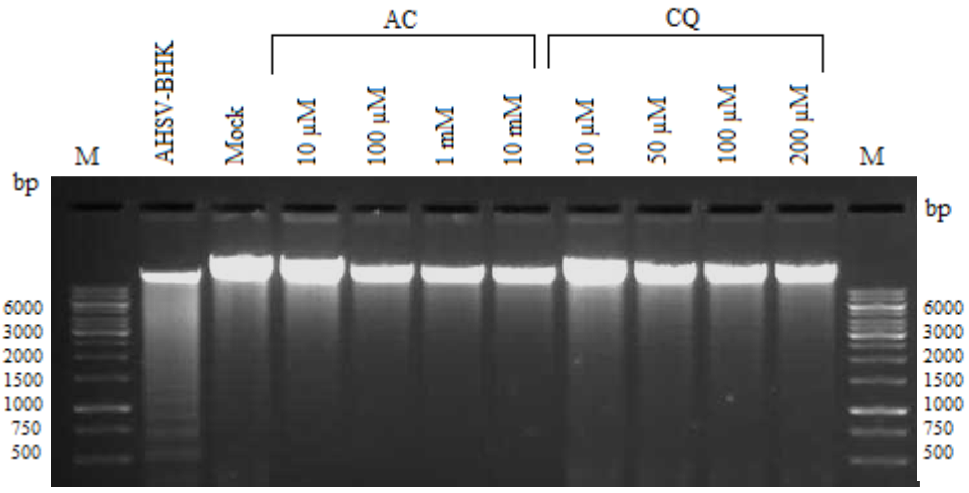

Fig. 3.8: Treatment of BHK-21 cells with the endosomal acidification inhibitors ammonium chloride (AC) and chloroquine (CQ). BHK-21 cell monolayers were treated with different concentrations of the respective endosomal acidification inhibitors and harvested at 24 h post-treatment. The chromosomal DNA was extracted and analyzed in a 1% (w/v) agarose gel for signs of DNA fragmentation. No chromosomal DNA fragmentation was observed at any of the inhibitor concentrations tested. Mock-infected BHK-21 cells and cells infected with AHSV-4 were included as controls of apoptosis in the assay. The sizes of the DNA molecular weight markers, O'GeneRuler™ 1kb DNA Ladder (Fermentas), are indicated to the left and right of the figure.

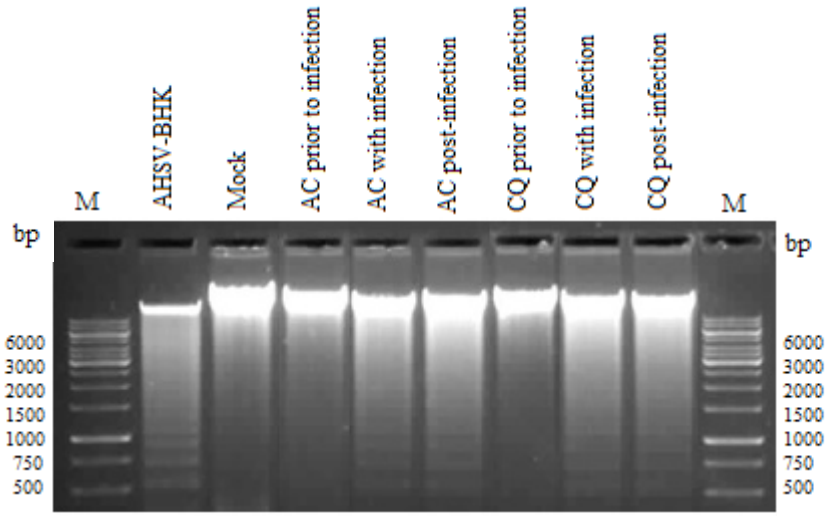

Fig. 3.9: The effect of inhibition of endosomal acidification on DNA fragmentation in BHK-21 cells infected with AHSV-4. BHK-21 cell monolayers were treated with the respective endosomal acidification inhibitors at the specified times and harvested at 24 h post-infection. The chromosomal DNA was extracted and analyzed in a 1% (w/v) agarose gel. DNA fragmentation, typical of apoptosis, was observed in cells treated with the inhibitors simultaneously with and following AHSV-4 infection. In contrast, no DNA fragmentation was visible in cells treated with the inhibitors prior to AHSV-4 infection. Mock-infected and AHSV-4 infected BHK-21 cells were included as negative and positive controls of apoptosis, respectively. The sizes of the DNA molecular weight markers, O'GeneRuler™ 1kb DNA Ladder (Fermentas), are indicated to the left and right of the figure.

3.4 DISCUSSION

African horse sickness virus (AHSV) is vectored by haematophagous *Culicoides* spp. to equids and causes severe oedema and haemorrhages in horses, but is asymptomatic in the vector insect (Wilson *et al*., 2009). This is also reflected in tissue culture where AHSV causes rapid cell death in infected mammalian cells in culture, whereas infection of insect cells is unapparent with no CPE (Osawa and Hazrati, 1965; Mirchamsy *et al.*, 1970). The basis for this differential host response is not known, but may be due to the induction of apoptosis in infected mammalian cells. Consequently, in this part of the investigation, a series of experiments were undertaken to examine the induction of apoptosis during AHSV-4 infection of mammalian cells and to identify possible initiators of AHSV-induced apoptosis.

Examination of AHSV-infected BHK-21 cells by light and transmission electron microscopy showed the presence of morphological hallmarks associated with the induction of apoptosis, which included cell shrinkage and detachment, nuclear chromatin condensation, blebbing of the plasma membrane and the formation of apoptotic bodies. These morphological alterations are a consequence of biochemical changes that occur during apoptosis (Wyllie *et al*., 1981; Kerr *et al*., 1984; Schwartzman and Cidlowski, 1993). Nuclear changes, *e.g.* chromatin condensation and apoptotic body formation, are the result of both DNA cleavage and proteolysis of key nuclear polypeptides (Earnshaw *et al*., 1999; Fischer *et al*., 2003). The loss of overall cell shape and integrity has been attributed to caspase cleavage of the cytoskeletal gelsolin and fodrin proteins, while detachment of cells from the surface has been attributed to caspase cleavage of the adherence junction proteins β-catenin and plakoglobin/γ-catenin (Brancolini *et al*., 1997; Kothakota *et al*., 1997; Herren *et al*., 1998). Moreover, caspase cleavage and subsequent activation of the proapoptotic kinase ROCK I results in blebbing of the plasma membrane (Coleman *et al*., 2001), whereas caspase-dependent cleavage of nuclear proteins, *e.g.* lamin-A and lamin-B, are associated with nuclear shrinkage and chromatin condensation (Rao *et al*., 1996; Buendia *et al*., 1999). It therefore follows that the morphological and ultrastructural changes observed during AHSV-4 infection of BHK-21 cells may have been due to the activity of activated cellular caspases, which play a key role in apoptosis (Li and Yuan, 2008).

During apoptosis, the excision of nucleosome chains is routinely used as a biochemical marker of apoptosis (Wyllie, 1980; Earnshaw, 1995). DNA fragmentation typically occurs in

two stages with initial cleavage of the genome into fragments ranging between 300 and 30 kb in size, followed by further cleavage of these DNA fragments to produce an oligonucleosomal ladder (Wyllie, 1980; Walker *et al*., 1991). The initial DNA cleavage is due to the action of Topoisomerase II and correlates with the collapse of the chromatin against the nuclear periphery (Walker *et al*., 1994), whereas internucleosomal DNA cleavage by DNase I/DNase II produces fragments in multiples of *ca*. 180-200 bp (Wyllie *et al*., 1980; Peitsch *et al*., 1993). More recently, caspase-activated deoxyribonuclease (CAD)/DNA fragmentation factor 40 (DFF40), a 40-kDa nuclear enzyme that is activated by caspase-3, was shown to also promote apoptotic DNA degradation (Cao *et al*., 2001). Consequently, BHK-21 cells infected with AHSV-4 were examined for chromosomal DNA fragmentation. In virus-infected cells the onset and timing of DNA fragmentation, as evidenced by the enrichment of mono- and oligonucleosomes in the cytoplasm of AHSV-infected cells, was observed at 12 h post-infection and reached a maximum at 24 h post-infection (Fig. 3.4). No further increase in DNA fragmentation was observed, indicating that at 24 h post-infection the chromosomal DNA had been fragmented in the majority of the infected cells. These results differ from those reported for BTV in which DNA fragmentation is observed at 36 h post-infection in BHK-21 cells (Mortola *et al*., 2004) and in Vero cells (Nagaleekar *et al*., 2007). Interestingly, it has also been observed previously that cells infected with AHSV display a much stronger CPE at early times after infection than cells infected with BTV, suggesting that these two orbiviruses may differ in virulence (Wirblich *et al*., 2006). It is tempting to speculate that the apparent difference in virulence may reflect on AHSV having to replicate as rapidly as possible (and by implication more rapidly than BTV) in order to avoid the cellular machinery being shut down by apoptosis. This may have the added benefit of rapid dissemination of progeny virions to neighbouring cells, following apoptosis-induced cell death and lysis. Alternatively, it may also be that the difference in virulence is due to differences in the cytotoxicity of different membrane permeabilizing viral proteins, such as NS3 and VP5 (Huismans *et al*., 2004).

Previous studies have reported that in mammalian cells the AHSV virions remain predominantly associated with cellular components and fewer virus particles are found in the extracellular medium (<30%), presumably as a result of release from death of infected cells (Meiring *et al*., 2009; Barnes, 2011). Therefore, it may be reasonable to propose that the intracellular accumulation of viral proteins and nascent viral particles could be responsible for triggering apoptosis in mammalian cells, resulting in cell death and subsequent virus

release. To investigate if this is the case, AHSV-4 was inactivated by UV treatment and then used to treat BHK-21 cells. The results indicated that apoptosis was triggered in response to treatment of the cells with UV-inactivated virus. Thus, it could be concluded that a productive viral replication cycle was not required to trigger apoptosis. However, in these experiments, at least twice as many UV-inactivated AHSV-4 as infectious AHSV-4 was required to elicit an apoptotic response. A plausible explanation for this difference may be that, in contrast to the inactivated virus, replication of AHSV-4 and subsequent release of progeny virus particles from infected cells may trigger multiple rounds of infection, thereby amplifying the proapoptotic signals.

The above results imply that an event(s) prior to viral protein synthesis and genome replication may trigger the induction of apoptosis in AHSV-infected mammalian cells. Consistent with the fact that expression of viral proteins is not required to trigger apoptosis, the intracellular expression of VP2 and/or VP5 had no proapoptotic effect. However, since intracellular protein expression from the recombinant pCMV-Script® constructs could not be verified by immunoblot analysis (Chapter 2), it might be that the expression levels were too low to allow for the induction of apoptotic pathways. Nevertheless, note should be taken that intracellular expression of the outer capsid proteins VP2 and VP5 in this way is a poor mimic for the events involved in viral entry, since during virus entry it is the extracellular side of the plasma membrane that is first exposed to these proteins. Thus, to test whether treatment of BHK-21 cells with VP2 and/or VP5 proteins was sufficient to trigger apoptosis, the cells were treated with soluble proteins expressed in the baculovirus system. Notably, neither VP2 nor VP5 alone was able to trigger apoptosis, but when a combination of these proteins was applied exogenously to the cells, an apoptotic response was observed. Similar results were observed, irrespective of whether the outer capsid proteins were obtained from an attenuated or virulent AHSV-4 isolate. It is therefore likely that the amino acid differences observed in the VP2 protein of the attenuated AHSV-4 isolate (Chapter 2, Table 2.2) had no influence on the biological activity or function of the protein.

Reports regarding apoptosis in BTV (Mortola *et al*., 2004), mammalian reovirus (Connolly and Dermody, 2002) and avian reovirus (Labrada *et al*., 2002) infections have indicated that receptor binding alone is not sufficient to elicit an apoptotic response and that downstream events dependent on acidification of the endosome, such as viral disassembly, are also necessary. Similarly, results obtained in this part of the investigation indicated that

ammonium chloride (AC) and chloroquine (CQ), two weakly basic lysosomotropic agents that neutralize vacuolar acidification (Seglen, 1983), inhibited apoptosis induced by AHSV infection. Although not yet reported for AHSV, it is generally accepted that the AHSV VP2 protein functions in a manner analogous to that of BTV, which has been shown to be involved in virus attachment (Hassan and Roy, 1999). During the course of this investigation, however, evidence was obtained for the involvement of AHSV-4 VP2 in cell binding and internalization by making use of an immunofluorescence technique combined with appropriate monospecific polyclonal antibodies (See Supplementary Material A1). Moreover, it was recently reported that the N-terminus of AHSV VP5 contains amphipathic α-helices that are capable of membrane permeabilization and thus may play a role in the release of the viral core from the endosomal vesicle (Stassen *et al*., 2011). It is therefore tempting to suggest that a complex of VP2 and VP5 is internalized in cells treated extracellularly with the respective outer capsid proteins and that it is this combination of receptor-binding activity of VP2 and the membrane permeabilizing activity of VP5 that is responsible for triggering apoptosis. In agreement with this hypothesis, apoptosis in response to infection of BHK-21 cells with AHSV-4 was inhibited by prior treatment of the cells with either AC or CQ (Fig. 3.9). Thus, activation of VP5 by acidification of endosomal vesicles is critical to the induction of apoptosis. In this regard, it is interesting to note that excessive leakage of endosomal enzymes into the cell cytoplasm and cytosol acidification have been reported to potentiate apoptotic signalling through procaspase activation, the release of proapoptotic factors from the mitochondria or through cytochrome *c*-mediated activation of caspases (Brunk *et al*., 1997; Li *et al*., 2000; Matsuyama *et al*., 2000; Turk *et al*., 2000).

In conclusion, the results obtained in this part of the investigation provided evidence for the induction of apoptosis following AHSV infection of mammalian cells and that the AHSV outer capsid proteins are specifically involved in this induction. It is most likely that apoptosis is induced during the very early stages of the virus infectious cycle through the combined receptor-binding and membrane permeabilization activities of the VP2 and VP5 proteins, respectively. Despite this progress, several aspects of AHSV-induced apoptosis remain to be elucidated, such as the cellular pathways involved. The details of these studies are presented in the following Chapter.

CHAPTER FOUR

AFRICAN HORSE SICKNESS VIRUS INDUCES APOPTOSIS IN MAMMALIAN CELLS BY BOTH EXTRINSIC AND INTRINSIC APOPTOTIC PATHWAYS

4.1 INTRODUCTION

Apoptosis is an evolutionary conserved process triggered by a variety of intracellular or extracellular signals to remove unwanted, damaged or infected cells (Kerr *et al*., 1972; Wyllie, 1980). There are two major pathways of apoptotic cell death induction: extrinsic signalling through death receptors and intrinsic signalling mainly through mitochondria (Xu and Shi, 2007; Duprez *et al*., 2009). The extrinsic pathway is triggered by the binding of external (death) ligands to their cognate (death) receptors on cell membranes, as exemplified by members of the tumour necrosis factor (TNF) superfamily (Duprez *et al*., 2009). Receptor-ligand engagement results in the formation of the death-inducing signalling complex (DISC), which allows for the activation of initiator caspase-8 and -10 (Takahashi *et al*., 2006). The intrinsic pathway is initiated by various apoptosis-inducing signals that directly or indirectly alter mitochondrial membrane permeability and cause the release of several proapoptotic proteins, including cytochrome *c* and the second mitochondria-derived activator of caspase (Smac, also known as DIABLO) (Finkel, 2001; Danial and Korsmeyer, 2004). The release of cytochrome *c* from mitochondria into the cytoplasm results in the formation of an apoptosome complex with Apaf-1 and procaspase-9, resulting in activation of the latter (Ahmad *et al*., 1997; Zou *et al*., 1999). The initiator caspases, caspase-8 and -10 in the extrinsic pathway and caspase-9 in the intrinsic pathway, are responsible for activating the effector caspases (caspase-3, -6 and -7), which execute the apoptotic process through the proteolytic cleavage of various intracellular substrates (Timmer and Salvesen, 2007; Li and Yuan, 2008). Cells undergoing apoptosis exhibit characteristic morphological and biochemical features that include cell shrinkage, membrane blebbing, apoptosome formation, chromatin condensation and DNA fragmentation (Kerr *et al*., 1972; Wyllie *et al*., 1981; Martelli *et al*., 2001).

Infection of host cells by most viruses triggers apoptosis, but the exact mechanism whereby this occurs and the specific pathways that are activated in the virus-infected cells remain poorly understood (Roulston *et al*., 1999; Danthi, 2011). For bluetongue virus (BTV), the prototype virus of the genus *Orbivirus* in the family *Reoviridae*, it has been reported that the virus triggers apoptosis in infected mammalian cells through both the extrinsic and intrinsic pathways, and furthermore requires signalling via the JNK signalling pathway and NF-κB is activated in virus-infected cells (Mortola *et al*., 2004; Nagaleekar *et al*., 2007; Stewart and Roy, 2010). The induction of apoptosis by other members of the *Reoviridae* family, such as

rotavirus (Sato *et al*., 2006) and reovirus (Richardson-Burns and Tyler, 2004), have also been investigated. Rotavirus attachment, cell penetration and subsequent gene expression induce apoptosis in mammalian cells through activation of the mitochondrial pathway (Chaïbi *et al*., 2005; Martin-Latil *et al*., 2007). Reovirus attachment and disassembly transiently activates NF-κB (Connolly *et al*., 2001; Danthi *et al*., 2010), as well as genes involved in apoptotic signalling (DeBiasi *et al*., 2003; Coffey *et al*., 2006). Moreover, reovirus infection activates TNFα-induced cell death via the release of TRAIL (TNF-related apoptosis inducing ligand) from infected cells, resulting in DISC formation, the activation of caspase-8 and consequently, activation of the effector caspases-3 and -7 (Clarke *et al*., 2001; Kominsky *et al*., 2002; Richardson-Burns *et al*., 2002). Activated caspase-8 was also reported to cleave Bid in reovirus-infected cells, thereby initiating activation of the mitochondrial apoptotic pathway (Clarke *et al*., 2000; Kominsky *et al*., 2002).

As indicated above, both BTV infection (Mortola *et al*., 2004) and reovirus infection (Connolly *et al*., 2001) results in the activation of NF-κB. Activation of NF-κB results in its translocation into the nucleus from the cytoplasm of infected cells, thereby promoting the expression of a variety of genes that are involved either in regulating the host survival immune responses or in apoptosis (Hayden and Ghosh, 2008). NF-κB exists as a heterodimer, which is sequestered in the cytoplasm of unstimulated cells through non-covalent interactions with a class of inhibitor proteins, called IκBs (Liu and Chen, 2011). These inhibitor proteins mask the nuclear localization signal of NF-κB. Signals that induce NF-κB activity cause the phosphorylation of IκB, their dissociation and subsequent degradation, thus allowing NF-κB proteins to enter the nucleus and induce gene expression.

In the previous Chapter it was shown that in infected mammalian cells AHSV-4 attachment and disassembly, but not replication triggers apoptosis. In addition, it was shown that extracellular treatment with a combination of both the outer capsid proteins, VP2 and VP5, is sufficient to trigger apoptosis. However, in contrast to BTV and other members of the *Reoviridae* family, no investigations into the apoptotic pathways induced in AHSV-infected cells have been undertaken. Consequently, the primary aim of this part of the investigation was to determine which apoptotic pathways are involved in AHSV-induced apoptosis in cultured mammalian cells. Furthermore, the activation of NF-κB during AHSV infection was also determined.

4.2 MATERIALS AND METHODS

4.2.1 Cells and virus

Baby Hamster Kidney-21 (BHK-21; ATCC CL-10) cells were propagated and maintained as monolayers in 75-cm^2 tissue culture flasks. The cells were cultured in Eagle's Minimal Essential Medium (EMEM) with Earle's Balanced Salt Solution (EBSS) and L-glutamine (Lonza, BioWhittaker®), supplemented with 5% (v/v) foetal bovine serum (FBS), 1% (v/v) non-essential amino acids (NEAA) and antibiotics (10 000 U/ml of penicillin, 10 000 µg/ml of streptomycin and 25 µg/ml of amphotericin B). The flasks were incubated at 37°C in a humidified incubator in the presence of 5% CO_2.

A virulent AHSV serotype 4 isolate [AHSV-4 (1)], isolated originally from a diseased horse, was supplied by Mr Flip Wege (Department of Genetics, University of Pretoria) and used for all cell infections. For infections, BHK-21 cell monolayers were rinsed twice with incomplete EMEM medium (lacking FBS and antibiotics) and then infected with AHSV-4 at a multiplicity of infection (MOI) of 1 pfu/cell. Virus infections were performed at 37°C for 1 h, followed by incubation of the cell monolayers in complete EMEM medium.

4.2.2 Caspase inhibition assays

4.2.2.1 Treatment of virus-infected BHK-21 cells with caspase inhibitor

Confluent BHK-21 cell monolayers in 6-well tissue culture plates were rinsed twice with incomplete EMEM medium (lacking FBS and antibiotics) and then incubated with 10 to 100 µM of the pan-caspase inhibitor, z-VAD-FMK (carbobenzoxy-valyl-alanyl-aspartyl-[O-methyl]-fluoromethylketone) (Promega). Following incubation at 37°C for 1 h, the cells were infected with AHSV-4 at a MOI of 1 pfu/cell. The infected BHK-21 cells were subsequently rinsed twice with incomplete EMEM medium. Following addition of complete EMEM medium containing the appropriate concentration of z-VAD-FMK, the tissue culture plates were incubated at 37°C in a CO_2 incubator. Uninfected BHK-21 cells treated with dimethyl sulfoxide (DMSO) (Sigma-Aldrich) and AHSV-infected BHK-21 cells were included in the assay as controls. At 24 h post-infection, the cells were harvested and processed for DNA fragmentation analysis, as described below.

4.2.2.2 DNA fragmentation analysis

Chromosomal DNA was extracted with the DNeasy® Blood and Tissue Kit (Qiagen), according to the manufacturer's instructions. Briefly, 2.5 × 10^6 cells were harvested by centrifugation at 2500 rpm for 10 min. The cell pellet was suspended in 200 µl of 1 × PBS (137 mM NaCl; 2.7 mM KCl; 4.3 mM $Na_2HPO_4.2H_2O$; 1.4 mM KH_2PO_4; pH 7.4), after which 20 µl of Proteinase K and 200 µl of the supplied Buffer AL were added to the sample. Following incubation at 56°C for 10 min, 200 µl of 96% ethanol was added to the sample and the mixture was centrifuged through a DNeasy Mini spin column at 8000 rpm for 1 min. The column was washed twice with the supplied buffers AW1 and AW2, respectively, after which the DNA was eluted in 100 µl of the supplied Buffer AE. Aliquots of the extracted DNA were analyzed by electrophoresis in a 1% (w/v) agarose gel.

4.2.3 Caspase activation assays

Caspase-3, -8 and -9 activation assays were performed with the ApoTarget™ Caspase Colorimetric Protease Assay range of kits (BioSource International), according to the manufacturer's instructions. BHK-21 cells were propagated in 25-cm^2 tissue culture flasks until 100% confluent and then infected with AHSV-4 at a MOI of 1 pfu/cell. At different times post-infection, *ca*. 2.5 × 10^6 cells were collected by centrifugation at 2500 rpm for 10 min and suspended in 50 µl of chilled Cell Lysis Buffer (supplied in the kits). Following incubation on ice for 10 min, cellular debris was pelleted by centrifugation at 12 200 rpm for 1 min. The protein concentration of each cytoplasmic extract was determined with the Quick Start Bradford Protein Assay kit (BioRad) and bovine serum albumin (BSA) as the standard. Each cytoplasmic extract was then diluted in 50 µl of Cell Lysis Buffer to yield *ca*. 100 µg total cellular protein and pipetted into the wells of a 96-well flat-bottom microtitre plate (Cellstar® Greiner Bio-one). Following addition of 50 µl of 2 × Reaction Buffer and 5 µl of the appropriate substrate, the microtitre plate was incubated at 37°C in the dark for 2 h. The substrates (4 mM each) comprised of DEVD-*p*NA for caspase-3, IETD-*p*NA for caspase-8 and LEHD-*p*NA for caspase-9. The samples were subsequently read at 405 nm against Reaction Buffer (containing the substrate) as the blank with a Multiscan Ascent v1.24 ELISA plate reader. The values of AHSV-infected samples were compared with uninfected BHK-21 controls to determine the increase in the caspase enzymatic activity. Two independent assays were performed for each of the respective caspases.

4.2.4 Detection of mitochondrial membrane depolarization

Mitochondrial membrane depolarization was assessed using DePsipher™ (5,5´,6,6´-tetrachloro-1,1´,3,3´-tetraethylbenzimidazolyl carbocyanin iodide) (Trevigen, Inc.), according to the manufacturer's instructions. DePsipher™ is a lypophilic cation that is susceptible to changes in mitochondrial membrane potential. It has the property of aggregating upon membrane polarization forming a red fluorescent compound with absorption/emission maxima of 585/590 nm. If the potential is disrupted, the dye cannot access the mitochondrial transmembrane space and remains in the cytoplasm in its green fluorescent monomeric form with absorption/emission maxima of 510/527 nm. To investigate, BHK-21 cells were propagated in 6-well tissue culture plates (1×10^6 cells/well) with or without glass coverslips and infected with AHSV-4 at a MOI of 1 pfu/cell. The tissue culture plates were incubated at 37°C in a CO_2 incubator and the cells were processed at different times post-infection for flow cytometric analysis or confocal microscopy, as described below. In these assays, uninfected BHK-21 cells were included as a control of healthy cells with polarized mitochondrial membranes, whereas BHK-21 cells incubated for 24 h with 20 µM FCCP (carbonyl cyanide *p*-[trifluoro-methoxy] phenylhydrazone) served as a positive control for cells with depolarized mitochondrial membranes (Heytler and Pritchard, 1962; Dispersyn *et al*., 1999).

4.2.4.1 Flow cytometry

At selected intervals post-infection, control and AHSV-infected BHK-21 cells were harvested by centrifugation at 1000 rpm for 5 min and suspended in 1 ml of DePsipher™ solution, which had been diluted in the supplied 1 × Reaction Buffer to a final concentration of 5 µg/ml. Following incubation of the samples at 37°C in the dark for 20 min in a CO_2 incubator, the cells were washed twice with 1 × PBS and suspended in 1 ml of the same buffer. Cell fluorescence was recorded with a BD FACSAria™ flow cytometer (BD Biosciences) equipped with a 488-nm argon laser and using neutral density filter 2. A minimum of 10 000 events were analyzed for each sample with FACSDiva™ v.6.1.1 software (BD Biosciences). Data collection was gated, utilizing forward light scatter and side light scatter, to exclude cell debris and cell aggregates. The green DePsipher™ monomer was detected using the fluorescein channel (FITC-A; FL1) and the red DePsipher™ aggregates were detected using the propidium iodide channel (PE-A; FL2). The results are presented as a green/red fluorescence ratio (geomean FL1/FL2), the increase of which indicates

mitochondrial membrane depolarization (Markovic *et al*., 2007; Isakovic *et al*., 2008). Two independent assays were performed.

4.2.4.2 Confocal laser scanning microscopy of AHSV-infected BHK-21 cells

At 24 h post-infection, the cell culture medium of control and AHSV-infected BHK-21 cells was aspirated and replaced with 1 ml of DePsipher™ solution (5 µg/ml). The tissue culture plates were incubated at 37°C in the dark for 20 min in a CO_2 incubator, after which the DePsipher™ solution was aspirated and the cells rinsed once with 1 ml of 1 × Reaction Buffer. The glass coverslips were removed from the tissue culture plates and the cells were examined with a Zeiss LSM S10 META confocal laser scanning microscope through the 40×1.3 objective, using bypass filters for fluorescein (505-550 nm) and rhodamine (560-615 nm). Fluorescent images were captured with a Zeiss Axiocam Series 5 digital camera and analyzed with Zeiss LSM Image Browser v.4.2.0.121 software.

4.2.5 Detection of NF-κB (p50 and p65)

4.2.5.1 Protein extraction

Confluent BHK-21 cell monolayers in 75-cm^2 tissue culture flasks were infected with AHSV-4 at a MOI of 1 pfu/cell. At different times post-infection, the infected BHK-21 cells were harvested by centrifugation at 2500 rpm for 10 min and nuclear proteins were extracted with the ProteoJET™ Cytoplasmic and Nuclear Protein Extraction Kit (Fermentas), according to the manufacturer's instructions. Briefly, the harvested cells were suspended in 650 µl of Cell lysis buffer, vortexed and incubated on ice for 10 min. To ensure cell lysis, the samples were passed through a 22G needle and incubated on ice for a further 10 min. Cytoplasmic proteins were removed by centrifugation of the samples at 610 rpm for 7 min at 4°C. To remove contaminating proteins and cell debris, the pelleted nuclei were washed twice with Nuclei washing buffer and the samples were incubated on ice for 2 min. Following incubation, the samples were centrifuged at 610 rpm for 7 min at 4°C and the pelleted nuclei were suspended in 150 µl of ice-cold Nuclei storage buffer. To lyse the nuclei, 15 µl of Nuclei lysis reagent was added to each suspension, vortexed briefly and incubated on ice for 2 h with intermittent vortexing. The nuclear lysates were cleared by centrifugation at 24 400 rpm for 5 min at 4°C, after which the supernatants, containing nuclear proteins, were carefully transferred to clean 1.5-ml Eppendorf tubes. The p50 and p65 subunits of activated NF-κB were subsequently detected by immunoblot analysis.

4.2.5.2 Immunoblot analysis

Prior to analysis, protein samples were mixed with an equal volume of 2 × PSB buffer (125 mM Tris-HCl [pH 6.8]; 4% [w/v] SDS; 20% [v/v] glycerol; 10% [v/v] 2-mercaptoethanol; 0.002% [w/v] bromophenol blue) and then denatured by heating to 95°C for 5 min in a boiling water bath. The proteins were resolved by electrophoresis in a discontinuous gel system (Laemmli, 1970), as described previously (Chapter 2, Section 2.2.13.1). Following SDS-polyacrylamide gel electrophoresis, proteins from the unstained gels were electroblotted onto Hybond™-C$^+$ nitrocellulose membranes (Amersham Pharmacia Biotech AB) at 28 V for 3 h with a Hoefer Mighty Small™ Transphor blotting apparatus. Following transfer, the membranes were washed once with 1 × PBS for 5 min and non-specific binding sites were blocked by incubating the membranes overnight in blocking solution (1% [w/v] fat-free milk powder in 1 × PBS). The membranes were transferred to 1 × PBS containing anti-p50 or anti-p65 antibodies, diluted 1:200 (Santa Cruz Biotechnology, Inc.). Following incubation at room temperature for 2 h with gentle agitation, the unbound primary antibodies were removed by washing the membranes three times for 5 min each with wash buffer (0.05% [v/v] Tween-20 in 1 × PBS). The secondary antibody, Protein-A conjugated to horseradish peroxidase (Sigma-Aldrich) and diluted 1:500 in 1 × PBS, was added to each membrane and then incubated at room temperature for 1 h with gentle agitation. The membranes were subsequently washed three times for 5 min each with wash buffer and once for 5 min with 1 × PBS. Finally, the membranes were immersed in a freshly prepared enzyme substrate solution (60 mg 4-chloro-1-naphtol in 20 ml of ice-cold methanol and 60 µl H_2O_2 in 100 ml of 1 × PBS, mixed just prior to use). Once the bands became visible, the membranes were rinsed with dH_2O and allowed to air dry.

4.3 RESULTS

4.3.1 AHSV-induced apoptosis in BHK-21 cells is caspase-dependent

In the previous Chapter it was shown that infection of BHK-21 cells with AHSV-4 resulted in morphological and biochemical hallmarks associated with the induction of apoptosis (Figs. 3.2 and 3.3). To investigate whether apoptosis induced by AHSV-4 infection was caspase-dependent, BHK-21 cells infected with AHSV-4 were incubated in the presence or absence of the pan-caspase inhibitor z-VAD-FMK. This tripeptide is a pseudo-substrate for several caspases, including caspase-3, which irreversibly blocks the caspase proteolytic cascade

(Nicholson and Thornberry, 1997). As a control, mock-infected BHK-21 cells were treated with DMSO. As the z-VAD-FMK inhibitor is provided in DMSO, this control served to assess the toxicity of DMSO to BHK-21 cells. At 24 h post-treatment, the control and virus-infected cells were harvested and analyzed for DNA fragmentation by electrophoresis in an agarose gel.

The results indicated that mock-infected BHK-21 cells treated with DMSO did not show DNA fragmentation, indicating that DMSO is not toxic to BHK-21 cells. In contrast, AHSV-infected cells incubated in the absence of the z-VAD-FMK inhibitor showed fragmentation of the chromosomal DNA, but no DNA fragmentation was observed when the virus-infected cells were incubated in the presence of the pan-caspase inhibitor (Fig. 4.1). These results therefore indicated that AHSV-induced apoptosis in BHK-21 cells was caspase-dependent.

4.3.2 Cellular caspases are activated in AHSV-infected BHK-21 cells

To characterize the activation of apoptotic pathways during AHSV-4 infection, BHK-21 cells were infected with AHSV-4 and the enzymatic activity of different cellular caspases in cytoplasmic extracts, prepared over a time course of 48 h, was measured by proteolytic cleavage of chromogenic substrates. These assays are based on the recognition and cleavage of different caspase-specific amino acid sequences linked to the chromatophore *p*-nitroanilide (*p*NA). Upon cleavage of the labeled peptide by the caspase, free *p*NA is released with a resulting increase in absorbance measurements. Comparison of the absorbance of released *p*NA from AHSV-infected cells with that of uninfected BHK-21 cells makes it possible to determine the increase in caspase activity.

In the first of these experiments, activation of caspase-3 was examined. Caspase-3 is a key agent of apoptosis and plays a central role in apoptosis by acting as an effector caspase in both the extrinsic and intrinsic apoptotic pathways (Xu and Shi, 2007; Duprez *et al.*, 2009). The results indicated that caspase-3 activity in AHSV-infected BHK-21 cells increased gradually from 0 until 12 h post-infection. From 12 h post-infection onwards, there was a steep increase in caspase-3 activity (Fig. 4.2a).

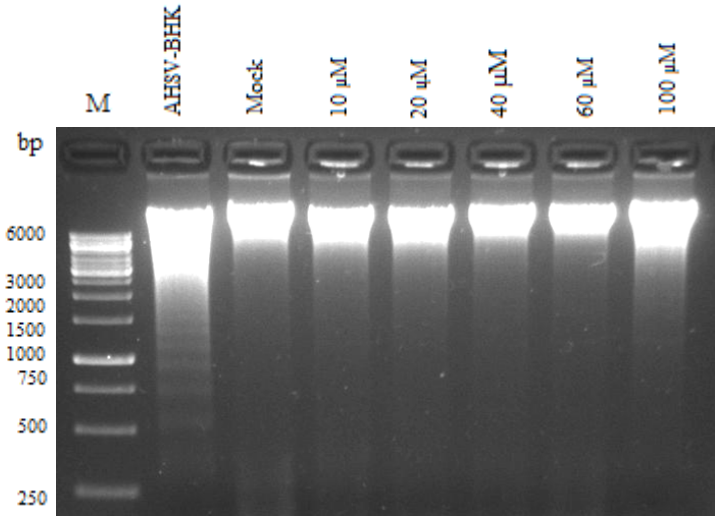

Fig. 4.1: The effect of caspase inactivation on DNA fragmentation in BHK-21 cells infected with AHSV-4. BHK-21 cells were infected with AHSV-4 in the absence or presence of the pan-caspase inhibitor z-VAD-FMK. The chromosomal DNA was extracted at 24 h post-infection and analyzed by electrophoresis in a 1% (w/v) agarose gel. In the presence of DMSO, mock-infected cells showed no DNA fragmentation, while DNA fragmentation, typical of cells undergoing apoptosis, was visible in AHSV-4 infected cells. In contrast, no DNA fragmentation was observed in virus-infected cells treated with the inhibitor at different concentrations, as indicated in the figure. The sizes of the DNA molecular weight marker, O'GeneRuler™ 1kb DNA Ladder (Fermentas), are indicated to the left of the figure.

Although the above data indicates that the executioner caspase, caspase-3, is activated during AHSV-4 infection of BHK-21 cells, it is, however, a common effector caspase to both the extrinsic and intrinsic apoptotic pathways. The assay therefore does not allow for any conclusions to be drawn regarding the exclusive involvement of the extrinsic or intrinsic pathways during AHSV-4 infection. Thus, to determine the role of the extrinsic pathway triggering AHSV-4 apoptosis, the activation of caspase-8 was examined. In AHSV-infected cells, caspase-8 activity increased gradually from 0 to 12 h post-infection. Between 12 and 24 h post-infection, there was a steep increase in caspase-8 activity and after 24 h post-infection, the caspase-8 activity showed a steady decrease (Fig. 4.2b).

To determine the activation of the intrinsic pathway by AHSV-infection, the activation of caspase-9 was examined. Caspase-9 is known to mediate the activation of apoptosis via the mitochondrial pathway (Hu *et al*., 1998; Prior and Salvesen, 2004). In AHSV-infected cells, caspase-9 activity was not detectable between 0 and 12 h post-infection. However, a steep increase in caspase-9 activity was observed between 12 and 24 h post-infection, whereafter the activity decreased (Fig. 4.2c). These results are similar to that obtained regarding caspase-8 activity, except that the caspase-9 activity was lower compared to that of caspase-8. Together, the data indicates that both the extrinsic and intrinsic apoptotic pathways are activated in AHSV-4 infected BHK-21 cells.

4.3.3 The mitochondrial membrane is depolarized in AHSV-infected BHK-21 cells

To elucidate the events preceding the activation of caspase-3 and to specifically evaluate the role of the mitochondria in this process, the mitochondrial transmembrane potential of AHSV-infected BHK-21 cells was examined. Depolarization of the mitochondrial outer membrane is an early, pivitol event in the intrinsic (or mitochondrial) apoptotic signalling pathway, resulting in the release of several proapoptotic proteins from the mitochondrial intermembrane space to the cytosol (Riedl and Salvesen, 2007; Duprez *et al*., 2009). This allows for the recruitment and activation of caspase-9, which, in turn, activates caspase-3, which is crucial for the execution of apoptotic cell death (Duprez *et al*., 2009). To investigate, BHK-21 cells were infected with AHSV-4 and the cells were stained with the lipophilic cation DePsipher™, which is used to indicate loss of mitochondrial membrane potential. The DePsipher™-stained virus-infected cells were analyzed by flow cytometry and confocal microscopy. In healthy cells with polarized membranes, the DePsipher™ reagent easily enters

(a)

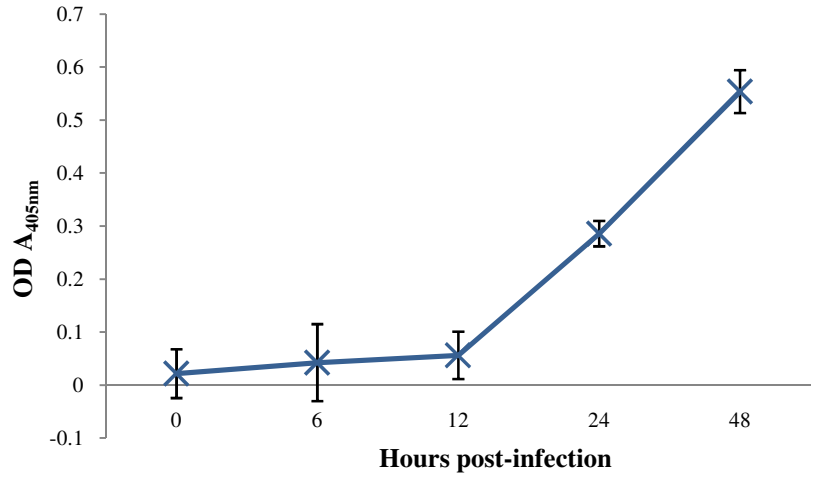

(b)

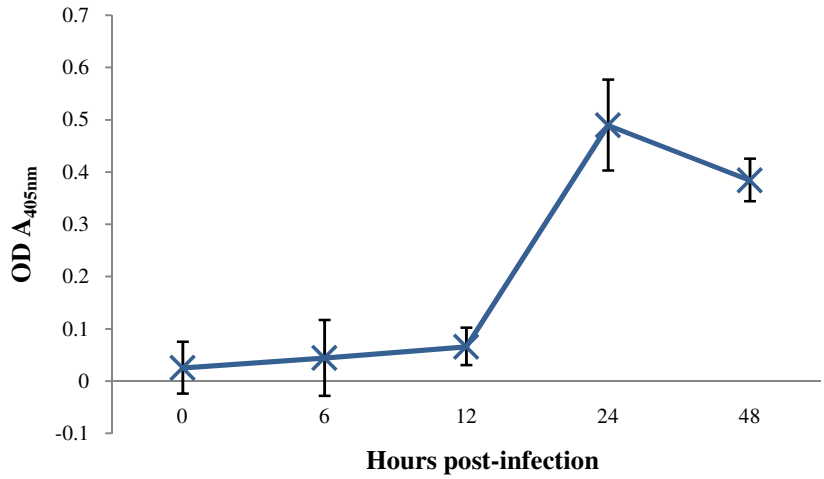

(c)

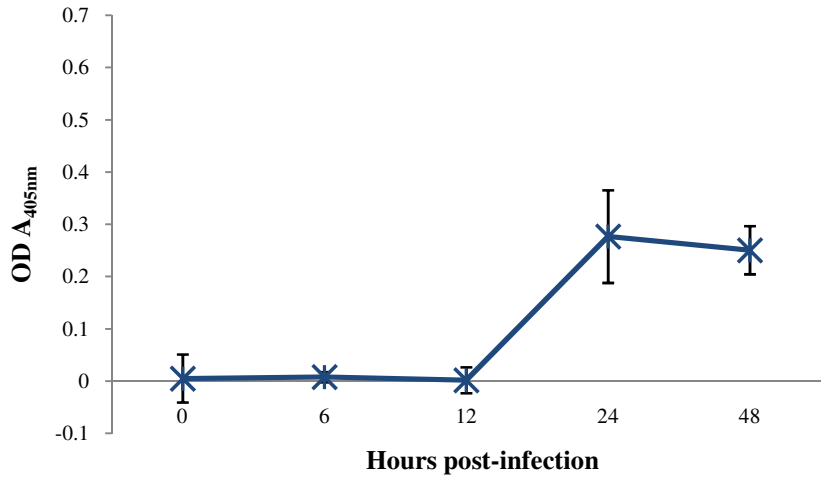

Fig. 4.2: Activation of different caspases associated with AHSV-induced apoptosis in BHK-21 cells. Cytoplasmic extracts, each containing 100 µg total protein, were prepared from uninfected and AHSV-infected BHK-21 cells at different times post-infection. Following incubation with the caspase-3 synthetic substrate DEVD-*p*NA (a), the caspase-8 synthetic substrate IETD-*p*NA (b) or the caspase-9 synthetic substrate LEHD-*p*NA (c), the liberated *p*NA was quantified at 405 nm with an ELISA plate reader. The data is presented as an increase in the activity of the respective caspases. Data are indicated as the means ± SD of two independent experiments.

cells and fluoresces brightly red in its multimeric form within healthy mitochondria. In apoptotic cells with a disturbed mitochondrial membrane potential, the dye cannot accumulate within the mitochondria and remains in the cytoplasm in its green fluorescent monomeric form. Thus, apoptotic cells showing primarily green fluorescence are readily differentiated from healthy cells that show red fluorescence. As a positive control, BHK-21 cells treated with the protonophore FCCP were included in the assays. FCCP is known for its ability to uncouple oxidative phosphorylation in mitochondria, thus resulting in depolarization of mitochondrial membranes (Heytler and Pritchard, 1962; Dispersyn *et al.*, 1999).

Flow cytometric analysis of AHSV-infected BHK-21 cells stained with the DePsipher™ reagent, over a time course of 30 h, indicated a progressive loss of mitochondrial potential from 6 to 30 h post-infection, as evidenced by an increase in the green-to-red (FL1/FL2) fluorescence form of the mitochondria-binding dye DePsipher™ (Fig. 4.3). To furthermore confirm these results, the control and AHSV-infected BHK-21 cells were examined by confocal microscopy at 24 h post-infection, following incubation of the cell monolayers with the DePsipher™ reagent. In uninfected BHK-21 cells, red fluorescent aggregates were observed in the mitochondria, indicative of a lack of apoptosis (Fig. 4.4a and b). In contrast, in AHSV-infected cells, green fluorescence was observed that was localized to the cell cytoplasm, indicating that the mitochondrial membrane potential was disturbed (Fig. 4.4c and d). These results are in agreement with those observed in BHK-21 cells treated with FCCP (Fig. 4.4e and f). Overall, these results indicate that infection of BHK-21 cells by AHSV-4 resulted in mitochondrial depolarization and furthermore confirmed that apoptosis induction involves the activation of the mitochondrial (intrinsic) apoptotic signalling pathway.

4.3.4 NF-κB is activated in AHSV-infected BHK-21 cells

To further characterize the induction of apoptosis, the activation of transcription factor NF-κB in response to AHSV-4 infection in BHK-21 cells was determined. Activation of NF-κB, a heterodimer composed of proteins p50 and p65, results in its translocation from the cytoplasm to the nucleus where it can potentiate the apoptotic response (Verma *et al.*, 1995; May and Ghosh, 1997; Liu and Chen, 2011). To investigate, BHK-21 cells were infected with AHSV-4 and the nuclear extracts from cells harvested over a time course of 24 h were subjected to immunoblot analysis using anti-p50 and anti-p65 antibodies.

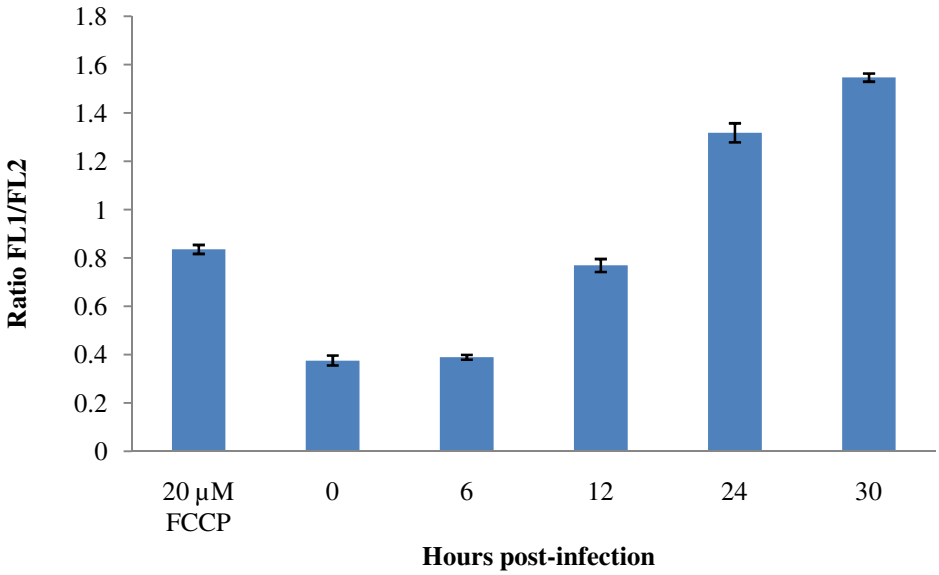

Fig. 4.3: Mitochondrial membrane depolarization in BHK-21 cells infected with AHSV-4. AHSV-infected BHK-21 cells were treated with DePsipher™ at the indicated times post-infection, and analyzed by flow cytometry. BHK-21 cells treated with FCCP were included as a positive control in the analysis. An increase in the ratio of green (FL1)/red (FL2) fluorescence is indicative of mitochondrial membrane depolarization. Results are mean values ± SD of two independent experiments.

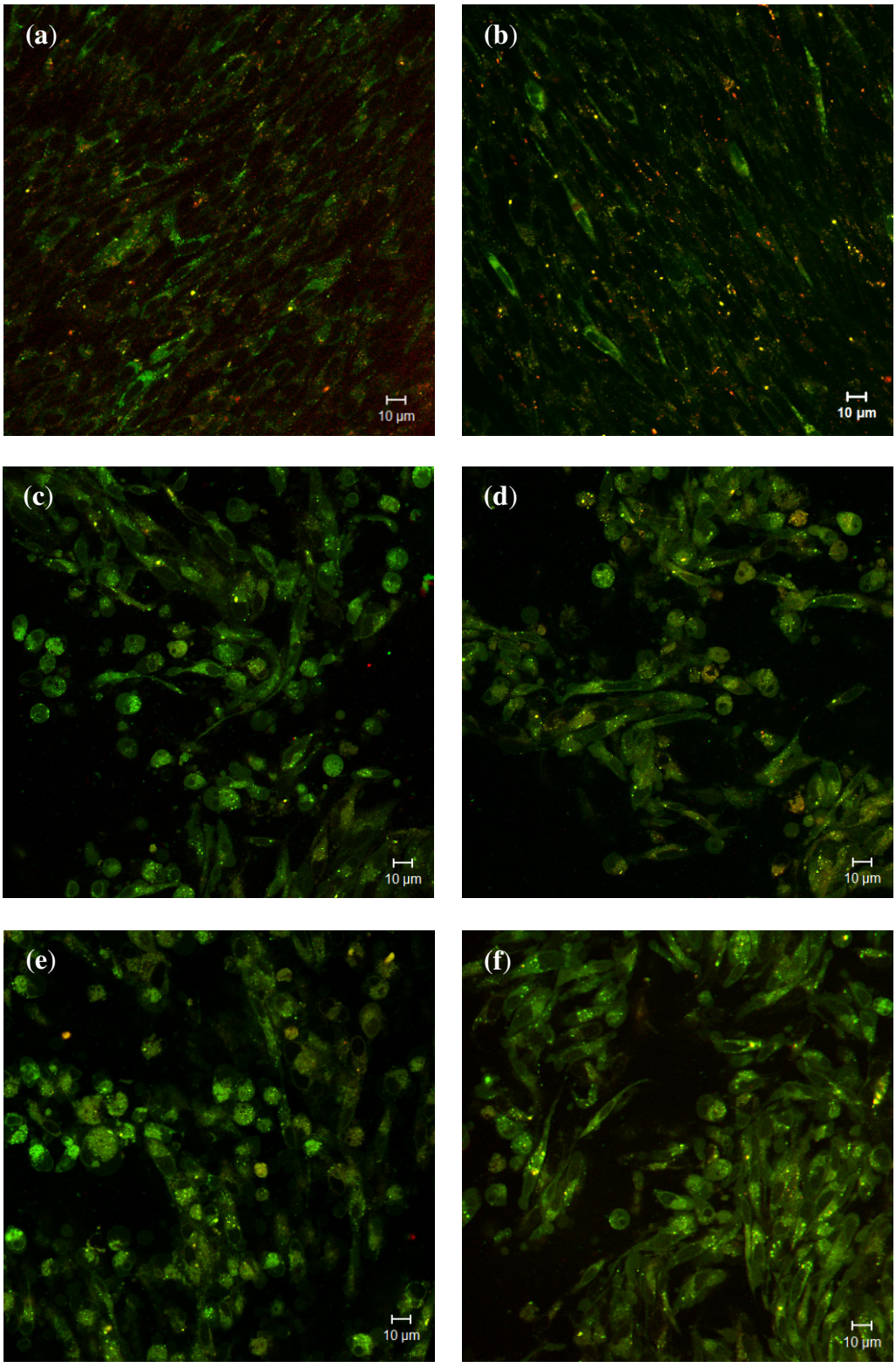

Fig. 4.4: Confocal laser scanning microscopy of AHSV-infected BHK-21 cells stained with DePsipher™. Uninfected BHK-21 cells (a and b), AHSV-infected BHK-21 cells (c and d) and BHK-21 cells treated with FCCP (e and f) were examined at 24 h post-infection with a Zeiss LSM S10 META confocal microscope fitted with bypass filters for fluorescein (505-550 nm) and rhodamine (560-615 nm).

The results, presented in Fig. 4.5, indicated clear signals for the activation of NF-κB in the AHSV-infected BHK-21 cells. Both the p50 and p65 subunits of NF-κB were detected in the nuclei of the cells from 6 h post-infection onwards, demonstrating the translocation of the NF-κB complex to the nuclei of cells. These results suggest that NF-κB may play a role in the AHSV-4 apoptotic machinery.

4.4 DISCUSSION

Various reports have indicated that infection of mammalian cells by viruses induces apoptosis, as well as a variety of signal transduction pathways (Roulston *et al*., 1999; Hay and Kannourakis, 2002; Danthi, 2011). There are two common pathways for the induction of apoptosis, *i.e.* the extrinsic pathway that is primarily initiated by virus attachment to receptors and the intrinsic pathway that is mediated by damage to the mitochondria (Xu and Shi, 2007; Duprez *et al*., 2009). In the previous Chapter it was shown that AHSV-4 induces apoptosis in infected BHK-21 cells, but the apoptotic pathways involved have not yet been investigated. To this end, a number of experiments were undertaken to examine the cellular activation of signalling pathways and thereby the induction of apoptosis during AHSV-4 infection.

Microscopy analysis of AHSV-4 infected BHK-21 cells revealed morphological and ultrastructural alterations indicative of cells undergoing apoptosis (Chapter 3, Figs. 3.1 and 3.2). Many of these alterations have been attributed to the action of caspase-3, a key executioner caspase of the caspase cascade responsible for cleavage of a variety of cellular and nuclear structural proteins (Barber, 2001; Li and Yuan, 2008). Results obtained in this part of the investigation verified that AHSV-induced apoptosis in BHK-21 cells was caspase-dependent, as was evidenced by a lack of chromosomal DNA fragmentation when virus-infected cells were incubated in the presence of the pan-caspase inhibitor z-VAD-FMK. These results were confirmed in a second independent assay in which BHK-21 cells infected with AHSV-4 were examined for caspase-3 activity. Notably, caspase-3 activity was detected from 12 h post-infection and coincided with the onset of DNA fragmentation in AHSV-infected BHK-21 cells (Chapter 3, Fig. 3.3).

The extrinsic pathway is directly linked to caspase-8, which is responsible for cleavage of downstream caspases, including caspase-3 and -7 (Micheau and Tschopp, 2003; Xu and

(a)

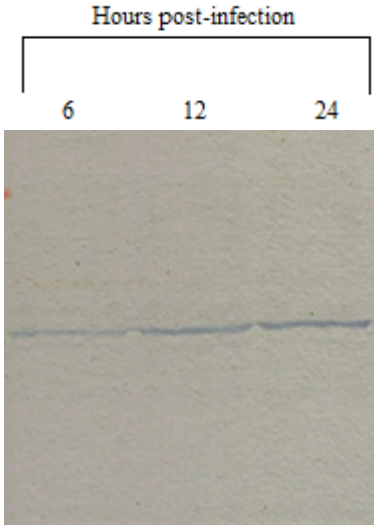

(b)

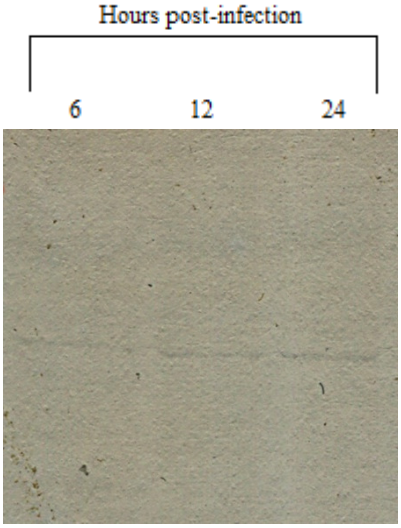

Fig. 4.5: Immunoblot analysis of NF-κB translocated to the nuclei in BHK-21 cells infected with AHSV-4. Nuclear extracts were prepared from AHSV-infected BHK-21 cells at the indicated times post-infection, resolved by SDS-PAGE and then electroblotted onto nitrocellulose membranes. The membranes were subjected to immunoblot analysis using anti-p50 (a) and anti-p65 (b) antibodies.

Shi, 2007). To determine if AHSV-induced apoptosis involves the activation of the death receptor pathway, caspase-8 activity was monitored over a time course of 48 h. The data indicated a steep increase in caspase-8 activity from 12 to 24 h post-infection in virus-infected cells. Since the primary activation of caspase-8 is due to receptor binding, it was expected that caspase-8 activation would occur relatively early after infection with AHSV-4. Nevertheless, the results are in agreement with that reported for BTV (Stewart and Roy, 2010). However, for both AHSV-4 and BTV, caspase-8 activation is somewhat delayed compared to mammalian reovirus (Kominsky *et al*., 2002). It was subsequently reported that c-FLIP, a cellular apoptotic inhibitor, regulates caspase-8 activity during reovirus infection (Clarke *et al*., 2005). It is thus tempting to speculate that the delay in caspase-8 activation in AHSV-infected cells may be due to regulation by c-FLIP. However, further investigation is required before such a conclusion can be reached.

In the intrinsic pathway, apoptosis is triggered by internal signals, primarily mediated and regulated by Bcl-2 family members, which leads to the disruption of the mitochondrial transmembrane potential (Riedl and Salvesen, 2007; Chipuk and Green, 2008). Once mitochondrial depolarization occurs, cell death is precipitated through the release of proapoptotic molecules from the intermembrane space, such as cytochrome *c* and Smac/DIABLO, and the formation of an apoptosome that leads to the activation of caspase-9 and subsequent effector caspase activation (Cain *et al*., 1999; Acehan *et al*., 2002). In this part of the investigation, data was also obtained demonstrating the involvement of the intrinsic pathway in AHSV-induced apoptosis. A steep increase in caspase-9 activity was detected between 12 and 24 h post-infection. To determine if AHSV-4 infection causes mitochondrial damage, virus-infected BHK-21 cells were examined by flow cytometry following incubation of the cells with DePsipher™, an indicator of mitochondrial depolarization. AHSV-4 infection of BHK-21 cells resulted in mitochondrial depolarization as early as 6 h post-infection and increased gradually until 30 h post-infection. These results thus indicated that the timing of mitochondrial damage precedes the activation of caspase-9 and furthermore confirms that the intrinsic mitochondrial signalling pathway is involved in AHSV-induced apoptosis. Moreover, the results are in agreement with those presented for mammalian reovirus (Kominsky *et al*., 2002) and BTV (Nagaleekar *et al*., 2007), both of which activate the intrinsic pathway following loss of mitochondrial potential. The early stage at which mitochondrial depolarization occurs in AHSV-infected BHK-21 cells is congruent with the earlier findings indicating that a virus-induced event early in the infection

cycle, such as viral disassembly in cellular endosomes (Chapter 3, Section 3.3.5), induces apoptosis in the infected cells.

The NF-κB family of transcription factors play a key role in regulating cellular stress responses (Hayden and Ghosh, 2008; Liu and Chen, 2011). The prototypical form of NF-κB exists as a heterodimer of proteins p50 and p65 (Staal *et al*., 2011). In this investigation, infection of BHK-21 cells with AHSV-4 was shown to be sufficient to trigger the translocation of NF-κB complexes containing the p50 and p65 subunits to the nucleus within 6 h post-infection. Activation of NF-κB by viral infection has been reported to result either in enhancement (Lin *et al*., 1995; Hong *et al*., 2008) or inhibition (Sciortino *et al*., 2008; Lin *et al*., 2010) of apoptosis. In mammalian reovirus infection, activation of NF-κB plays a significant role in virus-induced apoptosis (Connolly *et al*., 2000). Activation of NF-κB following virus infection was suggested to induce the expression of several proapoptotic members of the Bcl-2 family of proteins, thus leading to apoptosis of infected cells. In contrast to reovirus, NF-κB plays a minimal role, if any, in the induction of apoptosis in BTV-infected cells (Stewart and Roy, 2010). Following an initial early period of NF-κB activation (8 h post-infection), the response was not sustained and NF-κB activity was inhibited by viral proteins during the later stages of virus replication. It was subsequently shown that NF-κB activity acts to control virus replication during the early stages of the virus infectious cycle, suggesting that it may play a role in initiating an antiviral state through the induction of the innate immune response. Interestingly, for AHSV-4 infection, the p50 and p65 subunits were detected 24 h post-infection, indicating that NF-κB activity was sustained during the infection cycle. These results therefore suggest that, in contrast to BTV, NF-κB may play a significant role in AHSV-induced apoptosis. Similar to mammalian reovirus, activation of NF-κB may initiate the expression of several proapoptotic Bcl-2 proteins that culminate in apoptotic cell death. Interestingly, it appears that AHSV and mammalian reovirus may thus share a common strategy of apoptosis induction. However, further research is required to determine if this is indeed the case.

In conclusion, the results obtained in this part of the investigation represent the first to identify cellular pathways through which AHSV induces apoptosis in BHK-21 cells. DNA fragmentation was blocked by z-VAD-FMK, indicating that AHSV-4 requires the activation of caspases for the induction of apoptosis. The activation of caspase-8 and -9 and the loss of mitochondrial membrane potential in AHSV-infected BHK-21 cells indicate the involvement

of both caspase-dependent extrinsic and intrinsic apoptotic pathways. Moreover, sustained activation of NF-κB is suggestive of it playing an important role in the AHSV apoptotic machinery. It can be envisaged that a greater understanding of the signalling events that occur in AHSV infection may not only contribute new information regarding mechanisms by which AHSV causes cell death and disease, but may also aid in the identification of apoptosis inhibitors that may reduce disease severity.

CHAPTER FIVE

CONCLUDING REMARKS

Many viruses are capable of inducing programmed cell death, which results in apoptosis of infected cells (O'Brien, 1998; Roulston *et al.*, 1999; Hay and Kannourakis, 2002). In some cases, apoptosis triggered by virus infection may serve as a host defense mechanism to limit viral replication (Benedict *et al.*, 2002). In other instances, induction of apoptosis may enhance viral infection by facilitating virus spread or allowing the virus to evade host inflammatory or immune responses (Roulston *et al.*, 1999). Apoptosis also plays a role in viral pathogenesis and is an important mechanism for virus-induced tissue injury *in vivo* (O'Donnell *et al.*, 2005; Clarke and Tyler, 2009; Umeshappa *et al.*, 2010). Despite apoptosis being a common mechanism of cell death for many viruses, the mechanisms of virus-induced apoptosis remain largely unknown (Roulston *et al.*, 1999; Danthi, 2011). Consequently, the primary aims of this investigation were to determine whether African horse sickness virus (AHSV), a pathogen of veterinary importance, induces apoptosis in mammalian cells, and to identify the initiators and effectors of AHSV-induced apoptosis in mammalian cells. In this conclusion, the new information that has been obtained during the course of this investigation will be summarized and suggestions regarding future research will be made.

Data obtained regarding the initiators (Chapter 3) and effectors (Chapter 4) of AHSV-induced apoptosis in mammalian cells provided a basic model of the early events leading to the induction of apoptosis in AHSV-infected mammalian cells. In this proposed model (Fig. 5.1), apoptosis is induced through VP2-mediated attachment to an as yet unknown cellular receptor(s), followed by internalization of the virion into an endocytic vesicle and destabilization of the endosomal membrane by VP5. Subsequent steps in the virus replication cycle, such as protein synthesis and genome replication, are dispensable for the induction of apoptosis by AHSV in mammalian cells. Results obtained indicate that the extrinsic (death receptor) pathway is activated in AHSV-infected cells, as evidenced by the activation of caspase-8, which, in turn, activates the downstream effector caspase, caspase-3. Apoptotic stimuli resulting from AHSV infection also induce the intrinsic apoptotic pathway. These stimuli enhance mitochondrial membrane permeability that may permit translocation of cytochrome *c* and other proapoptotic molecules (*e.g.* Smac/DIABLO) from the mitochondria into the cytosol. Subsequently, a cytosolic complex that includes cytochrome *c* and Apaf-1 (apoptosome) activates caspase-9. Activated caspase-9, like activated caspase-8, can activate the downstream effector caspase, caspase-3. Subsequent caspase-dependent cleavage of various cellular substrates results in apoptosis of the AHSV-infected mammalian cells. Moreover, NF-κB complexes containing both p50 and p65 subunits are activated in the cells

in response to AHSV infection. It is unlikely that NF-κB activation is triggered solely by attachment of the virus to its cognate cellular receptor(s), as NF-κB activity follows virus adsorption by several hours. The delay in NF-κB activation raises the possibility that steps following viral attachment are required to activate NF-κB or, alternatively, it is also possible that AHSV infection induces a soluble factor that mediates activation of NF-κB.

Despite the progress that has been made in identifying initiators and effectors of AHSV-induced apoptosis in mammalian cells, several aspects regarding the cellular apoptotic mechanisms that are activated warrant further investigation. Further investigations are required to identify the cell surface death receptors and their ligands, as well as the mechanism by which they are activated. Moreover, it has been reported that caspase-8 dependent cleavage of Bid, a proapoptotic Bcl-2 family member (Youle and Strasser, 2008), allows the truncated protein to translocate to the mitochondrion where it directly or indirectly facilitates cytochrome *c* release (Luo *et al*., 1998; Korsmeyer *et al*., 2000). Thus, it would be of interest to determine if the intrinsic and extrinsic pathways are linked in this way or are activated independently from each other. It would furthermore be of interest to investigate the contribution of different mitochondrial proteins released into the cytosol following AHSV-induced apoptosis in greater detail. Although cytochrome *c*-dependent activation of caspase-9 is thought to be of central importance in the intrinsic apoptotic pathway (Acehan *et al*., 2002), it has been suggested that Smac/DIABLO release rather than caspase-9 activation may be a critical mitochondrial event in both TRAIL-induced (Deng *et al.*, 2002) and FasL-induced apoptosis (Sun *et al.*, 2002). In addition, since Smac/DIABLO interferes with the ability of inhibitor of apoptosis proteins (IAPs) to prevent caspase activation (Du *et al*., 2000; Ekert *et al*., 2001), the characterization of cellular levels of IAPs could provide insights into the regulatory mechanisms potentiating caspase activation during AHSV infection.

Although activation of NF-κB was detected in AHSV-infected cells, further research is required to clarify the mechanism by which AHSV activates NF-κB and to determine its role in AHSV apoptosis. For members of the *Reoviridae* family, such as mammalian reovirus, it has been reported that activation of NF-κB is required for virus-induced apoptosis (Connolly *et al.*, 2000), whereas for bluetongue virus (BTV) it was reported not to be linked to the induction of apoptosis (Stewart and Roy, 2010). However, the sustained activation of NF-κB in AHSV-induced apoptosis suggests that NF-κB may function to enhance the expression of proapoptotic genes. Several genes encoding proapoptotic proteins are induced by a variety of

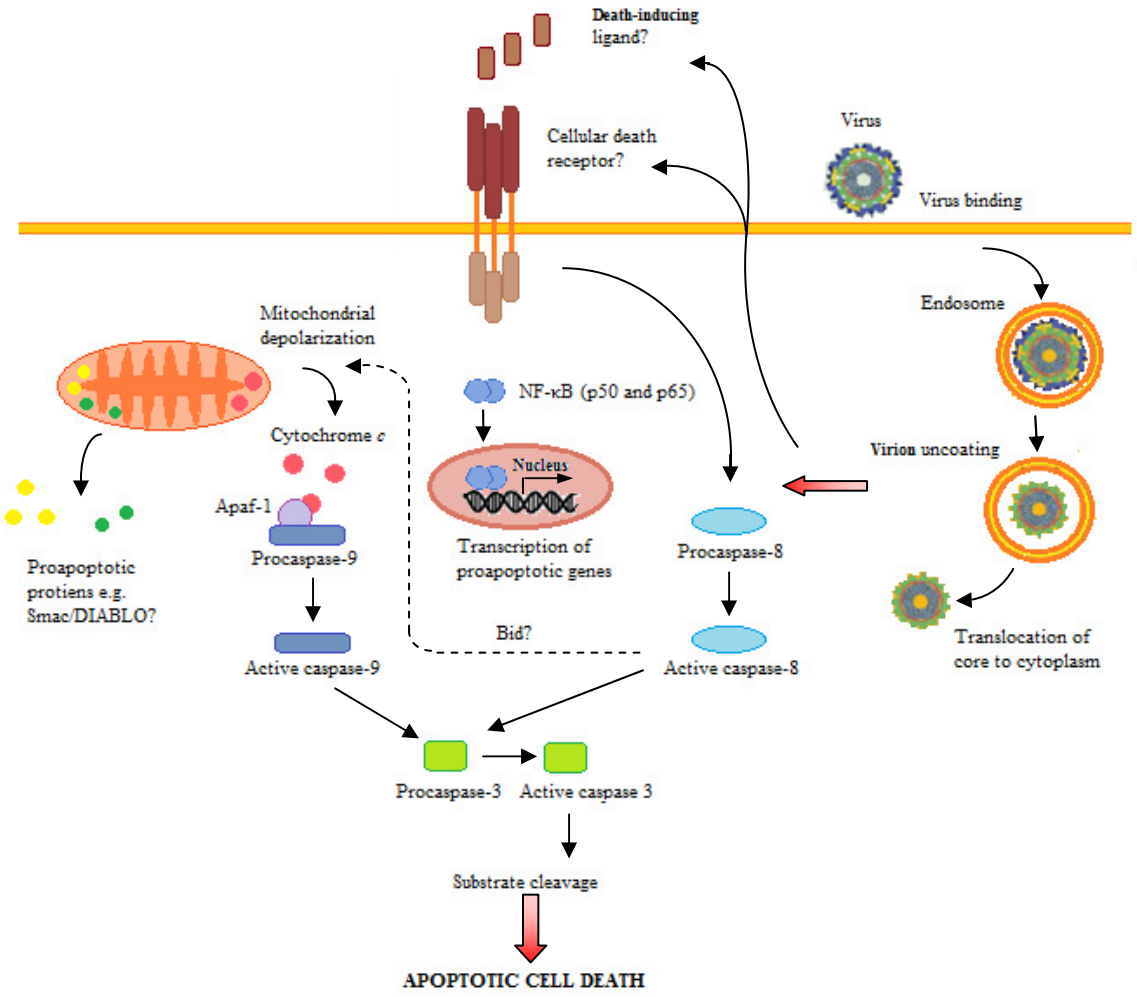

Fig. 5.1: Proposed model of the induction of apoptosis by AHSV in mammalian cells (with adaptations from Mertens, 2004 and Duprez *et al*., 2009). The AHSV outer capsid proteins trigger an apoptotic response through the receptor-binding activity of VP2 and the membrane permeabilization activity of VP5. Virion disassembly within the endosome, but not viral replication, is required for the induction of apoptosis by AHSV. Following AHSV infection, NF-κB is activated and translocates to the nucleus. Activation of the initiator caspases-8 and -9, as well as mitochondrial depolarization initiates extrinsic and intrinsic death signalling cascades, resulting in the activation of the executioner caspase-3. Caspase-dependent cleavage of various cellular substrates culminates in apoptotic cell death. This is observed in AHSV-infected mammalian cells by distinct morphological and biochemical alterations, which include cell rounding and surface detachment, plasma membrane blebbing, chromatin condensation and fragmentation, and the formation of apoptotic bodies.

stimuli regulated by NF-κB and include, amongst other, TRAIL/DR4/DR5 (Ravi *et al.*, 2001; Siegmund *et al.*, 2001) and FasL (Kasibhatla *et al.*, 1999). Activation of NF-κB following AHSV infection may thus induce the expression of one or more of these genes or other proapoptotic genes, which include effector or initiator caspases, and proapoptotic Bcl-2 family members such as Bax and Bad (Connolly *et al.*, 2000; Burnstein and Duckett, 2003). Studies aimed at examining the NF-κB-mediated up-regulation of these proapoptotic proteins could be undertaken in future. It has been suggested that virus-induced activation of NF-κB and its signalling pathway may represent a common pathway used by various viruses to achieve optimal virus replication and dissemination, while avoiding host inflammatory responses (Connolly *et al.*, 2000). Whether this also holds true for AHSV requires further investigation and may include the use of chemical inhibition assays, viral yield assays and mutant cell lines deficient for specific Rel subunits of NF-κB.

Results obtained during the course of this investigation suggest that the process of induction of apoptosis by AHSV may be very similar to that of mammalian reovirus (Tyler *et al.*, 1995; Connolly *et al.*, 2000; Connolly and Dermody, 2002; Kominsky *et al.*, 2002). This is particularly interesting, since there are significant differences in the host range and mode of transmission between these viruses. It is tempting to speculate that the common structural features of the multilayered capsid of members of the *Reoviridae* predispose the uncoating virion to trigger cellular responses to virus invasion. It is also interesting to note that although the AHSV virions trigger apoptotic responses in mammalian cells, infection of insect cells have been reported to be long-term and unapparent, despite productive virus replication (Mirchamsy *et al.*, 1970). Since apoptosis in insect cells has been documented (Clavería and Torres, 2003; Kornbluth and White, 2005), it may suggest that the signalling pathway for the induction of apoptosis is not triggered by AHSV infection of insect cells. Alternatively, it is plausible that the invasion, replication and dissemination strategy of AHSV may proceed differently in insect cells compared to mammalian cells. Indeed, one of the major morphological differences observed during infection of insect and mammalian cells in culture is that BTV appears to preferentially bud from the plasma membrane of insect cells, thus leaving the cells intact. In contrast, in mammalian cell culture, a high proportion of virus remains cell-associated, leading to eventual cell lysis (Hyatt *et al.*, 1989; Guirakhoo *et al.*, 1995). Future studies aimed at characterizing the replication cycle of AHSV in the vector insect, as well as the cellular responses of the vector insect during infection with AHSV may

provide novel insights into host vector-AHSV interactions and could possibly aid in the development of strategies to prevent or control virus infection.

To enable the identification of initiators of AHSV-induced apoptosis in mammalian cells, the outer capsid proteins of attenuated and virulent AHSV-4 isolates were expressed in the recombinant baculovirus expression system (Chapter 2). The methodology used to obtain soluble recombinant VP2 proteins represents not only a major improvement over previously reported methods (du Plessis *et al.*, 1998; Scanlen *et al.*, 2002), but also provided a means whereby the biological function of VP2 could be investigated (Supplementary Material A1). The results from preliminary cell surface attachment and internalization studies with an immunofluorescent assay system indicated that the VP2 protein is responsible for AHSV entry into permissive BHK-21 mammalian cells. Likewise, the VP2 protein of the attenuated AHSV-4 isolate also retained its ability to bind to and internalize the BHK-21 cells. Considering that apoptosis is induced in AHSV-infected cells through a combination of VP2 receptor-binding activity and endosomal membrane penetration by VP5, it is therefore not surprising that the outer capsid proteins of the attenuated isolate were capable of inducing apoptosis when added extracellularly to the mammalian cells. These results therefore indicate that the amino acid differences observed in the VP2 protein only of the attenuated AHSV-4 isolate do not influence its ability to engage the cellular receptor(s) and therefore do not affect its ability to induce apoptosis. Since a virus stock of the attenuated AHSV-4 isolate is not available and taking into account that apoptosis could therefore not be quantified for this virus isolate, the results do not exclude the possibility that there may be differences in the extent or severity of apoptosis induced by the attenuated virus compared to the virulent AHSV-4 isolate. The results do, however, suggest that the observed amino acid differences may not play a role in the ability of VP2 to bind to the cellular receptor(s). Notably, it has been reported that sialic acid-binding reovirus strains induce high levels of apoptosis, whereas non-sialic acid-binding reovirus strains induce little or no apoptosis (Connolly *et al.*, 2001). Interestingly, it has been reported that VP2 of BTV binds to sialic acid at the surface of permissive cells (Hassan and Roy, 1999; Zhang *et al.*, 2010). The ability to produce large amounts of soluble biologically active AHSV VP2 protein may thus aid further studies to determine if binding to sialic acid is required for the induction of apoptosis and to identify regions within VP2 that may be required for this binding activity.

In summary, this investigation is the first to characterize the induction of apoptosis in AHSV-infected mammalian cells. The results indicated that steps in receptor binding and virion disassembly, but not those in viral replication subsequent to endosomal membrane penetration are required to induce apoptosis following AHSV infection. Moreover, the cellular pathways involved in AHSV-induced apoptosis involves both the intrinsic (mitochondrial) and extrinsic (death receptor) apoptotic pathways, and NF-κB was also implicated as playing a role in the AHSV apoptotic machinery. This information not only provides new insights into AHSV-host interactions, but also provides a platform for the study of AHSV disease mechanisms and has the potential to lead to the development of novel antiviral therapeutics capable of blocking apoptosis.

REFERENCES

Acehan, D., Jiang, X., Morgan, D.G., Heuser, J.E., Wang, X. & Akey, C.W. 2002, Three-dimensional structure of the apoptosome: implications for assembly, procaspase-9 binding, and activation, *Molecular Cell*, vol. 9, pp. 423-432.

Ahmad, M., Srinivasula, S.M., Wang, L., Talanian, R.V., Litwack, G., Fernandes-Alnemri, T. & Alnemri, E.S. 1997, CRADD, a novel human apoptotic adaptor molecule for caspase-2, and FasL/tumor necrosis factor receptor-interacting protein RIP, *Cancer Research*, vol. 57, pp. 615-619.

Alnemri, E.S., Livingston, D.J., Nicholson, D.W., Salvesen, G.S., Thornberry, N.A., Wong, W.W. & Yuan, J., 1996, Human ICE/CED-3 protease nomenclature, *Cell*, vol. 87, pp. 171.

Alonso, C., Miskin, J., Hernaez, B., Fernandez-Zapatero, P., Soto, L., Canto, C., Rodriguez-Crespo, I., Dixon, L. & Escribano, J.M. 2001, African swine fever virus protein p54 interacts with the microtubular motor complex through direct binding to light-chain dynein, *Journal of Virology*, vol. 75, pp. 9819-9827.

Altschul, S.F., Madden, T.L., Schaffer, A.A., Zhang, J., Zhang, Z., Miller, W. & Lipman, D.J. 1997, Gapped BLAST and PSI-BLAST: a new generation of protein database search programs, *Nucleic Acids Research*, vol. 25, pp. 3389-3402.

Anfinsen, C.B. 1973, Principles that govern the folding of protein chains, *Science*, vol. 181, pp. 223-227.

Anonymous, 1991, African horsesickness, in: *Manual of recommended diagnostic techniques and requirements for biological products for lists A & B diseases*, vol. II, Office International des Epizooties, Paris, France.

Ashe, P.C. & Berry, M.D. 2003, Apoptotic signaling cascades, *Progress in Neuro-Psychopharmacology & Biological Psychiatry*, vol. 27, pp. 199-214.

Ashkenazi, A. & Dixit, V.M. 1999, Apoptosis control by death and decoy receptors, *Current Opinion in Cell Biology*, vol. 11, pp. 255-260.

Baeuerle, P. & Baltimore, D. 1988. IκB: a specific inhibitor of the NF-κB transcription factor, *Science*, vol. 242, pp. 540-546.

Bagchi, P., Dutta, D., Chattopadhyay, S., Mukherjee, A., Halder, U.C., Sarkar, S., Kobayashi, N., Komoto, S., Taniguchi, K. & Chawla-Sarkar, M. 2010, Rotavirus nonstructural protein 1 suppresses virus-induced cellular apoptosis to facilitate viral growth by activating the cell survival pathways during early stages of infection, *Journal of Virology*, vol. 84, pp. 6834-6845.

Banerjee, M. & Johnson, J.E. 2008, Activation, exposure and penetration of virally encoded, membrane-active polypeptides during non-enveloped virus entry, *Current Protein and Peptide Science*, vol. 9, pp. 16-27.

Baneyx, F. 1999, Recombinant protein expression in *Escherichia coli*, *Current Opinion in Biotechnology*, vol. 10, pp. 411-421.

Bao, Q. & Shi, Y. 2007, Apoptosome: a platform for the activation of initiator caspases, *Cell Death and Differentiation*, vol. 14, pp. 56-65.

Barber, G.N. 2001, Host defense, viruses and apoptosis, *Cell Death and Differentiation*, vol. 8, pp. 113-126.

Barnard, J.H. 1998, Epidemiology of African horse sickness and the role of the zebra in South Africa, *Archives of Virology Supplementary*, vol. 14, pp. 13-19.

Barnes, W.A. 2011, Mapping the function of the NS3 protein of African horsesickness virus using RNAi and yeast two-hybrid analyses, MSc dissertation, University of Pretoria.

Barton, E.S., Chappell, J.D., Connolly, J.L., Forrest, J.C. & Dermody, T.S. 2001a, Reovirus receptors and apoptosis, *Virology*, vol. 290, pp. 173-180.

Barton, E.S., Forrest, J.C., Connolly, J.L., Chappell, J.D., Liu, Y., Schnell, F.J., Nusrat, A., Parkos, C.A. & Dermody, T.S. 2001b, Junction adhesion molecule is a receptor for reovirus, *Cell*, vol. 104, pp. 441-451.

Basak, A.K., Gouet, P., Grimes, J., Roy, P. & Stuart, D. 1996, Crystal structure of the top domain of African horse sickness virus VP7: comparison with Bluetongue virus VP7, *Journal of Virology*, vol. 70, pp. 3797-3806.

Beaton, A.R., Rodriguez, J., Reddy, Y.K. & Roy, P. 2002, The membrane trafficking protein calpactin forms a complex with bluetongue virus protein NS3 and mediates virus release, *Proceedings of the National Academy of Sciences, USA*, vol. 99, pp. 13154-13159.

Becker, M.M., Peters, T.R. & Dermody, T.S. 2003, Reovirus σNS and μNS proteins form cytoplasmic inclusion structures in the absence of viral infection, *Journal of Virology*, vol. 77, pp. 5948-5963.

Beg, A.A., Ruben, S.M., Scheinman, R.I., Haskill, S., Rosen, C.A. & Baldwin, A.S. 1992, I kappa B interacts with the nuclear localization sequences of the subunits of NF-kappa B: a mechanism for cytoplasmic retention, *Genes and Development*, vol. 6, pp. 1899-1913.

Benedict, C.A., Norris, P.S. & Ware, C.F. 2002, To kill or be killed: viral evasion of apoptosis, *Nature Immunology*, vol. 3, pp. 1013-1018.

Benedict, C.A., Norris, P.S., Prigozy, T.I., Bodmer, J-L., Mahr, J.A., Garnett, C.T., Martinon, F., Tschopp, J., Gooding, L.R. & Ware, C.F. 2001, Three adenovirus E3 proteins cooperate to evade apoptosis by tumor necrosis factor-related apoptosis-inducing ligand receptor-1 and -2, *Journal of Biological Chemistry*, vol. 276, pp. 3270-3278.

Bentley, L., Fehrsen, J., Jordaan, F., Huismans, H. & du Plessis, D.H. 2000, Identification of antigenic regions on VP2 of African horsesickness virus serotype 3 by using phage-displayed epitope libraries, *Journal of General Virology*, vol. 81, pp. 993-1000.

Bhattacharya, B. & Roy, P. 2008, Bluetongue virus outer capsid virus protein VP5 interacts with membrane lipid rafts via a SNARE domain, *Journal of Virology*, vol. 82, no. 21, pp. 10600-10612.

Bhattacharya, B., Noad, R.J. & Roy, P. 2007, Interaction between bluetongue virus outer capsid protein VP2 and vimentin is necessary for virus egress, *Virology Journal*, vol. 4, no. 7, pp. 1-12.

Birnbaum, M.J., Clem, R.J. & Miller, L.K. 1994, An apoptosis-inhibiting gene from a nuclear polyhedrosis virus encoding a polypeptide with Cys/His sequence motifs, *Journal of Virology*, vol. 68, pp. 2521-2528.

Blommel, P.G. & Fox, B.G. 2007, A combined approach to improving large-scale production of tobacco etch virus protease, *Protein Expression and Purification*, vol. 55, pp. 53-68.

Boatright, K.M., Renatus, M., Scott, F.L., Sperandio, S., Shin, H., Pedersen, I.M., Ricci, J-E., Edris, W.A., Sutherlin, D.P., Green, D.R. & Salvesen, G.S. 2003, A unified model for apical caspase activation, *Molecular Cell*, vol. 11, pp. 529-541.

Borucki, M.K., Kempf, B.J., Blair, C.D. & Beaty, B.J. 2001, The effect of mosquito passage on the La Crosse virus genotype, *Journal of General Virology*, vol. 82, pp. 2919-2926.

Borucki, M.K., Kempf, B.J., Blitvich, B.J., Blair, C.D. & Beaty, B.J. 2002, La Crosse virus: replication in vertebrates and invertebrate hosts, *Microbes and Infection*, vol. 4, pp. 341-350.

Boyce, F.M. & Bucher, N.L. 1996, Baculovirus-mediated gene transfer into mammalian cells, *Proceeding of the National Academy of Sciences, USA*, vol. 93, pp. 2348-2352.

Boyce, M., Wehrfritz, J., Noad, R. & Roy P. 2004, Purified recombinant bluetongue virus VP1 exhibits RNA replicase activity, *Journal of Virology*, vol. 78, no. 8, pp. 3994-4002.

Brancolini, C., Lazarevic, D., Rodriguez, J. & Schneider, C. 1997, Dismantling cell-cell contacts during apoptosis is coupled to a caspase-dependent proteolytic cleavage of β-catenin, *Journal of Cell Biology*, vol. 139, pp. 759-771.

Bremer, C.W. 1976, A gel electrophoretic study of the protein and nucleic acid components of African horsesickness virus, *Onderstepoort Journal of Veterinary Research*, vol. 43, no. 4, pp. 193-199.

Bremer, C.W., Huismans, H. & Van Dijk, A.A. 1990, Characterization and cloning of the African horsesickness virus genome, *Journal of General Virology*, vol. 71, pp. 793-799.

Brockman, J.A., Scherer, D.C., McKinsey, T.A., Hall, S.M., Qi, X., Lee, W.Y. & Ballard, D.W. 1995, Coupling of a signal response domain in I kappa B alpha to multiple pathways for NF-kappa B activation, *Molecular and Cellular Biology*, vol. 15, no. 5, pp. 2809–2818.

Brojatsch, J., Naughton, J., Rolls, M.M., Zingler, K. & Young, J.A. 1996, CAR1, a TNFR-related protein, is a cellular receptor for cytopathic avian leukosis-sarcoma viruses and mediates apoptosis, *Cell*, vol. 87, pp. 845-855.

Brookes, S.M., Hyatt, A.D. & Eaton, B.T. 1993, Characterization of virus inclusion bodies in bluetongue virus-infected cells, *Journal of General Virology*, vol. 74, pp. 525-530.

Brown, C.C. & Dardiri, A.H. 1990, African horsesickness: A continuing menace, *Journal of the American Veterinary Medical Association*, vol. 196, pp. 2019-2021.

Brown, M. & Faulkner, P. 1977, A plaque assay for nuclear polyhedrosis viruses using a solid overlay, *Journal of General Virology*, vol. 36, pp. 361-364.

Brown, S.E., Morrison, H.G., Karabatsos, N. & Knudson, D.L. 1991, Genetic relatedness of two new Orbivirus serogroups: Orungo and Lebombo, *Journal of General Virology*, vol. 72, pp. 1065-1072.

Brunk, U.T., Dalen, H., Roberg, K. & Hellquist, H.B. 1997, Photo-oxidative disruption of lysosomal membranes causes apoptosis of cultured human fibroblasts, *Free Radical Biology and Medicine*, vol. 23, pp. 616-626.

Buendia, B., Santa-Maria, A. & Courvalin, J.C. 1999, Caspase-dependent proteolysis of integral and peripheral proteins of nuclear membranes and nuclear pore complex proteins during apoptosis, *Cell Science*, vol. 112, pp. 1743-1753.

Burger, L. 2006, Silencing African horsesickness virus VP7 protein expression *in vitro* by RNA interference, MSc dissertation, University of Pretoria.

Burrage, T.G., Trevejo, R., Stone-Marschat, M. & Laegreid, W.W. 1993, Neutralizing epitopes of African horsesickness virus serotype 4 are located on VP2, *Virology*, vol. 196, pp. 799-803.

Burroughs, J.N., O'Hara, R.S., Smale, C.J., Hamblin, C., Walton, A., Armstrong, R. & Mertens, P.P.C. 1994, Purification and properties of virus particles, infectious subviral particles, cores and VP7 crystals of African horsesickness virus serotype 9, *Journal of General Virology*, vol. 75, pp. 1849-1857.

Burstein, E. & Duckett, C.S. 2003, Dying for NF-κB? Control of cell death by transcriptional regulation of the apoptotic machinery, *Current Opinion in Cell Biology*, vol. 15, pp. 732-737.

Cain, K., Brown, D.G., Langlais, C. & Cohen, G.M. 1999, Caspase activation involves the formation of the apoptosome, a large (~700 kDa) caspase-activating complex, *Journal of Biological Chemistry*, vol. 274, pp. 22686-22692.

Calisher, C.H. & Mertens, P.P.C. 1998, Taxonomy of African horse sickness viruses, *Archives of Virology Supplementary*, vol. 14, pp. 3-11.

Callus, B.A. & Vaux, D.L. 2007, Caspase inhibitors: viral, cellular and chemical, *Cell Death and Differentiation*, vol. 14, pp. 73-78.

Cao, G., Pei, W., Lan, J., Stetler, R.A., Luo, Y., Nagayama, T., Graham, S.H., Yin, X-M., Simon, R.P. & Chen, J. 2001, Caspase-activated Dnase/DNA fragmentation factor 40 mediates apoptotic DNA fragmentation in transient cerebral ischemia and in neuronal cultures, *The Journal of Neuroscience*, vol. 21, pp. 4678-4690.

Carrascosa, A.L., Bustos, M.J., Nogal, M.L., Gonzalez de Buitrago, G. & Revilla, Y. 2002, Apoptosis induced in an early step of African swine fever virus entry into Vero cells does not require virus replication, *Virology*, vol. 294, pp. 372-382.

Castro, A.E., Montague, S.R., Dotson, J.F., Jessup, D.A. & DeForge, J.R. 1989, Susceptibility of a fetal tongue cell line derived from Bighorn sheep to five serotypes of Bluetongue virus and its potential for the isolation of viruses, *Journal of Veterinary Diagnostic Investigation*, vol. 1, pp. 247-253.

Celma, C.C.P. & Roy, P. 2009, A viral non-structural protein regulates bluetongue virus trafficking and release, *Journal of Virology*, vol. 83, pp. 6806-6816.

Chacon, M.R., Almazan, F., Nogal, M.L., Vinuela, E. & Rodriguez, J.F. 1995, The African swine fever virus IAP homolog is a late structural polypeptide, *Virology*, vol. 214, pp. 670-674.

Chai, J., Du, C., Wu, J.W., Kyin, S., Wang, X. & Shi, Y. 2000, Structural and biochemical basis of apoptotic activation by Smac/DIABLO, *Nature*, vol. 406, pp. 855-862.

Chaïbi, C., Cotte-Laffitte, J., Sandré, C., Esclatine, A., Servin, A.L., Quéro, A-M. & Géniteau-Legendre, M. 2005, Rotavirus induces apoptosis in fully differentiated human intestinal Caco-2 cells, *Virology*, vol. 332, pp. 480-490.

Chang, D.W., Xing, Z., Capacio, V.L., Peter, M.E. & Yang, X. 2003, Interdimer processing mechanism of procaspase-8 activation, *The EMBO Journal*, vol. 22, pp. 4132-4142.

Chen, G. & Goeddel, D.V. 2002, TNF-R1 signaling: a beautiful pathway, *Science*, vol. 296, pp. 1634-1635.

Chen, X., Kandasamy, K. & Srivastava, R.K. 2003, Differential roles of Rel A (p65) and c-Rel subunits of nuclear factor κB in tumor necrosis factor-related apoptosis-inducing ligand signaling, *Cancer Research*, vol. 63, pp. 1059-1066.

Cheng, E.H., Wei, M.C., Weiler, S., Flavell, R.A., Mak, T.W., Lindsten, T. & Korsmeyer, S.J. 2001, Bcl-2, Bcl-X_L sequester BH3 domain-only molecules preventing Bax- and Bak-mediated mitochondrial apoptosis, *Molecular Cell*, vol. 8, pp. 705-711.

Chinchar, V.G., Bryan, L., Wang, J., Long, S. & Chinchar, G.D. 2003, Induction of apoptosis in frog virus 3-infected cells, *Virology*, vol. 306, pp. 303-312.

Chipuk, J.E. & Green, D.R. 2008, How do Bcl-2 proteins induce mitochondrial outer membrane permeabilization, *Trends in Cell Biology*, vol. 18, pp. 157-164.

Chiti, F., Stefani, M., Taddei, N., Ramponi, G. & Dobson, C.M. 2003, Rationalization of the effects of mutations on peptide and protein aggregation rates, *Nature*, vol. 424, pp. 805-808.

Chitnis, N.S., D'Costa, S.M., Paul, E.R. & Bilimoria, S.L. 2008, Modulation of iridovirus-induced apoptosis by endocytosis, early expression, JNK, and apical caspase, *Virology*, vol. 370, pp. 333-342.

Chowdhury, I., Tharakan, B. & Bhat, G.K. 2006, Current concepts in apoptosis: the physiological suicide program revisited, *Cellular and Molecular Biology Letters*, vol. 11, pp. 506-525.

Chowdhury, I., Tharakan, B. & Bhat, G.K. 2008, Caspases – An update, *Comparative Biochemistry and Physiology*, Part B, vol. 151, pp. 10-27.

Chuma, T., Le Blois, H., Sanchez-Vizcaino, J.M., Diaz-Laviada, M. & Roy, P. 1992, Expression of the major core antigen VP7 of African horsesickness virus by a recombinant baculovirus and its use as a group-specific diagnostic reagent, *Journal of General Virology*, vol. 73, pp. 925-931.

Ciccarone, V.C., Polayes, D.A. & Luckow, V.A. 1997, Generation of recombinant baculovirus DNA in *E. coli* using baculovirus shuttle vector, Humana Press Inc., Totowa.

Clarke, P. & Tyler, K.L. 2003, Reovirus-induced apoptosis: A minireview, *Apoptosis*, vol. 8, pp. 141-150.

Clarke, P. & Tyler, K.L. 2009, Apoptosis in animal models of virus-induced disease, *Nature Reviews Microbiology*, vol. 7, pp. 144-155.

Clarke, P., DeBiasi, R.L., Meintzer, S.M., Robinson, B.A. & Tyler, K.L. 2005, Inhibition of NF-kappa B activity and cFLIP expression contribute to viral-induced apoptosis, *Apoptosis*, vol. 10, pp. 513-524.

Clarke, P., Meintzer, S.M., Gibson, S., Widmann, C., Garrington, T.P., Johnson, G.L. & Tyler, K.L. 2000, Reovirus-induced apoptosis is mediated by TRAIL, *Journal of Virology*, vol. 74, pp. 8135-8139.

Clarke, P., Meintzer, S.M., Wang, Y., Moffitt, L.A., Richardson-Burns, S.M., Johnson, G.L. & Tyler, K.L. 2004, JNK regulates the release of proapoptotic mitochondrial factors in reovirus-infected cells, *Journal of Virology*, vol. 78, pp. 13132-13138.

Clarke, P., Meintzer, S.M., Widmann, C., Johnson, G.L. & Tyler, K.L. 2001, Reovirus infection activates JNK and the JNK-dependent transcription factor c-Jun, *Journal of Virology*, vol. 75, pp. 11275-11283.

Clavería, C. & Torres, M. 2003, Mitochondrial apoptotic pathways induced by *Drosophila* programmed cell death regulators, *Biochemical and Biophysical Research Communications*, vol. 304, pp. 531-537.

Clem, R.J. 2007, Baculoviruses and apoptosis: a diversity of genes and responses, *Current Drug Targets*, vol. 8, pp. 1069-1074.

Clem, R.J., Fechheimer, M. & Miller, L.K. 1991, Control of programmed cell death by the baculovirus genes *p35* and *iap*, *Science*, vol. 254, pp. 1388-1390.

Coetzer, J.A.W. & Erasmus, B.J. 1994, African horsesickness, in: J.A.W. Coetzer, G.R. Thomson & R.C. Tustin (Eds.), *Infectious diseases of livestock with special reference to Southern Africa*, vol. 1, Oxford University Press, Cape town, pp. 460-475.

Coffey, C.M., Sheh, A., Kim, I.S., Chandran, K., Nibert, M.L. & Parker, J.S. 2006, Reovirus outer capsid protein μ1 induces apoptosis and associates with lipid droplets, endoplasmic reticulum, and mitochondria, *Journal of Virology*, vol. 80, pp. 8422-8438.

Cohen, G.M. 1997, Caspase: the executioners of apoptosis, *Biochemical Journal*, vol. 326, pp. 1-16.

Coleman, M.L., Sahai, E.A., Yeo, M., Bosch, M., Dewar, A. & Olson, M.F. 2001, Membrane blebbing during apoptosis results from caspase-mediated activation of ROCK I, *Nature Cell Biology*, vol. 3, pp. 339-345.

Connolly, J.L. & Dermody, T.S. 2002, Virion disassembly is required for apoptosis induced by reovirus, *Journal of Virology*, vol. 76, no. 4, pp. 1632-1641.

Connolly, J.L., Barton, E.S. & Dermody T.S. 2001, Reovirus binding to cell surface sialic acid potentiates virus-induced apoptosis, *Journal of Virology*, vol. 75, no. 9, pp. 4029-4039.

Connolly, J.L., Rodgers, S.E., Clarke, P., Ballard, D.W., Kerr, L.D., Tyler, K.L. & Dermody, T.S. 2000, Reovirus-induced apoptosis requires activation of transcription factor NF-κB, *Journal of Virology*, vol. 74, no. 7, pp. 2981-2989.

Cory, S. & Adams, J.M. 2002, The Bcl-2 family: regulators of the cellular life-or-death switch, *Nature Reviews Cancer*, vol. 2, pp. 647-656.

Courageot, M-P., Catteau, A. & Desprès, P. 2003, Mechanisms of Dengue virus-induced cell death, *Advances in Virus Research*, vol. 60, pp. 157-186.

Cowley, J.A. & Gorman, B.M. 1987, Genetic reassortants for identification of the genome segment coding for the bluetongue virus hemagglutinin, *Journal of Virology*, vol. 61, pp. 2304-2306.

Cowley, J.A., Walker, P.J. & Gorman, B.M. 1992, Recognition sites in assembly of bluetongue viruses, in: T.E. Walton & B.I. Osborn (Eds.), *Bluetongue, African horse sickness and related orbiviruses, Proceedings of the Second International Symposium*, CRC Press, London, pp. 423-432.

Dagert, M. & Ehrlich, S.D. 1979, Prolonged incubation in calcium chloride improves the competence of *Escherichia coli* cells, *Gene*, vol. 6, pp. 23-38.

Danial, N.N. & Korsmeyer, S.J. 2004, Cell death: critical control points, *Cell*, vol. 116, pp. 205-219.

Danthi, P. 2011, Enter the kill zone: initiation of death signaling during virus entry, *Virology*, vol. 411, pp. 316-324.

Danthi, P., Coffey, C.M., Parker, J.S., Abel, T.W. & Dermody, T.S. 2008a, Independent regulation of reovirus membrane penetration and apoptosis by the mu1 phi domain, *PLoS Pathogens*, vol. 4, e1000248.

Danthi, P., Kobayashi, T., Holm, G.H., Hansberger, M.W., Abel, T.W. & Dermody, T.S. 2008b, Reovirus apoptosis and virulence are regulated by host cell membrane penetration efficiency, *Journal of Virology*, vol. 82, no. 1, pp. 161-172.

Danthi, P., Pruijssers, A.J., Berger, A.K., Holm, G.H., Zinkel, S.S. & Dermody, T.S. 2010, Bid regulates the pathogenesis of neurotropic reovirus, *PLoS Pathogens*, vol. 6, e1000980.

de Waal, P.J. & Huismans, H. 2005, Characterization of the nucleic acid binding activity of inner core protein VP6 of African horse sickness virus, *Archives of Virology*, vol. 150, pp. 2037-2050.

DeBiasi, R.L., Clarke, P., Meintzer, S., Jotte, R., Kleinschmidt-Demasters, B.K., Johnson, G.L. & Tyler, K.L. 2003, Reovirus-induced alteration in expression of apoptosis and DNA repair genes with potential roles in viral pathogenesis, *Journal of Virology*, vol. 77, pp. 8934-8947.

Degterev, A., Boyce, M. & Yuan, J. 2003, A decade of caspases, *Oncogene,* vol. 22, pp. 8543-8567.

DeMaula, C.D., Jutila, M.A., Wilson, D.W. & MacLachlan, N.J. 2001, Infection kinetics, prostacyclin release and cytokine-mediated modulation of the mechanism of cell death during bluetongue virus infection of cultured ovine and bovine pulmonary artery and lung microvascular endothelial cells, *Journal of General Virology*, vol. 82, pp. 787-794.

Deng, Y., Lin, Y. & Wu, X. 2002, TRAIL-induced apoptosis requires Bax-dependent mitochondrial release of Smac/DIABLO, *Genes and Development*, vol. 16, pp. 33-45.

Devaney, M.A., Kendall, J. & Grubman, M.J. 1988, Characterization of a non-structural phosphoprotein of two orbiviruses, *Virus Research*, vol. 11, pp. 151-164.

Deveraux, Q.L. & Reed, J.C. 1999, IAP family proteins – suppressors of apoptosis, *Genes and Development*, vol. 13, pp. 239-252.

Deveraux, Q.L., Roy, N., Stennicke, H.R., Van Arsdale, T., Zhou, Q., Srinivasula, S.M., Alnemri, E.S., Salvesen, G.S. & Reed, J.C. 1998, IAPs block apoptotic events induced by caspase-8 and cytochrome *c* by direct inhibition of distinct caspases, *The EMBO Journal*, vol. 17, pp. 2215-2223.

Deveraux, Q.L., Takahashi, R., Salvesen, G.S. & Reed, J.C. 1997, X-linked IAP is a direct inhibitor of cell-death proteases, *Nature*, vol. 388, pp. 300-304.

Devin, A., Lin, Y., Yamaoka, S., Li, Z., Karin, M. & Liu, Z.G. 2001, The α and β subunits of IkB kinase (IKK) mediate TRAF2-dependent IKK recruitment to tumor necrosis factor (TNF) receptor 1 in response to TNF, *Molecular and Cellular Biology*, vol. 21, pp. 3986-3994.

DiDonato, J., Mercurio, F., Rosette, C., Wu-Li, J., Suyang, H., Ghosh, S. & Karin, M. 1996, Mapping of the inducible IkB phosphorylation sites that signal its ubiquitination and degradation, *Molecular and Cellular Biology*, vol. 16, pp. 1295-1304.

DiDonato, J.A., Hayakawa, M., Rothwarf, D.M., Zandi, E. & Karin, M. 1997, A cytokine-responsive IkB kinase that activates the transcription factor NF-κB, *Nature*, vol. 388, pp. 548-554.

Dill, K.A. 1990, Dominant forces in protein folding, *Biochemistry*, vol. 29, pp. 7133-7155.

Dirks, W., Schaper, F., Kirchhoff, S., Morelle, C. & Hauser, H. 1994, A multifunctional vector family for gene expression in mammalian cells, *Gene*, vol. 149, pp. 387-388.

Dispersyn, G., Nuydens, R., Connors, R., Borgers, M. & Geerts, H. 1999, Bcl-2 protects against FCCP-induced apoptosis and mitochondrial membrane potential depolarization in PC12 cells, *Biochimica et Biophysica Acta – General Subjects*, vol. 1428, pp. 357-371.

Dobson, C.M. 2004, Principles of protein folding, misfolding and aggregation, *Seminars in Cell & Developmental Biology*, vol. 15, pp. 3-16.

du Plessis, M. & Nel, L.H. 1997, Comparative sequence analysis and expression of the M6 gene, encoding the outer capsid protein VP5, of African horsesickness virus serotype nine, *Virus Research*, vol. 47, pp. 41-49.

du Plessis, M., Cloete, M., Aitchison, H. & van Dijk, A.A. 1998, Protein aggregation complicates the development of baculovirus-expressed African horsesickness virus serotype 5 VP2 subunit vaccines, *Onderstepoort Journal of Veterinary Research*, vol. 65, pp. 321-329.

du Toit, R.M. 1944, The transmission of bluetongue and horse-sickness by *Culicoides*, *Onderstepoort Journal of Veterinary Science and Animal Industry*, vol. 19, pp. 7-16.

Du, C., Fang, M., Li, Y., Li, L. & Wang, X. 2000, Smac, a mitochondrial protein that promotes cytochrome c-dependent caspase activation by eliminating IAP inhibition, *Cell*, vol. 102, pp. 33-42.

Duckett, C.S., Nava, V.E., Gedrich, R.W., Clem, R.J., van Dongen, J.L., Gilfillan, M.C., Shiels, H., Hardwick, J.M. & Thompson, C.B. 1996, A conserved family of cellular genes related to the baculovirus *iap* gene and encoding apoptosis inhibitors, *The EMBO Journal*, vol. 15, pp. 2685-2694.

Duprez, L., Wirawan, E., Vanden Berghe, T. & Vandenabeele, P. 2009, Major cell death pathways at a glance, *Microbes and Infection*, vol. 11, pp. 1050-1062.

Dyson, M., Shadbolt, S.P., Vincent, K.J., Perera, R.L. & McCafferty, J. 2004, Production of soluble mammalian proteins in *Escherichia coli*: identification of protein features that correlate with successful expression, *BMC Biotechnology*, vol. 4, doi: 10.1186/1472-6750-4-32.

Earnshaw, W.A., Martins, L.M. & Kaufmann, S.H. 1999, Mammalian caspases: structure, activation, substrates, and functions during apoptosis, *Annual Review of Biochemistry*, vol. 68, pp. 383-424.

Earnshaw, W.C. 1995, Nuclear changes in apoptosis, *Current Opinion in Cell Biology*, vol. 7, pp. 337-343.

Eaton, B.T., Hyatt, A.D. & Brookes, S.M. 1990, The replication of bluetongue virus, *Current Topics in Microbiology and Immunology*, vol. 162, pp. 89-118.

Eaton, B.T., Hyatt, A.D. & White, J.R. 1988, Localization of the nonstructural protein NS1 in bluetongue virus-infected cells and its presence in virus particles, *Virology*, vol. 163, pp. 527-537.

Ekert, P.G., Silke, J., Hawkins, C.J., Verhagen, A.M. & Vaux, D.L. 2001, DIABLO promotes apoptosis by removing MIHA/XIAP from processed caspase-9, *Journal of Cell Biology*, vol. 152, pp. 483-490.

Elmore, S. 2007, Apoptosis: a review of programmed cell death, *Toxicologic Pathology*, vol. 35, pp. 495-516.

Erasmus, B.J. 1976, A new approach to polyvalent immunization against African horsesickness, Proceedings of the Fourth International Conference of Equine Infectious Diseases, Lyon, Princeton, N.J. Veterinary Publications, Inc., pp. 401-403.

Erasmus, B.J., Young, E., Pieterse, L.M. & Boshoff, S.T. 1978, The susceptibility of zebra and elephants to African horsesickness virus, *Journal of Equine Medicine and Surgery Supplementary*, vol. 1, pp. 409-413.

Fesik, S.W. 2000, Insights into programmed cell death through structural biology, *Cell*, vol. 103, pp. 273-282.

Fink, A.L. 1998, Protein aggregation: folding aggregates, inclusion bodies and amyloid, *Folding and Design*, vol. 3, pp. R9-R23.

Finkel, E. 2001, The mitochondrion: is it central to apoptosis? *Science*, vol. 292, pp. 624-626.

Fischer, U., Jänicke, R.U. & Schulze-Osthoff, K. 2003, Many cuts to ruin: a comprehensive update of caspase substrates, *Cell Death and Differentiation*, vol. 10, pp. 76-100.

Forzan, M., Marsh, M. & Roy, P. 2007, Bluetongue virus entry into cells, *Journal of Virology*, vol. 81, pp. 4819-4827.

Forzan, M., Wirblich, C. & Roy, P. 2004, A capsid protein of non-enveloped Bluetongue virus exhibits membrane fusion activity, *Proceedings of the National Academy of Sciences, USA*, vol. 101, no. 7, pp. 2100-2105.

Francki, R.I.B., Fauquet, C.M., Knudson, D.L. & Brown, F. 1991, Classification and nomenclature of viruses. Fifth report of the International Committee on Taxonomy of Viruses, *Archives of Virology Supplementary*, Springer, Wein New York.

French, T.J., Inumaru, S. & Roy, P. 1989, Expression of two related nonstructural proteins of bluetongue virus (BTV) type 10 in insect cells by a recombinant baculovirus: production of polyclonal ascetic fluid and characterization of the gene product in BTV-infected BHK cells, *Journal of Virology*, vol. 63, pp. 3270-3278.

Fuentes-Prior, P. & Salvesen, G.S. 2004, The protein structures that shape caspase activity, specificity, activation and inhibition, *Biochemistry Journal*, vol. 384, pp. 201-232.

Georgiou, G. & Segatori, L. 2005, Preparative expression of secreted proteins in bacteria: status report and future prospects, *Current Opinion in Biotechnology*, vol. 16, pp. 538-545.

Georgiou, G. & Valax, P. 1996, Expression of correctly folded proteins in *Escherichia coli*, *Current Opinion in Biotechnology*, vol. 7, pp. 190-197.

Ghosh, S., May, M.J. & Kopp, E.B. 1998, NF-kappa B and Rel proteins: evolutionarily conserved mediators of immune responses, *Annual Review of Immunology*, vol. 16, pp. 225-260.

Golks, A., Brenner, D., Fritsch, C., Krammer, P.H. & Lavrik, I.N. 2005, C-FLIPR: a new regulator of death receptor-induced apoptosis, *Journal of Biological Chemistry*, vol. 280, pp. 14507-14513.

Gombart, A.F., Pearson, M.N., Rohrmann, G.F. & Beaudreau, G.S. 1989, A baculovirus polyhedral envelope-associated protein: genetic location, nucleotide sequence, and immunocytochemical characterization, *Virology*, vol. 169, pp. 182-193.

Gómez-Villamandos, J.C., Sánchez, C., Carrasco, L., Laviada, M.D., Bautista, M.J., Martínez-Torrecuadrada, J., Sánchez-Vizcaíno, J.M. & Sierra, M.A. 1999, Pathogenesis of African horse sickness: Ultrastructural study of the capillaries in experimental infection, *Journal of Comparative Pathology*, vol. 121, pp. 101-116.

Gorman, B.M. & Taylor, J. 1985, Orbiviruses, in: B.N. Fields & D.M. Knipe (Eds.), *Field's Virology*, Raven Press, New York, pp. 275-278.

Gorman, B.M. 1979, Variation in Orbiviruses, *Journal of General Virology*, vol. 44, pp. 1-15.

Gorman, B.M. 1983, On the evolution of Orbiviruses, *Intervirology*, vol. 20, pp. 169-180.

Gorman, B.M. 1985, Speciation in orbiviruses, *Progress in Clinical and Biological Research*, vol. 178, pp. 275-278.

Gorman, B.M. 1992, An overview of orbiviruses, in: T.E. Walton & B.I. Osburn (Eds.), *Bluetongue, African horse sickness and related orbiviruses, Proceedings of the Second International Symposium*, CRC Press, London, pp. 335-348.

Gould, A.R. & Hyatt, A.D. 1994, The orbivirus genus. Diversity, structure, replication and phylogenetic relationships, *Comparative Immunology, Microbiology and Infectious Diseases*, vol. 17, pp. 163-188.

Grimes, J.M., Burroughs, J.N., Gouet, P., Diprose, J.M., Malby, R. Ziéntara, S., Mertens, P.P.C. & Stuart, D.I. 1998, The atomic structure of the bluetongue virus core, *Nature*, vol. 395, pp. 470-478.

Gross, A., Yin, X.M., Wang, K., Wei, M.C., Jockel, J., Milliman, C., Erdjument-Bromage, H., Tempst, P. & Korsmeyer, S.J. 1999, Caspase-cleaved Bid targets mitochondria and is required for cytochrome c release, while Bcl-X_L prevents this release but not tumor necrosis factor-R1/Fas death, *Journal of Biological Chemistry*, vol. 274, pp. 1156-1163.

Grubman, M.J. & Lewis, S.A. 1992, Identification and characterization of the structural and non-structural proteins of African horse sickness virus and determination of the genome coding assignments, *Virology*, vol. 186, pp. 444-451.

Guirakhoo, F., Catalan, J.A. & Monath, T.P. 1995, Adaptation of bluetongue virus in mosquito cells results in overexpression of NS3 proteins and release of virus particles, *Archives of Virology*, vol. 140, pp. 967-974.

Guthrie, A.J. 2007, African horse sickness, in: D.C. Sellon & M.T. Long (Eds.), *Equine infectious diseases*, Saunders Elsevier, St Louis, pp. 164-171.

Hall, T.A. 1999, BioEdit: a user-friendly biological sequence alignment editor and analysis program for Windows 95/98NT, *Nucleic Acids Symposium*, Series 41, pp. 95-98.

Han, Z. & Harty, R.N. 2004, The NS3 protein of bluetongue virus exhibits viroporin-like properties, *Journal of Biological Chemistry*, vol. 279, pp. 43092-43097.

Hanon, E., Keil, G., van Drunen Littel-van den Hurk, S., Griebel, P., Vanderplasschen, A., Rijsewijk, F.A., Babiuk, L. & Pastoret, P.P. 1999, Bovine herpesvirus 1-induced apoptotic cell death: role of glycoprotein D, *Virology*, vol. 257, pp. 191-197.

Harrison, S.C. 2008, Viral membrane fusion, *Nature Structural and Molecular Biology*, vol. 15, pp. 690-698.

Hartley, J.A. 2005, Cloning technologies for protein expression and purification, *Current Opinion in Biotechnology*, vol. 17, pp. 359-366.

Hassan, S.H., Wirblich, C., Forzan, M. & Roy, P. 2001, Expression and functional characterization of bluetongue virus VP5 protein: role in cellular permeabilization, *Journal of Virology*, vol. 75, no. 18, pp. 8356-8367.

Hassan, S.S. & Roy, P. 1999, Expression and functional characterization of bluetongue virus VP2 protein: role in cell entry, *Journal of Virology*, vol. 73, no. 12, pp. 9832-9842.

Hay, S. & Kannourakis, G. 2002, A time to kill: viral manipulation of the cell death program, *Journal of General Virology*, vol. 83, pp. 1547-1564.

Hayama, E. & Li, J.K. 1994, Mapping and characterization of antigenic epitopes and the nucleic acid-binding domains of VP6 protein of bluetongue viruses, *Journal of Virology*, vol. 68, pp. 3604-3611.

Hayden, M.S. & Ghosh, S. 2008, Shared principles in NF-κB signaling, *Cell*, vol. 132, pp. 344-362.

Helenius, A. 2007, Virus entry and uncoating, in: D.M. Knipe & P.M. Howley (Eds.), *Fields Virology*, 5th Ed. Lippincott Williams & Wilkins, Philadelphia, pp. 99-118.

Hengartner, M.O. 2000, The biochemistry of apoptosis, *Nature*, vol. 407, pp. 770-776.

Hernáez, B., Diaz-Gil, G., Garćia-Gallo, M., Ignacio Quetglas, J., Rodŕiquez-Crespo, I., Dixon, L., Escribano, J.M. & Alonso, C. 2004, The African swine fever virus dynein-binding protein p54 induces infected cell apoptosis, *FEBS Letters*, vol. 569, pp. 224-228.

Herren, B., Levkau, B., Raines, E.W. & Ross, R. 1998, Cleavage of β-catenin and plakoglobin and shedding of VE-cadherin during endothelial apoptosis: evidence for a role for caspases and metalloproteinases, *Molecular Biology of the Cell*, vol. 9, pp. 1589-1601.

Hewat, E.A., Booth, T.F. & Roy, P. 1992, Structure of bluetongue virus particles by cyroelectron microscopy, *Journal of Structural Biology*, vol. 109, pp. 61-69.

Hewish, D.R. & Burgoyne, L.A. 1973, Chromatin substructure. The digestion of chromatin DNA at regularly spaced sites by a nuclear deoxyribonuclease, *Biochemical and Biophysical Research Communications*, vol. 52, pp. 504-510.

Heytler, P.G. & Prichard, W.W. 1962, A new class of uncoupling agents - carbonyl cyanide phenylhydrazones, *Biochemical and Biophysical Research Communications*, vol. 7, pp.272-275.

Hofmann, C., Sandig, V., Jennings, G., Rudolph, M., Schlag, P. & Strauss, M. 1995, Efficient gene transfer into human hepatocytes by baculovirus vectors, *Proceeding of the National Academy of Sciences, USA*, vol. 92, pp. 10099-10103.

Hong, J-R., Guan, B-J., Her, G.M., Evensen, O., Santi, N. & Wu, J-L. 2008, Aquatic birnavirus infection activates the transcription factor NF-κB via tyrosine kinase signalling leading to cell death, *Journal of Fish Diseases*, vol. 31, pp. 451-460.

Horscroft, N.J. & Roy, P. 2000, NTP binding and phosphohydrolase activity associated with purified bluetongue virus non-structural protein NS2, *Journal of General Virology*, vol. 81, pp. 1961-1965.

House, J.A. 1998, Future international management of African horse sickness vaccines, *Archives of Virology Supplementary*, vol. 14, pp. 297-304.

Howell, P.G. 1960, The 1960 epizootic in the Middle East and SW Asia, *Journal of the South African Veterinary Medical Association*, vol. 31, pp. 329-334.

Howell, P.G. 1962, The isolation and identification of further antigenic types of African horse sickness virus, *Onderstepoort Journal of Veterinary Research*, vol. 29, pp. 139-149.

Hu, Y., Ding, L., Spencer, D.M. & Nunez, G. 1998, WD-40 repeat region regulates Apaf-1 self-association and procaspase-9 activation, *Journal of Biological Chemistry*, vol. 273, pp. 33489-33494.

Huang, B., Eberstadt, M., Olejniczak, E.T., Meadows, R.P. & Fesik, S.W. 1996, NMR structure and mutagenesis of the Fas (APO-1/CD95) death domain, *Nature*, vol. 384, pp. 638-641.

Huang, Y., Rich, R.L., Myszka, D.G. & Wu, H. 2003, Requirement of both the second and third BIR domains for the relief of X-linked inhibitor of apoptosis protein (XIAP)-mediated caspase inhibition by Smac, *Journal of Biological Chemistry*, vol. 278, pp. 49517-49522.

Huismans, H. & Els, H.J. 1979, Characterization of the tubules associated with the replication of three different orbiviruses, *Virology*, vol. 92, pp. 397-406.

Huismans, H. & Erasmus, B.J. 1981, Identification of the serotype-specific and group-specific antigens of bluetongue virus, *Onderstepoort Journal of Veterinary Research*, vol. 48, pp. 1-58.

Huismans, H. 1979, Protein synthesis in bluetongue virus-infected cells, *Virology*, vol. 92, pp. 385-396.

Huismans, H., van der Walt, N.T., Cloete, M. & Erasmus, B.J. 1983, The biochemical and immunological characterization of bluetongue virus outer capsid polypeptides, in: R.W. Compans & D.H.L. Bishop (Eds.), *Double-stranded RNA Viruses*, New York, Elsevier, pp. 165-172.

Huismans, H., van Dijk, A.A. & Bauskin, A.R. 1987, *In vitro* phophorylation and purification of a nonstructural protein of bluetongue virus with affinity for single-stranded RNA, *Journal of Virology*, vol. 61, pp. 3589-3595.

Huismans, H., van Staden, V., Fick, W.C., van Niekerk, M. & Meiring, T.L. 2004, A comparison of different orbivirus proteins that could affect virulence and pathogenesis, *Veterinaria Italiana*, vol. 40, pp. 417-425.

Huynh, C.Q. & Zieler, H. 1999, Construction of modular and versatile plasmid vectors for the high-level expression of single or multiple genes in insects and insect cell lines, *Journal of Molecular Biology*, vol. 288, pp. 13-20.

Hyatt, A.D. & Eaton, B.T. 1988, Ultrastructural distribution of the major capsid proteins within bluetongue virus and infected cells, *Journal of General Virology*, vol. 69, pp. 805-815.

Hyatt, A.D., Eaton, B.T. & Brookes, S.M. 1989, The release of bluetongue virus from infected cells and their superinfection by progeny virus, *Virology*, vol. 173, pp. 21-34.

Hyatt, A.D., Eaton, B.T. & Lunt, R. 1987, The grid-cell-culture technique: the direct examination of virus-infected cells and progeny viruses, *Journal of Microscopy*, vol. 145, pp. 97-106.

Hyatt, A.D., Zhao, Y. & Roy, P. 1993, Release of bluetongue virus-like particles from insect cells is mediated by BTV nonstructural protein NS3/NS3A, *Virology*, vol. 193, pp. 592-603.

Inumaru, S., Ghiasi, H. & Roy, P. 1987, Expression of bluetongue virus group-specific antigen VP3 in insect cells by a baculovirus vector: its use for detection of bluetongue virus antibodies, *Journal of General Virology*, vol. 68, pp. 1627-1635.

Isakovic, A., Jankovic, T., Harhaji, L., Kostic-Rajacic, S., Nikolic, Z., Vajs, V. & Trajkovic, V. 2008, Antiglioma action of xanthones from *Gentiana kochiana*: mechanistic and structure-activity requirements, *Bioorganic & Medicinal Chemistry*, vol. 16, pp. 5683-5694.

Isler, J.A., Skalet, A.H. & Alwine, J.C. 2005, Human cytomegalovirus infection activates and regulates the unfolded protein response, *Journal of Virology*, vol. 79, pp. 6890-6899.

Itoh, M., Isegawa, Y., Hotta, H. & Homma, M. 1997, Isolation of an avirulent mutant of Sendai virus with two amino acid mutations from a highly virulent field strain through adaptation to LLC-MK2 cells, *Journal of General Virology*, vol. 78, pp. 3207-3215.

Itoh, N., Yonehara, S., Ishii, A., Yonehara, M., Mizushima, S.I., Sameshima, M., Hase, A., Seto, Y. & Nagata, S. 1991, The polypeptide encoded by the cDNA for human cell surface antigen Fas can mediate apoptosis, *Cell*, vol. 66, pp. 233-243.

Jackson, A.C. & Rossiter, J.P. 1997, Apoptosis plays an important role in experimental rabies virus infection, *Journal of Virology*, vol. 71, pp. 5603-5607.

Jan, J.T. & Griffin, D.E. 1999, Induction of apoptosis by Sindbis virus occurs at cell entry and does not require viral replication, *Journal of Virology*, vol. 73, pp. 10296-10302.

Jarvis, D.L. 2009, Baculovirus-insect cell expression systems, *Methods in Enzymology*, vol. 463, pp. 191-222.

Johnson, C.R. & Jarvis, W.D. 2004, Caspase-9 regulation: an update, *Apoptosis*, vol. 9, pp. 423-427.

Jonasson, P., Liljeqvist, S., Nygren, A. & Ståhl, S. 2002, Genetic design for facilitated production and recovery of recombinant proteins in *Escherichia coli*, *Biotechnology and Applied Biochemistry*, vol. 35, pp. 91-105.

Jung, E. & Williams, K.L. 1997, The production of recombinant glycoproteins with special reference to simple eukaryotes including *Dictyostelium discoideum*, *Biotechnology and Applied Biochemistry*, vol. 25, pp. 3-8.

Kar, A.K., Bhattacharya, B. & Roy, P. 2007, Bluetongue virus RNA binding protein NS2 is a modulator of viral replication and assembly, *BMC Molecular Biology*, vol. 8, no. 4.

Karin, M. & Lin, A. 2002, NF-kappaB at the crossroads of life and death, *Nature Immunology*, vol. 3, pp. 221-227.

Karpf, A.R. & Brown, D.T. 1998, Comparison of Sindbis virus-induced pathology in mosquito and vertebrate cell culture, *Virology*, vol. 240, pp. 193-201.

Kasibhatla, S., Genestier, L. & Green, D.R. 1999, Regulation of Fas-ligand expression during activation-induced cell death in T lymphocytes via nuclear factor κB, *Journal of Biological Chemistry*, vol. 274, pp. 987-992.

Kerr, J.F.R., Bishop, C.J. & Searle, J. 1984, Apoptosis, in: P.P. Anthony & R.N.M. MacSween (Eds.), *Recent Advances in Histo-pathology*, vol. 12, Churchill Livingstone, Edinburgh, pp. 1-15.

Kerr, J.F.R., Wyllie, A.H. & Currie, A.R. 1972, Apoptosis: a basic biological phenomenon with wide-ranging implications in tissue kinetics, *British Journal of Cancer*, vol. 26, pp. 239-257.

Kidd, I.M. & Emery, V.C. 1993, The use of baculoviruses as expression vectors, *Applied Biochemistry and Biotechnology*, vol. 42, pp. 137-159.

Kiefer, M.C., Brauer, M.J., Powers, V.C., Wu, J.J., Umansky, S.R., Tomei, L.D. & Barr, P.J. 1995, Modulation of apoptosis by the widely distributed Bcl-2 homologue Bak, *Nature*, vol. 374, pp. 736-739.

King, L.A. & Possee, R.D. 1992, The baculovirus expression system: A laboratory guide, Chapman & Hall, New York, NY (USA).

Kischkel, F.C., Lawrence, D.A., Tinel, A., LeBlanc, H., Virmani, A., Schow, P., Gazdar, A., Blenis, J., Arnott, D. & Ashkenazi, A. 2001, Death receptor recruitment of endogenous caspase-10 and apoptosis initiation in the absence of caspase-8, *Journal of Biological Chemistry*, vol. 276, pp. 46639-46646.

Knudson, D.L. & Monath, T.P. 1990, Orbiviruses, in: B.N. Fields & D.M. Knipe (Eds.), *Field's Virology*, Raven Press, New York, pp. 1405-1433.

Kominsky, D.J., Bickel, R.J. & Tyler, K.L. 2002, Reovirus-induced apoptosis requires both death receptor- and mitochondrial-mediated caspase-dependent pathways of cell death, *Cell Death and Differentiation*, vol. 9, pp. 926-933.

Kornberg, R.D. 1974, Chromatin structure: a repeating unit of histones and DNA, *Science*, vol. 184, pp. 868-871.

Kornbluth, S. & White, K. 2005, Apoptosis in *Drosophila*: Neither fish nor fowl (nor man, nor worm), *Journal of Cell Science*, vol. 118, pp. 1779-1787.

Korsman, J.N. 2007, Characterization and sequence variation of the virulence-associated proteins of different tissue culture isolates of African horsesickness virus serotype 4, MSc dissertation, University of Pretoria.

Korsmeyer, S.J., Wei, M.C., Saito, M., Weiler, S., Oh, K.J. & Schlesinger, P.H. 2000, Pro-apoptotic cascade activates Bid, which oligomerizes Bak or Bax into pores that results in the release of cytochrome c, *Cell Death and Differentiation*, vol. 7, pp. 1166-1173.

Kost, T.A. & Condreay, J.P. 1999, Recombinant baculoviruses as expression vectors for insect and mammalian cells, *Current Opinion in Biotechnology*, vol. 10, pp. 428-433.

Kothakota, S., Azuma, T., Reinhard, C., Klippel, A., Tang, J., Chu, K., McGarry, T.J., Kirschner, M.W., Koths, K., Kwiatkowski, D.J. & Williams, L.T. 1997, Caspase-3-generated fragment of gelsolin: effector of morphological change in apoptosis, *Science*, vol. 278, pp. 294-298.

Kucharczak, J., Simmons, M.J., Fan, Y. & Gelinas, C. 2003, To be, or not to be: NF-κB is the answer - role of Rel/NF-κB in the regulation of apoptosis, *Oncogene*, vol. 22, pp. 8961-8982.

Kuwana, T., Bouchier-Hayes, L., Chipuk, J.E., Bonzon, C., Sullivan, B.A., Green, D.R. & Newmeyer, D.D. 2005, BH3 domains of BH3-only proteins differentially regulate Bax-mediated mitochondrial membrane permeabilization both directly and indirectly, *Molecular Cell*, vol. 17, pp. 525-535.

Labrada, L., Bodelón, G., Viñuela, J. & Benavente, J. 2002, Avian reoviruses cause apoptosis in cultured cells: viral uncoating, but not viral gene expression, is required for apoptosis induction, *Journal of Virology*, vol. 76, pp. 7932-7941.

Laegreid, W.W., Burrage, T.G., Stone-Marschat, M. & Skowronek, A. 1992, Electron microscopic evidence for endothelial infection by African horsesickness virus, *Veterinary Pathology*, vol. 29, pp. 554-556.

Laemmli, U.K. 1970, Cleavage of structural proteins during the assembly of the head of bacteriophage T4, *Nature*, vol. 227, pp. 680-685.

Lamkanfi, M., Festjens, N., Declercq, W., Vanden Berghe, T. & Vandenabeele, P. 2007, Caspases in cell survival, proliferation and differentiation, *Cell Death and Differentiation*, vol. 14, pp. 44-55.

Le Blois, H., French, T., Mertens, P.P.C., Burroughs, J.N. & Roy, P. 1992, The expressed VP4 protein of bluetongue virus binds GTP and is the candidate guanylyl transferase of the virus, *Virology*, vol. 189, pp. 757-761.

Lewis, J., Wesselingh, S.L., Griffin, D.E. & Hardwick, J.M. 1996, Alphavirus-induced apoptosis in mouse brains correlates with neurovirulence, *Journal of Virology*, vol. 70, pp. 1828-1835.

Li, H., Zhu, H., Xu, C.J. & Yuan, J. 1998, Cleavage of Bid by caspase-8 mediates the mitochondrial damage in the Fas pathway of apoptosis, *Cell*, vol. 94, pp. 491-501.

Li, J. & Yuan, J. 2008, Caspases in apoptosis and beyond, *Oncogene*, vol. 27, pp. 6194-6206.
Li, P., Nijhawan, D., Budihardjo, I., Srinivasula, S.M., Ahmad, M., Alnemri, E.S. & Wang, X. 1997, Cytochrome c and dATP-dependent formation of Apaf-1/caspase-9 complex initiates an apoptotic protease cascade, *Cell*, vol. 91, pp. 479-489.

Li, S., Zhao, Y., He, X., Kim, T-H., Huharsky, D.K., Rabinowich, H., Chen, J., Du, C. & Yin, X-M. 2002, Relief of extrinsic pathway inhibition by the Bid-dependent mitochondrial release of Smac in Fas-mediated hepatocyte apoptosis, *Journal of Biological Chemistry*, vol. 277, pp. 26912-26920.

Li, W., Yuan, X., Nordgren, G., Dalen, H., Dubowchik, G.M., Firestone, R.A. & Brunk, U.T. 2000, Induction of cell death by the lysosomotropic detergent MSDH, *FEBS Letters*, vol. 470, pp. 35-39.

Licari, P. & Bailey, J.E. 1992, Modelling the population dynamics of baculovirus-infected insect cells: optimizing infection strategies for enhanced recombinant protein yields, *Biotechnology and Bioengineering*, vol. 39, pp. 433-441.

Lin, K.I., Lee, S.H., Narayanan, R., Baraban, J.M., Hardwick, J.M. & Ratan, R.R. 1995, Thiol agents and Bcl-2 identify an alphavirus-induced apoptotic pathway that requires activation of the transcription factor NF-kappa B, *The Journal of Cell Biology*, vol. 131, pp. 1149-1161.

Lin, P-Y., Liu, H-J., Liao, M-H., Chang, C-D., Chang, C-I., Cheng, H-L., Lee, J-W. & Shih, W-L. 2010, Activation of PI 2-kinase/Akt/NF-κB and Stat3 signaling by avian reovirus S1133 in the early stages of infection results in an inflammatory response and delayed apoptosis, *Virology*, vol. 400, pp. 104-114.

Linskens, M.H.K., Grootenhuis, P.D.J., Blaauw, M., Huisman-De Winkel, B., Van Ravestein, A., Van Haastert, P.J.M. & Heikoop, J.C. 1999, Random mutagenesis and screening of complex glycoproteins: expression of human gonadotropins in *Dictyostelium discoideum*, *The FASEB Journal*, vol. 13, pp. 639-645.

Liston, P., Roy, N., Tamai, K., Lefebvre, C., Baird, S., Cherton-Horvat, G., Farahani, R., McLean, M., Ikeda, J.E., MacKenzie, A.E. & Korneluk, R.G. 1996, Suppression of apoptosis in mammalian cells by NAIP and a related family of IAP genes, *Nature*, vol. 379, pp. 349-353.

Liu, S. & Chen, Z.J. 2011, Expanding role of ubiquitination in NF-κB signalling, *Cell Research*, vol. 21, pp.6-21.

Liu, Y., Cai, Y. & Zhang, X. 2003, Induction of caspase-dependent apoptosis in cultures rat oligodendrocytes by murine coronavirus is mediated during cell entry and does not require virus replication, *Journal of Virology*, vol. 77, pp. 11952-11963.

Liu, Z., Sun, C., Oleniczak, E.T., Meadows, R.P., Betz, S.F., Oost, T., Herrmann, J., Wu, J.C. & Fesik, S.W. 2000, Structural basis for binding of Smac/DIABLO to the XIAP BIR3 domain, *Nature*, vol. 408, pp. 1004-1008.

Loudon, P.T. & Roy, P. 1992, Interaction of nucleic acids with core-like and subcore-like particles of bluetongue virus, *Virology*, vol. 191, pp. 231-236.

Lowy, R.J. 2003, Influenza virus induction of apoptosis by intrinsic and extrinsic mechanisms, *International Reviews of Immunology*, vol. 22, pp. 425-449.

Lubroth, J. 1988, African horsesickness and the epizootic in Spain 1987, *Equine Practice*, vol. 10, pp. 26-33.

Luckow, V.A. & Summers, M.D. 1988, Trends in the development of baculovirus expression vectors, *Nature Biotechnology*, vol. 6, pp. 47-55.

Luckow, V.A., Lee, S.C., Barry, G.F. & Olins, P.O. 1993, Efficient generation of infectious recombinant baculoviruses by site-specific transposon-mediated insertion of foreign genes into a baculovirus genome propagated in *Escherichia coli*, *Journal of Virology*, vol. 67, pp. 4566-4579.

Luo, X., Budihardjo, I., Zou, H., Slaughter, C. & Wang, X. 1998, Bid, a Bcl-2 interacting protein, mediates cytochrome *c* release from mitochondria in response to activation of cell surface death receptors, *Cell*, vol. 94, pp. 481-490.

Lymperopoulos, K., Wirblich, C., Brierley, I. & Roy, P. 2003, Sequence specificity in the interaction of bluetongue virus non-structural protein 2 (NS2) with viral RNA, *Journal of Biological Chemistry*, vol. 278, pp. 31722-31730.

MacLachlan, N.J., Balasuriya, U.B., Davis, N.L., Collier, M., Johnston, R.E., Ferraro, G.L. & Guthrie, A.J. 2007, Experiences with new generation vaccines against equine viral arteritis, West Nile disease and African horse sickness, *Vaccine*, vol. 25, pp. 5577-5582.

Madden, D.R. & Safferling, M. 2007, Baculoviral expression of an integral membrane protein for structural studies, *Methods in Molecular Biology*, vol. 363, pp. 39-57.

Maiorella, B., Inlow, D., Shauger, A. & Horano, D. 1988, Large-scale insect cell culture for recombinant protein production, *Biotechnology*, vol. 6, pp. 1406-1410.

Makrides, S.C. 1999, Components of vectors for gene transfer and expression in mammalian cells, *Protein Expression and Purification*, vol. 17, pp. 183-202.

Malissard, M. & Berger, E.G. 2001, Improving solubility of catalytic domain of human β-1,4-galactosyltransferase 1 through rationally designed amino acid replacements, *European Journal of Biochemistry*, vol. 268, pp. 4352-4358.

Maree, F.F. & Huismans, H. 1997, Characterization of tubular structures composed of nonstructural protein NS1 of African horsesickness virus expressed in insect cells, *Journal of General Virology*, vol. 78, pp. 1077-1082.

Maree, S. & Paweska, J.T. 2005, Preparation of recombinant African horse sickness virus VP7 antigen via a simple method and validation of a VP7-based indirect ELISA for the detection of group-specific IgG antibodies in horse sera, *Journal of Virological Methods*, vol. 125, pp. 55-65.

Maree, S., Durbach, S. & Huismans, H. 1998, Intracellular production of African horsesickness virus core-like particles by expression of the two major core proteins, VP3 and VP7, in insect cells, *Journal of General Virology*, vol. 79, pp. 333-337.

Markovic, Z., Todorovic-Markovic, B., Kleut, D., Nikolic, N., Vranjes-Djuric, S., Misirkic, M., Vucicevic, L., Janjetovic, K., Isakovic, A., Harhaji, L., Babic-Stojic, B., Dramicanin, M. & Trajkovic, V. 2007, The mechanism of cell-damaging reactive oxygen generation by colloidal fullerenes, *Biomaterials*, vol. 28, pp. 5437-5448.

Marshall, J.J.A. & Roy, P. 1990, High level expression of the two outer capsid proteins of bluetongue virus serotype 10: their relationship with the neutralization of virus infection, *Virus Research*, vol. 15, pp. 189-195.

Martelli, A.M., Zweyer, M., Ochs, R.L., Tazzari, P.L., Tabellini, G., Narducci, P. & Bortul, R. 2001, Nuclear apoptotic changes: an overview, *Journal of Cellular Biochemistry*, vol. 82, pp. 634-646.

Martínez-Torrecuadrada, J.L., Diaz-Laviada, M., Roy, P., Sanchez, C., Vela, C., Sanchez-Vizcaino, J.M. & Casal, J.I. 1996, Full protection against African horsesickness (AHS) in horses induced by baculovirus-derived AHS virus serotype 4 VP2, VP5 and VP7, *Journal of General Virology*, vol. 77, pp. 1211-1221.

Martínez-Torrecuadrada, J.L., Iwata, H., Venteo, A., Casal, I. & Roy, P. 1994, Expression and characterization of the two outer capsid proteins of African horsesickness virus: the role of VP2 in virus neutralization, *Virology*, vol. 202, pp. 348-359.

Martínez-Torrecuadrada, J.L., Langeveld, J.P., Meloen, R.H. & Casal, J.I. 2001, Definition of neutralizing sites on African horse sickness virus serotype 4 VP2 at the level of peptides, *Journal of General Virology*, vol. 82, pp. 2415-2424.

Martínez-Torrecuadrada, J.L., Langeveld, J.P., Venteo, A., Sanz, A., Dalsgaard, K., Hamilton, W.D., Meloen, R.H. & Casal, J.I. 1999, Antigenic profile of African horse sickness virus serotype 4 VP5 and identification of a neutralizing epitope shared with bluetongue virus and epizootic hemorrhagic disease virus, *Virology*, vol. 257, pp. 449-459.

Martin-Latil, S., Mousson, L., Autret, A., Colbère-Garapin, F. & Blondel, B. 2007, Bax is activated during Rotavirus-induced apoptosis through the mitochondrial pathway, *Journal of Virology*, vol. 81, pp. 4457-4464.

Martinon, F., Hofmann, K. & Tschopp, J. 2001, The pyrin domain: a possible member of the death domain-fold family implicated in apoptosis and inflammation, *Current Biology*, vol. 11, pp. R118-R120.

Matsuura, Y., Possee, R.D., Overton, H.A. & Bishop, D.H.L. 1987, Baculovirus expression vectors: the requirement for high level expression of proteins, including glycoproteins, *Journal of General Virology*, vol. 68, pp. 1233-1250.

Matsuyama, S., Llopis, J., Deveraux, Q.L., Tsien, R.Y. & Reed, J.C. 2000, Changes in intra-mitochondrial and cytosolic pH: early events that modulate caspase activation during apoptosis, *Nature Cell Biology*, vol. 2, pp. 318-325.

May, M.J. & Ghosh, S. 1997, Rel/NF-kappa B and I kappa B proteins: an overview, *Seminars in Cancer Biology*, vol. 8, pp. 63-73.

McCarthy, S.A., Symonds, H.S. & Van Dyke, T. 1994, Regulation of apoptosis in transgenic mice by simian virus 40 T antigen-mediated inactivation of p53, *Proceedings of the National Academy of Sciences, USA*, vol. 91, pp. 3979-3983.

McIntosh, B.M. 1958, Immunological types of horse sickness virus and their significance in immunization, *Onderstepoort Journal of Veterinary Research*, vol. 27, pp. 465-538.

Meiring, T.L., Huismans, H. & van Staden, V. 2009, Genome segment reassortment identifies non-structural protein NS3 as a key protein in African horsesickness virus release and alteration of membrane permeability, *Archives of Virology*, vol. 154, pp. 263-271.

Mellor, P.S. & Hamblin, C. 2004, African horse sickness, *Veterinary Research*, vol. 35, pp. 445-466.

Mellor, P.S. 1994, Epizootiology and vectors of African horse sickness virus, *Comparative Immunology, Microbiology and Infectious Diseases*, vol. 17, pp. 287-296.

Mellor, P.S., Boorman, J. & Jennings, M. 1975, The multiplication of African horse sickness virus in two species of *Culicoides* (Diptera: *Ceratopogonidae*), *Archives of Virology*, vol. 47, pp. 351-356.

Mertens, P. 2004, The dsRNA viruses, *Virus Research*, vol. 101, pp. 3-13.

Mertens, P.P.C. & Diprose, J. 2004, The bluetongue virus core: a nano-scale transcription machine, *Virus Research*, vol. 101, pp. 29-43.

Mertens, P.P.C., Diprose, J., Maan, S., Singh, K.P., Attoui, H. & Samuel, A.R. 2004, Bluetongue virus replication, molecular and structural biology, *Veterinaria Italiana*, vol. 40, pp. 426-437.

Mi, J., Li, Z.Y., Ni, S., Steinwaerder, D. & Lieber, A. 2001, Induced apoptosis supports spread of adenovirus vectors in tumors, *Human Gene Therapy*, vol. 12, pp. 1343-1352.

Micheau, O. & Tschopp, J. 2003, Induction of TNF receptor I-mediated apoptosis via two sequential signaling complexes, *Cell*, vol. 114, pp. 181-190.

Mirchamsy, H., Hazrati, A., Bahrami, S. & Shafyi, A. 1970, Growth and persistent infection of African horse-sickness virus in a mosquito cell line, *American Journal of Veterinary Research*, vol. 31, pp. 1755-1761.

Mizukoshi, N., Sakamoto, K., Iwata, A., Tsuchiya, T., Ueda, S., Apiwatnakorn, B., Kamada, M. & Fukusho, A. 1993, The complete nucleotide sequence of African horsesickness virus serotype 4 (vaccine strain) segment 4, which encodes the minor core protein VP4, *Virus Research*, vol. 28, pp. 299-306.

Modrof, J., Lymperopoulos, K. & Roy, P. 2005, Phosphorylation of bluetongue virus non-structural protein 2 is essential for formation of viral inclusion bodies, *Journal of Virology*, vol. 79, pp. 10023-10031.

Mortola, E. & Larsen, A. 2010, Bluetongue virus infection: activation of the MAP kinase-dependent pathway is required for apoptosis, *Research in Veterinary Science*, vol. 89, pp. 460-464.

Mortola, E., Noad, R. & Roy, P. 2004, Bluetongue virus outer capsid proteins are sufficient to trigger apoptosis in mammalian cells, *Journal of Virology*, vol. 78, pp. 2875-2883.

Nagaleekar, V.K., Tiwari, A.K., Kataria, R.S., Bais, M.V., Ravindra, P.V. & Kumar, S. 2007, Bluetongue virus induces apoptosis in cultures mammalian cells by both caspase-dependent extrinsic and intrinsic pathways, *Archives of Virology*, vol. 152, pp. 1751-1756.

Nason, E.L., Rothagel, R., Mukherjee, S.K., Kar, A.K., Forzan, M., Prasad, B.V. & Roy, P. 2004, Interactions between the inner and outer capsids of bluetongue virus, *Journal of Virology*, vol. 78, pp. 8059-8067.

Nicholson, D.W. & Thornberry, N.A. 1997, Caspases: killer proteases, *Trends in Biochemical Sciences*, vol. 22, pp. 299-306.

Nieuwoudt, M.A. 2008, Silencing of African horse sickness virus NS2 gene expression using vector-derived short hairpin RNAs, MSc dissertation, University of Pretoria.

Nogal, M.L., Gonzalez de Buitrago, G., Rodriguez, C., Cubelos, B., Carrascosa, A.L., Salas, M.L. & Revilla, Y. 2001, African swine fever virus IAP homologue inhibits caspase activation and promotes cell survival in mammalian cells, *Journal of Virology*, vol. 75, pp. 2535-2543.

O'Brien, V. 1998, Viruses and apoptosis, *Journal of General Virology*, vol. 79, pp. 1833-1845.

O'Donnell, S.M., Hansberger, M.W., Connolly, J.L., Chappell, J.D., Watson, M.J., Pierce, J.M., Wetzel, J.D., Han, W., Barton, E.S., Forrest, J.C., Valyi-Nagy, T., Yull, F.E., Blackwell, T.S., Rottman, J.N., Sherry, B. & Dermody, T.S. 2005, Organ-specific roles for transcription factor NF-κB in reovirus-induced apoptosis and disease, *Journal of Clinical Investigation*, vol. 115, pp. 2341-2350.

O'Reilly, D.R., Miller, L.K. & Luckow, V.A. 1992, An overview of baculoviruses, choosing a transfer plasmid and parent virus, methods for vector construction and gene expression, in: D.R. O'Reilly, L.K. Miller & V.A. Luckow (Eds.), *Baculo-expression vectors: a laboratory manual*, W.H. Freeman and Company, New York, pp. 1-36.

Oberhaus, S.M., Smith, R.L., Clayton, G.H., Dermody, T.S. & Tyler, K.L. 1997, Reovirus infection and tissue injury in the mouse central nervous system are associated with apoptosis, *Journal of Virology*, vol. 71, pp. 2100-2106.

Oellermann, R.A., Els, H.J. & Erasmus, B.J. 1970, Characterisation of African horse sickness virus, *Archiv für die gesamte Virusforschung*, vol. 29, pp. 163-174.

Office International des Epizooties (OIE). (2004). Manual of diagnostic tests and vaccines for terrestrial animals, 5th Edition. OIE, Paris, France.

Oltvai, Z.N., Milliman, C.L. & Korsmeyer, S.J. 1993, Bcl-2 heterodimerizes *in vivo* with a conserved homolog, Bax, that accelerates programmed cell death, *Cell*, vol. 74, pp. 609-619.

Osawa, Y. & Hazrati, A. 1965, Growth of African horse sickness virus in monkey kidney cell cultures, *American Journal of Veterinary Research*, vol. 25, pp. 505-511.

Owens, R.J., Limm, C. & Roy, P. 2004, Role of an arbovirus nonstructural protein in cellular pathogenesis and virus release, *Journal of Virology*, vol. 78, pp. 6649-6656.

Pahl, H.L. 1999, Activators and target genes of Rel/NF-kappaB transcription factors, *Oncogene*, vol. 18, pp. 6853-6866.

Peitsch, M.C., Polzar, B., Stephan, H., Crompton, T., MacDonald, H.R., Mannherz, H.G. & Tschopp, J. 1993, Characterization of the endogenous deoxyribonuclease involved in nuclear DNA degradation during apoptosis (programmed cell death), *The EMBO Journal*, vol. 12, pp. 371-377.

Ping-Yuan, L., Hung-Jen, L., Meng-Jiun, L., Feng-Ling, Y., Hsue-Yin, H., Jeng-Woei, L. & Wen-Ling, S. 2006, Avian reovirus activates a novel proapoptotic signal by linking Src to p53, *Apoptosis*, vol. 11, pp. 2179-2193.

Pitti, R.M., Marsters, S.A., Ruppert, S., Donahue, C.J., Moore, A. & Ashkenazi, A., 1996, Induction of apoptosis by Apo-2 ligand, a new member of the tumor necrosis factor cytokine family, *Journal of Biological Chemistry*, vol. 271, pp. 12687-12690.

Pop, C. & Salvesen, G.S. 2009, Human caspases: activation, specificity, and regulation, *Journal of Biological Chemistry*, vol. 284, pp. 21777-21781.

Possee, R.D. 1997, Baculoviruses as expression vectors, *Current Opinion in Biotechnology*, vol. 8, pp. 569-572.

Potgieter, A.C., Cloete, M., Pretorius, P.J. & van Dijk, A.A. 2003, A first full outer capsid protein sequence data-set in the *Orbivirus* genus (family *Reoviridae*): cloning, sequencing, expression and analysis of a complete set of full-length outer capsid VP2 genes of the nine African horsesickness virus serotypes, *Journal of General Virology*, vol. 84, pp. 1317-1326.

Prasad, B.V.V., Yamaguchi, S. & Roy, P. 1992, Three-dimensional structure of single-shelled BTV, *Journal of Virology*, vol. 66, pp. 2135-2142.

Prior, F.P. & Salvesen, G.S. 2004, The protein structures that shape caspase activity, specificity, activation and inhibition, *Biochemistry Journal*, vol. 384, pp. 201-232.

Privé, G.G. 2007, Detergents for the stabilization and crystallization of membrane proteins, *Methods*, vol. 41, pp. 388-397.

Purse, B.V., Brown, H.E., Harrup, L., Mertens, P.P.C. & Rogers, D.J. 2008, Invasion of bluetongue and other orbivirus infections into Europe: the role of biological and climatic processes, *Revue Scientifique et Technique de L'Office International des Epizooties*, vol. 27, no. 2, pp.427-442.

Purse, B.V., Mellor, P.S., Rogers, D.J., Samuel, A.R., Mertens, P.P.C. & Baylis, M. 2005, Climate change and the recent emergence of bluetongue in Europe, *Nature Reviews Microbiology*, vol. 3, pp.171-181.

Puthalakath, H., Huang, D.C., O'Reilly, L.A., King, S.M. & Strasser, A. 1999, The proapoptotic activity of the Bcl-2 family member Bim is regulated by interaction with the dynein motor complex, *Molecular Cell*, vol. 3, pp. 287-296.

Ramadevi, N. & Roy, P. 1998, Bluetongue virus core protein VP4 has nucleotide triphosphate phosphohydrolase activity, *Journal of General Virology*, vol. 79, pp. 2475-2480.

Ramadevi, N., Burroughs, N.J., Mertens, P.P., Jones, I.M. & Roy, P. 1998, Capping and methylation of mRNA by purified recombinant VP4 protein of bluetongue virus, *Proceedings of the National Academy of Sciences, USA*, vol. 95, pp. 13537-13542.

Ramírez-Solís, R., Reséndez-Pérez, D., Alvidrez-Quihui, L.E., Rincón-Limas, D.E., Varela-Martínez, R., Martínez-Rodríguez, H.G. & Barrera-Saldaña, H.A. 1990, New vectors for the efficient expression of mammalian genes in cultured cells, *Gene*, vol. 87, pp. 291-294.

Ramsey-Ewing, A. & Moss, B. 1998, Apoptosis induced by a post-binding step of vaccinia virus entry into Chinese hamster ovary cells, *Virology*, vol. 242, pp. 138-149.

Rao, C.D., Kiuchi, A. & Roy, P. 1983, Homologous terminal sequences of the genome double-stranded RNAs of bluetongue virus, *Journal of Virology*, vol. 46, pp. 378-383.

Rao, L., Modha, D. & White, E. 1997, The E1B 19K protein associates with lamins *in vivo* and its proper localization is required for inhibition of apoptosis, *Oncogene*, vol. 15, pp. 1587-1597.

Rao, L., Perez, D. & White, E. 1996, Lamin proteolysis facilitates nuclear events during apoptosis, *Journal of Cell Biology*, vol. 135, pp. 1441-1455.

Ravi, R., Bedi, G.C., Engstrom, L.W., Zeng, Q., Mookerjee, B., Gelinas, C., Fuchs, E.J. & Bedi, A. 2001, Regulation of death receptor expression and TRAIL/APO2L-induced apoptosis by NF-κB, *Nature Cellular Biology*, vol. 3, pp. 409-416.

Reading, P.C., Khanna, A. & Smith, G.L. 2002, Vaccinia virus CrmE encodes a soluble and cell surface tumor necrosis factor receptor that contributes to virus virulence, *Virology*, vol. 292, pp. 285-2998.

Renatus, M., Zhou, Q., Stennicke, H.R., Snipas, S.J., Turk, D., Bankston, L.A., Liddington, R.C. & Salvesen, G.S. 2000, Crystal structure of the apoptotic suppressor CrmA in its cleaved form, *Structure*, vol. 8, pp. 789-797.

Revilla, Y., Cebrian, A., Baixeras, E., Martinez, C., Vinuela, E. & Salas, M.L. 1997, Inhibition of apoptosis by the African swine fever virus Bcl-2 homologue: role of the BH1 domain, *Virology*, vol. 228, pp. 400-404.

Richardson-Burns, S.M. & Tyler, K.L. 2004, Regional differences in viral growth and central nervous system injury correlate with apoptosis, *Journal of Virology*, vol. 78, pp. 5466-5475.

Richardson-Burns, S.M., Kominsky, D.J. & Tyler, K.L. 2002, Reovirus-induced neuronal apoptosis is mediated by caspase-3 and is associated with the activation of death receptors, *Journal of Neurovirology*, vol. 8, pp. 365-380.

Riedl, S.J. & Salvesen, G.S. 2007, The apoptosome: signalling platform of cell death, *Nature Reviews Molecular Cell Bio*logy, vol. 8, pp. 405-413.

Roos, H.J. 2009, Suppression of African horse sickness virus NS1 protein expression in mammalian cells by short hairpin RNAs, MSc dissertation, University of Pretoria.

Rothe, M., Pan, M.G., Henzel, W.J., Ayres, T.M. & Goeddel, D.V. 1995, The TNFR2-TRAF signaling complex contains two novel proteins related to baculoviral inhibitor of apoptosis proteins, *Cell*, vol. 83, pp. 1243-1252.

Roulston, A., Marcellus, R.C. & Branton, P.E. 1999, Viruses and apoptosis, *Annual Review of Microbiology*, vol. 53, pp. 577-628.

Roy, N., Deveraux, Q.L., Takahashi, R., Salvesen, G.S. & Reed, J.C. 1997, The c-IAP-1 and c-IAP-2 proteins are direct inhibitors of specific caspases, *The EMBO Journal*, vol. 16, pp. 6914-6925.

Roy, P. 1992, Bluetongue virus proteins, *Journal of General Virology*, vol. 73, pp. 3051-3064.

Roy, P. 2001, Orbiviruses, in: D.M. Knipe, P.M. Howley, D.E. Griffin, R.A. Lamb & M.A. Martin (Eds.), *Field's Virology*, 4th Ed., Lippincott Williams and Wilkins, Philadelphia, 2001, pp. 1852-1857.

Roy, P. 2008, Functional mapping of bluetongue virus proteins and their interactions with host proteins during virus replication, *Cell Biochemistry and Biophysics*, vol. 50, pp. 143-157.

Roy, P., Adachi, A., Urakawa, T., Booth, T.F. & Thomas, C.P. 1990, Identification of bluetongue virus VP6 protein as a nucleic acid-binding protein and the localization of VP6 in virus-infected vertebrate cells, *Journal of Virology*, vol. 64, pp. 1-8.

Roy, P., Bishop, D.H.L., Howard, S., Aitchison, H. & Erasmus, B. 1996, Recombinant baculovirus-synthesized African horsesickness virus (AHSV) outer-capsid protein VP2 provides protection against virulent AHSV challenge, *Journal of General Virology*, vol. 77, pp. 2053-2057.

Roy, P., Fukusho, A., Ritter, D.G. & Lyons, D. 1988, Evidence for genetic relationship between RNA and DNA viruses from the sequence homology of a putative polymerase gene of bluetongue virus with that of vaccinia virus: conservation of RNA polymerase genes from diverse species, *Nucleic Acids Research*, vol. 16, pp. 11759-11767.

Roy, P., Mertens, P.P.C., & Casal, I. 1994, African horse sickness virus structure, *Comparative Immunology, Microbiology and Infectious Diseases*, vol. 17, pp. 243-273.

Rudolph, R. & Lilie, H. 1996, *In vitro* folding of inclusion body proteins, *The Journal of the Federation of American Societies for Experimental Biology*, vol. 10, pp. 49-56.

Salvesen, G.S. & Duckett, C.S. 2002, IAP proteins: blocking the road to death's door, *Nature Reviews Molecular Cell Biology*, vol. 3, pp. 401-410.

Salvesen, G.S. & Riedl, S.J. 2007, Caspase mechanisms, *Advances in Experimental Medicine and Biology*, vol. 615, pp. 13-23.

Sambrook, J. & Russell, D.W. 2001, Molecular Cloning, A Laboratory Manual, 3rd Ed., Cold Spring Harbour Laboratory Press.

Sanchez-Vizcaino, J.M. 2004, Control and eradication of African horse sickness with vaccine, *Developments in Biologicals*, vol. 119, pp. 255-258.

Sato, A., Iizuka, M., Nakagomi, O., Suzuki, M., Horie, Y., Konno, S., Hirasawa, F., Sasaki, K., Shindo, K. & Watanabe, S. 2006, Rotavirus double-stranded RNA induces apoptosis and diminishes wound repair in rat intestinal epithelial cells, *Journal of Gastroenterology and Hepatology*, vol. 21, pp. 521-530.

Sattar, R., Ali, S.A. & Abbasi, A. 2003, Molecular mechanism of apoptosis: prediction of three-dimensional structure of caspase-6 and its interactions by homology modelling, *Biochemical and Biophysical Research Communications*, vol. 308, pp. 497-504.

Scaffidi, C., Medema, J.P., Krammer, P.H. & Peter, M.E. 1997, FLICE is predominantly expressed as two functionally active isoforms, caspase-8/a and caspase-8/b, *Journal of Biological Chemistry*, vol. 272, pp. 26953-26958.

Scanlen, M., Paweska, J.T., Verschoor, J.A. & van Dijk, A.A. 2002, The protective efficacy of a recombinant VP2-based African horsesickness subunit vaccine candidate is determined by adjuvant, *Vaccine*, vol. 20, pp. 1079-1088.

Schaak, J. 2005, Induction and inhibition of innate inflammatory responses by adenovirus early region proteins, *Viral Immunology*, vol. 18, pp. 79-88.

Schein, C.H. 1990, Solubility as a function of protein structure and solvent compounds, *Nature Biotechnology*, vol. 8, pp. 308-317.

Schein, C.H. 1993, Solubility and secretability, *Current Opinion in Biotechnology*, vol. 4, pp. 456-461.

Schwartzman, R.A. & Cidlowski, J.A. 1993, Apoptosis: the biochemistry and molecular biology of programmed cell death, *Endocrine Reviews*, vol. 14, pp. 133-151.

Sciortino, M.T., Medici, M.A., Marino-Merlo, F., Zaccaria, D., Giuffrè-Cuculletto, M., Venuti, A., Grelli, S., Bramanti, P. & Mastino, A. 2008, Involvement of gD/HVEM interaction in NF-κB-dependent inhibition of apoptosis by HSV-1 gD, *Biochemical Pharmacology*, vol. 76, pp. 1522-1532.

Seddon, A.M., Curnow, P. & Booth, P.J. 2004, Membrane proteins, lipids and detergents: not just a soap opera, *Biochimica et Biophysica Acta - Biomembranes*, vol. 1666, pp. 105-117.

Seglen, P.O. 1983, Inhibitors of lysosomal function, *Methods in Enzymology*, vol. 96, pp. 737-764.

Shen, Y. & Shenk, T.E. 1995, Viruses and apoptosis, *Current Opinion in Genetics and Development*, vol. 5, pp.105-111.

Shi, Y. 2002a, Mechanisms of caspase activation and inhibition during apoptosis, *Molecular Cell*, vol. 9, pp. 459-470.

Shi, Y. 2002b, A conserved tetrapeptide motif: potentiating apoptosis through IAP-binding, *Cell Death and Differentiation*, vol. 9, pp. 93-95.

Shih, W.L., Hsu, H.W., Liao, M.H., Lee, L.H. & Liu, H.J. 2004, Avian reovirus σC protein induces apoptosis in cultured cells, *Virology*, vol. 321, pp. 65-74.

Shisler, J., Yang, C., Walter, B., Ware, C.F. & Gooding, L.R. 1997, The adenovirus E3-10.4K/14.5K complex mediates loss of cell surface Fas (CD95) and resistance to Fas-induced apoptosis, *Journal of Virology*, vol. 71, pp. 8299-8306.

Siegel, R.M., Frederiksen, J.K., Zacharias, D.A., Chan, F.K.-M., Johnson, M., Lynch, D., Tsien, R.Y. & Lenardo, M.J. 2000, Fas pre-association required for apoptosis signaling and dominant inhibition by pathogenic mutations, *Science*, vol. 288, pp. 2354-2357.

Siegmund, D., Hausser, A., Peters, N., Scheurich, P. & Wajant, H. 2001, Tumor necrosis factor (TNF) and phorbol ester induce TNF-related apoptosis-inducing ligand (TRAIL) under critical involvement of NF-κB essential modulator (NEMO)/IKKγ, *Journal of Biological Chemistry*, vol. 276, pp. 43708-43712.

Smith, C.A., Farrah, T. & Goodwin, R.G. 1994, The TNF receptor superfamily of cellular and viral proteins: activation, co-stimulation, and death, *Cell*, vol. 76, pp. 959-962.

Smith, G.E., Summers, M.D. & Fraser, M.J. 1983, Production of human beta interferon in insect cells infected with a baculovirus expression vector, *Molecular and Cellular Biology*, vol. 12, pp. 2156-2165.

Sørensen, H.P. & Mortensen, K.K. 2005, Advanced genetic strategies for recombinant protein expression in *Escherichia coli*, *Journal of Biotechnology*, vol. 115, pp. 113-128.

Sprick, M.R., Rieser, E., Stahl, H., Grosse-Wilde, A., Weigand, M.A. & Walczak, H. 2002, Caspase-10 is recruited to and activated at the native TRAIL and CD95 death-inducing signalling complexes in a FADD-dependent manner but cannot functionally substitute caspase-8, *The EMBO Journal*, vol. 21, pp. 4520-4530.

Srinivasula, S.M. & Ashwell, J.D. 2008, IAPs: What's in a name? *Molecular Cell*, vol. 30, pp. 123-135.

Staal, J., Bekaert, T. & Beyaert, R. 2011, Regulation of NF-κB signalling by caspases and MALT1 paracaspase, *Cell Research*, vol. 21, pp. 40-54.

Stassen, L., Huismans, H. & Theron, J. 2007, Silencing of African horse sickness virus VP7 protein expression in cultured cells by RNA interference, *Virus Genes*, vol. 35, pp. 777-783.

Stassen, L., Huismans, H. & Theron, J. 2011, Membrane permeabilization of the African horse sickness virus VP5 protein is mediated by two N-terminal amphipathic α-helices, *Archives of Virology*, vol. 156, pp. 711-715.

Stäuber, N., Martinez-Costas, J., Sutton, G., Monastyrskaya, K. & Roy P. 1997, Bluetongue virus VP6 protein binds ATP and exhibits an RNA-dependent ATPase function and a helicase activity that catalyze the unwinding of double-stranded RNA substrates, *Journal of Virology*, vol. 71, pp. 7220-7226.

Stehlik, C., de Martin, R., Kumabashiri, I., Schmid, J.A., Binder, B.R. & Lipp, J. 1998, Nuclear factor (NF)-κB-regulated X-chromosome-linked *iap* gene expression protects endothelial cells from tumor necrosis factor α-induced apoptosis, *Journal of Experimental Medicine*, vol. 188, pp. 211-216.

Stennicke, H.R., Ryan, C.A. & Salvesen, G.S. 2002, Reprieval from execution: the molecular basis of caspase inhibition, *Trends in Biochemical Sciences*, vol. 27, pp. 94-101.

Stewart, M.E. & Roy, P. 2010, Role of cellular caspases, nuclear factor-kappa B and interferon regulatory factors in Bluetongue virus infection and cell fate, *Virology Journal*, vol. 7, pp. 1-16.

Stoltz, M.A., van der Merwe, C.F., Coetzee, J. & Huismans, H. 1996, Subcellular localization of the nonstructural protein NS3 of African horsesickness virus, *Onderstepoort Journal of Veterinary Research*, vol. 63, pp. 57-61.

Stone-Marschat, M.A., Moss, S.R., Burrage, T.G., Barber, M.L., Roy, P. & Laegreid, W.W. 1996, Immunization with VP2 is sufficient for protection against lethal challenge with African horsesickness virus type 4, *Virology*, vol. 220, pp. 219-222.

Stratagene 2006, pCMV-Script® Vector, Instruction Manual, Revision #056003c, Stratagene.

Stuart, D.I. & Grimes, J.M. 2006, Structural studies on Orbivirus proteins and particles, *Current Topics in Microbiology and Immunology*, vol. 309, pp. 221-244.

Stuart, D.I., Gouet, P., Grimes, J., Malby, R., Diprose, J., Zientara, S., Burroughs, J.N. & Mertens, P.P. 1998, Structural studies of orbivirus particles, *Archives in Virology Supplementary*, vol. 14, pp. 235-250.

Suda, T., Takahashi, T., Golstein, P. & Nagata, S. 1993, Molecular cloning and expression of the Fas ligand, a novel member of the tumor necrosis factor family, *Cell*, vol. 75, pp. 1169-1178.

Summers, M.D. & Smith, G.E. 1987, A manual of methods for Baculovirus vectors and insect cell culture procedures, *Texas Agricultural Experiment Station Bulletin*, no. 1555.

Summers, M.D. 2006, Milestones leading to the genetic engineering of baculoviruses as expression vector systems and viral pesticides, *Advances in Virus Research*, vol. 68, pp. 3-73.

Sun, X.M., Bratton, S.B., Butterworth, M., MacFarlane, M. & Cohen, G.M. 2002, Bcl-2 and Bcl-XL inhibit CD95-mediated apoptosis by preventing mitochondrial release of Smac/DIABLO and subsequent inactivation of X-linked inhibitor-of-apoptosis protein, *Journal of Biological Chemistry*, vol. 277, pp. 11345-11351.

Sundararajan, R. & White, E. 2001, E1B 19K blocks Bax oligomerization and tumor necrosis factor alpha-mediated apoptosis, *Journal of Virology*, vol. 75, pp. 7506-7516.

Suzuki, Y., Imai, Y. Nakayama, H., Takahashi, K., Takio, K. & Takahashi, R. 2001, A serine protease, HtrA2, is released from the mitochondria and interacts with XIAP, inducing cell death, *Molecular Cell*, vol. 8, pp. 613-621.

Takahashi, K., Kawai, T., Kumar, H., Sato, S., Yonehara, S. & Akira, S. 2006, Cutting edge: roles of caspase-8 and caspase-10 in innate immune responses to double-stranded RNA, *Journal of Immunology*, vol. 176, pp. 4520-4524.

Takahashi, R., Deveraux, Q., Tamm, I., Welsh, K., Assa-Munt, N., Salvesen, G.S. & Reed, J.C. 1998, A single BIR domain of XIAP sufficient for inhibiting caspases, *Journal of Biological Chemistry*, vol. 273, pp. 7787-7790.

Tang, G., Minemoto, Y., Dibling, B., Purcell, N.H., Li, Z., Karin, M. & Lin, A. 2001, Inhibition of JNK activation through NF-κB target genes, *Nature*, vol. 414, pp. 313-317.

Taraporewala, Z.F., Chen, D. & Patton, J.T. 2001, Multimers of the bluetongue virus non-structural protein, NS2, possess nucleotidyl phosphatase activity: similarities between NS2 and rotavirus NSP2, *Virology*, vol. 280, pp. 221-231.

Tartaglia, L., Weber, R., Figari, I., Reynolds, C., Palladino, M. & Goeddel, D. 1991, The two different receptors for tumor necrosis factor mediate distinct cellular responses, *Proceedings of the National Academy of Sciences, USA*, vol. 88, pp. 9292-9296.

Tartaglia, L.A., Ayres, T.M., Wong, G.H., Goeddel, D.V. 1993, A novel domain within the 55 kd TNF receptor signals cell death, *Cell*, vol. 74, pp. 845-853.

Taylor, M.B., van der Meyden, C.H., Erasmus, B.J., Reid, R., Labuschagne, J.H., Dreyer, L. & Prozesky, O.W. 1992, Encephalitis and chorioretinitis associated with neurotropic African horse sickness virus infection in laboratory workers. Part IV. Experimental infection of the vervet monkey *Cercopithecus pygerythrus*, *South African Medical Journal*, vol. 81, pp. 462-467.

Theron, J. & Nel, L.H. 1997, Stable protein-RNA interaction involves the terminal domains of bluetongue virus mRNA, but not the terminally conserved sequences, *Virology*, vol. 229, pp. 134-142.

Thomas, C.P., Booth, T.F. & Roy, P. 1990, Synthesis of bluetongue viral-coded phosphoprotein and formation of inclusion bodies by recombinant baculovirus in insect cells: it binds the single-stranded RNA species, *Journal of General Virology*, vol. 71, pp. 2073-2083.

Timmer, J.C. & Salvesen, G.S. 2007, Caspase substrates, *Cell Death and Differentiation*, vol. 14, pp. 66-72.

Trevino, S.R., Scholtz, J.M. & Pace, C.N. 2007, Amino acid contribution to protein solubility: Asp, Glu, and Ser contribute more favourably than the other hydrophilic amino acids in RNase Sa, *Journal of Molecular Biology*, vol. 366, pp. 449-460.

Tsai, B. 2007, Penetration of nonenveloped viruses into the cytoplasm, *Annual Review of Cell Developmental Biology*, vol. 23, pp. 23-43.

Tsunoda, I., Kurtz, C.I. & Fujinami, R.S. 1997, Apoptosis in acute and chronic central nervous system disease induced by Theiler's murine encephalomyelitis virus, *Virology*, vol. 228, pp. 388-393.

Tsunoda, I., Libbey, J.E. & Fujinami, R.S. 2007, TGF-β1 suppresses T cell infiltration and VP2 puff B mutation enhances apoptosis in acute polio-encephalitis induced by Theiler's virus, *Journal of Neuroimmunology*, vol. 190, pp. 80-89.

Tucker, P.C., Strauss, E.G., Kuhn, R.J., Strauss, J.H. & Griffin, D.E. 1993, Viral determinants of age-dependent virulence of Sindbis virus for mice, *Journal of Virology*, vol. 67, pp. 4605-4610.

Turk, B., Turk, D. & Turk, V. 2000, Lysosomal cysteine proteases: more than scavengers, *Biochimica et Biophysica Acta*, vol. 1477, pp. 98-111.

Turnbull, P.J., Cormack, S.B. & Huismans, H. 1996, Characterization of the gene encoding core protein VP6 of two African horsesickness virus serotypes, *Journal of General Virology*, vol. 77, pp. 1421-1423.

Tyler, K.L., Squier, M.K.T., Rodgers, S.E., Schneider, B.E., Oberhaus, S.M., Grdina, T.A., Cohen, J.J. & Dermody, T.S. 1995, Differences in the capacity of reovirus strains to induce apoptosis are determined by the viral attachment protein σ1, *Journal of Virology*, vol. 69, pp. 6972-6979.

Uitenweerde, J.M., Theron, J., Stoltz, M.A. & Huismans, H. 1995, The multimeric nonstructural NS2 protein of Bluetongue virus, African horsesickness virus, and Epizootic hemorrhagic disease virus differ in their single-stranded RNA-binding ability, *Virology*, vol. 209, pp. 624-632.

Umeshappa, C.S., Singh, K.P., Nanjundappa, R.H. & Pandey, A.B. 2010, Apoptosis and immune-suppression in sheep infected with bluetongue virus serotype-23, *Veterinary Microbiology*, vol. 144, pp. 310-318.

Urakawa, T., Ritter, G.D. & Roy, P. 1989, Expression of largest RNA segment and synthesis of VP1 protein of bluetongue virus in insect cells by recombinant baculoviruses: association of VP1 protein with RNA polymerase activity, *Nucleic Acids Research*, vol. 17, pp. 7395-7401.

Urbano, P. & Urbano, F.G. 1994, The *Reoviridae* family, *Comparative Immunology, Microbiology and Infectious Diseases*, vol. 17, pp. 151-161.

Vallejo, L.F. & Rinas, U. 2004, Strategies for the recovery of active proteins through refolding of bacterial inclusion body proteins, *Microbial Cell Factories*, vol. 3, doi: 10.1186/1475-2859-3-11.

van Niekerk, M., Smit, C.C., Fick, W.C., van Staden, V. & Huismans, H. 2001, Membrane association of African horsesickness virus nonstructural protein NS3 determines its cytotoxicity, *Virology*, vol. 279, pp. 499-508.

van Staden, V. & Huismans, H. 1991, A comparison of the genes which encode nonstructural protein NS3 of different orbiviruses, *Journal of General Virology*, vol. 72, pp. 1073-1090.

van Staden, V., Stoltz, M.A. & Huismans, H. 1995, Expression of nonstructural protein NS3 of African horsesickness virus (AHSV): evidence for a cytotoxic effect of NS3 in insect cells, and characterization of the gene products in AHSV-infected Vero cells, *Archives of Virology*, vol. 140, pp. 289-306.

Venter, G.J. & Meiswinkel, R. 1994, The virtual absence of *Culicoides imicola* (Diptera: *Ceratopogonidae*) in a light-trap survey of the colder, high-lying area of the eastern Orange Free State, South Africa, and implications for the transmission of arboviruses, *Onderstepoort Journal of Veterinary Research*, vol. 61, pp. 327-340.

Venter, G.J., Graham, S.D. & Hamblin, C. 2000a, African horse sickness epidemiology: vector competence of South African *Culicoides* species for virus serotypes 3, 5 and 8, *Medical and Veterinary Entomology*, vol. 14, pp. 245-250.

Venter, M., Napier, G. & Huismans, H. 2000b, Cloning, sequencing and expression of the gene that encodes the major neutralization-specific antigen of African horsesickness virus serotype 9, *Journal of Virological Methods*, vol. 86, pp. 41-53.

Verma, I.M., Stevenson, J.K., Schwarz, E.M., Van Antwerp, D. & Miyamoto, S. 1995, Rel/NF-kappa B/I kappa B family: intimate tales of association and disassociation, *Genes and Development*, vol. 9, pp. 2723-2735.

Verwoed, D.W. & Huismans, H. 1969, On the relationship between bluetongue, African horsesickness and reoviruses: hybridization studies, *Onderstepoort Journal of Veterinary Research*, vol. 36, pp. 175-179.

Verwoerd, D.W., Els, H.J., De Villiers, E.M. & Huismans, H. 1972, Structure of bluetongue virus capsid, *Journal of Virology*, vol. 10, pp. 783-794.

Villaverde, A. & Carrío, M.M. 2003, Protein aggregation in recombinant bacteria: biological role of inclusion bodies, *Biotechnology Letters*, vol. 25, pp. 1385-1395.

Vreede, F.T. & Huismans, H. 1994, Cloning, sequencing and expression of the gene that encodes the major neutralization-specific antigen of African horsesickness virus serotype 3, *Journal of General Virology*, vol. 75, pp. 3629-3633.

Vreede, F.T. & Huismans, H. 1998, Sequence analysis of the RNA polymerase gene of African horse sickness virus, *Archives of Virology*, vol. 143, pp. 413-419.

Walker, P.R., Kokileva, L., LeBlanc, J. & Sikorska, M. 1994, Detection of the initial stages of DNA fragmentation in apoptosis. *BioTechniques*, vol. 15, pp.1032-1040.

Walker, P.R., Smith, C., Youdale, T., Leblanc, J., Whitfield, J.F. & Sikorska, M. 1991, Topoisomerase II-reactive chemotherapeutic drugs induce apoptosis in thymocytes, *Cancer Research*, vol. 51, pp.1078-1085.

Wang, C-Y., Mayo, M.W., Korneluk, R.G., Goeddel, D.V. & Baldwin, A.S. 1998, NF-κB antiapoptosis: induction of TRAF1 and TRAF2 and c-IAP1 and c-IAP2 to suppress caspase-8 activation, *Science*, vol. 281, pp. 1680-1683.

Wang, K., Yin, X.M., Chao, D.T., Milliman, C.L. & Korsmeyer, S.J. 1996, Bid: a novel BH3 domain-only death agonist, *Genes and Development*, vol. 10, pp. 2859-2869.

Wang, X.W., Gibson, M.K., Vermeulen, W., Yeh, H., Forrester, K., Sturzbecher, H.W., Hoeijmakers, J.H.J. & Harris, C.C. 1995, Abrogation of p53-induced apoptosis by the hepatitis B virus x gene, *Cancer Research*, vol. 55, pp. 6012-6016.

Waugh, D.S. 2006, Making the most of affinity tags, *Trends in Biotechnology*, vol. 23, pp. 316-320.

Weber, C.H. & Vincenz, C. 2001, The death domain superfamily: a tale of two interfaces? *Trends in Biochemical Sciences*, vol. 26, pp. 475-481.

Weyer, U., Possee, R.D. 1991, A baculovirus dual expression vector derived from the *Autographa californica* nuclear polyhedrosis virus polyhedrin and p10 promoters: co-expression of two influenza virus genes in insect cells, *Journal of General Virology*, vol. 72, pp. 2967-2974.

White, E. 1998, Regulation of apoptosis by adenovirus E1A and E1B oncogenes, *Seminars in Virology*, vol. 8, pp. 505-513.

White, J.M., Delos, S.E., Brecher, M. & Schornberg, K. 2008, Structures and mechanisms of viral membrane fusion proteins: multiple variations on a common theme, *Critical Reviews in Biochemistry and Molecular Biology*, vol. 43, pp. 189-219.

Whitford, W.G. & Mertz, L.M. 1998, Multiplicity of baculoviral infection and recombinant protein production in *Sf*9 cells, *Focus*, vol. 18, pp. 75-76.

Wiley, S.R., Schooley, K., Smolak, P.J., Din, W.S., Huang, C.P., Nicholl, J.K., Sutherland, G.R., Smith, T.D., Rauch, C., Smith, C.A. & Goodwin, R.G. 1995, Identification and characterization of a new member of the TNF family that induces apoptosis, *Immunity*, vol. 3, pp. 673-682.

Wilson, A., Mellor, P.S., Szmaragd, C. & Mertens, P.P.C. 2009, Adaptive strategies of African horse sickness virus to facilitate vector transmission, *Veterinary Research*, vol. 40, doi: 10.1051/vetres:2008054.

Wirblich, C., Bhattacharya, B. & Roy P. 2006, Nonstructural protein 3 of bluetongue virus assists virus release by recruiting ESCRT-I protein Tsg101, *Journal of Virology*, vol. 80, pp. 460-473.

Wisniewski, M.L., Werner, B.G., Hom, L.G., Anguish, L.J., Coffey, C.M. & Parker, J.S. 2010, Reovirus infection or ectopic expression of outer-capsid protein μ1 induces apoptosis independently of the cellular proapoptotic proteins Bax and Bak, *Journal of Virology*, vol. 85, pp. 296-304.

Wood, A.R. & McInnes, C.J. 2003, Transcript mapping of the 'early' genes of *Orf* virus, *Journal of General Virology*, vol. 84, pp. 2993-2998.

Wu, V., Chen, S., Iwata, H., Compas, R. & Roy, P. 1992, Multiple glycoproteins synthesized by the smallest RNA segment (S10) of bluetongue virus, *Journal of Virology*, vol. 12, pp. 7104-7112.

Wyllie, A.H. 1980, Glucocorticoid-induced thymocyte apoptosis is associated with endogenous endonuclease activation, *Nature*, vol. 284, pp. 555-556.

Wyllie, A.H., Beattie, G.J. & Hargreaves, A.D. 1981, Chromatin changes in apoptosis, *Histochemical Journal*, vol. 13, pp. 681-692.

Wyllie, A.H., Kerr, J.F.R. & Currie, A.R. 1980, Cell death: the significance of apoptosis, *International Review of Cytology*, vol. 68, pp. 251-306.

Xiao, S.Y., Guzman, H., Zhang, H., Travassos da Rosa, A.P. & Tesh, R.B. 2001, West Nile virus infection in the golden hamster (*Mesocricetus auratus*): a model for West Nile encephalitis, *Emerging Infectious Diseases*, vol. 7, pp. 714-721.

Xu, G. & Shi, Y. 2007, Apoptosis signaling pathways, *Cell Research*, vol. 17, pp. 759-771.

Xu, G., Cirilli, M., Huang, Y., Rich, R.L., Myszka, D.G. & Wu, H. 2001, Covalent inhibition revealed by the crystal structure of the caspase-8/p35 complex, *Nature*, vol. 410, pp. 494-497.

Yang, E., Zha, J., Jockel, J., Boise, L.H., Thompson, C.B. & Korsmeyer, S.J. 1995, Bad, a heterodimeric partner for Bcl-X_L and Bcl-2, displaces Bax and promotes cell death, *Cell*, vol. 80, pp. 285-291.

Yang, J.S., Ramanathan, M.P., Muthumani, K., Choo, A.Y., Jin, S.H., Yu, Q.C., Hwang, D.S., Choo, D.K., Lee, M.D., Dang, K., Tang, W., Kim, J.J. & Weiner, D.B. 2002, Induction of inflammation by *West Nile virus* capsid through the caspase-9 apoptotic pathway, *Emerging Infectious Diseases*, vol. 8, pp. 1379-1384.

Yang, X., Chang, H.Y. & Baltimore, D. 1998a, Essential role of CED-4 oligomerization in CED-3 activation and apoptosis, *Science*, vol. 281, pp. 1355-1357.

Yang, X., Chang, H.Y. & Baltimore, D. 1998b, Autoproteolytic activation of procaspases by oligomerization, *Molecular Cell*, vol. 1, pp. 319-325.

Yin, J., Li, G., Ren, X. & Herrler, G. 2007, Select what you need: A comparative evaluation of the advantages and limitations of frequently used expression systems for foreign genes, *Journal of Biotechnology*, vol. 127, pp. 335-347.

Youle, R.J. & Strasser, A. 2008, The Bcl-2 protein family: opposing activities that mediate cell death, *Nature Reviews Molecular Cell Biology*, vol. 9, pp. 47-59.

Zhang, S.Q., Kovalenko, A., Cantarella, G. & Wallach, D. 2000, Recruitment of the IKK signalosome to the p55 TNF receptor: RIP and A20 bind to NEMO (IKKγ) upon receptor stimulation, *Immunity*, vol. 12, pp. 301-311.

Zhang, X., Boyce, M., Bhattacharya, B., Zhang, X., Schein, S., Roy, P. & Hong Zhou, Z. 2010, Bluetongue virus coat protein VP2 contains sialic acid-binding domains, and VP5 resembles enveloped virus fusion proteins, *Proceedings of the National Academy of Sciences, USA*, vol. 107, pp. 6292-6297.

Zhou, L. 2005, The 'unique key' feature of the IAP-binding motifs in RHG proteins, *Cell Death and Differentiation*, vol. 12, pp. 1148-1151.

Zou, H., Li, Y., Liu, X. & Wang, X. 1999, An Apaf-1.cytochrome *c* multimeric complex is a functional apoptosome that activates procaspase- 9, *Journal of Biological Chemistry*, vol. 274, pp. 11549-11556.

APPENDICES

A1 PROTEIN BINDING AND INTERNALIZATION ASSAYS

During the course of this investigation, evidence was obtained indicating that extracellular co-administration of the outer capsid proteins VP2 and VP5 of AHSV-4 induces apoptosis in BHK-21 mammalian cells (Chapter 3). Since treatment of the cells with the individual proteins did not induce apoptosis, these results suggest that the uptake of VP2-VP5 complexes is required to trigger apoptosis. Although the biological role of the VP5 protein of AHSV was recently investigated (Stassen *et al.*, 2011), no similar information exists for the VP2 protein. However, of the seven structural proteins, VP2 is the most likely candidate virus attachment protein due to its outermost location on the virion (Roy *et al.*, 1994). The availability of soluble recombinant baculovirus-expressed VP2 thus provided an opportunity to determine the host cell binding and internalization activity of the protein. These properties were assessed in AHSV-permissive BHK-21 cells with an immunofluorescence assay, together with appropriate monospecific polyclonal antibodies. For comparative purposes, the assay was performed using the outer capsid proteins of virulent and attenuated AHSV-4 isolates. The following provides a brief report of these findings.

MATERIALS AND METHODS

Indirect immunofluorescence

- **Preadsorption of antisera**

To minimize non-specific cross-reactions, AHSV-4 VP2 EpiB and anti-βgal-VP5 antisera were adsorbed against cell lysates prepared from wild-type baculovirus-infected *Sf*9 cells and uninfected BHK-21 cells, as described by Lee *et al*. (1996) with modifications. Briefly, 10 µl of the antiserum and 1 ml of the *Sf*9 cell lysate were incubated on ice for 2 h. Following centrifugation at 4000 rpm for 10 min at 4°C, the supernatant was retained and then adsorbed against the BHK-21 cell lysate using the same method. The preadsorbed antisera were stored at -20°C until use.

- **Confocal microscopy**

BHK-21 cells, seeded at 20% confluency on glass coverslips in 6-well tissue culture plates, were treated with 10 µg of VP2 and also in combination with 5 µg of VP5. Protein binding to the cell surface was performed at 4°C for 1 h, whereas protein internalization was carried out

at 37°C for an additional 1 h (Hassan and Roy, 1999). For surface membrane immunofluorescence, cells were washed twice with 1 × PBS and then fixed in an isotonic solution of 2% paraformaldehyde at room temperature for 2 min. For intracellular staining, following washing twice with 1 × PBS, the cells were permeabilized by ice-cold methanol:acetone (1:1 [v/v]) at room temperature for 3 min (Matthews and Russell, 1998). Subsequently, the cell monolayers were washed twice with 1 × PBS and incubated for 30 min in blocking solution (5% [w/v] fat-free milk powder in 1 × PBS). The cells were then incubated overnight at 4°C with either AHSV-4 VP2 EpiB antiserum or a mixture of AHSV-4 VP2 EpiB and anti-βgal-VP5 antisera, which were each diluted 1:100 in 1% (w/v) blocking solution. After removal of the unbound antibodies by three washes for 5 min each with wash buffer (0.5% [v/v] Tween-20 in 1 × PBS), the coverslips were incubated for 1 h with a labeled secondary antibody or a mixture of labeled secondary antibodies. These comprised of TRITC-conjugated anti-guinea pig IgG for VP2 and FITC-conjugated anti-chicken IgY (IgG) for VP5, which were diluted 1:160 and 1:320 in 1% (w/v) blocking solution, respectively. Following incubation, the cells were washed twice with wash buffer and twice with 1 × PBS. BHK-21 cells infected with AHSV-4 at a MOI of 1 pfu/cell, as well as BHK-21 cells treated with a soluble protein extract from *S. frugiperda* (*Sf*9) insect cells infected with wild-type baculovirus were prepared identically and included in the assay as controls. The coverslips were mounted on glass slides and the cells were examined with a Zeiss LSM S10 META confocal laser scanning microscope through the 63×1.4 objective, using bypass filters for fluorescein (467-498 nm) and rhodamine (532-554 nm). Images were captured with a Zeiss Axiocam Series 5 digital camera and analyzed with Zeiss LSM Image Browser v.4.2.0.121 software.

RESULTS AND CONCLUSIONS

To determine if AHSV-4 VP2 is capable of binding to and being internalized into host cells, the experimental approach outlined above was followed. In these experiments, soluble protein extracts prepared from recombinant baculovirus-infected cells were used, since it was not possible to purify the recombinant VP2 and VP5 proteins to homogeneity. In addition to the cell attachment and penetration experiments carried out with VP2, internalization assays were also performed using a combination of the VP2 and VP5 proteins. In the binding assays, only VP2 antigens on the cell surface were probed with antibody, but in the internalization

assays the plasma membranes of the cells were permeabilized to allow detection of both the VP2 and VP5 antigens within the cells. The results of these assays are presented in Fig. A1.1.

In the VP2 binding assays performed, antigens detected on the surface of cellular plasma membranes were typically observed as a fluorescent signal outlining the cells. When the cells were incubated at 37°C for a further 1 h to allow internalization to occur, a fluorescent pattern indicative of internalization, *i.e.* staining of the cytoplasm, was observed. Moreover, internalization assays performed with co-administered VP2 and VP5 proteins indicated the presence of both proteins within the cells. These results are similar to those obtained for BHK-21 cells infected with AHSV-4, in which both VP2 and VP5 could be detected in the infected cells. No differences in the results were observed, irrespective of using the outer capsid proteins of a virulent or an attenuated AHSV-4 isolate.

Control binding and internalization assays were also performed, the results of which are shown in Fig. A1.1. No fluorescence signal was observed for BHK-21 cells without the addition of VP2. Likewise, no signal was achieved in internalization assays by making use of BHK-21 cells treated with a soluble protein extract prepared from wild-type baculovirus-infected *Sf*9 cells. These results thus confirmed that the preadsorbed antisera did not cross-react with BHK-21 cellular proteins or with either *S. frugiperda* insect cell or wild-type baculovirus-expressed proteins.

Based on the ability of VP2 to bind to BHK-21 cells, in the absence of other viral proteins, and its subsequent internalization, it may be concluded that the VP2 protein is capable of mediating virus entry into mammalian cells. The results furthermore indicate that the soluble VP2 proteins of the virulent and attenuated AHSV-4 isolates expressed in the recombinant baculovirus expression system were appropriately folded, and that the observed amino acid differences present in the VP2 protein of the attenuated AHSV-4 isolate did not influence its biological function. Finally, the results also present evidence for the internalization of VP2-VP5 protein complexes, which was suggested to trigger apoptosis when co-administered extracellularly to uninfected BHK-21 cells.

REFERENCES

Hassan, S.S. & Roy, P. 1999, Expression and functional characterization of bluetongue virus VP2 protein: role in cell entry, *Journal of Virology*, vol. 73, no. 12, pp. 9832-9842.

Lee, T.H., Kato, H., Kogure, K. & Itoyama, Y. 1996, Temporal profile of nerve growth factor-like immunoreactivity after transient focal cerebral ischemia in rats, *Brain Research*, vol. 713, pp. 199-210.

Matthews, D.A. & Russell, W.C. 1998, Adenovirus core protein V interacts with p32 – a protein which is associated with both the mitochondria and the nucleus, *Journal of General Virology*, vol. 79, pp. 1677-1685.

Roy, P., Mertens, P.P.C., & Casal, I. 1994, African horse sickness virus structure, *Comparative Immunology, Microbiology and Infectious Diseases*, vol. 17, pp. 243-273.

Stassen, L., Huismans, H. & Theron, J. 2011, Membrane permeabilization of the African horse sickness virus VP5 protein is mediated by two N-terminal amphipathic α-helices, *Archives of Virology*, vol. 156, pp. 711-715.

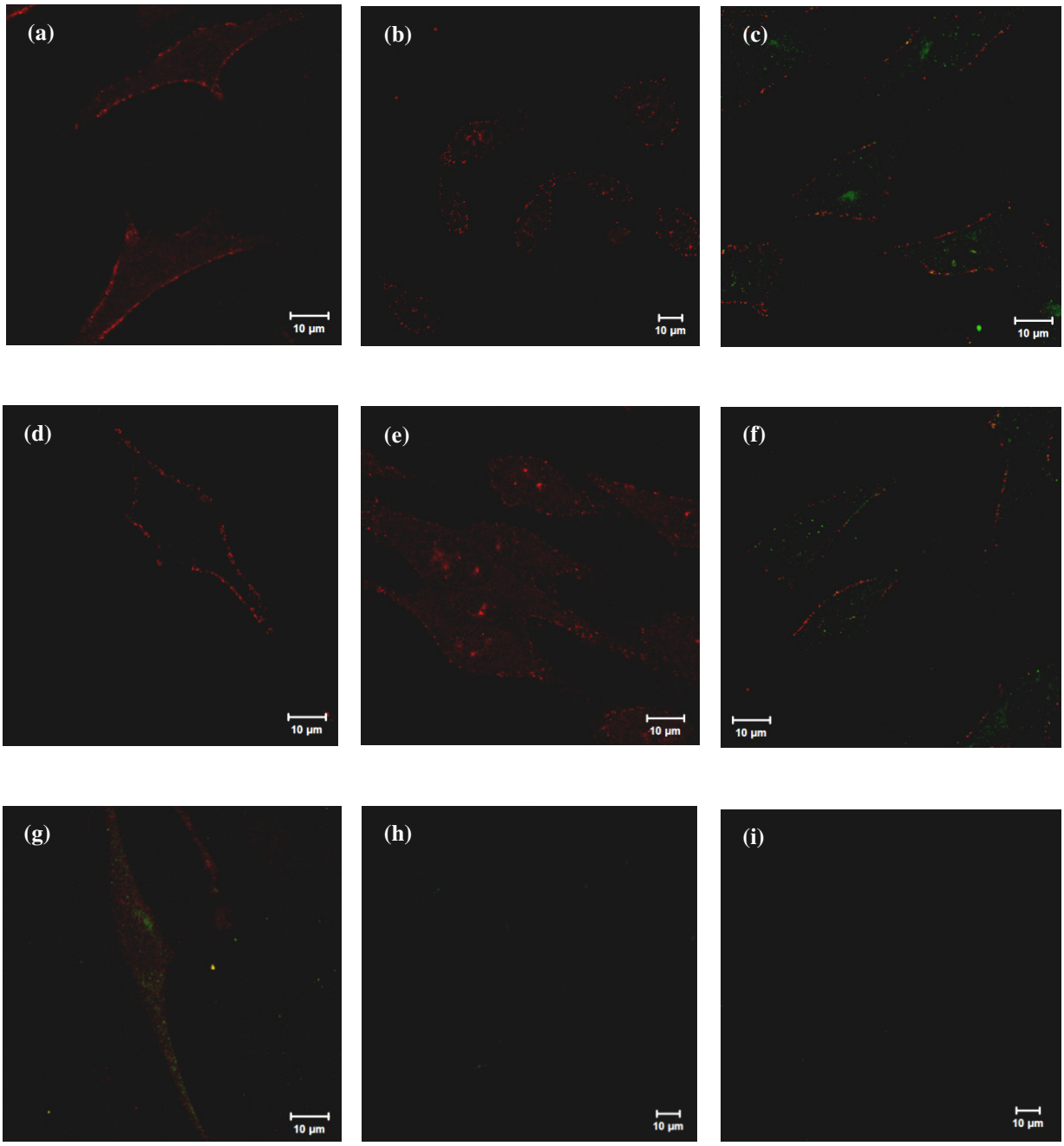

Fig. A1.1: Indirect immunofluorescent staining showing binding to and internalization of BHK-21 cells by VP2 and co-administered VP2 and VP5. (a and b) Binding of VP2 of an attenuated AHSV-4 isolate to BHK-21 cells and internalization by VP2 of the BHK-21 cells. (c) Internalization of BHK-21 cells by extracellularly co-administered VP2 and VP5 proteins of an attenuated AHSV-4 isolate. (d and e) Binding of VP2 of a virulent AHSV-4 isolate to BHK-21 cells and internalization by VP2 of the BHK-21 cells. (f) Internalization of BHK-21 cells by extracellularly co-administered VP2 and VP5 proteins of a virulent AHSV-4 isolate. (g) Internalization of BHK-21 cells by AHSV-4. (h and i) Controls for the binding assay in BHK-21 cells in the absence of VP2 and in the internalization assay of BHK-21 cells treated extracellularly with a soluble extract prepared from wild-type baculovirus-infected cells. Either an anti-VP2 antibody (a, b, d, e and h) or mixture of anti-VP2 and anti-VP5 antibodies (c, f, g and i) were used in the assays.

A2 NUCLEOTIDE AND AMINO ACID SEQUENCE ALIGNMNETS

(a)

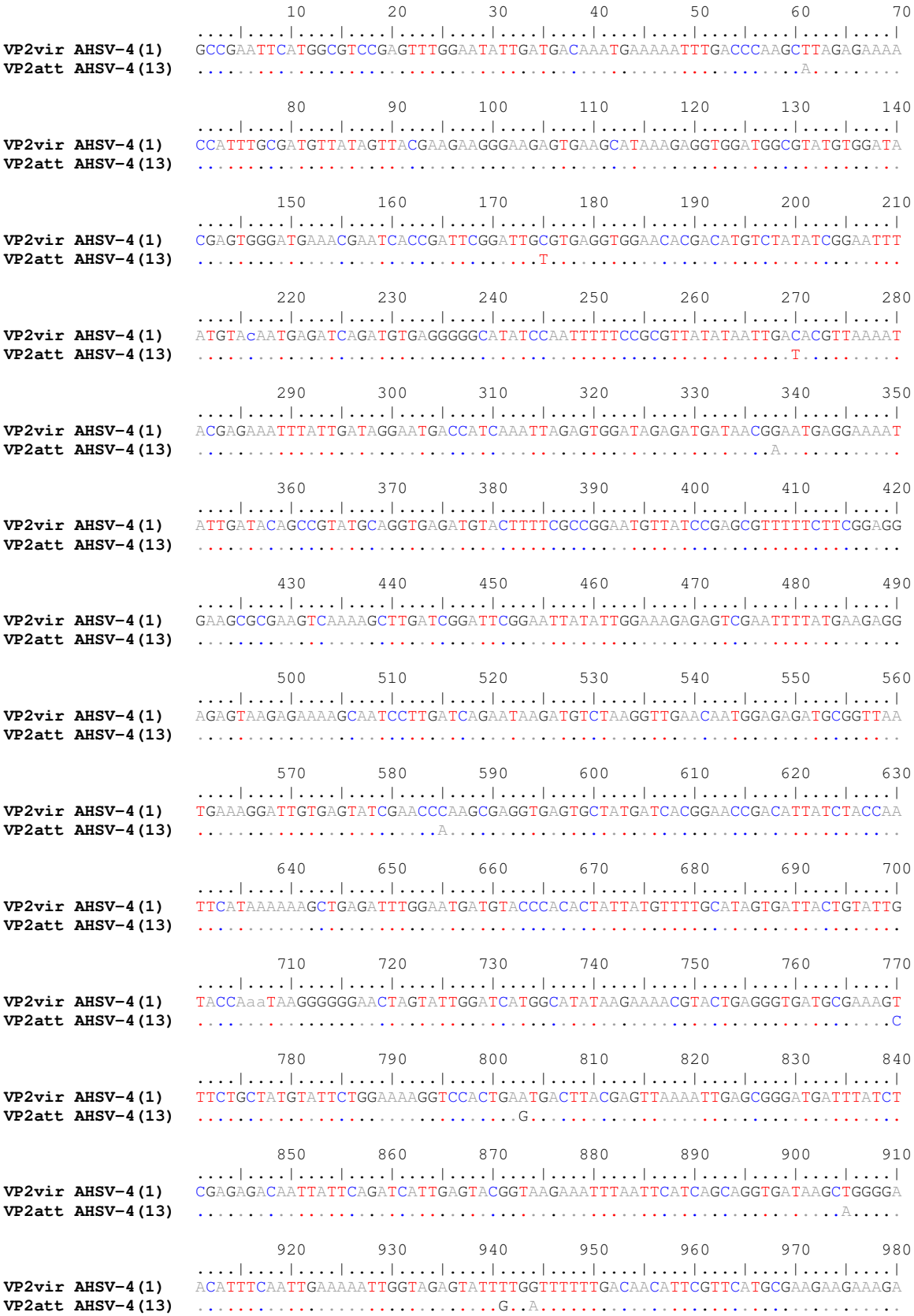

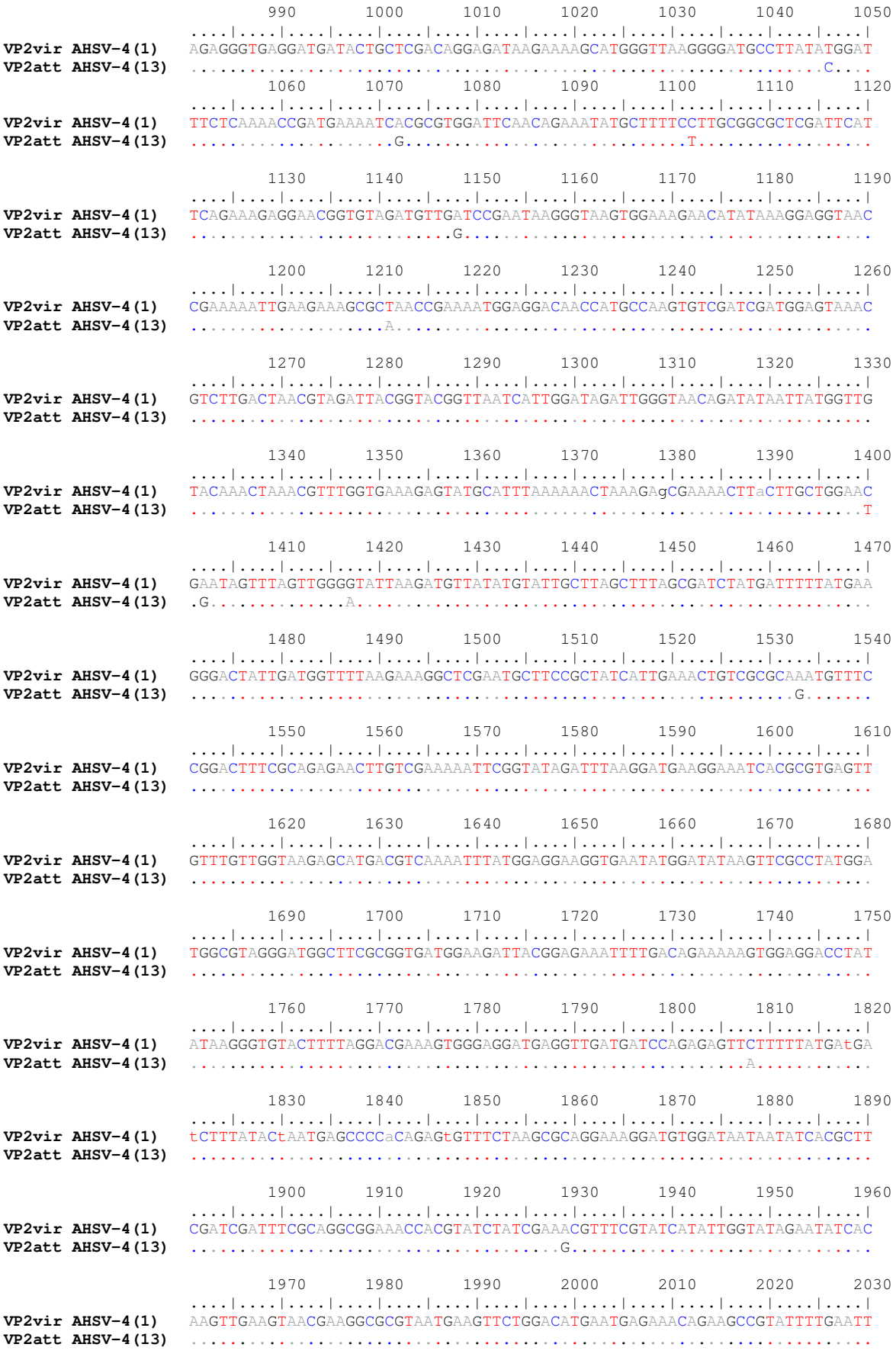

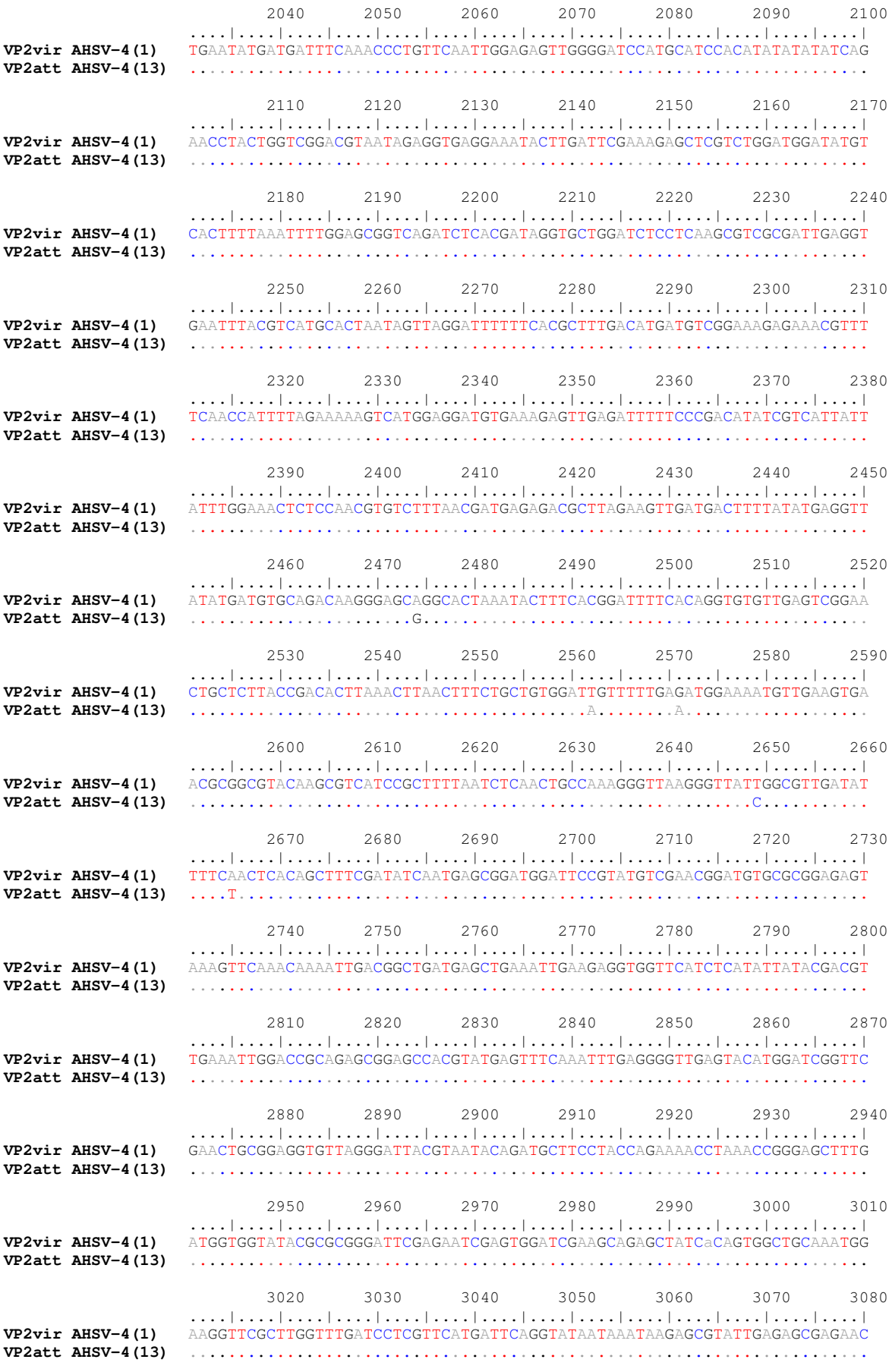

```
                          3090       3100       3110       3120       3130       3140       3150
                   ....|....|....|....|....|....|....|....|....|....|....|....|....|....|....|....|
VP2vir AHSV-4(1)   TCTGAAAATTTACAATaGGGGTTCGATGGATACTTTAATTCTaATTTCGAGTGGAGTTTACACTTTCGGA
VP2att AHSV-4(13)  ...........................................................................

                          3160       3170       3180       3190       3200
                   ....|....|....|....|....|....|....|....|....|....|.
VP2vir AHSV-4(1)   AATAAATTCTTGTTGTCGAAGTTACTCGCAAAAACAGAATAGGGTACCGCC
VP2att AHSV-4(13)  ..........................G..............
```

(b)

```
                            10         20         30         40         50         60         70
                     ....|....|....|....|....|....|....|....|....|....|....|....|....|....|....|....|
VP5vir AHSV-4(1)     CCCGCGGCCGCATGGGAAAGTTCACATCTTTTTTGAAGCGCGCGGGCAATGCGACCAAGAGGGCGCTGAC
VP5att AHSV-4(13)    ...................................................................................

                            80         90        100        110        120        130        140
                     ....|....|....|....|....|....|....|....|....|....|....|....|....|....|....|....|
VP5vir AHSV-4(1)     GTCGGATTCAGCAAAGAAGATGTATAAGTTGGCGGGGAAAACGTTACAGAGAGTGGTAGAAAGTGAAGTT
VP5att AHSV-4(13)    ...................................................................................

                           150        160        170        180        190        200        210
                     ....|....|....|....|....|....|....|....|....|....|....|....|....|....|....|....|
VP5vir AHSV-4(1)     GGAAGTGCAGCGATCGATGGCGTGATGCAGGGGGCGATACAAAGCATAATACAAGGCGAAAACCTTGGTG
VP5att AHSV-4(13)    ...................................................................................

                           220        230        240        250        260        270        280
                     ....|....|....|....|....|....|....|....|....|....|....|....|....|....|....|....|
VP5vir AHSV-4(1)     ATTCAATTAAGCAGGCGGTTATTTTAAATGTTGCGGGGACATTGGAATCGGCGCCAGACCCGTTGAGCCC
VP5att AHSV-4(13)    ...................................................................................

                           290        300        310        320        330        340        350
                     ....|....|....|....|....|....|....|....|....|....|....|....|....|....|....|....|
VP5vir AHSV-4(1)     AGGGGAGCAGCTCCTTTACAATAAGGTTTCTGAAATCGAGAAAATGGAAAAAGAGGATCGAGTGATTGAA
VP5att AHSV-4(13)    ...................................................................................

                           360        370        380        390        400        410        420
                     ....|....|....|....|....|....|....|....|....|....|....|....|....|....|....|....|
VP5vir AHSV-4(1)     ACACACAATGCGAaAATAGAAGAAAAATTTGGTAAAGATTTATTAGCGATTCGAAAGATTGTGAAAGGCG
VP5att AHSV-4(13)    ...................................................................................

                           430        440        450        460        470        480        490
                     ....|....|....|....|....|....|....|....|....|....|....|....|....|....|....|....|
VP5vir AHSV-4(1)     AGGTTGATGCAGAAAAGCTGGAAGGTAACGAAATTAAGTACGTAGAAAAAGCGCTTAGCGGTTTGCTGGA
VP5att AHSV-4(13)    ...................................................................................

                           500        510        520        530        540        550        560
                     ....|....|....|....|....|....|....|....|....|....|....|....|....|....|....|....|
VP5vir AHSV-4(1)     GATAGGGAAAGATCAGTCAGAACGCATTACAAAGCTATATCGCGCGTTACAAACAGAGGAAGATTTGCGG
VP5att AHSV-4(13)    ...................................................................................

                           570        580        590        600        610        620        630
                     ....|....|....|....|....|....|....|....|....|....|....|....|....|....|....|....|
VP5vir AHSV-4(1)     ACACGAGATGAGACTAGAATGATAAACGAATATAGAGAAAaATTTGACGCGTTGAAAGAAGCGATTGAAA
VP5att AHSV-4(13)    ...................................................................................

                           640        650        660        670        680        690        700
                     ....|....|....|....|....|....|....|....|....|....|....|....|....|....|....|....|
VP5vir AHSV-4(1)     TCGAGCAGCAAGCGACACATGATGAGGCGATTCAAGAGATGCTCGACTTaAGCGCGGAAGTAATTGAGAC
VP5att AHSV-4(13)    ...................................................................................

                           710        720        730        740        750        760        770
                     ....|....|....|....|....|....|....|....|....|....|....|....|....|....|....|....|
VP5vir AHSV-4(1)     TGCGTCGGAGGAGGTACCAATCTTCGGCGCTGGGGCGGCGAACGTTATCGCCACAACCCGCGCAATACAG
VP5att AHSV-4(13)    ...................................................................................

                           780        790        800        810        820        830        840
                     ....|....|....|....|....|....|....|....|....|....|....|....|....|....|....|....|
VP5vir AHSV-4(1)     GGGGGGTTAAAACTAAAGGAAATTGTTGATAAGCTTACGGGCATAGATTTGAGCCATTTGAAGGTGGCCG
VP5att AHSV-4(13)    ...................................................................................
```

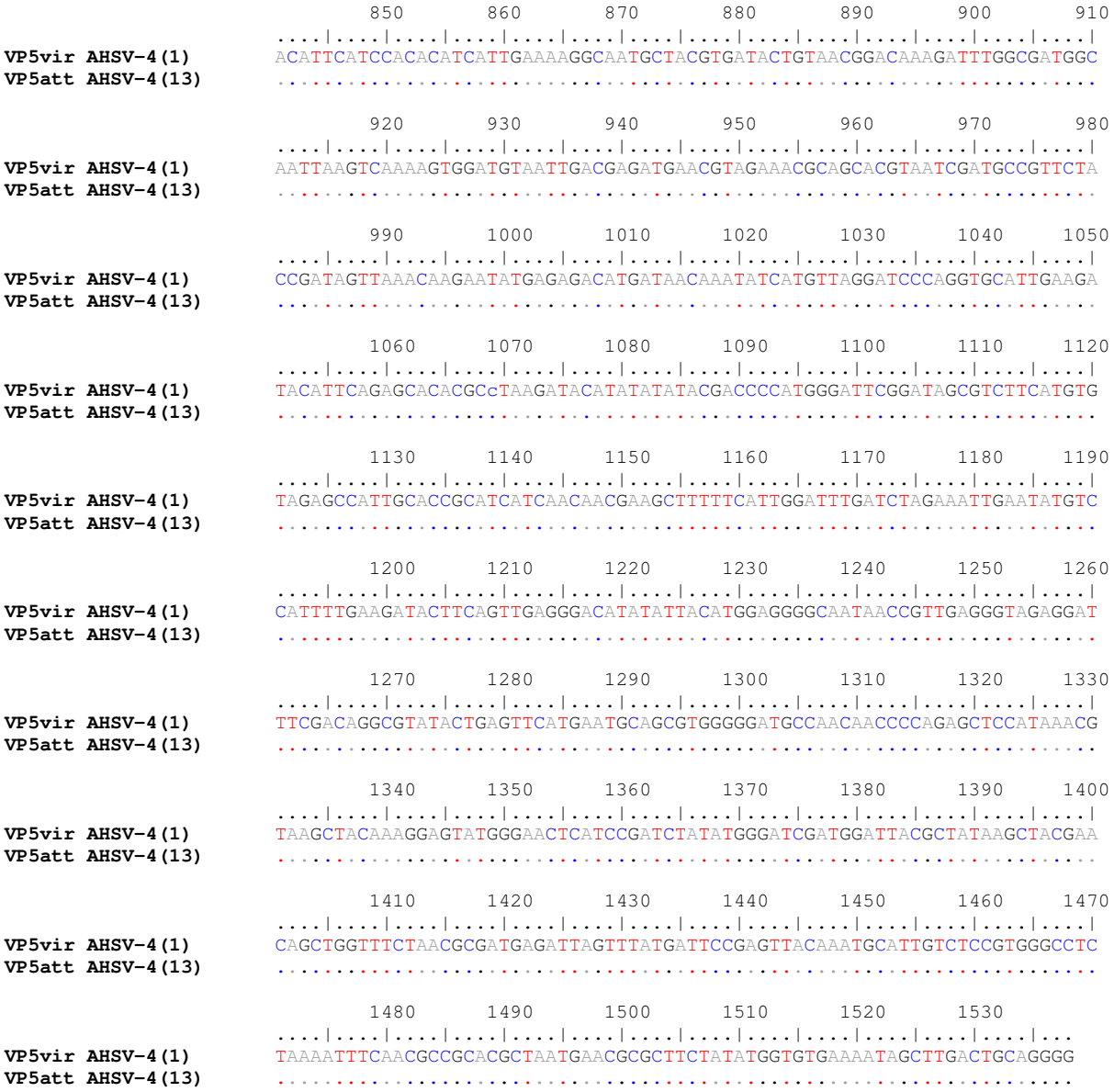

Fig. A2.1: Nucleotide sequence alignments of the VP2 (a) and VP5 (b) genes of a virulent and an attenuated AHSV-4 isolate. The nucleotide sequences were analyzed with BioEdit Sequence Alignment Editor software. Dots denote identical nucleotides.

(a)

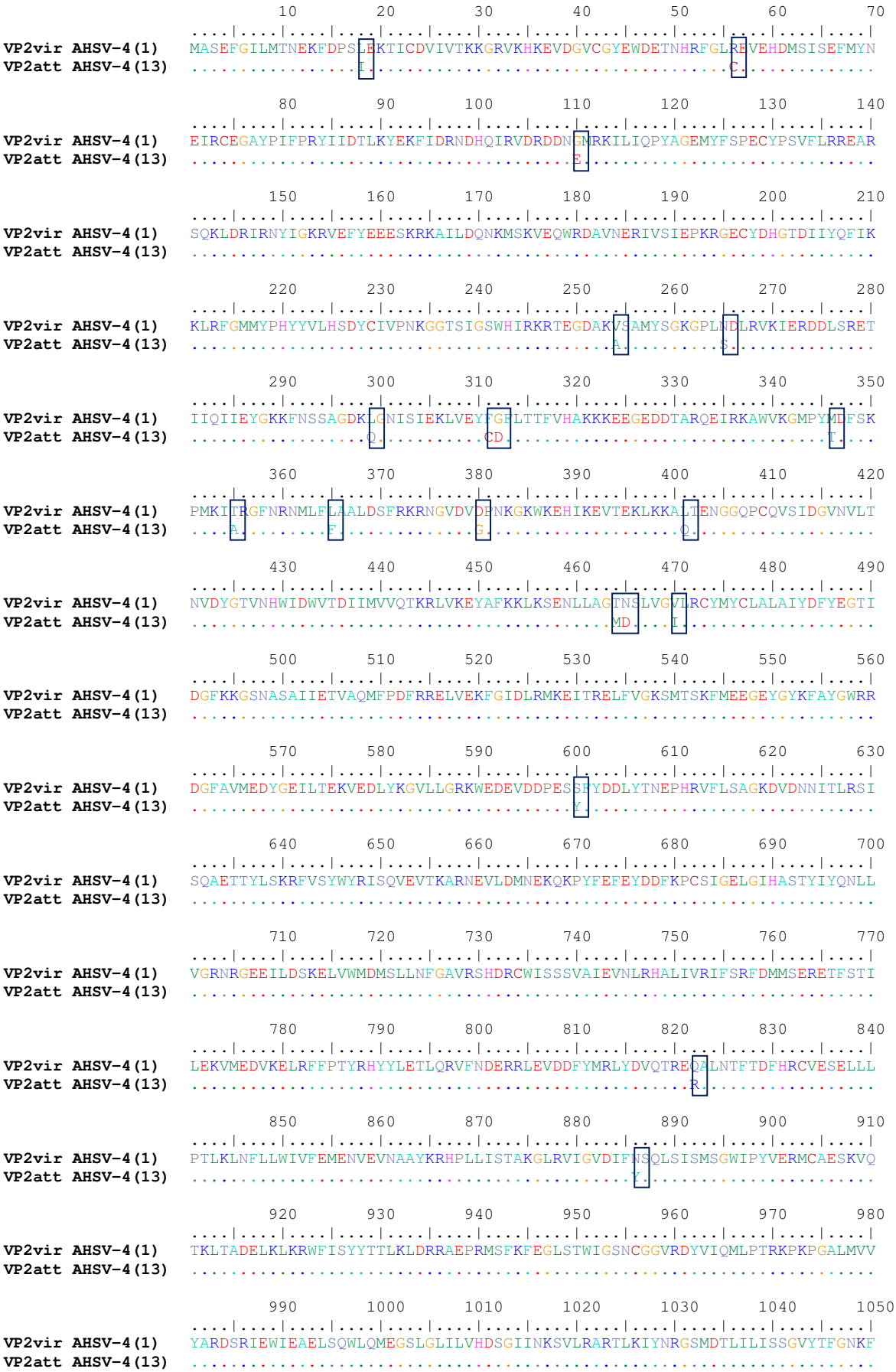

```
                          1060
                 ....|....|....
VP2vir AHSV-4(1)    LLSKLLAKTE*GTA
VP2att AHSV-4(13)   ..........*...
```

(b)

```
                          10        20        30        40        50        60        70
                 ....|....|....|....|....|....|....|....|....|....|....|....|....|....|
VP5vir AHSV-4(1)    MGKFTSFLKRAGNATKRALTSDSAKKMYKLAGKTLQRVVESEVGSAAIDGVMQGAIQSIIQGENLGDSIK
VP5att AHSV-4(13)   ..............................................................................

                          80        90       100       110       120       130       140
                 ....|....|....|....|....|....|....|....|....|....|....|....|....|....|
VP5vir AHSV-4(1)    QAVILNVAGTLESAPDPLSPGEQLLYNKVSEIEKMEKEDRVIETHNAKIEEKFGKDLLAIRKIVKGEVDA
VP5att AHSV-4(13)   ..............................................................................

                         150       160       170       180       190       200       210
                 ....|....|....|....|....|....|....|....|....|....|....|....|....|....|
VP5vir AHSV-4(1)    EKLEGNEIKYVEKALSGLLEIGKDQSERITKLYRALQTEEDLRTRDETRMINEYREKFDALKEAIEIEQQ
VP5att AHSV-4(13)   ..............................................................................

                         220       230       240       250       260       270       280
                 ....|....|....|....|....|....|....|....|....|....|....|....|....|....|
VP5vir AHSV-4(1)    ATHDEAIQEMLDLSAEVIETASEEVPIFGAGAANVIATTRAIQGGLKLKEIVDKLTGIDLSHLKVADIHP
VP5att AHSV-4(13)   ..............................................................................

                         290       300       310       320       330       340       350
                 ....|....|....|....|....|....|....|....|....|....|....|....|....|....|
VP5vir AHSV-4(1)    HIIEKAMLRDTVTDKDLAMAIKSKVDVIDEMNVETQHVIDAVLPIVKQEYERHDNKYHVRIPGALKIHSE
VP5att AHSV-4(13)   ..............................................................................

                         360       370       380       390       400       410       420
                 ....|....|....|....|....|....|....|....|....|....|....|....|....|....|
VP5vir AHSV-4(1)    HTPKIHIYTTPWDSDSVFMCRAIAPHHQQRSFFIGFDLEIEYVHFEDTSVEGHILHGGAITVEGRGFRQA
VP5att AHSV-4(13)   ..............................................................................

                         430       440       450       460       470       480       490
                 ....|....|....|....|....|....|....|....|....|....|....|....|....|....|
VP5vir AHSV-4(1)    YTEFMNAAWGMPTTPELHKRKLQRSMGTHPIYMGSMDYAISYEQLVSNAMRLVYDSELQMHCLRGPLKFQ
VP5att AHSV-4(13)   ..............................................................................

                         500
                 ....|....|....|....
VP5vir AHSV-4(1)    RRTLMNALLYGVKIA*LQG
VP5att AHSV-4(13)   ..............*...
```

Fig. A2.2: Amino acid sequence alignments of the VP2 (a) and VP5 (b) proteins of a virulent and an attenuated AHSV-4 isolate. Amino acid sequences were deduced from the obtained nucleotide sequences. Dots denote identical amino acids and asterisks denote stop codons. For VP2, the boxes indicate amino acid differences between the VP2 proteins of a virulent and an attenuated AHSV-4 isolate.